MECHANISMS OF POLYOMAVIRUS TRANSFORMATION OF THE MOUSE MAMMARY GLAND

By

MARC A. WEBSTER, B.Sc.

A Thesis

Submitted to the School of Graduate Studies

in Partial Fulfillment of the Requirements

for the Degree

Doctor of Philosophy

McMaster University

POLYOMAVIRUS-MEDIATED MAMMARY TUMORIGENESIS

DOCTOR OF PHILOSOPHY (1996)

(Biology)

McMASTER UNIVERSITY

Hamilton, Ontario, Canada

TITLE: Mechanisms of polyomavirus transformation of the mouse mammary gland

AUTHOR: Marc A. Webster, B.Sc. (McMaster University)

SUPERVISOR: Professor W.J. Muller

NUMBER OF PAGES: xv, 216

Polyomavirus infection of newborn rodents results in the rapid induction of tumor formation in a number of tissues. One of the prominent target organs for Polyomavirus-mediated transformation is the mammary gland. The transforming potential of Polyomavirus (PyV) resides in the cellular expression of three tumor antigens (large, middle, and small) immediately following viral absorption. Due to the potent transforming ability of these T antigens in the mouse mammary gland, and given the extensive characterization of cellular proteins which interact with the various T antigens, I sought to exploit the use of these viral oncogenes to elucidate cellular proteins critical in this transformation process.

To analyze the functional significance of large T antigen expression in the mouse mammary gland, I generated transgenic mice harboring the PyV LT antigen cDNA under transcriptional control of the mouse mammary tumor virus long terminal repeat (MMTV LTR). While PyV LT expression was correlated with the genesis of mammary dysplasia, the latency, frequency, and focal nature with which tumors arise suggests that PyV LT is not sufficient to induce malignant conversion of the primary mammary epithelial cell.

PyV MT efficiently transforms the mouse mammary epithelium. To better elucidate which signal transduction pathways central to this process, I have generated mouse models which effectively demonstrate the *in vivo* role(s) of three MT-associated proteins in mammary tumorigenesis - Src, SHC, and phosphatidylinositol 3-kinase. To directly assess the effect of mammary gland-specific expression of activated c-Src, I established transgenic mice which carry a constitutively activated form of *c-src* under the transcriptional control of the MMTV LTR. The roles of both SHC and PI3'K were investigated through functional inactivation of the corresponding binding sites for these proteins on PyV MT. These mutant MT isoforms were used to generate MMTV/MT Y250F and MMTV/MT Y315/22F strains respectively. Similar to PyV LT transgenic strains, Src527F, MT Y250F, and MT Y315/22F strains all were debilitated in mammary tumor formation compared to wild-type PyV MT transgenic animals.

Acknowledgements

There are many people whom I would like to thank for making my extended stay here at McMaster memorable and (mostly) enjoyable. Dr. William Muller, my supervisor, consistently provided me with encouragement and provided me with every possible opportunity to succeed. His willingness to help me through many situations both in and out of the laboratory truly made him a fantastic friend. I don't think I could ever repay you for all you've done for me Bill - thanks. I'd also like to give a special thanks to co-workers Monica Graham, Peter Siegel, David Dankort, Chantale Guy, and Senthil Muthuswamy (Moochosalami) and many others for making otherwise mundane lab work that much more interesting and enjoyable. Thanks also to committee members Dr. John Hassell and Dr. Colin Nurse for their helpful comments and guidance throughout my Ph.D.

I cannot even begin to express how thankful I am for all the personal support from all my close friends and my family (both the Websters and the Taylors). Finally, I would like to thank my loving wife Janice who had to put up me during some fairly rough times. Without you I really could not have done it. I love you very much.

Thanks everyone!

CONTRIBUTION BY OTHERS

Some of the work described herein was generated with the help of others. In particular I would like to list the following contributions:

Figure 3.3 Polyomavirus large T-antigen expression in the brain of transgenic strain MMTV/LTN-7 results in severe hypomyelination in the central nervous system, was performed by Dr. Colin Nurse and Dr. Richard Butler in collaboration.

Figure 5.1 Construct MT Y315/22F was generated by Senthil Muthuswamy, a fellow Ph.D. graduate student in the laboratory.

Figure 5.31 Southern blot analyses used to distinguish between mT mutant transgene carriers, was performed by Monica Graham, a technician in the laboratory.

Table 1.1 Generation of MMTV/LT transgenic animals LT-1, LT-2, LT-3 was accomplished by Chantale Guy, a fellow PhD graduate student in the laboratory.

Table 5.4 Janice Webster helped in the data collection from the focus forming assays.

CHAPTER 1

CHAPTER 2 No Figures

CHAPTER 3

CHAPTER 4

CHAPTER 5

INTRODUCTION

1.1. Normal mammary gland biology

Mammary tissue from virtually all mammalian species demonstrate remarkable similarities in embryonic development and subsequent tissue rearrangements associated with puberty and/or pregnancy (reviewed in Borellini et al., 1989, Kratochwil, 1969, Williams et al., 1983). The mouse thus serves as an ideal model with which to study both the normal and malignant development of the human mammary epithelium. During embryogenesis, the future mammary gland presents itself as an ectodermal thickening on both sides of the trunk known as the mammary band. Following birth, a cord of epithelial cells extends below the surface ectoderm into the surrounding mesenchyme. Gradually this cord of cells becomes canalized, opening at the apex where the future nipple forms. Two distinct growth phases associated with prepubertal and pubertal development are evident. Prepubertal growth is associated with isometric growth of the mammary anlage while pubertal growth results in allometric expansion of the mammary tissues compared to whole body growth rate. The rapid mammary gland expansion is associated with increased end bud formation and ductal elongation. Secondary and tertiary branching from the main epithelial ducts give rise to the characteristic tree-shaped pattern of the virgin mammary gland (Figure 1.1). Further epithelial differentiation is associated with the onset of pregnancy. Systemic hormone changes associated with pregnancy make way for another round of epithelial proliferation in the mammary gland. Epithelial branching combined with lobuloalveolar development of the terminal end bud structures prepares for the eventual secretion of milk for the newborn. While systemic hormones play a significant role in the development of the mammary gland, they are by no means the sole influence. Indeed local factors mediated by epithelial and stromal interactions determines both the extent of growth and the overall architecture of the gland. The combination of systemic hormones coupled to the interplay of local heterotypic cell interactions allows for a coordinated and highly organized development of the mammary gland.

Figure 1.1. Subgross morphology of the developing mouse mammary gland. Photomicrograph of a hematoxylin/eosin-stained wholemount preparation from a four week old normal mouse mammary gland. Note the secondary and tertiary ductal branching (indicated with an open-ended arrow) as well as the densely stained epithelial end buds (indicated with a closed-end arrow). Magnification, (2.5X)

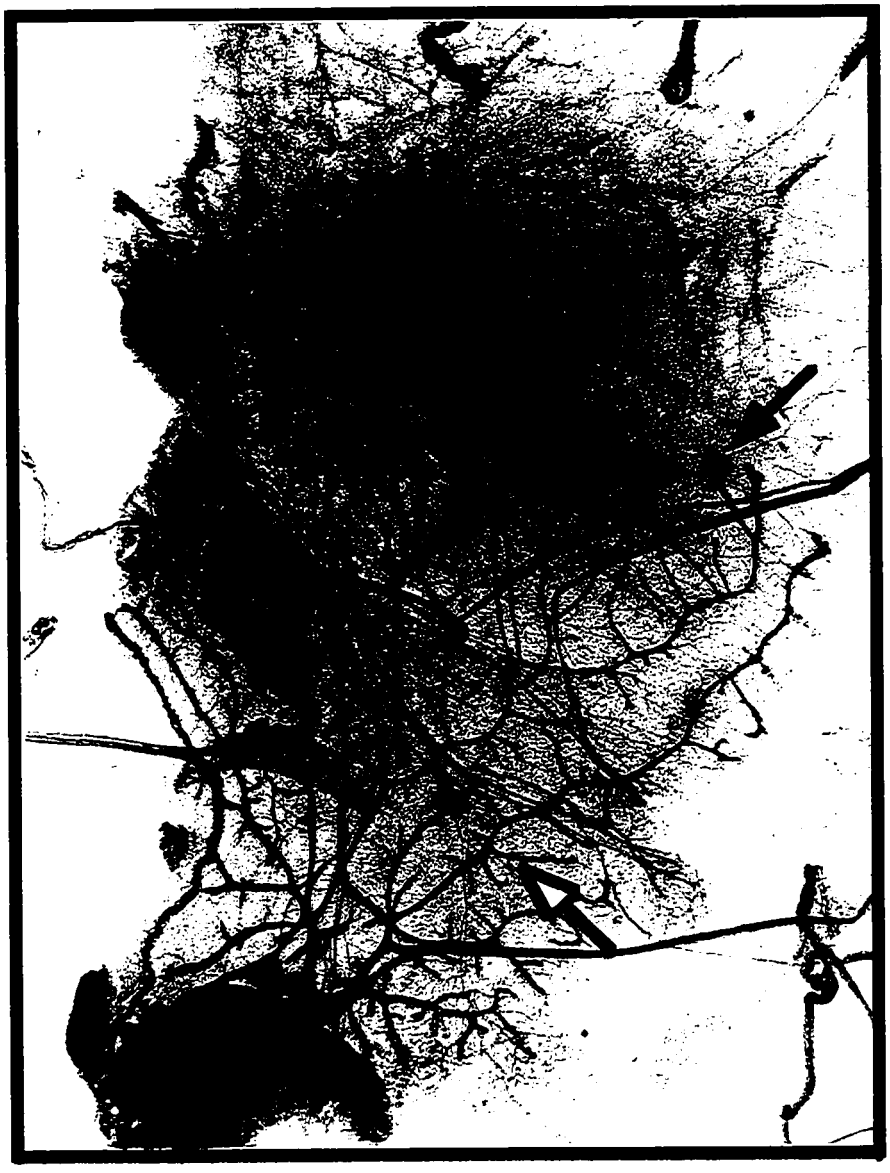

influenced by any one or combination of a large number of factors affecting mammary epithelial cell growth.

1.2. Mammary Tumorigenesis

Mammary tumorigenesis is viewed as a multistep process. The presence of overt carcinoma is the terminal phase of disease progression prior to metastasis. Estimates place the number of women affected by breast cancer as high as 1 in 9 (Dickson et al., 1991). Given the high incidence of this type of tumor there is a need to better understand the underlying mechanisms through which this disease progresses in order to facilitate the development of preventative treatments. Many of the advances to date have resulted the culmination of a wide variety of cellular genes whose altered and/or amplified products have been implicated as progressive factors in mammary carcinogenesis. The receptor tyrosine kinase *neu/erbB2/her2* amplification and /or overexpression has been reported in 9 to 33% of breast carcinomas and as a result has yielded one of the most useful genetic markers correlating tumor progression with prognosis (Coussens et al., 1985, King, 1985). *c-erbB* , the hallmark receptor tyrosine kinase of this family of proteins, is amplified in 6-32% of primary breast carcinoma samples analyzed (Garcia, 1989, Slamon et al., 1987, Van de Vijver, 1989, Varley, 1987). Other protein families which have been cited as possible candidates in this multistep transformation process include growth factors: TGF-alpha, IGFI, IGFII, PDGF, *Wnt* -1, *int* - 2, αFGF, βFGF and FGF-5; growth factor receptors: IGF-I and II receptors; non-receptor tyrosine kinase Src; GDP/GTP-binding protein Ras ; transcription factor Myc; and numerous cyclin and cyclin dependent kinases (for reviews see Dickson et al., 1991,Van de Vijver et al., 1991). Most of these gene products are involved in the normal proliferation of mammary anlage during development and therefore represent targets for mutational activation.

Loss of heterozygosity (LOH) in tumor DNA, on the other hand, is typically indicative of mutations which specifically impair or inactivate gene products whose function resides in negative

3p, 11p, 13q and 17 in 29%, 30% 20-27%, 7-19% and 70% respectively (for review see Callahan, 1989). Most genes responsible for the observed LOHs are as yet uncharacterized with exception to the p53 (Donehower et al., 1992), BRCA1 (Miki et al., 1994), and RB (T'Ang et al., 1988, Varley et al., 1989) loci of chromosomes 17p, 17q and 13q respectively.

1.3 The Transgenic Mouse as a Model for Mammary Tumorigenesis

The transgenic mouse has served as a powerful model with which to investigate the *in vivo* effects of many genes thought to be responsible for cancer progression. Indeed, many such mouse models have recapitulated the etiology of most human malignancies from a variety of tissue origins. The identity of proteins leading to malignancy in addition to the availability of an *in vivo* model has improved our understanding of events leading to tumorigenesis and facilitated the design of potential therapeutic interventions. A number of transgenic mouse strains have been created which predispose animals to formation of mammary carcinomas (Table 1.1). Most studies have utilized highly tissue-specific promoters/enhancers to limit the site(s) of expression of the transgene. Of particular interest to the study of mammary tumorigenesis are promoter/enhancer elements derived from the mouse mammary tumor virus (MMTV) long terminal repeat or the whey acidic protein (WAP)(reviewed in Muller, 1991). Both DNA elements when linked to heterologous genes enables high levels of transcription primarily in mouse mammary epithelial tissues. While both promoters drive high levels of transcription within the mouse mammary gland, the temporal pattern of expression and the epithelial cell type that sustains this transcription differs. Transgenes under transcriptional control of the WAP promoter are restricted to later stages of pregnancy coincident with the natural expression of endogenous WAP. In effect, this temporal restriction limits the study of transgenes to a well-differentiated state of the mammary gland. The MMTV LTR on the other hand maintains low levels of transcription throughout the hormonally induced morphogenic alterations of the mammary gland with levels peaking at parturition (Hagar,

Table 1.1 Comparison of MMTV/ and WAP/oncogene transgenic strains.

Summary of current transgenic strains demonstrating various mammary gland pathologies, the latency associated with the pathology and nature of tumor occurrence (i.e. stochastic versus synchronous multifocal appearance of tumors (if applicable)).

Comparison of MMTV and WAP oncogene transgenic strains

nstruct	Pathology*	Tumor occurence[b]	Onset	References
-myc	m.gl. tumors, B&T-cell lymphomas	stochastic	325 days	Sinn, 1987 ; Stewart, 1984 ; Leder, 1986
-Ha-ras,N-ras	m.gl. tumors, lymphomas, sal.gl. tumors, har. gl. hyperplasia, lung tumors, epididymal hyperplasia	stochastic	168 days	Sinn, 1987 ; Tremblay, 1989 Mangues, 1990
a-ras[a] / c-myc	m. gl. tumors, sal. gl. tumor[a]	stochastic	3-6 months	Andres, 1987 ; Andres, 1988 ; Schonenberger, 1988
ctivated neu	m. gl. tumors, sal. gl. hyperplasia, epididymal hyperplasia	single-step or rapid progression	89 days	Muller, 1988
ctivated neu	m. gl. tumor, epididymal hyperplasias, har. gl. hyperplasia	stochastic	5-10 months	Bouchard, 1989
-erbB-2 / neu	lymphomas, facial adenocarcinoma	stochastic	ND	Suda, 1990
eu	m. gl. tumors, lung metastases	stochastic	7-8 months	Guy, 1992b
et	m. gl. adenocarcinoma	stochastic	6-7 months	Iwamoto, 1990
nt-1	m. gl. hyperplasia, m. gl. tumors, sal. gl. tumors	stochastic	3-7 months	Tsukamoto, 1988
nt-2	m. gl. hyperplasia, m. gl. tumors, prostate and epididymal hyperplasia	stochastic	>18 months	Muller, 1990 ; Omitz, 1991 Stamp, 1992
nt-3	m. gl. tumors, epididymal hyperplasia, sal. gl. tumor	stochastic	2-7 months	Jhappan, 1992
GF α	m. gl. tumors	stochastic	3-5 months	Matsui, 1990
ionein / TGF α	m. gl. tumors, pancreatic metaplasia, liver tumors	stochastic	7-14 months	Jhappan, 1990 ; Sandgren, 1990
SV40 large T	lymphomas, lung and kidney adenocarcinomas, m. gl. adenocarinomas	stochastic	ND	Choi, 1988
E1A and E1B	gastric tumors		ND	Koike, 1989
PyV middle T	m. gl. tumors, lung metastases	single-step or rapid progression	60 days	Guy, 1992a
GH	precocious m. gl. development			Bchini, 1991

iations: mammary gland = m. gl. , salivary gland = sal. gl., harderian gland = har. gl.; ND,not done
to mammary tumors

WAP/H-*ras* transgenic mice rarely develop mammary tumors, while mice transgenic for the same oncogene under transcriptional control of the MMTV LTR demonstrate frequent mammary tumor formation (Mangues et al., 1990, Sinn et al., 1987, Tremblay et al., 1989). A similar phenomenon was observed in transgenic mice expressing the *int-2* oncogene under the transcriptional control of either the wild-type or a truncated version of the MMTV LTR (Muller et al., 1990). In the latter transgenic strains, *int-2* expression could be detected in the mammary glands of pregnant animals but was absent in virgin animals. In contrast, transgenic animals carrying the wild-type MMTV LTR/*int-2* fusion gene expressed the transgene in both virgin and pregnant mammary glands (Muller et al., 1990). All the wild-type MMTV LTR/*int-2* animals developed severe mammary gland hyperplasias that eventually led to the stochastic development of mammary tumors (Muller et al., 1990, Ornitz et al., 1991). Interestingly, animals carrying the truncated LTR/*int-2* developed benign well-differentiated mammary epithelial hyperplasias which rarely progressed to full malignancy (Muller et al., 1990). These two examples demonstrate the underlying significance of temporal patterns of transgene expression with respect to mammary gland differentiation.

1.4 Multistep model of tumorigenesis

Remarkable progress has been made towards understanding the mechanisms through which normal cells escape the highly regulated and coordinated events which maintains the cell in an appropriate state of homeostasis with respect to tissue (and ultimately organ) development and function. Underlying the origin of tumorigenesis is the intrinsic presence of genetic damage within cancer cells. These events are typically manifest through either 'gain of function' mutations associated with deregulated proto-oncogenes and/or through 'loss of function' mutations resulting from recessive lesions in tumor suppressor genes. In general, tumorigenesis of most, if not all tissues, requires multiple genetic alterations in order to successfully breach the cells' restrictive growth controls. It has been estimated that the mean number of 'activating mutations' (including

transform any given cell is 5 or 6 (Peto et al., 1975).

The first evidence suggesting collaborative transforming effects in response to co-expression of oncogenes derives from studies with Polyomavirus transforming (T) antigens large-sized T antigen (PyV LT) and middle-sized T antigen (PyV MT). While individual expression of either T-antigen in Rat embryo fibroblasts rarely results in transformation, co-expression of PyV MT and PyV LT is capable of efficiently transforming these cells (Rassoulzadegan et al., 1982). Since then, numerous studies have highlighted the co-operative *in vitro* transforming effects of various oncogenic products including *ras/myc*, *ras/E1a*, *int-1/int-2* oncogene combinations (reviewed in Hunter, 1991). It has been noticed that given appropriate experimental conditions, some oncogenic products are sufficient to induce full transformation. Indeed, *src*, *ras* and PyV MT if linked to strong transcriptional promoters are capable of transforming rat embryo fibroblasts, albeit, at reduced efficiency (Dotto et al., 1988,Land et al., 1986,Spandidos et al., 1984).

While these *in vitro* studies have identified many candidate genes which when expressed in established cell lines confers a transformed phenotype, this is not always reflective of their *in vivo* potential. Indeed the immediate cellular environment is likely to influence the mitogenic capacity of oncogene-expressing cells. Local paracrine interactions from adjacent epithelial or stromal cells and/or more distant hormonal influences are factors which can positively or negatively affect growth potential. While oncogenes such as *myc*, *ras* and *src* demonstrate powerful transforming effects *in vitro* (reviewed in Weinberg, 1985), examination of their transforming potential in the mammary glands of transgenic animals has revealed that their expression is not sufficient to induce widespread transformation of the mammary epithelium (Leder et al., 1986, Schonenberger et al., 1988, Sinn et al., 1987, Stewart et al., 1984, Tremblay et al., 1989, Webster et al., 1995). Tumors which arise in these transgenic strains are focal in origin and arise next to histologically hyperplastic mammary tissue. Furthermore, there is almost always a significant latency associated with the appearance of mammary tumors. Taken together, these observations suggest that additional genetic events are required to complement the

vivo.

1.5. Single-step/rapid progression oncogenes in mammary gland tumorigenesis

Although mammary epithelial expression of most oncogenes is not sufficient to induce malignant transformation of the mammary gland, there are several notable exceptions in which high level expression of certain classes of oncogenes can lead to the rapid induction of multifocal mammary tumors. For example, expression of a constitutively active version of Neu in several transgenic strains leads to the rapid induction of multifocal mammary tumors (Guy et al., 1996, Muller et al., 1988). Bouchard and colleagues (Bouchard et al., 1989) describe a similar transgenic model, however, the appearance of tumors was stochastic rather than global in nature. These conflicting results may be reflective of relative transgene level differences between these transgenic mice. In effect, there may be a putative threshold tolerance intrinsic to mammary epithelial cells for which expression levels influence cellular fate (Cardiff et al., 1993). Another transgenic mouse model which demonstrates similar tumor kinetic profiles are the MMTV/MT strains (Guy et al., 1992). These animals harbor the Polyomavirus middle sized T-antigen under transcriptional control of the MMTV LTR. Indeed, detection of PyV MT transcript is tightly correlated with the presence of mammary carcinoma *in situ* (Guy et al., 1992 ; Chapter 5).

1.6 Polyomavirus

1.6.1 Polyomavirus overview

Polyomavirus was initially isolated serendipitously as a cell-free extract (prepared from a high-incidence leukemic mouse strain Ak) that was capable of inducing parotid tumors in AKR or C3H mouse strains (reviewed in Eddy, 1969, Gross, 1970). The intent of the authors was to study the etiologic agent giving rise to lymphomas frequently observed in this strain of mice. The parotid malignancy was somewhat of a surprise given the fact that Ak mice rarely develop parotid malignancies. Further evaluation revealed the co-habitation of distinct tumor-bearing viruses with the lymphoma-generating virus being phenotypically dominant. *In vitro* cultivation of the parotid

rodent hosts and causing malignancies in a wider variety of tissues. The range of tissues infected following inoculation can be quite extensive involving over 30 different cell types. From these affected tissues more than a dozen may give rise to tumor formation, collectively known as the Polyoma tumor constellation. Tumors are generally mesenchymal or epithelial in origin depending on the strain of virus, route of infection, and the genetic background of recipient animals (Dawe et al., 1987, Dubensky et al., 1991, Gross, 1970). For example, low tumor-incidence strains RA and A3 almost exclusively give rise to tumors of mesenchymal origin (primarily bone) while the highly oncogenic variant strains PTA and A2 display roughly equal incidence of epithelial and mesenchymal malignancies (Dawe et al., 1987). The viral proteins responsible for cellular transformation appear early following viral absorption. All three 'T' or tumor antigens share a common transcript with differential splicing giving rise to three functionally distinct T-antigens: large T(PyV LT), middle T(PyV MT), and small T(PyV ST). Genetic and biochemical analyses of Polyomavirus-mediated transformation revealed that the early region encoding these T-antigens is responsible for the potent transforming nature of the virus. Indeed functional inactivation in any one of these viral T-antigens greatly reduces the *in vivo* capacity of the virus to transform (Benjamin et al., 1990, Fluck, 1987).

1.6.2. Polyomavirus large T-antigen

PyV LT antigen has been employed extensively by researchers as a means to immortalize primary cell cultures (Rassoulzadegan, 1983). Its immortalizing capacity likely resides in its ability to manipulate nuclear regulatory factors so as to maintain the cell in a constant state of cycling thereby impeding cellular quiescence. Two such regulatory proteins found complexed to PyV LT are the retinoblastoma gene product (Dyson et al., 1990) and the homologue of Drosophila homeoprotein Cut1 (Chapter 3, section 3.2.5.) (see Figure 1.2A). PyV LT is homologous to SV40 large T antigen sharing features with SV40 LT shown to be essential for its

Figure 1.2. Diagrammatic representation of Polyomavirus T-antigen associated cellular proteins

(A) Cellular proteins which associate with PyV LT. The stippled object represents the viral T antigen. Multiple protein family members which have been shown to complex PyV LT are indicated on the same object separated by a slash.

(B) Cellular proteins which associate with PyV MT. The stippled object represents the viral T antigen. Multiple protein family members which have been shown to complex PyV MT are indicated on the same object separated by a slash.

(C) Cellular proteins which associate with PyV ST. The stippled object represents the viral T antigen.

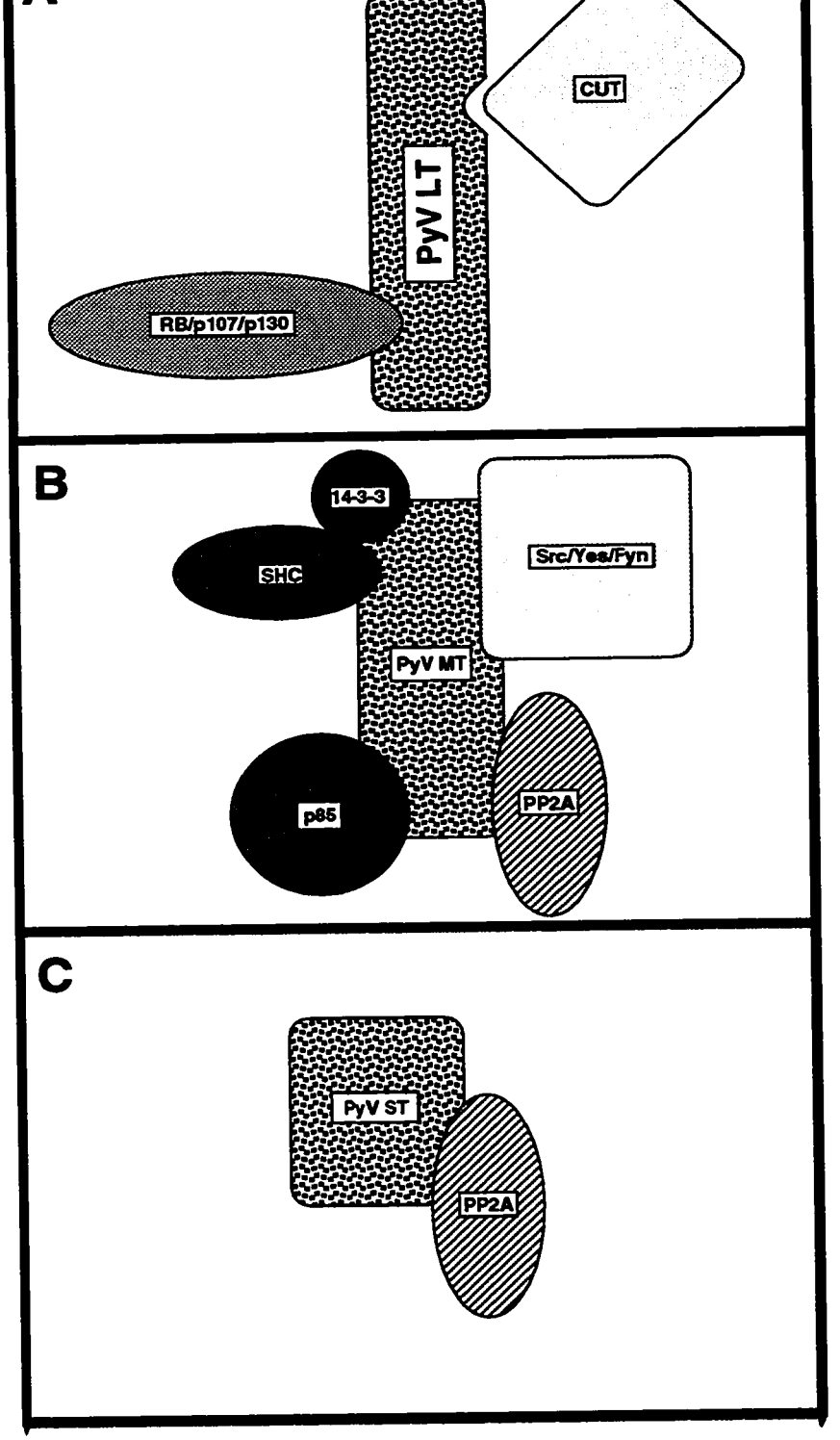
A
CUT
PyV LT
RB/p107/p130
B
14-3-3
SHC
Src/Yes/Fyn
PyV MT
p85
PP2A
C
PyV ST
PP2A

between these T antigens from different viruses, PyV LT expression alone is weakly oncogenic in cells in contrast to SV40's potent transforming ability. The differences in tumorigenic potential between these proteins may in part reside in the ability of SV40 to bind and functionally inactivate the cellular protein p53 (Linzer et al., 1979). Unlike other DNA tumor viruses, polyomavirus (more specifically PyV LT) has thus far shown to be incapable of complexing p53. Moreover, SV40 has been demonstrated to complex with other RB-family members (i.e. p107) which could also influence its transforming potential (Dyson et al., 1989). To achieve complete transformation in polyomavirus infection, PyV LT expression requires the concerted expression of PyV MT and perhaps PyV ST. In viral infection, PyV LT modulates early and late transcription as well as functioning in the initiation of viral DNA replication through its ability to bind to specific sites in the regulatory region of the viral genome (Tooze, 1981).

1.6.3 Polyomavirus middle T-antigen

i) PyV MT associates with several cellular signaling proteins

PyV MT is characteristically known as the transforming antigen of Polyomavirus. It is a 56kDa phosphoprotein with no intrinsic biochemical function and is found primarily associated with cell membranes. A higher 58 kDa PyV MT species is thought to result from extensive serine and threonine phosphorylation mediated by protein kinase C (PKC) (Matthews et al., 1986). The significance of this post-translational modification with respect to PyV MT-mediated transformation, however, is unclear. The lack of intrinsic biochemical activity is compensated for by its ability to serve as a scaffold enabling the recruitment of many distinct signaling proteins. A number of host cellular cytosolic factors are found associated with PyV MT including the p85 regulatory subunit of phosphatidylinositol 3' kinase (PI3'K) (Whitman et al., 1985), the catalytic and regulatory subunits of protein phosphatase 2A (Pallas et al., 1990, Walter et al., 1990), SHC (Campbell et al., 1994, Dilworth et al., 1994), 14-3-3 (Pallas et al., 1994), members of the Src kinase family (Courtneidge & Smith, 1983 , Kornbluth et al., 1987, Cheng et al., 1988, Kypta et

transforming nature of this protein both *in vitro* and *in vivo* is likely due to its ability to assemble such diverse signaling proteins into multimeric complexes. Indeed, similar to MMTV/activated Neu transgenic mice, mammary gland expression of PyV MT in MMTV/MT transgenic animals is coincident with the synchronous formation of multifocal mammary tumors with rapid onset (Guy et al., 1992a). Tumors arising in these animals demonstrated a high propensity to metastasize to the lungs offering for the first time, an *in vivo* model which recapitulates all stages of breast cancer progression. Although the mammary phenotype was striking, it is perhaps not all that surprising given the potent transforming nature of the parent virus.

ii) PyV MT associates with members of the src family of tyrosine kinases

The first associated biochemical activity associated with PyV MT was the tyrosine kinase activity of Src. Interaction of PyV MT with Src or Src family members (*c-yes, fyn*), renders the tyrosine kinase activities of these proteins constitutively active (Courtneidge & Smith, 1983 , Kornbluth et al., 1987, Cheng et al., 1988, Kypta et al., 1988, Horak et al., 1989). The mechanism of Src kinase activation resembles that employed by the retrovirally transduced homologue v-*src* in that the negatively regulating tyrosine within the carboxyl terminus is prevented from forming intramolecular interactions with the Src homology 2 (SH2) region. While v-*src* removes the terminal regulatory tyrosine (Cooper et al., 1993, Kmiecik et al., 1987), PyV MT masks this site, effectively preventing its phosphorylation by a family of tyrosine kinases demonstrating specificity for this site (Csk, Lsk, Ntk)(Chow et al., 1994, McVicar et al., 1994, Okada et al., 1991). The association of Src or Src family members with PyV MT is critical for viral transformation. Mutants incapable of Src complex formation are transformation incompetent both *in vitro* and *in vivo* (Markland et al., 1987, Cook & Hassell, 1990). Similarly, tissues which fail to express Src can show a marked reduction in the ability of PyV MT to transform these cells. This is made particularly evident by the lack of mammary tumor formation seen in PyV MT strains bearing constitutive homozygous deletion of both c-*src* alleles (Guy et al., 1994). Hyperplasias and the

family members Yes or Fyn (Guy et al., 1994). PyV MT-mediated signaling, however, appears to primarily target Src in the transformation of mammary epithelium, as PyV MT expression in mice lacking functional Yes protein have comparable rates of tumor formation to wild-type PyV MT transgenics (Guy et al., 1994).

iii) PyV MT associates with the regulatory subunit of PI3'K

While the ability to complex and activate Src is important, it alone is not sufficient to produce full transformation. PyV MT mutants dl1015, Py1178-T, pT250 are among a number of PyV MT proteins fully capable of activating Src and Src family members yet which fail to transform cells (Markland & Smith, 1987). It appears as though PyV MT requires the concerted action of still other associated cellular proteins including PI3'K and SHC to efficiently transform cells. Following association with Src, PyV MT serves as a Src substrate becoming phosphorylated on several tyrosine resides including the major tyrosine phosphorylated site at 315 and minor sites at 322 and 250 (Kaplan et al., 1988). These phosphorylated tyrosines subsequently serve as docking sites for Src homology (SH) 2 containing cellular proteins. SH2 and SH3 domains are highly conserved protein motifs which mediate protein:protein interactions. While SH2 domains demonstrate remarkable specificity for tyrosine phosphorylated residues and immediate adjacent downstream residues (Songyang et al., 1993), SH3 domains demonstrate an affinity for poly-proline sequences (Yu et al., 1994). The p85 regulatory subunit of PI3'K contains one SH3 domain flanked by two SH2 domains (Skoinik et al., 1991) which makes contact with tyrosine phosphorylated site(s) 315 and possibly 322 of PyV MT (Carpenter et al., 1993). The binding of p85 facilitates the recruitment and activation of the catalytic subunit of PI3'K allowing phosphorylation of inositol lipids at the D3 position (Whitman et al., 1987). These phosphorylated lipids are thought to comprise a second messenger signaling system analogous to the phosphoinositol/diacylglycerol generation following activation of phospholipase C family members. Among the proteins influenced by elevated PI3'P levels include serine/threonine kinase

kinase (Dahl, 1996). PyV MT mutants deficient in p85 binding are severely impaired in their ability to transform both *in vitro* (reviewed in Markland & Smith, 1987) and *in vivo* (Freund et al., 1992).

It has been observed by others that tyrosine residue 322 may contribute to the association and consequent activation of PI3'K. Using various mono or dual phosphorylated peptides derived from PyV MT sequences spanning sites Y315 and Y322, Carpenter and colleagues demonstrated the increased efficacy with which doubly phosphorylated peptide activates PI3'K *in vitro* over singly phosphorylated peptides at either site (Carpenter et al., 1993). Many proteins known to activate PI3'K contain clusters of tyrosine phosphorylated residues thought to be relevant in this activation process. Indeed, IRS-1 and the PDGF-β receptor both contain several tyrosine phosphorylated residues important for PI3'K association (Escobedo et al., 1991, Sun et al., 1991).

Recent observations confound the molecular interactions at this site by suggesting that tyrosine phosphorylation of PyV MT residue 322 creates a binding site for PLC-γ (Su et al., 1995). Further, this interaction appears to increase the *in vivo* tyrosine phosphorylation of PLC-γ consistent with activation and the consequent increase in IP3 and DAG products associated with PyV MT transformed cells. Deletion of this residue appears to marginally affect the transforming nature of this protein compared to its parental isoform as judged by focus forming ability in BALB/3T3 cells. If, however, serum concentrations are lowered, the decrease in focus formation is exacerbated. While Su et al. demonstrate that this site allows for specific and selective association of PLC-γ, Brizuela et al. failed to detect this association with murine PyV MT (unpublished observations). This interaction, however, was readily detected with the highly homologous Hamster MT (Brizuela et al., 1995).

Similar to its murine homologue, HaMT when exposed to newborn animals, results in the rapid induction of malignancies with high penetrance. In stark contrast to murine PyV MT, however, the malignancies are primarily lymphoid in origin (Kiefer et al., 1994). Analysis of associated biochemical activities with HaMT reveal similar tyrosine kinase, phosphatase, and

While tyrosine kinase activity with murine PyV MT reflects the association and activation of Src family members Src, Yes and Fyn, HaMT exclusively activates Fyn. Given the importance of Fyn and PLC-γ activities in the activation of T-cells (Sefton et al., 1994, Noh et al., 1995), Brizuela and colleagues suggest that these inherent biochemical differences between PyV MT family members governs the tissue origin susceptible to transformation. Indeed direct comparison of the ability of PyV MT family members to activate IL-2 transcription in murine T-cell line EL4, highlights these differences. While PyV MT failed to stimulate transcription from an IL-2 responsive reporter plasmid, HaMT efficiently induced transcription. Furthermore, murine PyV MT failed to elevate IP3 levels beyond those in control cells unlike the significant elevation observed in HaMT transfected cells. These analyses are consistent with a weak interaction of PLC-γ with murine PyV MT and a comparatively stronger interaction with HaMT (although this may simply be reflective of the ability of murine PyV MT to activate Fyn in these cells).

iv) PyV MT activates ras through the recruitment of adapter protein SHC

In addition to the major tyrosine phosphorylation site, a minor tyrosine phosphorylation site located within middle T-antigen (tyrosine residue 250) was recently shown to serve as a high affinity binding site for the SH2/phosphotyrosine binding domain (PTB) containing protein SHC (Campbell et al., 1995,Dilworth et al., 1994). Unlike SH2 domains, PTB domains recognize tyrosine phosphorylated proteins in context of immediate upstream residues of the phosphorylated tyrosine (van der Geer et al., 1996). SHC exists in multiple isoforms (46kDa, 52kDa and 66kDa) arising from the use of alternative start sites in the native gene (Rozakis-Adcock et al., 1992). This adapter protein becomes highly phosphorylated on tyrosine residues following growth factor receptor activation. Tyrosine residue 317 of SHC, when phosphorylated, creates a consensus GRB2 SH2-mediated binding site (Rozakis-Adcock et al., 1992). GRB2, another adapter-type protein containing two SH3 domains flanking a single SH2 domain, is found constitutively complexed to the GTP exchange protein SOS through interactions with the GRB2

complex to the plasma membrane allows conversion of Ras from its inactive GDP-bound conformation to its active GTP-bound form. Active Ras, in turn, mediates sequential activation of Raf and proteins involved in the mitogen activated protein kinase (MAPK) pathway (reviewed in Seger et al., 1995). MAPK cascades facilitate the transduction of signals received at the plasma membrane to the generation of transcriptional responses in the nucleus. This kinase cascade consists of a 'core' group of three sequentially activated protein kinases which is conserved from yeast to man (reviewed in Waskiewicz et al., 1995). To date three such pathways in mammalian cells have been unveiled and evidence for yet others exists. Activation of MAPK cascades appears to be a central feature in many biological processes including tumorigenesis. It is therefore not surprising that deletion or substitution of the PyV MT residues which mediate SHC binding to PyV MT drastically reduces the tumorigenicity of PyV MT in cells (Campbell et al., 1995, Dilworth et al., 1994).

(v) Polyomavirus middle T-antigen binds phosphatase 2A and members of the 14-3-3 family

While genetic manipulation of PyV MT coding sequences which ablate binding of SHC or PI3'K allows functional identification of the roles these associated cellular proteins play in MT-mediated tumorigenesis, similar studies with PyV MT mutants incapable of complexing PP2A have proven uninformative. Mutations which interfere with PP2A binding also affects binding of all other PyV MT associating proteins (Campbell et al., 1995,Glenn et al., 1995). Indeed, PP2A appears to be one of the first associated cellular protein with PyV MT. Evidence for this derives from the production of monoclonal antibodies which differentiate between PyV MT protein complexes harboring PP2A and/or Src. Of the panel of antibodies generated, none could detect the presence of MT/Src complexes in the absence of PP2A while the converse was readily observed (i.e. MT/PP2A complexes in the absence of Src) (Dilworth et al., 1993). The lack of PyV

PP2A in PyV MT-mediated tumorigenesis.

Recently Pallas et al. described the identification of two previously undescribed PyV MT associated cellular proteins (Pallas et al., 1994). Both proteins proved to be members of the 14-3-3 gene family - a large family of ubiquitously expressed genes. These proteins were initially identified by virtue of their abundance and chomatograph migration in brain tissue preparations (Boston et al., 1980). While a functional role for 14-3-3 proteins has yet to be assigned, 14-3-3 proteins are found in complexes with several distinct signaling proteins including cdc25 proteins (Conklin et al., 1995), Raf (Freed et al., 1994), protein kinase C (Aitken et al., 1995), Bcr (Braselmann et al., 1995), and tryptophan hydroxylases (Ichimura et al., 1995). 14-3-3 core binding sequences have recently revealed the importance of phosphorylated serine residues in 14-3-3 binding proteins (Muslin et al., 1996). The functional significance of 14-3-3 binding to PyV MT is unclear, although as described in Chapter 5, the isolation of a PyV MT deletion mutant which alters the putative core 14-3-3 binding sequence transforms just as well as wild-type MT suggesting that interaction with 14-3-3 family members may be dispensable for MT-mediated transformation.

1.6.4 Polyomavirus small T-antigen

The small T transcript shares the splice donor site of PyV MT and the splice acceptor site of PyV LT and encodes a 22 kDa cytoplasmic and nuclear localized protein. The amino terminus of PyV ST binds to the cellular serine/threonine phosphatase 2A (PP2A)(Pallas et al., 1990)(see Figure 1.2 C). The functional consequence of this interaction is not known, however, it may facilitate activation of mitogen activating protein kinase pathways by preventing dephosphorylation and consequent inactivation of members of the dual specificity kinase family - the MAPKKs or MEKs. Indeed, expression of homologous SV40 small T antigen in fibroblasts was consistent with an elevation in MAPK activation (Sontag et al., 1993). Similar to PyV ST, SV40 ST binds PP2A. However, the levels of SV40 PyV ST required for MAPK activation far

observations). These conflicting observations may be reconciled by the fact that PyV MT can also bind PP2A allowing a concerted sequestration of PP2A. An alternative or additional function of PyV ST resides in its putative supportive role to PyV LT in the initiation of tumorigenesis (Fluck et al., 1979).

Of the three known T antigens expressed following Polyomavirus infection, PyV ST function is the least understood. Indeed in many experimental systems PyV ST expression may be eliminated without consequence on tumor initiation or progression (Cherington et al., 1986, Rassoulzadegan et al., 1982). In still other studies, the co-expression of PyV ST with PyV MT obviated the requirement for PyV LT (Asselin et al., 1986, Fluck & Benjamin, 1979). Regardless of its involvement in tumorigenesis, PyV ST does appear to be necessary for productive infection of wild-type virus by boosting the levels of viral DNA synthesis, and consequently, infectious virus (Berger et al., 1986, Turler et al., 1985).

1.7. Experimental Rationale

Polyomavirus is a potent tumor-inducing virus in newborn rodents. One tissue which demonstrates remarkable sensitivity to Polyomavirus transformation is the mammary gland. While it is well known that the immediate early proteins are essential for viral propagation, it is unclear whether all three immediate early gene products are essential for the tumorigenic potential of the virus. *In vitro* studies suggest that the small T antigen likely plays a supportive role to the actions of large and middle T antigens in Polyomavirus transformation. While significant attention has been focused on PyV MT, little is known about what role, if any, LT serves in this transformation process. Support for its potential involvement in mammary tumorigenesis derives from the observation that LT can bind and functionally inactivate the negative regulatory gene product RB (Dyson et al., 1990). Indeed, many viral oncogenes gain a proliferative advantage through their ability to complex RB or RB family members (Nevins, 1994)(see Figure 1.2A). Furthermore, cytogenetic analyses of primary breast tumor samples has revealed that a significant proportion

1989). Taken together, these data argue that functional inactivation of RB (or RB family members) plays an important role in mammary tumorigenesis. By taking advantage of the ability of PyV LT to bind RB (and possibly other RB family members), I have generated transgenic mouse strains which express PyV LT in the mammary epithelium. Generation of these animals will allow assessment of the role of PyV LT, and by extension, RB's role in mammary gland development and tumorigenesis.

Because PyV MT has been demonstrated as the principal transforming agent in Polyomavirus infected cells *in vitro* (Markland et al., 1987) and within the mouse mammary gland *in vivo* (Guy et al., 1992), I was interested in analyzing the biochemical nature by which PyV MT mediates these effects. PyV MT in many ways resembles activated receptor tyrosine kinases in the ability to recruit key cellular proteins to facilitate the transmission of proliferative signals to the nucleus. Indeed, PyV MT has evolutionarily selected the minimal requirements to push the cell out of quiescence to the benefit of viral production. Similar to the activated Neu receptor tyrosine kinase (RTK), PyV MT complexes cellular proteins SHC, Src, PI3'K, and possibly PLC-gamma (see Figure 1.2B). In contrast to RTK's, PyV MT does not appear to encode redundant signaling mechanisms. Disruption of any one PyV MT-associated cellular protein results in debilitation of its transforming capacity. Many RTKs can incur multiple mutations but retain the ability to signal. This redundancy is manifested by the presence of compensating phosphorylation sites and/or receptor heterodimerization. This presents an inherent complication in identifying which signaling proteins are crucial for tumorigenesis. PyV MT thus presents itself as an ideal model system with which to analyze the steps leading to tumor formation. By genetic manipulation of PyV MT, we can assess the importance of individual signaling pathways in malignant progression.

Although Src activation is essential for PyV MT-mediated mammary transformation (Guy et al., 1994), Src activation is by no means restricted to PyV MT-mediated mammary tumorigenesis. Indeed, several observations suggest that Src activation is a common and perhaps underlying event in mammary tumorigenesis. In a number of primary mammary tumors

breast carcinomas over matched normal mammary tissues. (Jacobs et al., 1983; Ottenhoff-Kalli et al., 1992, Rosen et al., 1986). Moreover, Neu-mediated mammary tumorigenesis is correlated with, on average, a 6.8 fold elevation in the levels of Src kinase activity over matched adjacent normal epithelium (Muthuswamy et al., 1994). The elevated Src kinase levels observed in Neu-derived mammary tumors likely derives from the ability of tyrosine phosphorylated Neu to directly bind Src (Muthuswamy et al., 1995). Given these observations, we wished to examine the *in vivo* consequence of constitutive Src activity in the mouse mammary gland. As described in Chapter 4, a chimeric MMTV-driven expression cassette harboring an activated version of c-*src* was used in the generation of transgenic mice. These animals were used to identify what role, if any, Src activation plays in mammary tumorigenesis.

Results from Chapter 4 argue that activation of Src alone, while necessary for transformation, is not sufficient to produce transformation of the primary mammary epithelial cell. The observation that PyV MT recruits additional signaling molecules implies that the concerted action of several distinct signaling pathways is required for PyV middle T-mediated transformation.

Because Ras activation has been implicated in the genesis of many human cancers including those of the mammary gland (Sinn et al., 1987, Tremblay, 1989), we sought to identify the role Ras activation plays in PyV MT-mediated mammary tumorigenesis. To accomplish this task, I generated transgenic mice harboring a PyV MT mutant protein with tyrosine residue 250 substituted for by a phenylalanine residue (see Chapter 5). This mutant impairs the ability of PyV MT to bind SHC and activate Ras-mediated signaling pathways. Expression of this particular mutant in the mammary gland of transgenic mice will address whether this molecular interaction is relevant to PyV MT-mediated mammary tumorigenesis.

While PI3'K activation has yet to be directly linked to mammary gland tumorigenesis, the observation that the transforming potential of PyV MT closely correlates with its ability to complex this signaling molecule argues that PI3'K likely plays an important role in this transformation

tumorigenesis, I created transgenic strains harboring a PyV MT mutant lacking tyrosines residues necessary for complex formation with this lipid kinase (Chapter 5). This particular PyV MT mutant should allow further characterization of PI3'K in mammary carcinogenesis.

2.1. DNA constructions

To derive the pMMTV LTN construct, plasmid MTLT (obtained from J. Hassell) bearing the cDNA encoding PyV LT (bounded by nucleotides 154 to 4632) was excised with BamHI and BglII, rendered blunt end with the Klenow fragment of DNA polymerase I following which BclI linkers were added. The target PA-9-derived expression vector, pMMTV-SV40 (206), was prepared by restriction at the unique EcoRI site, rendered blunt end with Klenow fragment to which BclI linkers were added. The latter construct was established by first inserting the PstI-to-BamHI fragment bearing the simian virus 40 (SV40) small T splicing and polyadenylation signal from CDM8 (Seed et al., 1987) into the corresponding sites in plasmid Bluescript KS (Stratagene) and then cloning the MMTV LTR containing SalI-to-BamHI fragment derived from plasmid pMMTV neuNT (Muller et al., 1988) into the corresponding sites of Bluescript KS.

To derive the pMMTV LT construct, a 2.3 kbp BamHI fragment derived from the PA-9 derived expression vector containing the MMTV promoter/enhancer sequences (lacking the v-Ha-ras untranslated sequences present in pMMTV LTN) was cloned into the unique BamHI site of plasmid pSP72 (Promega). The BamHI-BglII fragment containing the PyV LT coding sequences was subsequently cloned into the BamHI site of this hybrid vector. Polyadenylation signals derive from parent vector MTLT.

To derive the pSRC527F construct, plasmid pcSRC527 (a generous gift from Dr. D. Shalloway), containing the virally transduced cellular chicken *src* homologue, was excised as an NcoI-BglII fragment and rendered blunt-end following incubation with the Klenow fragment of DNA polymerase I. EcoRI linkers were added and the cDNA was inserted in the correct orientation into the unique EcoRI site of p206 (Guy et al., 1992a).

To derive MMTV/MT Y315/22F construct, PyV MT cDNA derived from plasmid pMMTV/MT was subcloned into the HindIII and EcoRI sites of Bluescript KS. Standard M13

(tgtccaaaaacagatcc). These oligonucleotides allow conversion of wild-type MT tyrosine residues #315 and #322 to phenylalanine residues. Automated sequence analyses confirmed the presence the nucleotide substitutions allowing for the coding of a phenylalanine residues at sites #315 and #322 of MT. The mutant cDNA was subsequently cloned directionally into the HindIII-EcoRI sites of p206.

To derive plasmid pMMTV/MT Y250F, oligonucleotides AB3705 (ccagcggttctgcagaatgcc), AB3706 (tcataacagaaaaggtcggg), AB3595 (gcctaagactgccgagtcttctgagcaacccgacctttctgttatg) and AB3596 (atgagccctctgcaaatcccgaagaatcagaccctcccatgg) were employed in a PCR-based strategy to generate a tyrosine to phenylalanine residue substitution at amino acid residue #250 of PyV MT sequence. Briefly, matched sets of oligonucleotides harboring the necessary nucleotide changes were used to amplify sequences upstream (AB3705+AB3706) and downstream (AB3595+AB3596) of the target mutation site. These PCR products overlap and were subsequently PCR amplified with oligonucleotides AB3705 and AB3596 to generate a PCR product harboring the desired mutation. Restriction of the PCR product with PstI and NcoI followed by a three way ligation resulted in generation of pMMTV/MT Y250F. Automated sequence analyses confirmed the presence of the nucleotide substitution allowing for the coding of a phenylalanine residue at MT site 250.

MoMLV based MT and MT mutant expression cassettes were generated by subcloning the desired MT cDNA via from the MMTV-derived plasmids via unique HindIII and EcoRI sites into the corresponding site of MoMLV-based expression cassette J4-Ω (a gift from B. Rowley).

The PyV large T and middle T-antigen ribonucleotide protection probe (riboprobe) pSP65mT (MTR) was obtained from J. Hassell and contains a 203 bp HindIII-to-AccI fragment of the PyV early region (PyV nucleotides 165 to 368)(Soeda, 1980) inserted into the HindIII and AccI sites of pSP65 (Promega). To generate antisense probe, the plasmid MTR was cleaved with HindIII and RNA polymerase SP6 was employed. The SV40 polyadenylation-specific riboprobe (SPA) contains an 847 bp BamHI-HindIII fragment of SV40 polyadenylation signals (SV40

To generate antisense probe, the plasmid SPA was cleaved with HindIII and RNA polymerase SP6 was employed. The PGK-1 internal control riboprotection probe was obtained from M. Rudnicki and contains the AccI-PstI fragment from the mouse phosphoglycerate kinase cDNA (bounded by nucleotides 939-1633) in the PstI site of pSP64 (Promega). To generate antisense probe, the plasmid PGK1 was cleaved with EcoNI and RNA polymerase SP6 was employed. The 3' β-casein riboprobe contains a 421 nucleotide fragment of β-casein (bounded by nucleotides 153-574) and is cloned into the PstI site of pSP64 (Promega). To generate antisense probe, the plasmid 3'β-casein was cleaved with BamHI and RNA polymerase SP6 was employed. MTsn301 riboprobe used to distinguish between MT mutant MT Y315/22F and MT Y250F contains an 513 nucleotide fragment (bounded by nucleotides 727-1240) in the SphI and NcoI sites of plasmid vector pSL301 (Promega). To generate antisense probe, the plasmid MTsn301 was cleaved with XbaI and RNA polymerase T3 was employed. The *myc* riboprobe pMycExon1 (a generous gift from A. Nepveu) contains an 917 nucleotide fragment (bounded by nucleotides -400 to +517) in the SmaI and SacI sites of plasmid vector pSP65 (Promega). To generate antisense probe, the plasmid pMycExon1 was cleaved with HindIII and RNA polymerase SP6 was employed.

All oligonucleotide synthesis and automated DNA sequencing was performed by Dinsdale Gooden and Brian Allore at the MOBIX Main Central Facility, McMaster University.

2.2. Generation and identification of transgenic mice.

DNA was prepared for microinjection by digestion with 4U each of SalI and SpeI per μg for 1.5 h. The DNA was electrophoresed through a 1% agarose gel and purified as described previously (Sinn et al., 1987). FVB female mice (Taconic Farms, Germantown, Pa) were mated with FVB/N males the night before injection. After isolation of the fertilized one-cell mouse embryos, the pronuclei of these zygotes were injected with 0.5 to 1 pl of DNA solution (5μg/ml). Following microinjection, viable eggs were transferred to the oviducts of pseudo-pregnant Swiss-Webster mice (Taconic Farms).

as described by Muller et al. (Muller et al., 1988). The nucleic acid pellet was resuspended in 100 µl of distilled water at an approximate DNA concentration of 1 µg/ml, and 15 µl of the DNA solution was digested with 30 units of BamHI for 1.5h. Following gel electrophoresis and Southern blot transfer (Southern, 1975) to Gene-Screen filters (Dupont), the filters were hybridized with transgene radiolabeled with [α-^{32}P]dCTP (Dupont) by random priming (Feinberg et al., 1983). MT cDNA sequences derived from pMTR were used to identify both MMTV/LT and MMTV/MT transgenic strains. To identify dual MT mutant transgenic carriers, tail DNA was restricted with PstI following which radiolabeled DNA sequences from p206SPA was used as a probe. MMTV/src527F transgenic progeny were identified by probing genomic DNA after Southern blot transfer with a c-*src* specific probe.

2.3. RNA Analysis.

RNA was isolated from various tissues by the procedure described by Chirgwin et al. (Chirgwin et al., 1979), using the CsCl sedimentation gradient modification. Tissue was flash frozen in liquid nitrogen and stored at -80°C or immediately homogenized in 3 ml of guanidine isothiocyanate (GIT, BRL) solution (4M GIT, 25 mM sodium citrate and 0.1M β-mercaptoethanol). The homogenate was layered onto 4 mls of 5.7 M CsCl containing 25 mM sodium acetate (pH 5.2), and RNA pelleted by ultracentrifugation at 32,000 rpm @ 20°C using an SW41Ti rotor (Beckman) for greater than 17 hours. GIT and CsCl layers were aspirated off and the bottom of the tube cut off using a razor blade. RNA was resuspended in 500 µl of sterile water plus 300 mM sodium acetate (pH 5.2) and precipitated with 2 volumes ice cold ethanol. RNA yield was determined by UV absorption at 260 nm (1 OD260 = 40 µg/ml RNA).

Ribonucleotide protection probes were made with either the Bluescript (Stratagene) or pSP64/65 vectors prepared by restriction with blunt end or 5'-OH overhangs. Linearized riboprobe was analyzed by agarose gel electrophoresis to ensure restriction was complete. Linearized DNA was extracted from the agarose using NaI/glass milk purification (Geneclean, Biocan) and 1 µg

polymerase (SP6, T3, T7) was added to 25 µl of transcription cocktail (200 mM Tris pH 7.5, 30 mM MgCl, 20 mM spermidine.HCl, 15 mM DTT, 40 U RNasin (Pharmacia), 100 µCi [α-32P] UTP [10 mCi/ml, 3000 mCi/mmol], 1 mM each of rCTP, rGTP, rATP and 0.1 mM rUTP) and incubated for 45 min. at 37°C. The reaction was quick chilled on ice and another 30-60 U of RNA polymerase was added. The reaction was allowed to proceed for another 30 min. at 37°C. Transcription was terminated by destruction of the DNA template through the addition of 20U of RNase-free DNaseI, 1 µl of 0.5 mM MgCl and 20 µl of water and incubated at 37°C for 10 min. After bringing the volume of the reaction to 100 µl with water, an equal amount of phenol:chloroform (1:1) was added, the aqueous phase extracted and precipitated with the addition of 300mM sodium acetate (pH 5.2), 20 µg RNase-free tRNA (MRE 600, Boehringer Mannheim) and 2-4 volumes ethanol and resuspended in 100 µl water. Percent radiolabel incorporation was assessed by spotting in duplicate 1 µl of riboprobe onto Whatman-DE81 ion exchange filters whereupon one filter was washed one time each with 5 mls of 0.5 M sodium phosphate buffer, water, and ethanol to remove unincorporated nucleotide. Both filters were subsequently placed in scintillation cocktail (Beckman) and radioactivity measured in a scintillation counter (Beckman).

RNase protection assays were performed as described by Melton et al. (Melton et al., 1984), using 30 µg of total cellular RNA per tissue (except where noted) incubated with 1 µl prepared riboprobe in hybridization buffer (80% formamide, 40 mM piperazine-N,N'-bis (2-ethanesulfonic acid)(PIPES) pH 6.4, 1 mM EDTA pH 8.0, and 400 mM NaCl) at 85°C for 5 min. following which the water bath temperature was reduced to 50°C. RNA was allowed to anneal for greater than 8 hours at 50°C. Hybridization mixtures were quick-chilled and spun at 4°C. RNA digestion conditions were as follows: (i) under normal conditions: 300 µl RNase digestion buffer (300 mM NaCl, 10 mM Tris pH 7.4, 5 mM EDTA pH 8.0, 2 µg/ml RNase T1, and 40 µg/ml RNase A) was added and incubated for 20 min. at 37°C or (ii) conditions used to detect pyrimidine mismatches or deletions: 120 µg/ml RNase A was used in the absence of RNase T1 and

tRNA and 500 µl phenol:chloroform (1:1) followed by ethanol precipitation. RNA pellets were dried for 10 min. in a speed vac, resuspended in 10 µl of formamide loading buffer (80% formamide, 10 mM EDTA pH 8.0, 1 mg/ml xylene cyanol FF, 1 mg/ml bromophenol blue) boiled for 7 min. at 95°C and resolved on a 6% urea polyacrylamide gel (40% acrylamide: 2% N,N'-methylene-bis-acrylamide, 7 M urea, 0.001% ammonium persulfate and 0.0005% N,N,N',N'-tetramethyl-ethylenediamine (TEMED)) electrophoresed at 60-80 amps in 1X TBE running buffer (0.1 M Tris, 0.08 M boric acid, 0.002 M EDTA pH 8.0). The gel was dried and exposed at -70°C against Kodak XAR-5 film in the presence of intensifying screens.

2.4. Antibodies

Antibodies used include mouse monoclonal pAb762 and rat monoclonal pAb701 for PyV MT (a generous gift from S. Dilworth), rabbit polyclonal N16 (Transduction) and mouse monoclonal 7D10 (Quality Biotech) for Src, rat monoclonals pAb820 (a generous gift from J. Bolen), pAb701 for PyV LT and Cut-specific antisera including monoclonals A, W3, 10B, AX, AK and polyclonal antibodies raised against the amino or carboxy sequences. Also used in these studies were antibodies specific for SHC - rabbit polyclonal (Transduction, Cat# S14620) and mouse monoclonal (Transduction, Cat# S14630), the p85 subunit of phosphatidylinositol 3-kinase- rabbit polyclonal (Transduction, Cat# P13030) and mouse monoclonal (Transduction, Cat# P13020), phospholipase C-γ1 - mouse monoclonal mixture (UBI, Cat# 05-163) in addition to antisera specific for phosphorylated tyrosine residues - PY20 (Transduction, Cat# P11120), rabbit polyclonal (Transduction, Cat# P11230). Antibodies specific for Erk1 and Erk2: rabbit polyclonal (residues 191-211, NEB, Cat# 9102) and tyrosine phosphorylated versions of Erk1/2 (NEB, Cat# 9101S) were also used.

Tissue samples were flash frozen in liquid nitrogen and ground to a fine powder with chilled mortar and pestle. Cells were lysed on ice for 30 min. in TNE lysis buffer (20 mM Tris pH 8.0, 150 mM NaCl, 1% Nonidet P-40, 2.5 mM EDTA, 1 mM sodium orthovanadate, 10 mM sodium fluoride, 10 mM aprotinin, 10 mM leupeptin) with constant agitation. Lysates were cleared twice by centrifugation at 13,000 xg for 5 min. each. Supernatants were aspirated and protein concentration assessed using the Bradford assay kit (Biorad).

2.6. Immunoblotting

Unless otherwise specified a total of 100 μg total protein lysate was used for each sample analyzed. An equal volume of 2X protein sample loading buffer (62.5 mM Tris pH 6.8, 2% SDS, 10% glycerol, 5% β-mercaptoethanol, 0.02% bromophenol blue) was added and mixtures were boiled for 10 min. at 95°C. Proteins were resolved on SDS-polyacrylamide gels, transferred electrophoretically (Biorad) onto polyvinylidine difluoride (PVDF) membranes (Immobilon-P, Millipore). Membranes were incubated overnight in 3% low-fat powdered skim milk in TBS (20 mM Tris pH 7.5, 150 mM NaCl, 5 mM KCl) or 3% BSA (Sigma) in TBS for anti-phosphotyrosine immunoblots. Membranes were subsequently incubated for 2 hours at room temp. with antibodies (1:1000 for all monoclonal antibody preparations and 1:250 for all polyclonal antibody preparations). After washing four times (10 min. each) in TBS plus 0.01% Tween 20 (TBST), membranes were incubated for 1 hour room temp. with the appropriate secondary antibody conjugated to horseradish peroxidase (HRP, Biocan Scientific) at 1:2500-1:5000 dilution. The membrane was washed four more times in TBST and proteins were detected using the enhanced chemiluminescence detection system (ECL, Amersham).

2.7. Immunoprecipitations

Immunoprecipitations were performed by preincubating antigen-specific antibody (1-2 μg monoclonal; 5-10 μg polyclonal) with 30 to 40 μl of Protein G Sepharose fast flow (Pharmacia) in

4°C on a rotating platform. Antibody-bound beads were washed 1X 1ml PBS and 1X 1ml lysis buffer. 500ug to 1 mg of total protein lysate was added to a total volume of 700 µl and incubated with the pre-bound beads for 1 to 5 hrs at 4°C on a rotating platform. Beads were subsequently washed 5X in lysis buffer following which bound antigen could subsequently be analyzed.

2.8. Preparation of GST fusion proteins

An overnight culture of *E. Coli.* harboring the GSTag fusion proteins were diluted 1:10 in 50 ml culture media, incubated for 1 hour whereupon IPTG was added to 1 mM and further cultured for 4 hours. Bugs were spun and resuspended in 500 µl MTPBS (150 mM NaCl, 16 mM Na_2HPO_4, 4 mM NaH_2PO_4 pH7.3, 10 µg/ml aprotinin, 10 µg/ml leupeptin) and sonicated on ice. Triton X-100 was added to 1% and lysate was centrifuged at 4°C for 5 min. and supernatant saved. Fusion proteins were immobilized on glutathione Sepharose beads washed extensively with MTPBS.

2.9. Direct binding assay

Analyses were performed as described previously (Ron et al., 1992,Stein et al., 1994). Briefly, 10 µl of glutathione beads representing 15-20 µg of GSTag fusion protein was washed once with DK phosphorylation buffer (50 mM potassium phosphate pH 7.15, 10 mM MgCl, 5 mM NaF, 4.5 mM DTT) and resuspended in 60 µl of reaction mixture containing 500 µCi g-32P ATP (6000Ci/mM, Dupont NEN) in DK buffer. To this 0.2 U/µl of protein kinase A (Sigma) was added and the reaction incubated at 30°C for 30 min. Unincorporated nucleotides were removed by 5 sequential 1 ml PBS plus 5 mM NaF washes. Immunoprecipitates were resolved on SDS-PAGE and transferred to PVDF membranes. Membranes were incubated at 25°C for 3 hours in blocking buffer (20 mM Hepes pH 7.5, 5 mM KCl, 0.02% sodium azide, 5 mM DTT, 5% skim milk). The membranes were probed for 2 hours at 25°C in blocking buffer containing $1x10^6$ cpm/ml

while monitoring the extent of radiolabel removal with a hand held Geiger counter.

2.10. *In vitro* kinase assays

Mouse anti-SRC avian-specific antibody (Upstate Biotechnology) was used for immunoprecipitations (3µg / 500µg protein lysate) with Src-derived tissues and 2 µg pAb762/1 mg protein lysate was employed on MT-derived tissues. Immune complexes were washed as described above and once in KB buffer (5 mM MgCl, 20 mM morpholinepropanesulfonic acid [pH 7.0]). Beads were resuspended in 25µl KB buffer supplemented with 5 µCi of [γ-^{32}P] ATP, incubated at 30°C for 20 min. For phosphorylation of an exogenous substrate 10 µg of acid denatured enolase (Boehringer) was included in the kinase reaction mixture. Kinase reactions were terminated with the addition of an equal volume of 2X protein sample loading buffer , boiled and separated on SDS-PAGE. Gels were fixed in 25% methanol, 7% acetic acid for 30 min. followed by incubation with 1N KOH at 45°C for 30 min. and neutralized in 40% methanol 10% acetic acid for 30 min. 25°C. Gels were dried on a slab drier at 80°C for no longer than 40 min. Dried gels were subjected to autoradiography and/or PhosphorImager screens and quantitated by PhosphorImager analysis (Molecular Dynamics, Sunny vale, CA).

2.11. Phosphatidylinositol 3-kinase analysis

MT and MT mutant immune complexes were washed in 1 ml each of: 3 times in TNE, once in PBS (140 mM NaCl, 2.7 mM KCl, 4.3 mM Na_2HPO_4, 1.4 mM KH_2PO_4), once in 0.5 M LiCl plus 0.1 M Tris pH 7.5, once in water, once in0.1 M NaCl plus 1 mM EGTA pH 8 plus 20 mM Tris pH 7.5 and 2 times in PI kinase buffer (20 mM Tris pH 7.5, 100 mM NaCl, 0.5 mM EGTA pH 8.0). Immune complexes were resuspended in 50 µl PI kinase buffer supplemented with 10 µg bovine liver phosphatidylinositol. After incubation at 25°C for 10 min. the kinase reaction was begun following the addition of 20 mM $MgCl_2$ with 5 µCi of [γ-^{32}P] ATP. The kinase reaction was incubated at room temp. for 10 min. and the reaction was terminated with the sequential addition

chloroform. The mixture was briefly vortexed and phases separated by pulse centrifugation. The top phase was discarded and 150 µl of solution 2 (methanol : 1N HCl (1:1)) was added to the organic phase. Following brief vortex and centrifugation the aqueous phase was decanted to a fresh tube where liquid was evaporated in a speed vac for 20 min. with no heat. Lipid product was resuspended in 15 µl chloroform and subsequently spotted onto Silica gel 60 hard plates (Bodman). Phosphorylated lipid products were separated by thin layer chromatography in a chamber containing 46% CHCl3, 41% MeOH, 5.5% NH4OH (28%), and 7.5% water. Plates were air dried and were subjected to autoradiography and/or PhosphorImager screens and quantitated by PhosphorImager analysis.

2.12. Histological evaluation.

Complete autopsies were performed and both gross and microscopic examinations were done. Four mice at each time point (day 5 pregnant, day 11 pregnant, day 15 pregnant, day 1 postpartum) from both the wild-type background strain FVB/n (Taconic Farms, Germantown, Pa) and the transgenic strain SRC-2 were used to study the lactation deficiency (the presence of a copulation plug was designated day 1 of pregnancy). Five mice from each time point (4 weeks, 8 weeks, 12 weeks, 16 weeks) from transgenic strains MMTV/MT, MMTV/MT Y250F, MMTV/MT Y315/22F, and non-transgenic FVB/n were analyzed. Upper left mammary fat pad (#2L) tissues were fixed in 4% paraformaldehyde, blocked in paraffin, sectioned at 5µm, stained with hematoxylin and eosin, and examined. Wholemount preparations were prepared using the upper right mammary fat pad (#2R) as described by Vonderhaar et. al.(Vonderhaar et al., 1979). Briefly, resected tissue was spread out on glass slides and allowed to air dry overnight. Glands were fixed and defatted by overnight incubation in acetone. To enhance the defatting process, glands were squeezed between glass slides and placed in fresh acetone the next morning. Harris modified hematoxylin was added for overnight staining of the glands. Destain solution (1% conc. HCl in 75% ethanol) was added and discarded until the epithelial component of the mammary

sec. wash in 0.002% ammonium hydroxide. Slides were then transferred to 75% ethanol for 5 min. and then 100% ethanol for several hours. Glands were cleared overnight in xylenes and mounted in Permount.

multiple distinct tumor types.

3.1 INTRODUCTION

Genetic and biochemical analyses of DNA tumor viruses have demonstrated that gene products of the early regions play a pivotal role in inducing cellular transformation. For example, the large, middle and small T antigens of Polyomavirus are the principle viral oncoproteins involved Polyomavirus-mediated cellular transformation (Benjamin, 1990). Recent studies suggest that viral oncoproteins induce cellular transformation through remarkably similar mechanism(s) (Nevins, 1994). For example, the Papillomavirus E7 protein, SV40 large T antigen, Adenovirus early protein E1A, and PyV large T (LT) have all have been shown to physically complex and functionally inactivate members of the RB family (Dyson, 1990). This family currently comprises the product of the retinoblastoma susceptibility gene RB (p105), (Lee et al., 1987), p107 (Ewen et al., 1992) and p130 (Mayol et al., 1993). While the molecular mechanism(s) through which members of the RB family function remains uncertain, they are thought to regulate cell cycle progression (Sherr, 1994). Thus the capability of attenuating the function of these cell cycle control genes within virally infected cells lends a selective growth advantage to the virus by inducing entry into the cell cycle.

The RB gene product has gained significant attention over the past few years as the prototype tumor suppressor gene. Initially, constitutional homozygous deletion of this gene within retinoblasts was blamed as the causative factor in childhood retinoblastoma (Friend et al., 1986). In addition, RB loss of function has been observed in several other cancers including: osteosarcomas, small cell carcinomas of the lung, bladder, and breast carcinomas (Marshall, 1991). The evidence implicating RB in mammary tumorigenesis has stemmed from several independent groups. T'ang et al. and Varley reported that 7-19% of primary breast tumor DNAs had LOHs at the RB-1 locus. Moreover, immunohistochemical analysis revealed 29% of 56 breast

Similarly Lundberg et al. (Lundberg et al., 1987) showed LOH on chromosome 13 (harboring the RB gene locus) in 4 out of 14 breast carcinomas. With the exception of these few studies describing indirect evidence for RB involvement in breast cancer, there is relatively little known concerning the physiological role RB plays in normal mammary gland development and in tumorigenesis.

Given the potential importance of the RB family in mammary tumorigenesis, the generation of an animal model in which endogenous levels of functional RB family are greatly attenuated within the mammary epithelium would prove useful. To accomplish this, I have taken advantage of the observation that PyV large T can functionally inactivate members of the retinoblastoma gene family by forming specific complexes with these proteins (Dyson et al., 1990). In an attempt to reduce the functional levels of RB specifically in the mammary gland, I have generated 8 transgenic mouse strains expressing Polyomavirus large T antigen under transcriptional control of the mouse mammary tumor virus promoter/enhancer. Although mammary epithelial-specific expression of the PyV large T strains was initially not associated with any apparent phenotype, older female transgenic mice developed mammary tumors, albeit, with low penetrance.

In addition to the mammary phenotype, many male and female transgenic progeny developed a number of reproductive tract neoplasms including testicular tumors (of Leydig cell origin) and uterine tumors (leiomyomas). Because human leiomyomas are associated with the loss of chromosomal region 7q22 (Sargent et al., 1994, Ozisik et al., 1993) which encompasses the human Cut gene (Lemieux et al., 1994), we examined whether the expression of Cut was altered in both PyV large - induced leiomyomas and mammary tumors. Results revealed that the levels of Cut were elevated in both tumor tissues analyzed compared to adjacent normal tissues. This increase in the levels of Cut were further correlated with the formation of specific protein complexes between the cellular Cut protein and PyV large T in both mammary and uterine

complex is involved in tumorigenesis.

3.2. RESULTS

3.2.1. Generation and characterization of transgenic mice expressing the PyV large T antigen in the mammary epithelium.

To allow high mammary gland-specific expression of PyV LT antigen, we chose the MMTV LTR promoter/enhancer as the transcriptional control element responsible for transgene expression. Because the MMTV LTR is expressed throughout all stages of mammary gland development with further induction during gestation (Muller, 1991), we are able to examine the effect of transgene expression throughout mammary gland differentiation. A PyV LT cDNA derived from plasmid pMTLT (plasmid obtained from J. Hassell) was excised and subcloned into MMTV expression cassette plasmid pMMTV-LTR in the correct transcriptional orientation (Figure 3.1A). Transgenic strains established with this particular expression cassette resulted in poor mammary gland-specific expression. In an effort to enhance the *in vivo* transgene expression levels, a second MMTV-driven PyV LT expression plasmid was constructed - p206LT (Figure 3.1B). Although both expression vectors contain identical MMTV LTR sequences, the second construct includes the presence of 5' v-Ha-*ras* untranslated sequences upstream of the transcription start site in addition to the inclusion of a 3' splicing cassette derived from the SV40 small T intron (compare Figures 3.1A and 3.1B). These modifications reportedly enhance the levels of translatable transcript (Huang et al., 1981) and constitute the only differences between these plasmids. Both expression cassettes were released from plasmid sequences and microinjected into one-cell mouse embryos. Four independent transgenic strains were generated with each plasmid construct.

The tissue specificity of transgene expression was assessed by RNase protection using 30 μg of total RNA isolated from a variety of organs (Figure 3.2B). The riboprobes used in these

Figure 3.1 Transgene constructs pMMTV LT and pMMTV LTN used in the generation of Polyomavirus large T-antigen transgenic mice

(A) Structure of the pMMTV LT expression vector. Vector backbone sequences shown by the single line refer to sequences from pSP72 (Promega). The horizontal slashed region corresponds to the MMTV-LTR derived from the original plasmid CDM8 (Seed & Aruffo, 1987). The shaded region indicates the PyV LT cDNA derived from expression vector MTLT (obtained from J. Hassell). The hatched region 3' to the PyV LT cDNA refers to SV40-derived polyadenylation signals also derived from plasmid MTLT.

(B) Structure of pMMTV LTN expression vector. Backbone vector sequences (shown by single line from BamHI to SalI site shown) are from Bluescript SK plus (Promega). The horizontal slashed region corresponds to the MMTV-LTR derived from the original plasmid CDM8 (Seed & Aruffo, 1987). The solid region shown between the MMTV-LTR and the PyV LT cDNA refers to an inert fragment derived from the original pA9 clone containing untranslated v-Ha-ras sequences (Muller et al., 1988). The shaded region refers to the PyV LT cDNA derived from plasmid MTLT while the hatched region adjacent to the PyV LT cDNA represents SV40-derived polyadenylation/splicing sequences.

A

pMMTV/LT

B

pMMTV/LTN

Figure 3.2 Tissue specificity of transgene expression in the MMTV/LTN-5 transgenic strain.

(A) Structure of the pMMTV LTN transgene and identification of riboprobes used in expression analyses. The thin solid line refers to the backbone sequences of the p206 vector derived from Bluescript SK plus. The hatched region corresponds to the MMTV-LTR while the shaded region indicates SV40-derived polyadenylation and splicing signals. The stippled region corresponds to the Polyomavirus large-T antigen cDNA (LT) is indicated. The bent arrow on top of the transgene denotes the location and direction of the transcription start site. Also shown below the transgene structure are locations of riboprobes used to assess PyV LT expression in tissue RNA. Riboprobe MTR protects a 203 nucleotide fragment corresponding to the first 203 nucleotides of PyV LT coding sequences while riboprobe pSPA protects a 628 nucleotide fragment corresponding to nucleotides #2599 to #4556 of SV40 untranslated sequences of the processed transcript.

(B) RNA transcripts corresponding to the MMTV / PyV LT transgene in various organs of the MMTV/LTN-5 transgenic strain as assessed by RNase protection. Tissues were derived from: a multiparous tumor-bearing female (#681, lanes13-15), a lactating (day 1 post-parturition) female (#5920, lanes 1-11) a male (#3754, lanes 19-21), a virgin female (#609, lanes 12,17) and a leiomyoma-bearing virgin female (#5584, lane 17). The antisense probe used in this RNase protection analysis (MTR) protects a 203 nucleotide fragment corresponding to the amino terminus of PyV LT and is marked by LT and the arrows. Also shown below is an RNase protection analyses on identical RNA samples with an antisense probe directed against phosphoglycerate kinase which protects a 124 nucleotide fragment indicated by PGK and an arrow.

A

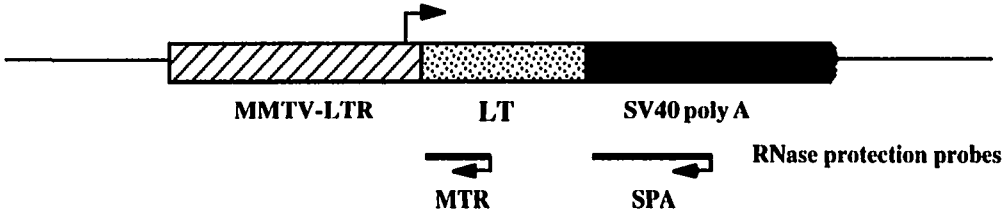
MMTV-LTR
LT
SV40 poly A
RNase protection probes
MTR
SPA

B

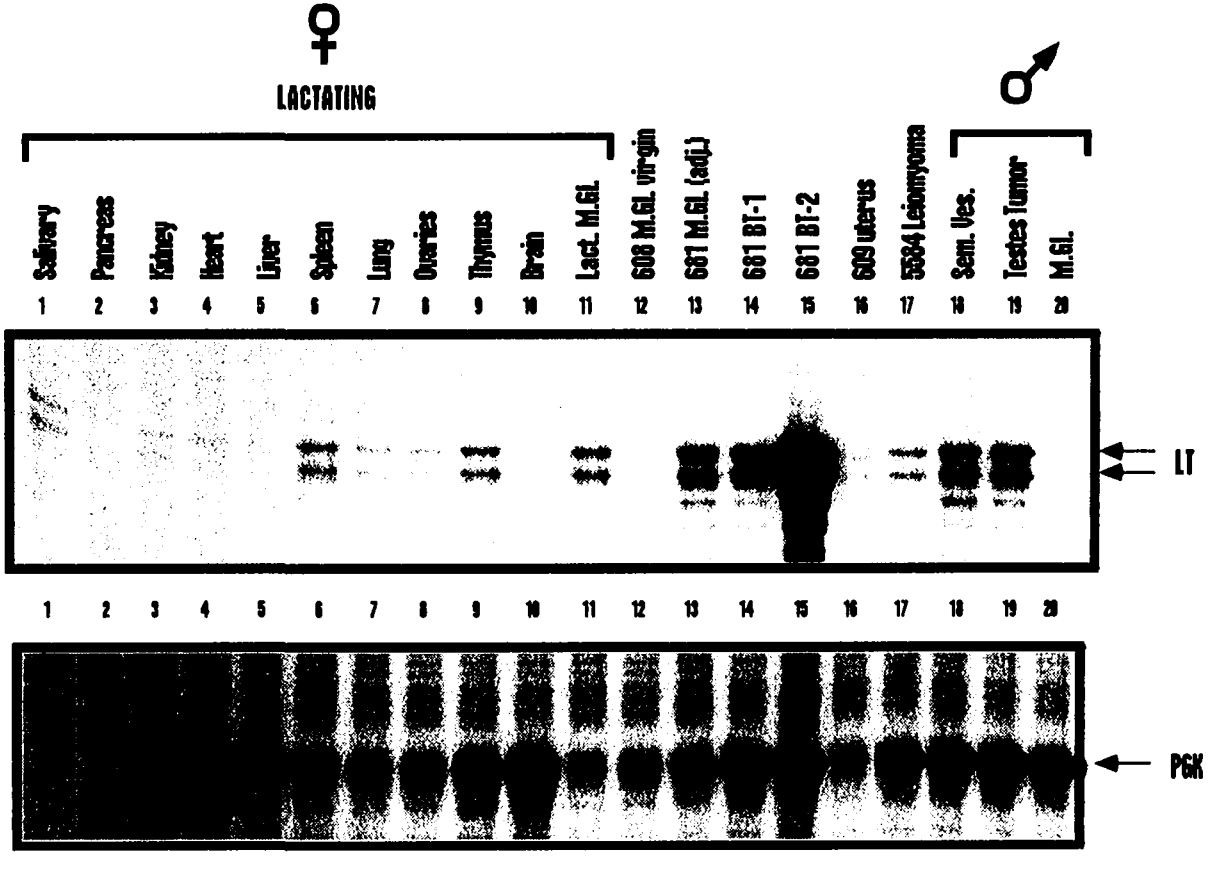
♀
LACTATING
♂
Salivary
Pancreas
Kidney
Heart
Liver
Spleen
Lung
Ovaries
Thymus
Brain
Lact. M.Gl.
608 M.Gl. virgin
681 M.Gl. (adj.)
681 BT-1
681 BT-2
609 uterus
5584 Leiomyoma
Sem. Ves.
Testes Tumor
M.Gl.
1 2 3 4 5 6 7 8 9 10 11 12 13 14 15 16 17 18 19 20
LT
1 2 3 4 5 6 7 8 9 10 11 12 13 14 15 16 17 18 19 20
PGK

specific for PyV LT coding sequences (nt 165 to 368)) and riboprobe pSPA (which protects a 625 nucleotide fragment corresponding to transcribed non-coding SV40 polyadenylation signals (Figure 3.2A, Muller et al., 1988)). Both riboprobes demonstrated transgene specificity and provided identical results when utilized on the same set of tissues in RNase protection assays. In general, transgenic strains which harbor the expression cassette derived from plasmid p206LT express higher detectable transgene levels in all expressing tissues analyzed when compared to strains created with plasmid pMMTV LT. This is in agreement with the transcript enhancing properties attributed to the modifications present in plasmid p206LT. In addition to low transgene levels detected within mammary glands, appreciable levels were also seen in the brain and in male reproductive tissues (particularly the testes and seminal vesicles) of transgenic carriers from several strains. Tissue-specific expression of PyV LT in all transgenic strains is summarized in Table 3.1.

3.2.2. Severe central nervous system hypomyelination results from neurogenic expression of PyV LT

Offspring from one line (LTN-7 #2892) exhibited a severe neurological pathology which resulted in recurrent seizures of progressive duration ultimately leading to asphyxiation. In an attempt to identify the factor(s) responsible for the disorder, PyV LT expression was assessed in brain tissue of affected animals. Although the severity of phenotype observed in this strain was not seen in comparable independently derived strains, aggressive behavior coupled with occasional whole body seizures was observed in two other strains. These observations argue that the phenotype witnessed in transgenic strain LTN-7 was likely not a consequence of a transgene site integration effect, but rather reflects a PyV LT-mediated pathology. In an effort to assess the underlying pathophysiological basis of this disorder, fixed and sectioned cerebellar samples were stained with the myelin-specific dye Kluver-Barrera luxol fast blue-creysl violet stain. In comparison to wild-type control specimens, there appeared to be a significant reduction in the

Table 3.1 Transgene expression in MMTV/LT and MMTV/LTN transgenic mice.

Thirty micrograms of total cellular RNA isolated from a variety of tissues from male and female transgenic mice were analyzed for expression of PyV MT-specific transcript by RNase protection analyses. The riboprobe used in these analyses (MTR, figure 3.2A) recognizes the first 203 coding nucleotides of PyV MT. Phosphoglycerate kinase (PGK) levels were measured to internally control for RNA loading.

TABLE 1.1. Transgene expression and onset of tumors in MMTV /PYLT mice*

e	Expression of transgene						Average onset of mammary tumors in days (# animals)	Tumor types & Hyperplasias (# animals)
	M.Gl.T	M.GL. N	Uterus	Brain	Testes	Sem. Ves.		
-1	NA	-	-	++	-	+	none	Unilateral testicular tumors
-2	NA	+	ND	+	++	+	none	Hyperplastic Alveolar Nodules Seminal Vesicle Hyperplasia Bilateral Testicular Tumors
-3	-	-	-	-	-	-	none	NA
-4	-	-	-	-	-	-	none	NA
N-5	+++	++	+	+	+++	+++	449 (n=5)	M.Gl. Adenocarcinomas Hyperplastic Alveolar Nodules Seminal Vesicle Hyperplasia Bilateral Testicular Tumors
N-6	-	-	-	-	-	-	none	NA
N-7	NA	+	+	+	+++	+++	none	Severe Demyelination of CNS Seminal Vesicle Hyperplasia Bilateral Testicular Tumors
N-8	+++	+	+	++	+++	+++	453 (n=3)	M.Gl. Adenocarcinomas Hyperplastic Alveolar Nodules Seminal Vesicle Hyperplasia Bilateral Testicular Tumors

RNase protection analysis was performed on 20 μg of total RNA isolated from a variety of organs in the MMTV / PyLT strains as described in aterials and Methods. Relative levels of transgene expression (as determined by quantitative phosphorimager analysis) are indicated by - (not tected) + (low) ++ (intermediate) +++ (high). M.GL.N, normal mammary gland; M.GL.T, mammary gland tumor; Sem. Ves.; seminal sicles; NA, not applicable; ND, not determined; n, number of animals analyzed.

optic nerves from affected and control animals were examined by electron microscopy for ultrastructural analysis (Figure 3.3). Demyelination is clearly evident in the transgenic animal displaying incompletely or poorly formed sheaths of myelin surrounding nerve bundles when compared to those in the control wild-type animal (see arrows). These observations argue that expression of PyV large T in the central nervous system can lead to severe demyelination.

3.2.3. Expression of PyV LT results in the induction of tumors in several distinct tissues.

Histological analysis of mammary glands from virgin PyV LT expressing mice, by in large, failed to reveal the presence of tumors or preneoplastic lesions. Ductal ectasia or widening of the ductal lumen was frequently associated with PyV LT expression. Occasionally, however, elevated transgene expression was coincident with mammary tumor occurrence. Mammary tumors originating from these transgenic strains are histologically characterized as discrete focal secretory adenomatous carcinomas which arise adjacent to morphologically normal epithelium (Figure 3.4A). The incidence of mammary tumor formation appears to directly correlate with both age and parity of female transgenic carriers. Indeed, of the virgin animals analyzed for tumor formation, only 6.6% (4/61) developed mammary carcinoma, while 23.8% of multiparous animals (5/23) from the same strain demonstrated neoplasia of the mammary gland. Given that transgene levels are increased during pregnancy, it is possible that transgene level and/or differentiation state of the PyV LT-expressing mammary epithelial cell are factors in determining whether carcinoma results. Alternatively, the recurrent tissue remodeling associated with multiple pregnancies may also influence tumor progression in these animals. The latency with which tumors arise, however, (449 days±120) and the focal nature in which they develop, suggest that expression of transgene alone appears insufficient to achieve full transformation of the mammary gland.

Despite the relatively poor transforming nature of PyV LT in the mammary gland, PyV LT expression in select tissues of non-mammary origin demonstrate susceptibility to transformation.

Figure 3.3 Polyomavirus large T-antigen expression in the brain of transgenic strain MMTV/LTN-7 results in severe hypomyelination in the central nervous system.

(A) Electron micrograph showing a cross-sectional view of a normal FVB/N optic nerve. Note the oligodendrocytic-derived myelin sheaths that surround the axons (see arrows) (optic nerve, FVB/N, 24 days, electron micrograph).

(B) Hypomyelination of the optic nerve in LTN-7 mice. Compare with (A). Note the conspicuous deficiency of well-formed myelin sheaths encompassing the nerve axons (optic nerve, LTN-7 #5702, 24 days, electron micrograph).

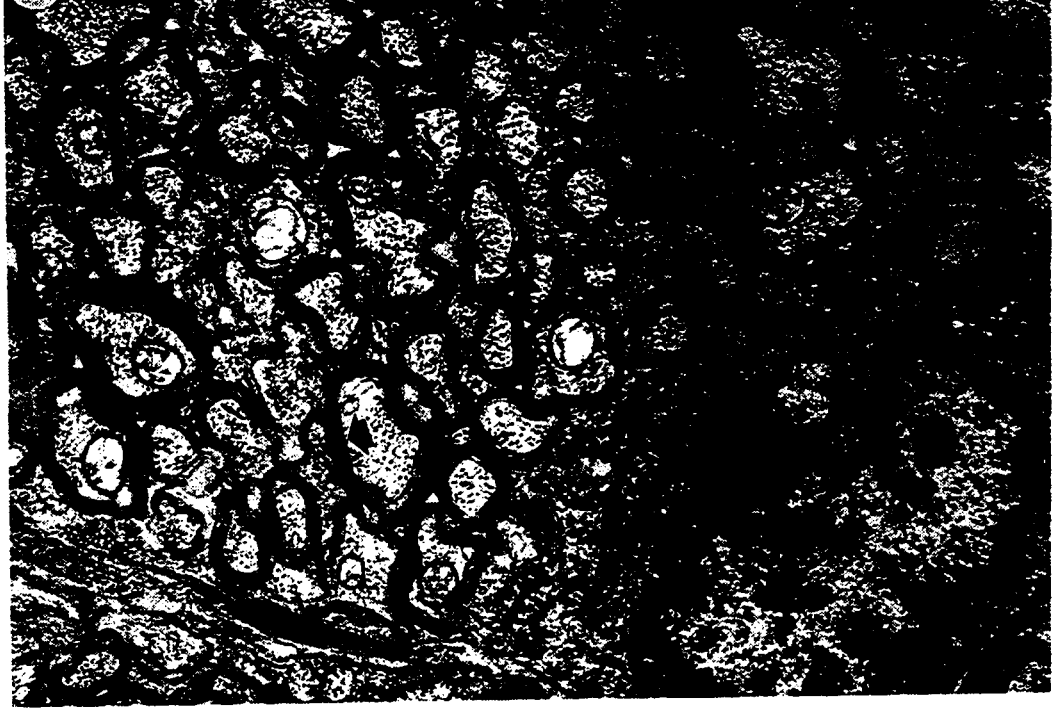

1µm

Figure 3.4 Histopathology of proliferative disorders frequently observed in MMTV/LT transgenic mice

(A) Mammary tumor. Hematoxylin and eosin stained tissues show expansile, papillary and cystic neoplastic masses with varying amounts of eosinophilic debris. Note the large spaces lined by cells which have secretory vacuoles and form papillae. Although not seen in this photomicrograph, the rest of the mammary epithelium shows a secretory hyperplasia (X87 magnification, mammary tissue, LTN-8 #6705, multiparous female, 8 months, hematoxylin eosin stained)

(B) Leiomyoma. This benign tumor is composed of whorling bundles of smooth muscle cells that resemble the architecture of the uninvolved myometrium.(X87 magnification, leiomyoma, female, LTN-6#7822, 10- months, hematoxylin and eosin stained)

(C) Seminal vesicle adenomatous hyperplasias. The seminal vesicles are dilated and distorted by small focal proliferations of small back to back glands lined with cells with large regular round to oval nuclei. The glands are associated with edema and fibrosis of some of the normal components of the vesicles. (X87 magnification, testicle tumor, male, LTN-6#7226, 8 months, hematoxylin and eosin stained)

(D) Testicular tumors. The tumor is composed of sheets of small round cells with eosinophilic cytoplasm. The interstitial origin of these tumors is evident given the remnants of the seminiferous tubules seen here. (X87 magnification, testicle tumor, male, LTN-8#5706, 10 months, hematoxylin and eosin stained).

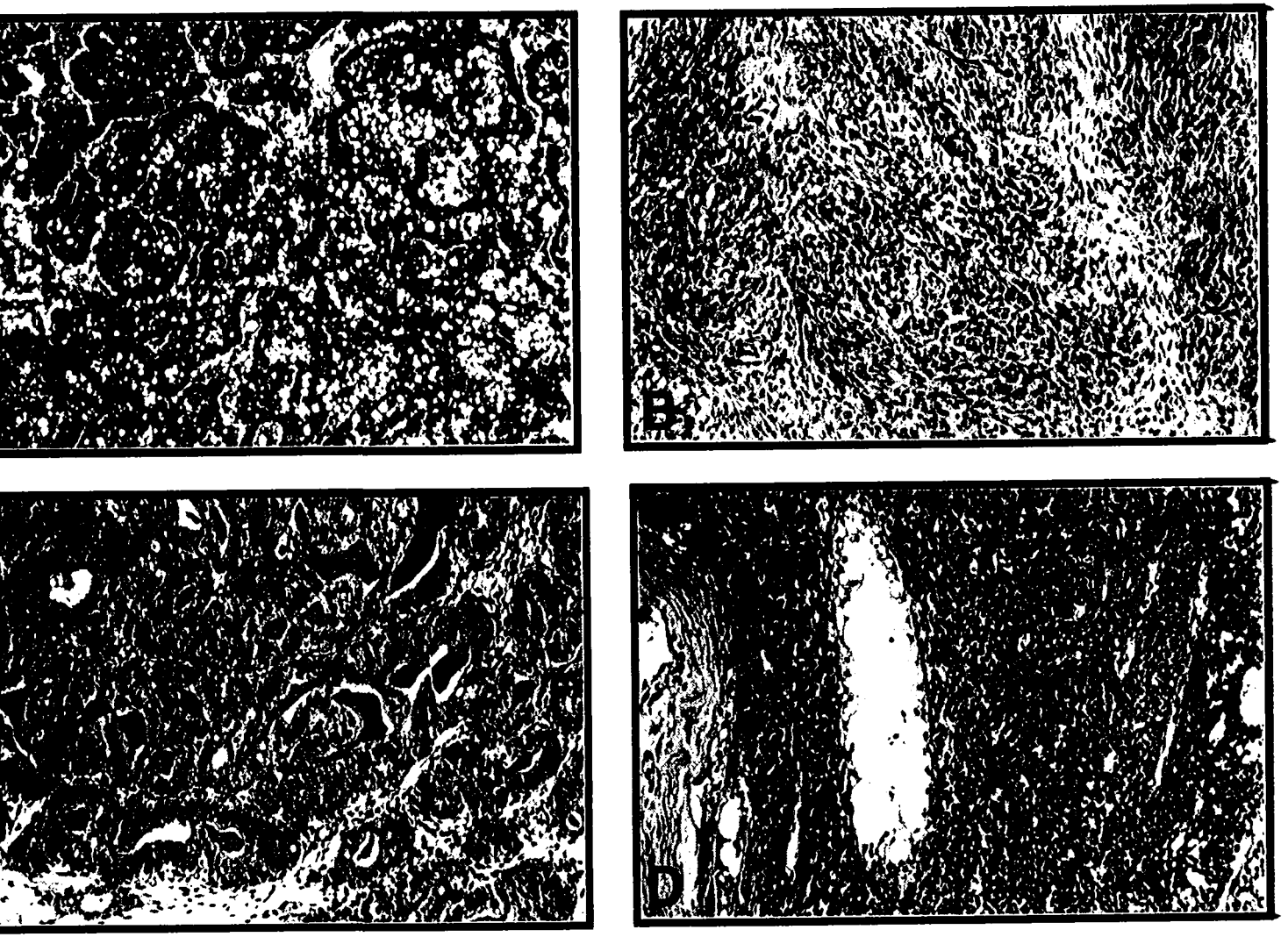
B
D

leiomyomas (benign endometrial neoplasia) in a high percentage of transgenic carriers. This phenotype has been seen reproducibly in three independently derived PyV LT expressing strains and is histologically characterized as whorling bundles of smooth muscle (Figure 3.4B). Up to 50% of virgin transgenic carriers develop leiomyomas while only 24% of multiparous animals develop this tumor type. Interestingly, mammary tumor-bearing animals fail to demonstrate abnormality of uterine tissues, yielding thus far, mutually exclusive tumor phenotypes.

The relatively high levels of transgene detected in the seminal vesicles and testes correlates with histological hyperplasia and transformation respectively of the analyzed tissue. Seminal vesicles from affected animals are distorted by a proliferation of small back-to-back glands lined with cells with large regular round-to-oval nuclei. The proliferation is associated with edema and fibrosis of some of the normal components of the vesicles (Figure 3.4C). Usually co-incident with hyperplasia of the seminal vesicles is associated transformation of one or both testes. Over time, testicular tumor formation occurs with complete penetrance and typically involves both testes. The testes tumor is composed of sheets of small round cells with eosinophilic cytoplasm which are interstitial in origin (Leydig cells)(Figure 3.4D). Tumor transplant into syngeneic animals grow, albeit, very slowly. Histology of the resultant tumor transplant is indistinguishable from the primary neoplasm. As a result of transformation of these tissues, male transgenic animals become increasingly infertile with advancing age with males over the age of 8 months rarely reproducing.

To determine whether increased levels PyV LT protein correlate with neoplasia, protein extracts from various tumor and adjacent normal tissues was analyzed by immunoblot analysis using PyV LT-specific antisera. The results reveal that tumor tissues possess elevated levels of PyV large T protein compared to adjacent normal tissues (Figure 3.5). These observations suggest that induction of mammary, testicular, and uterine tumors is associated with elevated levels of PyV large T antigen.

Figure 3.5 Immunoblot analysis of Polyomavirus large T-antigen expression in transgene expressing tissues.

Seventy five micrograms of total protein lysate was analyzed for PyV LT protein using antisera specific for PyV LT. Shown is PyV LT-specific immunoblot indicating PyV LT protein product marked by the arrow and LT. Included as a non-specific control is a protein lysate derived from a day 1 post-parturition FVB/n (non-transgenic) mouse (lane 7).

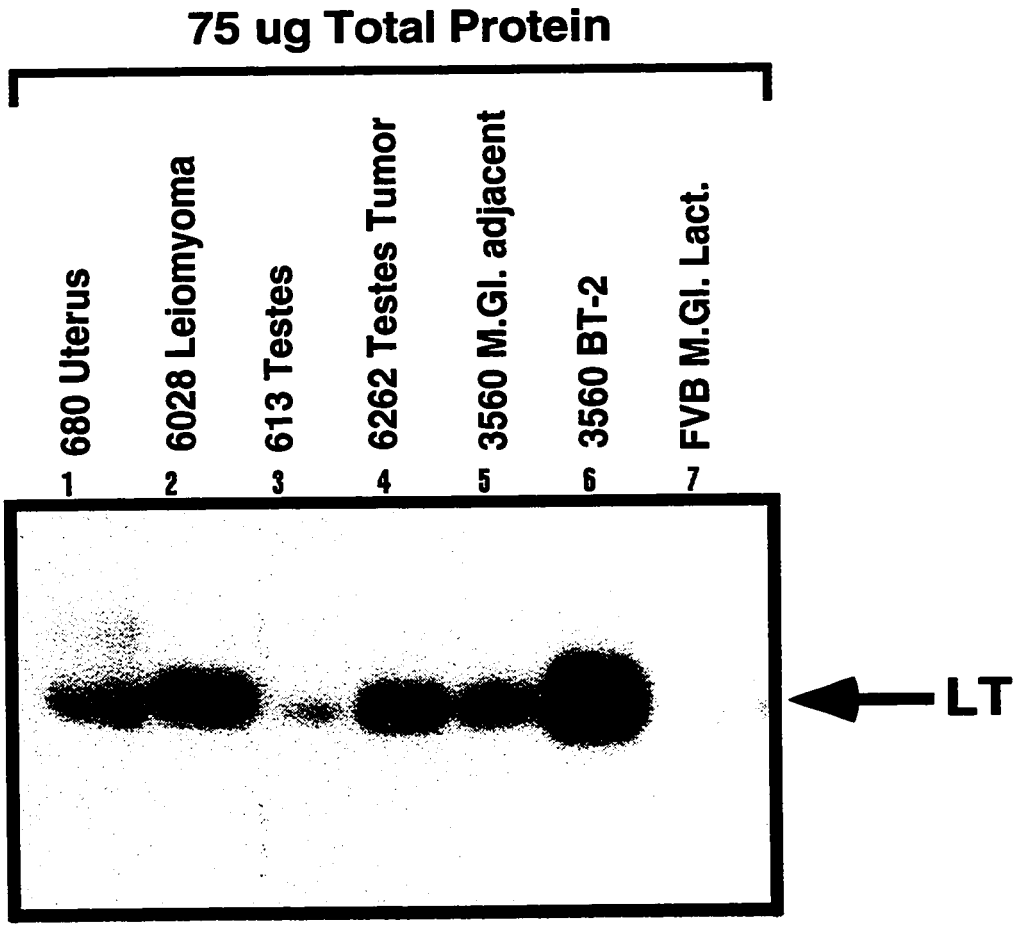
75 ug Total Protein
1 680 Uterus
2 6028 Leiomyoma
3 613 Testes
4 6262 Testes Tumor
5 3560 M.GI. adjacent
6 3560 BT-2
7 FVB M.GI. Lact.
LT

tumors.

Because the immortalizing and growth supportive properties of PyV LT likely resides in the ability to complex RB (Larose et al., 1991), we assessed whether RB or RB family members were complexed to PyV LT in mammary tumors derived from PyV LT-expressing strains. To this end, co-immunoprecipitation studies utilizing antibodies specific for RB family members RB, p107 and p130 demonstrated that PyV LT could be detected in complexes with all three family members (Figure 3.6 lanes 1, 3, 5). To control for non-specific interactions, protein lysate from an MMTV/Neu-induced mammary tumor was included (Figure 3.6 lanes 2, 4, 6). A cross-reacting protein of slightly faster mobility was detected in these immunoprecipitates and likely represents a non-specific interaction. These observations confirm that PyV LT antigen is complexed with members of the RB family in mammary tumors.

3.2.5. The mouse homologue of Drosophila homeoprotein Cut co-immunoprecipitates with PyV LT

Another potential mediator of the observed tumor phenotype in PyV large T expressing tissues is the Cut protein. Previous observations have shown that chromosomal region 7q22 which spans the human Cut gene is frequently deleted in human leiomyomas (Lemieux et al. 1994, Sargent et al., 1994, Ozisik et al., 1993). To examine whether Cut expression is modified in PyV LT affected tissues, immunoprecipitation followed by immunoblotting with antibodies specific for murine Cut was performed on all PyV LT affected tissues (Figure 3.7). Interestingly, Cut protein levels appeared particularly elevated in a mammary tumor derived from a PyV LT transgenic animal when compared to Cut levels observed in a Neu-induced mammary tumor (compare lanes 9 and 10). Similar high levels of Cut were seen in leiomyomas (lane 8). With notable exception of the testes tumor, increased PyV LT protein levels correlates directly with elevated levels of Cut protein.

Figure 3.6 PyV LT is found associated with the retinoblastoma gene product (p105) in addition to retinoblastoma family members p107 and p130.

PyV LT immunoblot analyses of p105(RB) (lanes 1, 2), p107 (lanes 3, 4), and p130 (lanes 5, 6) immunoprecipitates derived from an MMTV/LTN-5 mammary tumor-bearing animal (lanes 1, 3, 5). As a non-specific control, protein lysate derived from MMTV/Neu (#6144) mammary tumor was included (lanes 2, 4, 6). Indicated by the arrow and PyV LT designation is a 100kDa band corresponding to PyV LT antigen.

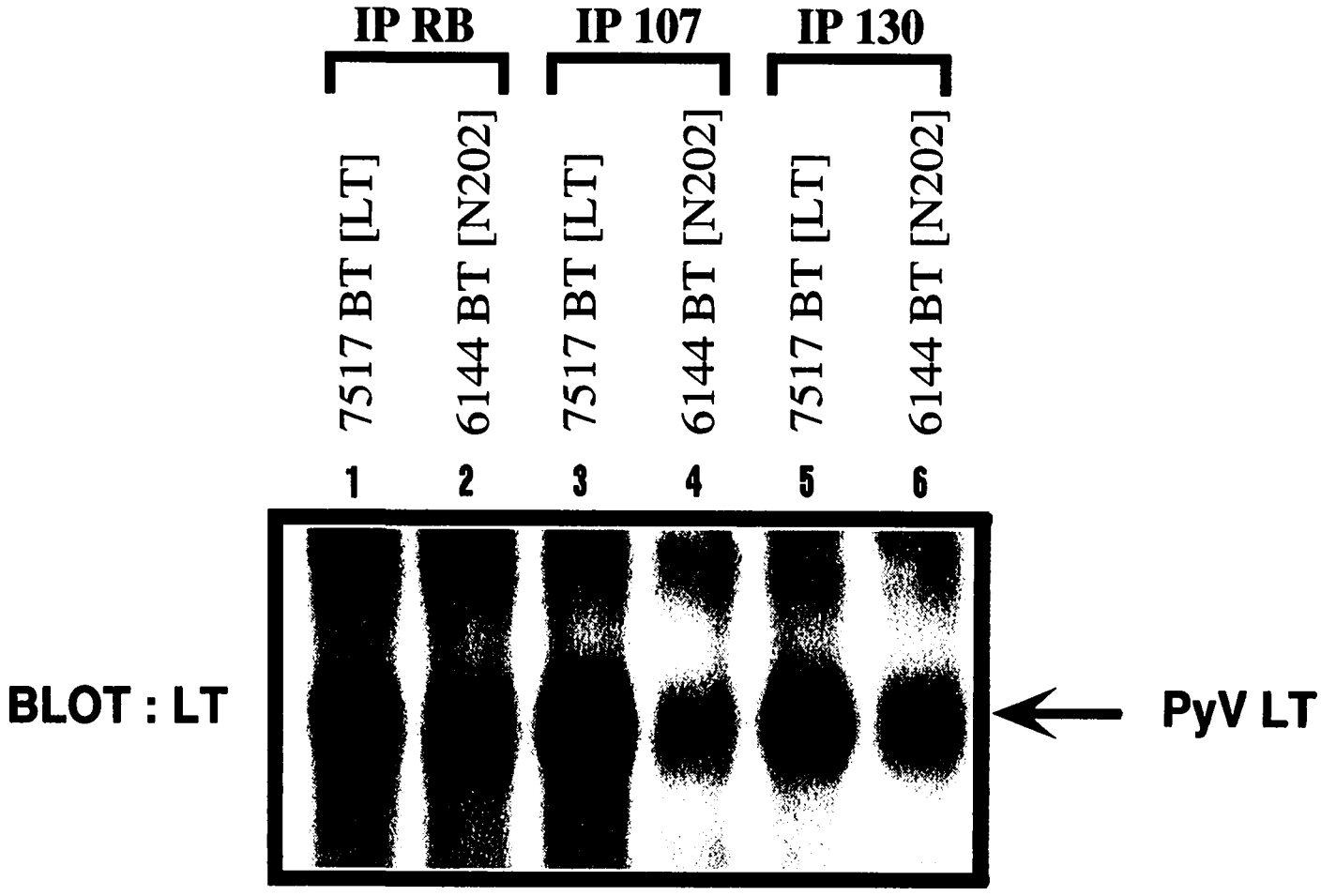
IP RB
IP 107
IP 130
7517 BT [LT]
6144 BT [N202]
7517 BT [LT]
6144 BT [N202]
7517 BT [LT]
6144 BT [N202]
1
2
3
4
5
6
BLOT : LT
PyV LT

Figure 3.7 Cut protein levels are elevated in PyV LT transformed tissues of the uterus and mammary gland.

Cut immunoblot analyses of Cut immunoprecipitates derived from: MMTV/LTN tissues (lanes 1-6, 8, 9), non-transgenic (FVB/n) lactating mammary tissue (lane 7), and MMTV/Neu-derived mammary tumor tissue (#9066, lane 10). MMTV/LTN tissues include: normal uterus (#680), leiomyoma (#6028), normal testes (#613), testicular tumor (#6262), adjacent 'normal' and transformed mammary tissue (#3560).

sue Origin :
IP: CUT
BLOT: CUT
1 UTERUS
2 LEIOMYOMA
3 TESTE
4 TESTES TUMOR
5 BREAST
6 BREAST TUMOR
7 FVB BREAST (LACT)
8 LEIOMYOMA
9 BREAST TUMOR
10 N202 BREAST TUMOR
PyLT
FV B
PyLT
N2 0 2

conceivable that the elevated levels of Cut observed in these tumor tissues is due to its direct interaction with PyV large T antigen. To explore this possibility, co-immunoprecipitation analyses with both Cut and PyV large T antisera was performed on protein extracts derived from either tumor or adjacent normal tissues. Immunoprecipitation with antisera specific for murine Cut followed by immunoblotting for PyV LT revealed the presence of co-precipitating PyV LT in leiomyomas and mammary tumors (Figure 3.8). To control for possible non-specific interaction, tumor extracts from leiomyomas or mammary tumors were immunoprecipitated with a non-specific antibody (6.14) or no antibody (lanes 3, 7 and 2, 6 respectively). PyV LT co-precipitated protein was clearly evident in Cut immunoprecipitated lysates which directly correlated with levels of immunoprecipitated Cut. However, on longer exposure of the autoradiogram, a low level co-migrating species was evident in both negative control lanes. These observations suggest that the formation of specific complexes of PyV large T and Cut may be involved in the induction of both mammary tumors and leiomyomas.

3.2.6. Measurement of Myc transcript levels in various normal and tumor-derived MMTV/LT tissues.

The promoter region of Myc contains core Cut binding sequences and has been shown to be negatively regulated by Cut (Dufort et al., 1994). To determine the effect of PyV LT expression on c-*myc* transcription, RNase protection analyses was used to assess the relative levels of c-*myc* transcript in normal and transformed PyV LT tissues. To control for non-specific increases in epithelial cell content, mammary tumors from other MMTV/oncogene (onc)-derived strains were included. Results from these analyses demonstrated that the levels of c-*myc* varied considerably between different tissue types. On average, mammary tumors derived from MMTV/LT transgenic strains demonstrated slightly elevated c-*myc* levels (1.2 fold) when compared to mammary tumors from either MMTV/MT or MMTV/Neu transgenic strains (Figure 3.9, compare lanes 15, 16, 24, 25, 27 with lanes 8-11)(values are normalized to PGK levels). c-*myc* levels were, however,

Figure 3.8 Detection of Cut:PyV LT complexes in mammary and uterine tumors derived from MMTV/LTN transgenic animals

PyV LT immunoblot analyses of Cut (lanes 1, 4, 5) immunoprecipitates from: MMTV/Neu-derived mammary tumor (#9066, lane 1), MMTV/LTN-derived mammary tumor (#3560, lane 5) or MMTV/LTN-derived leiomyoma (#6028, lane 4). Also included are beads alone control (lane 2, 6) or the use of non-specific Neu antisera (lanes 3, 7). Tissues are derived from: MMTV/LTN mammary tumor (#3560, lanes 5-7), MMTV/LTN leiomyoma (#6028, lanes 2-4), MMTV/Neu mammary tumor (#9066, lane 1). The lower panel is the same immunoprecipitates immunoblotted for Cut.

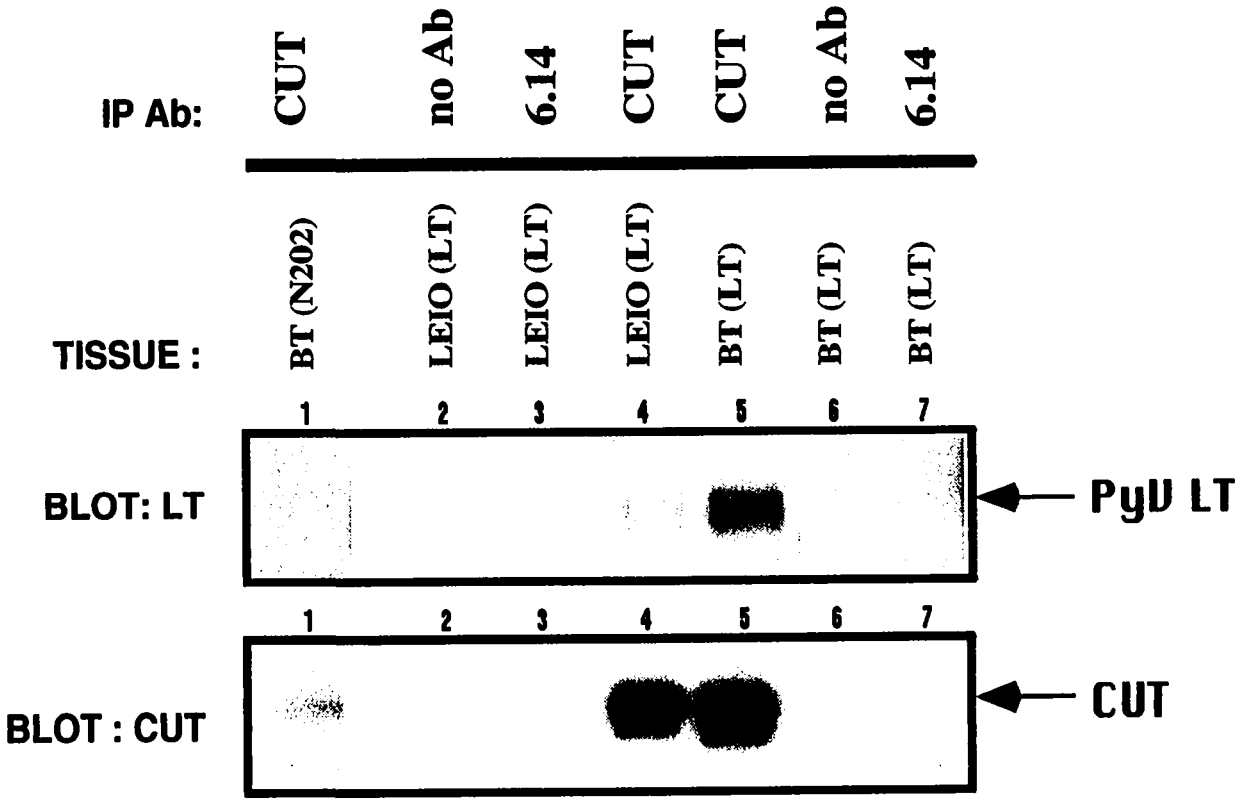
IP Ab:
CUT
no Ab
6.14
CUT
CUT
no Ab
6.14
TISSUE :
BT (N202)
LEIO (LT)
LEIO (LT)
LEIO (LT)
BT (LT)
BT (LT)
BT (LT)
1
2
3
4
5
6
7
BLOT: LT
PyV LT
1
2
3
4
5
6
7
BLOT : CUT
CUT

levels are reduced in leiomyomas when compared to normal non-transgenic FVB uterine tissue (Figure 3.9, compare lanes 18 and 22 with lane 5). Importantly, however, histologically normal uterus derived from a MMTV/LT transgenic mouse demonstrated a 2 fold elevation in c-myc levels when normalized to PGK levels and compared to normal non-transgenic FVB uterus (Figure 3.9, compare lane 17 with lane 5). While these results are preliminary, they suggest that PyV LT may influence c-*myc* transcription levels to promote cell growth through functional inactivation of Cut.

3.3 DISCUSSION

The generation of a neoplasm generally involves several biochemically distinct cell transition phases including immortilization, hyperproliferation, and ultimately development of an overt cancer. Each of these phases represents the culmination of selective genetic alterations which permits bypass of normal growth restrictions allowing clonal expansion of a selected cell population. Because tumor kinetics in the mouse closely parallel human tumor kinetics (in proportion to life span), the transgenic mouse has served as an invaluable tool in the study of many tumor types. RB is implicated as a causative factor in mammary tumorigenesis (Lundberg et al., 1987, T'Ang et al., 1988, Varley et al., 1989). Given the lack of a suitable animal model with which to study the role of RB in the generation of this neoplasm, I exploited the inherent ability of PyV LT to complex and functionally inactivate RB to generate transgenic animals which express PyV LT in the mammary gland.

Not unlike other MMTV/onc transgenic animals, expression of the PyV LT transgene was detected in the mammary gland of female transgenic carriers in addition to reproductive tract tissues from both sexes. Curiously, though, brain-specific PyV LT transcript was seen in several independently derived transgenic strains.

Figure 3.9 Measurement of Myc transcript levels from various MMTV/onc transformed and corresponding normal tissues

Myc transcript levels were assessed by RNase protection analyses using riboprobe pMycExon1 (HindIII cut). This riboprobe protects two fragments (355 nucleotides (corresponding to c-myc nucleotide positions +162 to +517) and 377 nucleotides(corresponding to c-myc nucleotide positions +140 to +517)) owing to the use of two independent transcription start sites (P1 and P2) present in the c-myc gene locus. Thirty micrograms of total cellular RNA derived from various transgenic (1, 6-27) and non-transgenic tissues (lanes2-5) was assessed. MMTV/onc tissue origins are shown above brackets. Also shown is an RNase protection analyses on identical RNA samples with an antisense probe directed against phosphoglycerate kinase which protects a 124 nucleotide fragment indicated by PGK and an arrow.

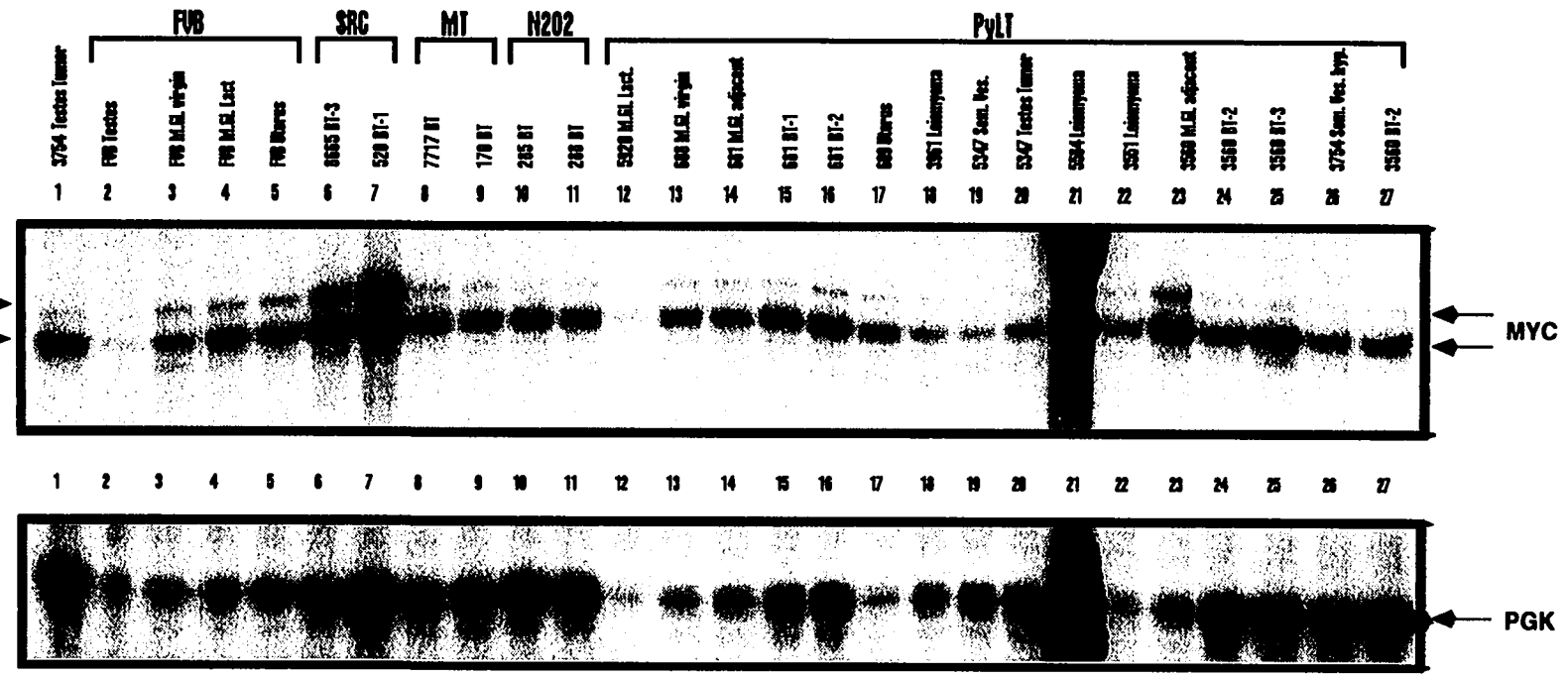
FVB
SRC
MT
N202
PyLT
3754 Testes Tumor
FVB Testes
FVB M.G. virgin
FVB M.G. Lact
FVB Uterus
8855 BT-3
520 BT-1
7717 BT
170 BT
285 BT
288 BT
5820 M.G. Lact.
600 M.G. virgin
601 M.G. adjacent
611 BT-1
611 BT-2
600 Uterus
3571 Leiomyoma
5347 Sem. Ves.
5347 Testes Tumor
5804 Leiomyoma
3571 Leiomyoma
3560 M.G. adjacent
3560 BT-2
3560 BT-3
3754 Sem. Ves. hyp.
3560 BT-2
1 2 3 4 5 6 7 8 9 10 11 12 13 14 15 16 17 18 19 20 21 22 23 24 25 26 27
MYC
1 2 3 4 5 6 7 8 9 10 11 12 13 14 15 16 17 18 19 20 21 22 23 24 25 26 27
PGK

neurological phenotype particularly evident in one strain. The neuropathology associated with offspring from the strain LTN-7#2892 likely results from PyV LT expression within a specific cell type in the brain of these animals. Support for this argument stems from several transgenic studies in which neural-specific expression of viral large T antigens results in either tumorigenesis of the expressing tissue or inhibition of normal differentiation. For example, SV40 large T expression in the choroid plexus results in transformation (Palmiter, 1985). In contrast, JC virus large T-antigen expressing transgenic mice develop severe demyelinating disorders associated with brain-specific expression of the transgene (Small, 1986). Similarly, Baron-Van Evercooren et al. have shown that one particular transgenic mouse strain expressing PyV LT under its own promoter develop severe demyelinating disorders identical in phenotype to JCV large T transgenics and to progeny derived from strain LTN-7#2892 described here. The demyelination shown by Baron-Van Evercooren et. al. proved to be linked to PyV LT expression in astrocytes resulting in arrest of oligodendriglial maturation and hypomyelination within the central nervous system. It is reasonable to assume that PyV LT expression and consequent hypomyelination within the CNS in progeny from LTN-7#2892 likely results from a similar mechanism. To validate that PyV LT expression is in fact an effector of the demyelination phenotype, myelin-specific analyses should be performed with other PyV LT expressing strains which demonstrate a less severe neurologic phenotype manifested by infrequent whole body seizures.

The behavior of the PyV LT gene in mammary epithelium provides an informative model with which to study malignant transformation of this tissue. Its effect on mammary gland growth varies from induction of a hyperplastic state to stochastic tumor formation. Because PyV LT is thought to induce cellular proliferation through the binding and inactivation of cellular RB, sufficient levels of the PyV LT product within a cell would be necessary in order to significantly reduce the population of functional RB protein to induce cell proliferation. This is consistent with elevated PyV LT levels seen in all mammary neoplasias analyzed thus far. Although PyV LT is known to bind RB, it is conceivable that binding to other RB family members may also influence

complexes with RB and RB family members p107 and p130. Similarly, E1A proteins of adenovirus are found complexed with RB, p107 and p130 (Devoto, 1992) and SV40 large T antigen is found in complexes with both RB and p107 (Harlow, 1986). The ability to complex RB family members likely represents a common strategy employed by several distinct viruses in the generation of neoplasia.

Two lines of evidence, however, suggest that mammary gland-specific expression of PyV LT antigen is not sufficient for mammary tumorigenesis. First, the tumors that arise in transgene carriers arise adjacent to morphologically normal epithelium that expresses appreciable quantities of PyV LT. Secondly, tumors and epithelial hyperplasias which arise, do so only after long latencies. Similar observations have been made with other transgenic strains harboring MMTV/c-onc fusion genes. For example, transgenic mice carrying activated versions of the *ras* or *myc* oncogenes under MMTV or WAP transcriptional control, develop focal tumors after long latency (Andres et al., 1987,Leder, 1986,Schonenberger, 1988,Tremblay et al., 1989). Given the latency and the clonal nature of tumors arising from these transgenic models, evidence suggests that additional genetic lesions in concert with transgene expression are necessary for tumorigenesis.

Literature has cited that the function of PyV LT in carcinogenesis resides in its role as an initiating agent in the transformation process and not in the maintenance or progression of the neoplastic state. Since carcinogenesis is generally viewed as a multistep progressive disorder requiring several genetic mutations involving both inactivation of tumor suppressor genes as well as activating mutations to proto-oncogenes, such a model could conceivably account for the resultant phenotypes observed with these transgenic strains. In other words, introduction of the PyV LT transgene into mice has served as an initiating event or a primary genetic lesion rendering these animals increasingly susceptible to further sporadic mutational events leading to neoplastic transformation. In Polyomavirus infection, the MT antigen (and possibly ST) serves as a means to obviate the need for additional mutagenic events required for the full tumor phenotype.

uterus. Indeed, greater than 50% of MMTV/LT transgenic mice from two independently derived strains developed benign leiomyomas. Leiomyomas represent the most common pelvic tumor in women with frequencies approaching one in four (Roboy et al., 1988). Indeed, occurrence of these tumors is the main cause for hysterectomy. Cytogenetic analysis of leiomyomas has identified region q22 on chromosome 7 as a frequently deleted region in these tumors (Ozisik et al., 1993, Sargent et al., 1994). One gene which maps to this region is the homeobox containing protein CDP/Cut/Clox/Cux. Cut was initially identified as a negative regulator of transcription in promoter regions of *myc*, gp91-phox, and Ncam genes (Skalnik et al., 1991, Valarche et al., 1993, Dufort et al., 1994, Lemieux et al., 1994). One mechanism by which PyV LT may influence cellular growth is through its potential ability to manipulate Cut protein activity. Co-immunoprecipitation analyses of mammary tumors or leiomyomas revealed the presence of PyV LT in Cut-specific immunoprecipitates suggesting a possible direct interaction. However, given the observation that other PyV LT expressing tissues or cell lines failed to co-precipitate these proteins argues for a more indirect and possibly tissue-specific association. Indeed, while co-immunoprecipitations revealed the presence of PyV LT:Cut protein complexes, no equivalent complexes were detected in testicular tumors dispite the presence of high levels of PyV LT protein (Figure 3.7, lane 4). Conceivably, a direct or even indirect association could alter Cut function allowing a de-repression of many Cut regulated gene products. One of the functional consequences of PyV LT binding Cut may be to relieve its negative regulatory influence on c-*myc* transcription. Indeed, c-myc transcript levels demonstrate, on average, higher basal levels in PyV LT expressing tissues when compared to corresponding non-transgenic FVB tissue. Additional support stems from observations using reporter plasmids for measuring Cut-mediated repression. Co-transfection of PyV LT with either murine or human Cut expression cassettes into fibroblasts relieves Cut-mediated repression of the reporter constructs (unpublished observations, A. Nepveu). Furthermore, PyV LT homologue SV40 LT is similarly found complexed to Cut in cell lines expressing SV40 LT (unpublished observations, A. Nepveu). Given that many human

observation that PyV LT physically interacts with Cut, suggests that functional inactivation of Cut plays a role in uterine and possibly mammary neoplastic progression.

In addition to the PyV LT induced proliferative disorders observed in the mammary gland, expression of PyV LT in other tissues has a significant effect. The observation that all transgenic strains which expressed PyV LT in the testes and seminal vesicles went on to develop tissue dysplasia in that particular organ, demonstrates the sensitivity of these tissues to PyV LT transformation. Two other groups studying PyV LT transgenic mice transcriptionally controlled by the metallothionine (MT) and PyV early promoters respectively (Evercooren, A.B.-V. et al. 1992), have observed similar phenotypes. In contrast, Wang et. al. in their characterization of transgenic mice carrying the entire polyomavirus early region, obtained no tumor formation in the testes despite high expression levels of PyV LT in this organ (Wang et al, 1991). One obvious possible explanation for this discrepancy may be due to the fact that high expressing transgene carriers die of hemagenomas before the testicle phenotype is evident.

While Cut levels and perhaps Cut function may directly or indirectly influence tumorigenesis (particularly in mammary gland and uterine tissues), the ability of PyV LT to bind and functionally inactivate RB remains a formidable and well characterized means by which PyV LT manipulates cell growth. Indeed, PyV LT mutants which fail to bind RB, also fail to immortalize rat embryo fibroblasts (Larose et al., 1991). Several cellular proteins are known to associate with RB. Of particular interest is associated E2F transcriptional activity due to its involvement in both cellular proliferation and differentiation. E2F consists of a heterocomplex of E2F subunits (of which 5 exist in mice and 1 in Drosophila) and DP subunits (3 of which exist in mammals and 1 in invertebrates)(Lam & La Thangue, 1994). Coincident with an exit from G0, cyclin E and/or cyclin D phosphorylate and consequently disrupt the physical association of RB from the E2F complex allowing either transcriptional activation of a subset of genes or repression of yet others (Lam & La Thangue, 1994). This in effect alters the composition of the molecular machinery to prepare for the advent of cellular division. Interestingly, homozygous deletion of E2F1 in mice does not

malignancies (including predominantly uterine sarcomas, lung adenocarcinomas, and lymphomas) in addition to atrophy of yet other tissues (particularly the testes)(Yamasaki et al., 1996). The organs affected by the deletion of E2F1 bear striking similarity to those affected in transgenic animals bearing the PyV LT transgene - specifically the testes and uterus. Interestingly, while there is significant atrophy of the testes in homozygous null E2F1 animals, the number of Leydig cells remained the same or elevated in more severely affected animals. Similarly the occurrence of uterine dysplasia parallels that seen in the PyV LT transgenics. One might anticipate that PyV LT mimics the effect of the knock-out by somehow affecting the normal function of E2F in these tissues likely through its ability to sequester RB or RB family members.

Induction of mammary epithelial hyperplasias and mammary tumors in transgenic mice expressing an MMTV/activated *c-src* fusion gene.

4.1. INTRODUCTION

The *c-src* proto-oncogene encodes a 60-kDa cytoplasmic protein that is a member of the nonreceptor tyrosine kinase family (Bolen, 1993). Activation of the c-Src tyrosine kinase has been observed in a number of human malignancies. For example, activation of human c-Src has been observed in a large proportion of human breast and colon carcinomas (Rosen et al., 1986) (Ottenhoff-Klaff et al., 1992). In addition, mammary epithelial-specific expression of the polyomavirus (PyV) middle T (MT) oncogene, which is known to associate with and activate members of the c-Src tyrosine kinase family, leads to the development of metastatic mammary tumors in transgenic mice (Guy et al., 1992a) (Guy et al., 1994). The importance of c-Src in mammary tumorigenesis is further highlighted by the observation that mice expressing the MMTV/PyV middle T transgene in a *c-src* deficient background rarely develop mammary tumors whereas tumor formation remains unaffected in a *c-yes* deficient background (Guy et al., 1994).

Additional support for a role of c-Src in mammary tumorigenesis originates from observations with established cell lines and primary mammary tumors expressing the *neu/c-erbB2* proto-oncogene. Primary murine mammary tumors overexpressing Neu possess elevated c-Src activity by comparison to adjacent morphologically normal epithelium (Muthuswamy et al., 1994). Moreover, human mammary tumor cell lines expressing elevated levels of either Neu or the epidermal growth factor receptor (EGFR) exhibit enhanced c-Src kinase activity (Luttrell et al., 1994). Because overexpression of *c-erbB2* is a frequent event in human breast cancer, these observations suggest that activation of c-Src in these tumors likely occurs through its association with ErbB2 (Muthuswamy & Muller, 1995).

While these studies strongly suggest that c-Src may be involved in the induction of breast cancer, direct evidence supporting this contention is lacking. To directly test the oncogenic

MMTV/activated *c-src* fusion gene were derived. Overexpression of activated c-Src in the mammary epithelium of three of these lines resulted in the induction of mammary epithelial hyperplasias which eventually lead to the induction of focal mammary tumors. In addition, these transgenic strains exhibited a severe lactation deficiency due to a defect in normal mammary epithelial development. These observations support the hypothesis that activation of c-Src is involved in the induction of mammary epithelial hyperplasias and tumors.

4.2. RESULTS

4.2.1. Generation and tissue site expression of MMTV/Src527F transgenic mouse strains

To directly test whether activation of c-Src is sufficient for the induction of mammary tumors, we established 7 lines of transgenic mice which carry an activated version of *c-src* under the transcriptional control of the MMTV LTR (Figure. 4.1A). Because of a substitution of a tyrosine residue at amino acid position 527 with a phenylalanine residue (527F) in the c-Src regulatory domain, this mutant version of *c-src* has previously been shown to possess constitutive tyrosine kinase activity (Cartwright et al., 1987, Kmiecik & Shalloway, 1987, Piwnica-Worms et al., 1987). Of the seven founder animals, four passed the transgene to their progeny in a Mendelian fashion. The remaining three male founder animals failed to reproduce.

To assess the tissue specificity of transgene expression, 20 µg of total RNA from several different tissues of the various MMTV/activated *c-src* strains were subjected to RNase protection with a transgene specific probe comprising the SV40 polyadenylation-splicing signals (Figure. 4.1A, (Muller et al., 1988)). Representative results from these RNase protection experiments for the Src-2 strain are shown in Figure 4.1B. The results revealed that the major sites of transgene expression included the mammary glands of both virgin and lactating female animals and the Harderian glands of both male and female transgene carriers. Lower amounts of the transgene transcript were detected in the salivary glands, epididymis, and seminal vesicles following longer

Figure 4.1 Structure of transgene and tissue specificity of transgene expression.

(A) Transgene structure. The Bluescript vector backbone is represented by a thin line on either side of the expression cassette with the cross-hatched region corresponding to the MMTV LTR derived from plasmid pA9 (Sinn et al., 1987), the stippled portion to avian *c-src* c-DNA with an activating phenylalanine substitution at amino acid position 527, and the solid region specifies the transcriptional processing sequences derived from the SV40 early transcription unit. Transcription start site is indicated by the arrow. Also shown is the antisense probe, its position within the SV40 polyadenylation sequences the size (285bp) and the direction of RNA transcription used in its synthesis.

(B) RNA transcripts corresponding to the MMTV / *c-src*527F transgene in various organs of the Src-2#8222 transgenic strain. Tissues were derived from: a multiparous tumor bearing Src-2 female (#9087), a virgin female (#8637), a female at postpartum day 1 (#5964) and a male (#8645). The antisense probe used in this RNase protection analysis protects a 285 bp fragment corresponding to SV40 polyadenylation signals on the *c-src*527F transcript.

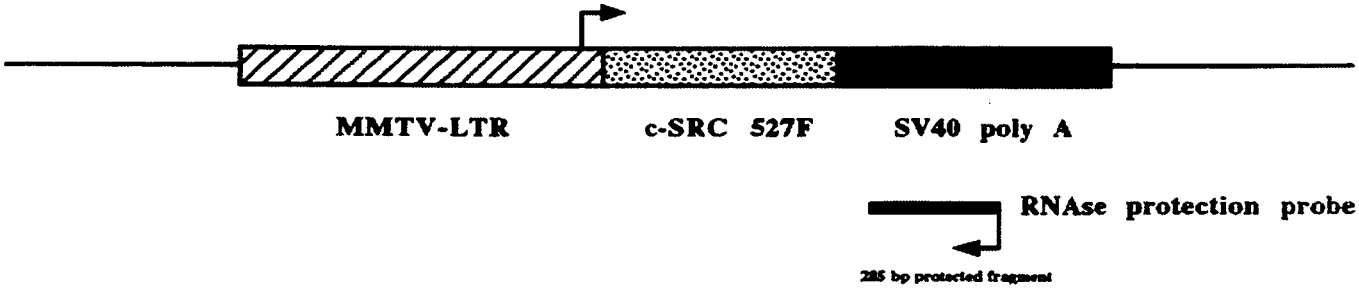
MMTV-LTR
c-SRC 527F
SV40 poly A
RNAse protection probe
285 bp protected fragment

B.

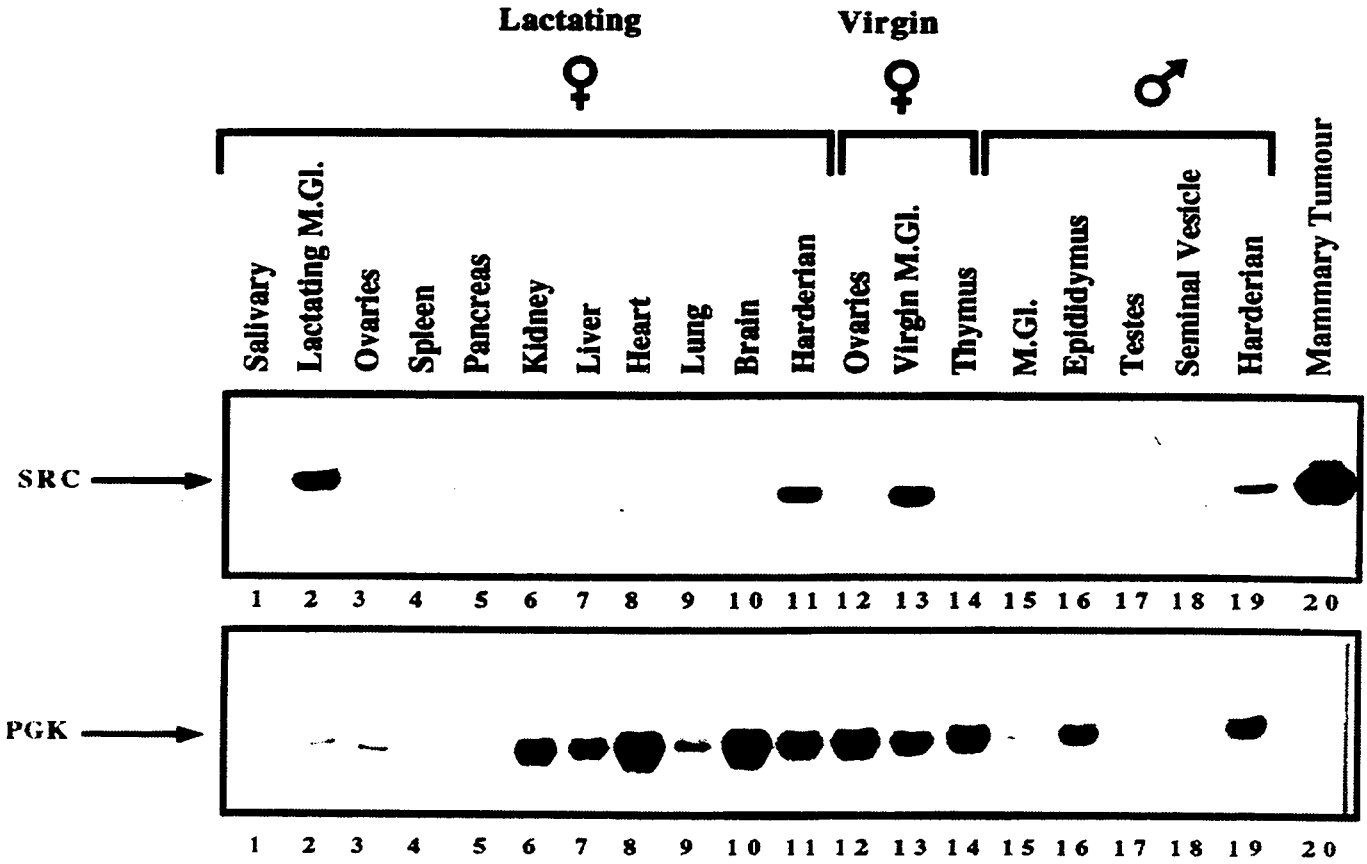
Lactating
Virgin
Salivary
Lactating M.Gl.
Ovaries
Spleen
Pancreas
Kidney
Liver
Heart
Lung
Brain
Harderian
Ovaries
Virgin M.Gl.
Thymus
M.Gl.
Epididymus
Testes
Seminal Vesicle
Harderian
Mammary Tumour
SRC
PGK
1 2 3 4 5 6 7 8 9 10 11 12 13 14 15 16 17 18 19 20

distribution of expression was also noted in the four other independent strains (Table 4.1).

4.2.2. Expression of the MMTV SRC527F transgene induces epithelial hyperplasias and focal mammary tumors.

Expression of activated c-Src in both the mammary and Harderian glands correlated with the appearance of epithelial hyperplasias. The induction of Harderian and focal mammary epithelial hyperplasias could be detected as early as 8 weeks which progressively became more involved as the animals aged. Histological examination of the mammary fat pads of these transgenic mice revealed multiple focal epithelial hyperplasias that resemble the hyperplastic alveolar nodules (HANs) found in MMTV infected mice (Figure 4.2A, (Morris et al., 1990)). Although expression of the activated *c-src* transgene was initially associated with the induction of mammary epithelial hyperplasias, focal mammary tumors began to appear in these strains as early as 200 days of age. In our two best characterized strains (Src-2, and Src-5), 50% of the female transgenic mice developed tumors at 345 and 292 days respectively (Table 4.1). One of the major histological mammary tumor types (50%) observed in the MMTV/activated *c-src* strains is scirrhous carcinomas (Figure 4.2B). These epithelial carcinomas are surrounded by dense sclerotic connective tissue (Figure 4.2B). In addition to the sclerosing mammary tumor phenotype, the remaining mammary tumors examined possessed either an acinar or papillary phenotype (Table 4.1). In the majority of the mammary tumors examined the levels of *c-src*527F transgene transcript were elevated compared to that observed in either virgin or lactating mammary epithelium (Figure 4.1B, compare lane 20 to lanes 2 and 13). In addition to the mammary epithelial hyperplasias, 6 of the 7 transgenic lines developed Harderian epithelial hyperplasias which were bilateral and involved all transgene carriers (Table 4.1). While there was some variation in transgene expression between the different transgenic strains, the epithelial hyperplasias and tumors expressed elevated levels of the transgene.

Table 4.1 Transgene expression and tumor onset in MMTV / Src527F transgenic mice.

Thirty micrograms of total cellular RNA isolated from a variety of tissues from male and female transgenic mice were analyzed for expression of PyV MT-specific transcript by RNase protection analyses. The riboprobe used in these analyses (SPA, Section 2.1) recognizes a 628 nucleotide fragment specific for SV40 polyadenylation signals (bounded by nucleotides 2599-4556). All normal tissues were derived from 8-10 week old mice while tumorous tissue derives from animals whose age was greater than the average onset at which respective neoplasias were first detected.

TABLE 4.1. Transgene expression and onset of tumors in MMTV / SRC527F mice*

	Expression of transgene							Average onset of mammary tumors in days (# animals)	Tumor types & Hyperplasias (# animals)
	M.Gl.T (female)	M.GL. N (female)	M.Gl. N (male)	Sal.	Epidid.	Sem. Ves.	Harderian		
	NA	NA	-	+	+	+	++	none	Bilateral Harderian hyperplasias
er)	+++	++	-	+	+	+	++	345 (n=12)	M.Gl. Adenocarcinomas (Scirrhous, Acinar, Papillary) Hyperplastic Alveolar Nodules Myeloid Leukemia, Malignant Lymphoma (n=2) Bilateral Harderian hyperplasias
	NA	NA	-	+	+	+	++	none	Bilateral Harderian hyperplasias
ler)	NA	NA	-	+	+	+	++	none	Bilateral Harderian hyperplasias
ler)	+++	++	-	+	+	+	++	292 (n=16)	M.Gl. Adenocarcinomas (Scirrhous, Acinar, Papillary) Hyperplastic Alveolar Nodules Myeloid Leukemia, Malignant Lymphoma (n=2) Bilateral Harderian hyperplasias
	NA	-	-	-	-	-	-	none	NA
	ND	+	-	ND	ND	ND	ND	366 (n=3)	Bilateral Harderian hyperplasias

ase protection analysis was performed on 20 µg of total RNA isolated from a variety of organs in the MMTV / SRC527F strains as
ibed in Materials and Methods. Relative levels of transgene expression (as determined by quantitative phosphorimager analysis) are indicated
(not detected) + (low) ++ (intermediate) +++ (high). M.GL.N, normal mammary gland; M.GL.T, mammary gland tumor; Sal., salivary
l; Epidid., epididymus; Sem. Ves.; seminal vesicles; Harderian, Harderian gland; NA, not applicable; ND, not determined; n, number of
als analyzed.

Figure 4.2 Histopathology of MMTV/src527F mammary glands.

Photomicrographs of hematoxylin and eosin stained 7 μm thick paraffin sections. Illustrating:

(A) a hyperplastic alveolar focus from a mammary gland of a *c-src*527F female with inflammation in the center of the field. Compare this focus with the portions of normal mammary duct in the upper right corner in the midst of the fat.

(B) a scirrhous adenocarcinoma from a mammary gland of a *c-src*527F female invading skeletal muscle.

(C) a section of mammary gland from a normal, non-transgenic FVB female mouse one day after delivery of litter. Note crowded alveoli with the large number of clear lipid vacuoles in the cytoplasm and in the lumen of the acini.

(D) a section of mammary gland from a *c-src*527F female one day after delivery of litter. Note the relative lack of luminal contents, the lack of clear lipid vacuoles and the mature residual fat.

50μm
D
100μm
B

protein kinase levels.

To establish whether the elevated levels of transgene expression observed in the tumor tissues resulted in a corresponding increase in the levels of protein, protein lysates from mammary tumors, adjacent mammary epithelium and Harderian gland hyperplasias from two independent transgenic strains were subjected to immunoblot analyses with c-Src specific antibodies. The results revealed that the levels of c-Src protein present in the tumor tissue were considerably higher that those observed in the adjacent mammary epithelium or Harderian hyperplasias (Figure 4.3B, compare lanes 5 and 8 to lanes 3, 4 and 6, 7 respectively). In addition to the authentic 60kDa c-Src, upper Src related proteins were also noted in both normal (on longer exposure) and tumor tissues (Figure 4.3B, lanes 5 and 8). These upper bands have been observed by others (Taylor et al., 1994, Migliaccio et al., 1993) and are likely extensive serine/threonine phosphorylations of the full length c-Src protein. Lower amounts of the endogenous c-Src protein was observed in normal FVB mammary tissues (Figure 4.3B, lanes 1 and 2) and middle T and Neu induced mammary tumors (Figure 4.3B, lanes 9 and 10) after longer exposure of the autoradiograms.

Because the potent transforming properties of activated c-Src are closely associated with activation of its tyrosine kinase activity, we also measured the Src kinase activity in these tissue samples by performing an *in vitro* kinase assay using avian-specific c-Src antisera (Figure 4.3A). Although tyrosine phosphorylated bands corresponding to the c-Src protein species could be detected in both the epithelial hyperplasias and tumors, the levels of c-Src tyrosine kinase activity observed in the tumor tissues were considerably higher (Figure 4.3A, compare lanes 5 and 8 to lanes 4 and 7 respectively). As expected, the avian-specific Src antibody did not recognize any comparable autophosphorylated species in virgin or lactating non-transgenic mammary tissues (Figure. 4.3A, lanes 1 and 2) or in PyV middle T and Neu induced mammary tumors (Figure. 4.3A, lanes 9 and 10). These observations indicate that the c-Src-induced mammary tumors possess elevated c-Src kinase activity.

Figure 4.3 Expression of Src protein and associated kinase activity in tumor and adjacent mammary epithelium.

(A) *In vitro* kinase activities of wild-type FVB/n virgin and day 1 postpartum breast, Src transgenic tissues, and control mammary tumors derived from middle-T and Neu transgenic animals (Guy et al., 1992a)(Guy et al., 1992b). Protein extracts were incubated with an avian-specific monoclonal antibody and immune complexes were incubated with [γ-^{32}P] as described in materials and methods.

(B) Immunoblot analysis of control and transgenic tissues with a Src-specific rabbit polyclonal antibody of the same samples described above. Positions of avian Src species is indicated by arrows and migration of protein standards is indicated on the right in kDa.

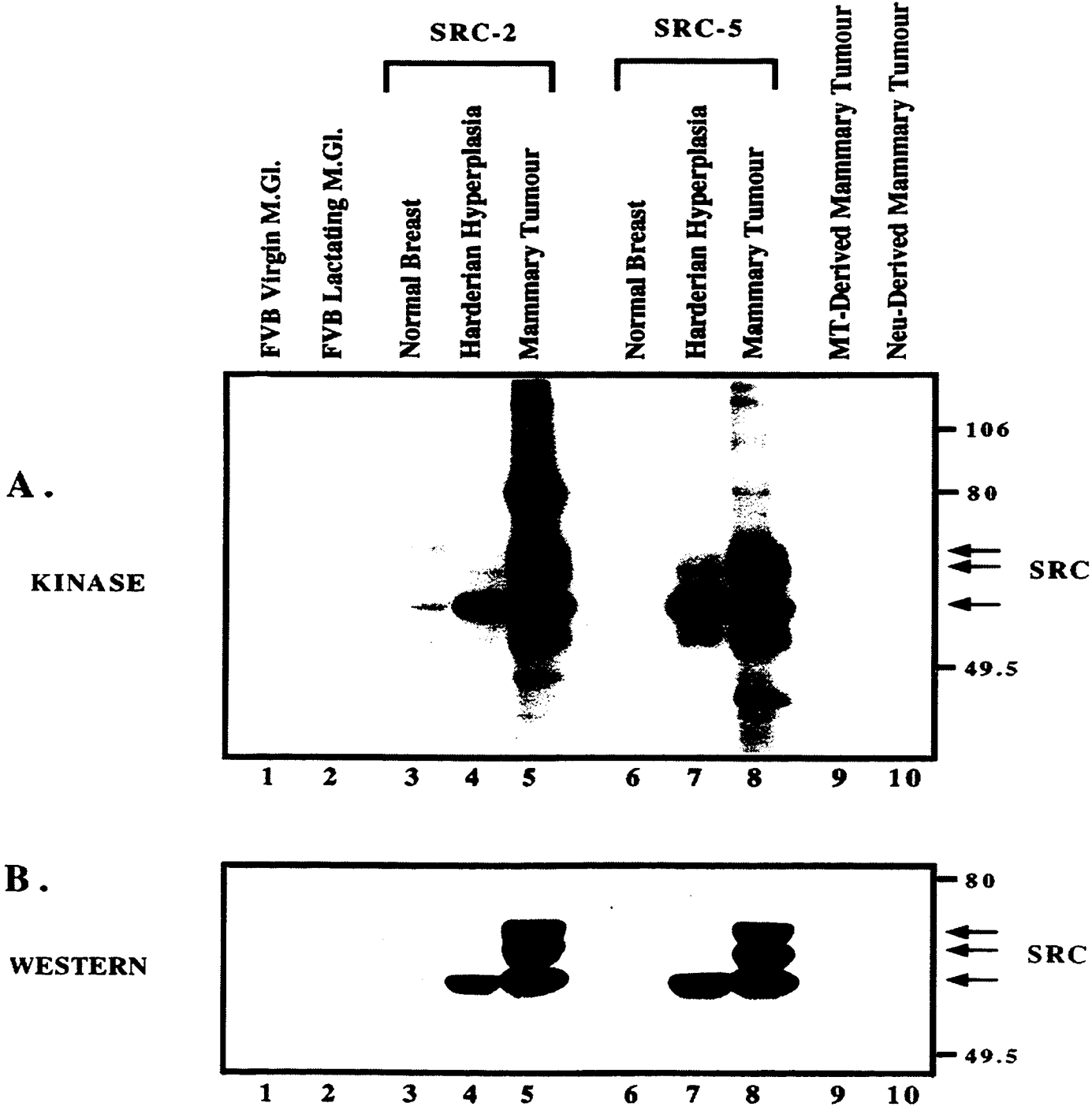
SRC-2
SRC-5
FVB Virgin M.Gl.
FVB Lactating M.Gl.
Normal Breast
Harderian Hyperplasia
Mammary Tumour
Normal Breast
Harderian Hyperplasia
Mammary Tumour
MT-Derived Mammary Tumour
Neu-Derived Mammary Tumour
A.
KINASE
106
80
SRC
49.5
1 2 3 4 5 6 7 8 9 10
B.
WESTERN
80
SRC
49.5
1 2 3 4 5 6 7 8 9 10

mammary epithelial development.

Another major phenotype exhibited by female mice expressing the activated *c-src* transgene is a severe lactational defect. To further explore the nature of this defect, we examined and compared mammary epithelial development in 5, 11, and 15 day pregnant and 1 day post-partum Src-2 and normal FVB female mice by wholemount and histological analyses (Figure 4.4). The day 5 pregnant female *c-src*527F and FVB mammary glands superficially appeared similar. However, on closer histological examination, one noticeable difference between the Src-2 female mice and wild-type FVB controls is that the side buds of the transgenic females did not extend into the surrounding fat pad. Inspection of the mammary fat pads derived from day 15 pregnant transgenic and wild-type mice revealed indications of gross abnormalities in the developing MMTV/Src527F mammary glands (compare Figure. 4.4A and 4.4B). By contrast to the uniform development of the wild-type mammary gland, the development of the *c-src*527F transgenic mammary gland was irregular and not uniform with many of the epithelial branches failing to extend to the edge of the mammary fat pad.

Following parturition there was a dramatic and obvious difference in the extent of lobulo-alveolar development in the mammary gland of the transgenic mice by comparison to the wild-type controls (compare Figure 4.4C and 4.4D). In contrast to wild-type day 1 post-partum mice in which most of the fat pad is occupied by lobular units, the mammary fat pads derived from transgenic mice expressing the activated *c-src*527F transgene demonstrated little lobulo-alveolar development. Histological analyses of these alveolar epithelial cells revealed very little cytoplasmic lipid vesicles by comparison to FVB control animals taken at identical stages of post-parturition (Figure. 4.2C and 4.2D).

Because expression of the milk gene proteins such as the caseins are useful differentiation markers, we assessed the levels of the β-casein transcripts in mammary epithelium of both transgenic and control mammary glands. Although there was obvious differences in alveolar development between these mammary glands, these RNA analyses revealed little

Figure 4.4 Expression of the MMTV/Src527F transgene in the mammary gland of transgenic mice results in a failure to differentiate in response to lactogenic stimulation.

Slide-mounted, whole-mount preparations of hematoxylin stained mammary glands comparing the subgross morphology of non-transgenic FVB (Figures A and C) with transgenic *c-src*527F (Figures B and D) females 15 days after conception (Figure A and B) and one day after delivery of the litter (Figures C and D). Note that the mid-pregnant transgenic *c-src*527F mammary gland (Figure B) has fewer developing lobules than the normal FVB (Figure A). The few developing lobules stand out from the background as hyperplastic foci. The lactating mammary gland of the FVB (Figure C) fills the fat pad while the transgenic *c-src*527F mammary gland (Figure D) has very few fully developed lobules.

D
1mm
B

mammary epithelial differentiation appears to occur after the β-casein gene has been induced. Taken together, these observations suggest that expression of activated c-Src can interfere with normal mammary epithelial development.

4.3. DISCUSSION

Our observations provide direct evidence that expression of activated c-Src in the mammary epithelium of transgenic mice can induce mammary epithelial hyperplasias that eventually progress into mammary tumors. In addition, our results further suggest that mammary epithelial expression of activated c-Src can interfere with normal mammary epithelial development.

The initial morphological abnormalities exhibited by virgin MMTV/activated *c-src* mice were the appearance of focal mammary hyperplasias and bilateral Harderian gland hyperplasias. The appearance of these epithelial hyperplasias was strictly correlated with expression of *c-src*527F transcripts in both these tissues (Figure.4.1 and Figure. 4.3). One interesting pathological feature of the mammary epithelial hyperplasias, is that they histologically resemble hyperplastic alveolar nodules (HANs) that have been observed in both chemically and MMTV induced mammary tumorigenesis (Figure 4.2, (Morris et al., 1987)). Because these hyperplastic lesions are immortal but not transplantable subcutis, HANs have been viewed as representing one of the early steps in neoplastic progression (Cardiff, 1984). Interestingly, one of the initial events during chemical induced transformation of Syrian hamster embryo cells is the induction of the tyrosine kinase activity of c-Src (Kanner et al., 1989). These observations suggest that elevation of c-Src kinase activity in the mammary epithelium of these mice is involved in the initial stages of mammary tumorigenesis.

Although expression of activated c-Src in the mammary epithelium of these transgenic mice is sufficient to induce mammary epithelial hyperplasias, tumors which develop in these strains arise stochastically and appear to be focal in origin (Table 4.1). These results are

Figure 4.5 RNase protection analyses of beta-casein levels in mammary glands from FVB/n and MMTV/Src527F transgenic mice at different stages of development.

Mammary glands from three or four mice at various stages of pregnancy were analyzed for beta-casein using riboprobe 3' β-casein. The top panel shows results from these analyses. The bottom panel illustrates levels of MMTV/Src527F transgene as assessed by RNase protection analyses with riboprobe pSPA. Wild-type non-transgenic animals are indicated by bracket and FVB/N. P.C. indicates post-conception while P.P. indicates post-parturition.

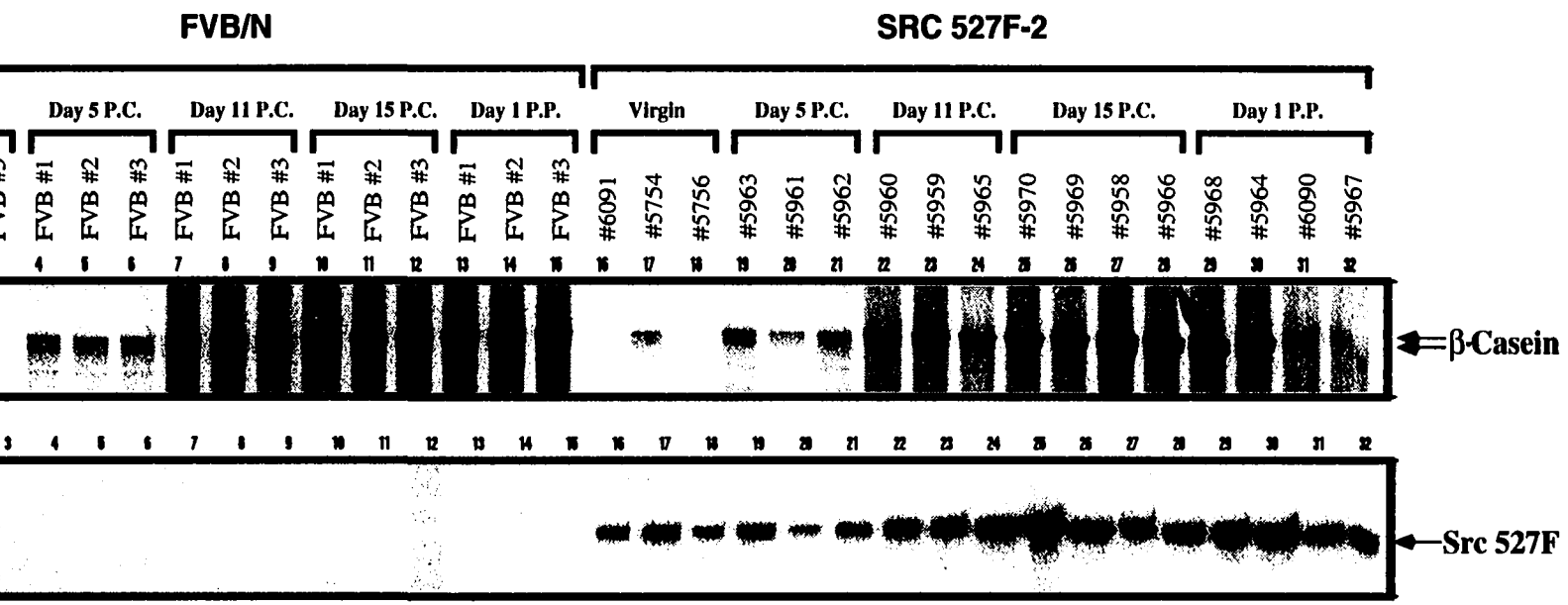
FVB/N
SRC 527F-2
Day 5 P.C.
Day 11 P.C.
Day 15 P.C.
Day 1 P.P.
Virgin
Day 5 P.C.
Day 11 P.C.
Day 15 P.C.
Day 1 P.P.
FVB #1
FVB #2
FVB #3
#6091
#5754
#5756
#5963
#5961
#5962
#5960
#5959
#5965
#5970
#5969
#5958
#5966
#5968
#5964
#6090
#5967
β-Casein
Src 527F

mammary carcinoma. Rather these data suggest that additional genetic events are required to convert the mammary epithelial cell to the transformed phenotype. By contrast to these observations, mammary epithelial specific expression of PyV middle T antigen which is known to activate the c-Src family kinases can induce multifocal metastatic mammary tumors with apparent one-step kinetics (Guy et al., 1992a). Moreover, the function of c-Src is required for transformation of the mammary epithelium since transgenic mice expressing PyV middle T antigen in a *c-src* deficient background rarely develop mammary tumors (Guy et al., 1994). One possible explanation for the difference in phenotypes observed between the MMTV/*c-src*527F and MMTV/PyV middle T mice is that in addition to activating c-Src, PyV middle T is also involved in the activation of the phosphatidylinositol 3' kinase (PI-3' kinase) (Whitman et al., 1985) (Yoakim et al., 1992) and the cellular SHC protein (Dilworth et al., 1994, Campbell et al., 1994). Consistent with this hypothesis, mammary specific expression of mutant PyV middle T antigens capable of activating c-Src but unable to complex either the 85 kDa subunit of PI-3' kinase or SHC are severely impaired in their capacity to induce mammary tumors (Chapter 5). Taken together these observations argue that while activation of c-Src is required for the induction of mammary carcinoma, its elevated expression is not sufficient for tumorigenesis.

In addition to the induction of mammary hyperplasias and neoplasias, mammary epithelial-specific expression of activated c-Src interferes with normal mammary epithelial development (Figure 4.4). Consistent with these observations, other investigators have reported that overexpression of Src, Ras, Mos and Fos interferes with the ability of several immortalized mammary epithelial cells to express differentiation markers in response to lactogenic hormone stimulation (Jehn et al., 1992). However, unlike these *in vitro* studies, the primary mammary epithelium derived from the activated *c-src*527F transgenics are still capable of expressing differentiation specific genes such as β-casein (Figure 4.5), suggesting that the block in mammary epithelial differentiation occurs after β-casein expression is induced. Although it is clear that

mechanism by which this is accomplished is unclear.

The observation that a large proportion of human breast cancers express elevated levels of activated c-Src (Jacobs & Rubsamen, 1983) (Rosen et al., 1986) and the results of these transgenic experiments suggest that activation of c-Src tyrosine kinase may be a crucial step in the induction of mammary carcinomas. Consistent with this notion, both human and transgenic mammary cancers overexpressing the *neu* proto-oncogene also possess elevated c-Src activity (Muthuswamy et al., 1994) (Luttrell et al., 1994). In fact, activation of c-Src by Neu likely occurs through its direct physical association with tyrosine phosphorylated Neu (Muthuswamy et al., 1994, Muthuswamy & Muller, 1995). In addition, it has also been reported that the 80/85 kDa *v-src* substrate EMS-1 is amplified and overexpressed in human mammary carcinomas (Schuuring et al., 1993). Taken together, these observations suggest that activation of the c-Src tyrosine kinase plays an integral role in induction of human breast cancer. In this regard, the MMTV/activated *c-src* transgenic mice may serve as excellent model system to elucidate the mechanism by which c-Src induces mammary cancers.

The role of the PyV middle T-mediated activation of the PI-3' kinase and SHC signaling pathways in mammary tumorigenesis

5.1. INTRODUCTION:

Mammary epithelial-specific expression of the PyV middle T (MT) oncogene in transgenic mice results in the induction of multifocal mammary tumors involving 100% of the transgene carriers. In addition, these tumor bearing mice frequently develop pulmonary metastases (Guy et al., 1992a). Because expression of PyV MT alone is likely sufficient to induce malignant conversion of the mammary gland, identification of the molecular mechanisms by which PyV MT induces this tumor phenotype will provide important insight into the molecular basis for breast cancer. The potent transforming properties of PyV MT is due to its ability to associate with and activate a number cellular signaling proteins. One class of cellular enzymes activated by PyV MT are members of the Src family of tyrosine kinases (c-Src and c-Yes) (Cheng et al., 1988, Courtneidge & Smith, 1983, Horak et al., 1989, Kornbluth et al., 1987, Kypta et al., 1988). Indeed, the observation that expression of PyV MT in mammary glands of Src deficient mice rarely results in the induction of mammary tumors suggests that activation of Src by PyV MT is required for this potent transforming phenotype (Guy et al., 1994). However, I have demonstrated that mammary epithelial-specific expression of a constitutively active version of Src leads to the development of mammary epithelial hyperplasias which rarely progress to full malignancy ((Webster et al., 1995), Chapter 4). Taken together, these observations suggest that although activation of the Src tyrosine kinase pathway by PyV MT oncogene is required for the multifocal mammary tumor phenotype, expression of a constitutively active version of Src in the mammary gland is clearly not sufficient to induce global transformation of the mammary gland.

One possible explanation for these observations is that in addition to activation of the Src tyrosine kinase, PyV MT must recruit additional cellular signaling pathways to effect malignant transformation of the mammary epithelial cell. Indeed, PyV MT is known to physically associate

signal transduction. For example, PyV MT can associate with the 85kDa regulatory subunit of PI-3' kinase resulting in its catalytic activation (Whitman et al., 1985). The association of PI-3'kinase with PyV MT is thought to occur through the binding of p85 SH2 domains with specific tyrosine phosphorylation sites (tyrosine residues 315 and 322) located in PyV MT coding sequences (Whitman et al., 1985). More recently, specific complexes between the SHC adaptor protein and PyV MT antigen have been reported to occur through the binding of the SHC PTB domain to the tyrosine phosphorylated 'NPTY' motif of PyV MT (MT residues 247-250) (Campbell et al., 1995, Dilworth et al., 1994). Indeed, specific mutations affecting either tyrosine residues 250 or 315/322 in PyV MT coding sequences which interferes with binding of SHC or PI-3' kinase respectively, results in a dramatic impairment of the transforming potential of the PyV MT oncogene (Markland & Smith, 1987). In addition, stable complexes between protein phosphatase 2A (regulatory), 2C (catalytic) (Pallas et al., 1990, Walter et al., 1990), PLC-γ (Su et al., 1995) and 14-3-3 proteins (Pallas et al., 1994) have also been observed. However, the role of these proteins in PyV MT-mediated transformation is not known.

To address the functional significance of PI3'K and the adapter molecule SHC in PyV MT-mediated mammary tumorigenesis, we have generated specific PyV MT mutants that are not able to associate with either the SHC or PI-3' kinase pathways. Because phosphorylation of tyrosine 250 is required for the interaction of SHC with PyV MT (Campbell et al., 1994, Dilworth et al., 1994), a tyrosine to phenylalanine substitution at this site should specifically ablate SHC interaction without affecting its association with other cellular signaling pathways. Similarly, the major tyrosine phosphorylation site of MT (tyrosine 315) is required for its association with the p85 subunit of PI-3'K. Additional tyrosine phosphorylation at tyrosine 322 may be involved in creating a high affinity binding site for the SH2 domains of p85 (Carpenter et al., 1993). Thus substitution of both tyrosines 315 and 322 for phenylalanines should result in a MT mutant defective in associating with PI3'K without affecting its ability to interact with other associated proteins.

mammary tumorigenesis, individual PyV MT cDNAs containing phenylalanine substitutions at tyrosine 250 (MT Y250F) or tyrosines 315 and 322 (MT Y315/322F) were placed under transcriptional control of the MMTV promoter / enhancer and microinjected into one-cell mouse embryos to derive transgenic mice expressing these mutant PyV MT antigens. Mammary epithelial-specific expression of either mutant PyV MT cDNAs resulted in the induction of widespread mammary epithelial hyperplasias which led to a lactation defect. Although the initial phenotype exhibited by both sets of transgenic mice were global mammary hyperplasias, mammary tumors eventually arose in both MT Y250F and MT Y315/322F female mice. However, in contrast to the parental MMTV/wild-type MT transgenic mice which rapidly developed multifocal mammary tumors, tumors arising in these mutant strains were focal in origin and arose with delayed onset. Taken together, these observations argue that recruitment of these additional signaling pathways play a pivotal role in the induction of mammary tumors through either of these tyrosine phosphorylation sites.

5.2. RESULTS

5.2.1. Generation and characterization of PyV MT mutants debilitated in their capacity to associate and activate either the PI-3' kinase or SHC adaptor.

The generation of mutant PyV MT cDNA containing phenylalanine substitutions at tyrosine 315/322 (MT 315/322F) (Figure 5.1C) was generated by standard M13 *in vitro* mutagenesis using wild-type PyV MT containing plasmid E8 (MMTV/PyV MT) (Guy et al., 1992a) as a template (Figure 5.1A). The tyrosine to phenylalanine substitution at position 250 was generated by a PCR-based strategy employing site directed mutagenesis with overlap extension (SOE) (Figure 5.1B) on the same parental plasmid (E8). DNA sequence analyses was performed to verify that the corresponding mutations were present in each construct (see Chapter 2). To examine the *in vitro* transforming activities of each mutant, MT Y250F, MT Y315/22F and wild-

Figure 5.1 Structure of PyV MT and PyV MT mutant cDNAs

A. Structure of the wild-type PyV MT cDNA. Relevant tyrosine residues are indicated. Also shown are a pair of cysteine clusters in addition to the hydrophobic carboxyl tail. Both indicated structures are indispensable for PyV MT function.

B. Structure of the MT Y250F cDNA. Tyrosine residue 250 of wild-type PyV MT is substituted for by a non-phosphorylatable phenylalanine residue.

C. Structure of the MT Y315/22F cDNA. Tyrosine residues 315 and 322 of wild-type PyV MT are substituted for by non-phosphorylatable phenylalanine residues.

A. WT MT

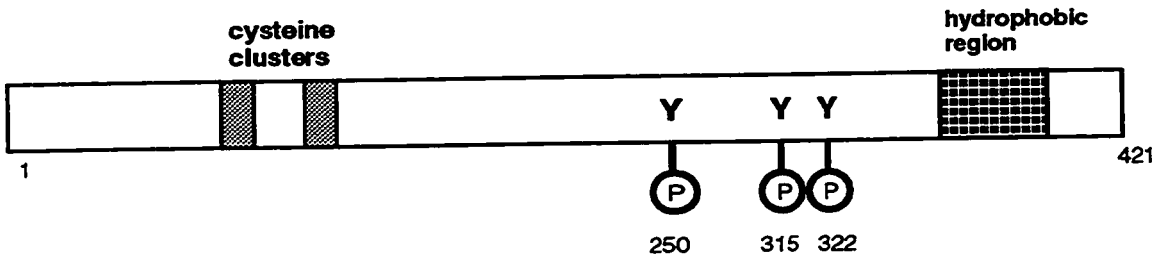

B. MT Y250F

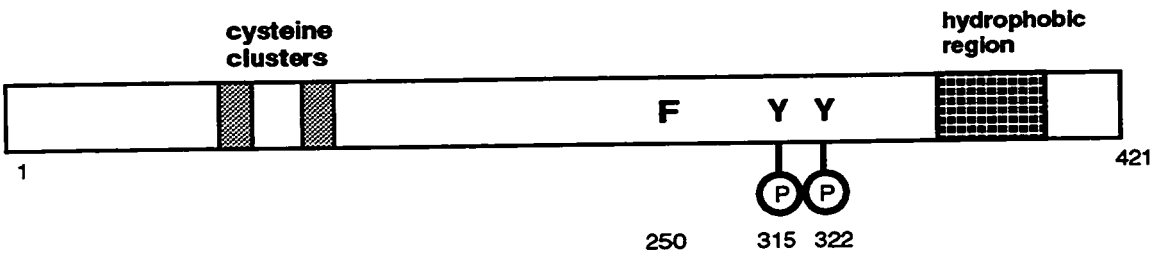

C. MT Y315/22F

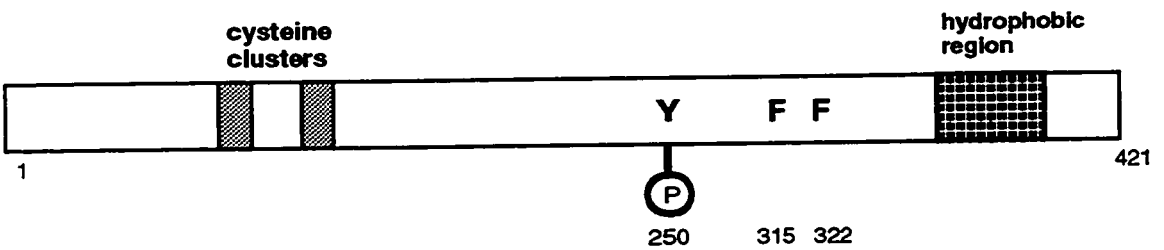

form foci in Rat-1 fibroblasts. The results from these analyses are depicted in Table 5.1. Consistent with previous studies (Markland & Smith, 1987), mutation of either tyrosine 250 or 315/322 resulted in a dramatic impairment of transforming activity. The MT Y250F mutant was able to induce transformed foci at 5.7% the levels observed in wild-type MT whereas the MT Y315/22F mutant induced transformed foci at 9.1% the levels of wild-type MT (Table 5.1). For subsequent biochemical characterization of these mutant PyV MT proteins, stable G418 resistant cell lines (provided for by co-transfected selectable marker plasmid pSV2neo) were also generated. To confirm expression of PyV MT transcript, RNA isolated from clonal cell lines was subjected to RNase protection analyses using a riboprobe spanning the amino terminal 203 nucleotides (pMTR, Figure 5.2A). The results showed that many of the co-transfectants expressed either the introduced PyV MT mutant or wild-type PyV MT transcripts (Figure 5.2B). Several independent cell lines expressing comparable levels of PyV MT transcript were subsequently selected for further biochemical characterization (Figure 5.2, lanes 35, 37 and 43).

5.2.2. Biochemical characterization of MT and MT mutant cell lines

To assess whether cell lines expressing the PyV MT transcripts produced comparable levels of PyV MT protein, protein lysates from a representative cell line for each construct transfected was subjected to immunoprecipitation followed by immunoblot analyses using antisera specific for PyV MT. As shown in Figure 5.3A, a single 56 kDa species corresponding to MT was observed in each of the clonal Rat-1 cell lines derived. To confirm that the introduction of the various phenylalanine mutations did not interfere with PyV MT associated kinase activity, identical protein extracts were subjected to an *in vitro* kinase assay (Figure 5.3B).The results of these analyses revealed that the extent of kinase activity corresponded directly to the levels of PyV MT expressed . These observations suggest that associated kinase activity is not compromised in the MT mutants. To ensure that the mutant cDNAs resulted in MT proteins

Table 5.1 Transformation potential of wild-type PyV MT and PyV MT mutants in Rat-1 cells.

Established fibroblast cell line Rat-1 was used to assess the *in vitro* transforming properties of PyV MT and PyV MT mutants. MoMLV expression cassettes harboring the MT cDNAs (or empty vector alone) were electroporated into Rat-1 cells following which monolayers were analyzed for focus formation after 14 days.

TABLE 5.1. Transformation of Rat-1 cells [a]

ession nid	Focus assay 1 [b] Average no. of foci [f]	Average no. of G418 colonies [g]	% Transformation of pJ4Ω MT [h]	Focus assay 2 [c] Average no. of foci [f]	Average no. of G418 colonies [g]	% Transformation of pJ4Ω MT [h]
	0	85±6	0	0	85±6	0
ΩMT Y250F	3±1	85±9	2.8	2±1	85±9	5
ΩMT Y315/22F	8±4	89±15	6.7	3±1	89±15	8.1
ΩMT	106±7	77±6	100	32±3	77±6	100

ession nid	Focus assay 3 [d] Average no. of foci [f]	Average no. of G418 colonies [g]	% Transformation of pJ4Ω MT [h]	Focus assay 4 [e] Average no. of foci [f]	Average no. of G418 colonies [g]	% Transformation of pJ4Ω MT [h]
	0	347±11	0	0	347±11	0
ΩMT Y250F	22±4	157±1	6.9	34±2	157±1	8.1
ΩMT Y315/22F	43±5	182±9	11.6	47±2	182±9	9.8
ΩMT	487±22	242±8	100	825±44	242±8	100

tive transforming ability [i]	
Ω	0.0
ΩMT Y250F	5.7
ΩMT Y315/22F	9.1
ΩMT	100.0

Four independent focus assays were performed with Rat-1 fibroblasts. All transfections performed with CsCl purified DNA preparations. MT and all mutant MT cDNAs inserted into plasmid pJ4Ω under transcriptional control of the Moloney murine leukemia virus long terminal repeat. pJ4Ω represents parent empty vector used for mock transfections. Two plates from each transfection were treated with 40 ug/ml G418. All plates fixed in 10% phosphate buffered formalin and stained with Giemsa 14 days following transfection.

pJ4Ω plasmid concentration per 100 mm plate is 500ng. pSV2neo plasmid concentration is 50ng per 100 mm plate. 20 ug salmon sperm per 100mm plate

pJ4Ω plasmid concentration per 100 mm plate is 100ng. pSV2neo plasmid concentration is 50ng per 100 mm plate. 20 ug salmon sperm per 100mm plate

pJ4Ω plasmid concentration per 100 mm plate is 500ng. pSV2neo plasmid concentration is 50ng per 100 mm plate.

pJ4Ω plasmid concentration per 100 mm plate is 750ng. pSV2neo plasmid concentration is 50ng per 100 mm plate.

Values are the mean numbers of foci counted on four plates ± the standard error

Values are the mean number of G418 resistant colonies counted from 2 plates ± the standard error.

Values represent the ratio of foci obtained for each construct with respect to wild-type MT (pJ4Ω MT) normalized to the number of G418 resistant colonies obtained per transfection ± the standard error.

Values represent the mean transforming efficiencies over four transfections normalized to the number of G418 resistant colonies obtained per transfection ± the standard error.

Figure 5.2 Identification of clonal Rat-1 cell lines expressing PyV MT, PyV MT Y250F or PyV Y315/22F cDNAs by RNase protection.

A. Diagrammatic representation of the PyV MT cDNA (shaded bar) and the riboprobe used to detect PyV MT RNA transcripts (line under shaded bar). Also shown is the direction of transcription used in the *in vitro* generation of antisense RNA transcript (arrow below line). This probe protects the first 203 nucleotides of PyV MT coding sequences.

B. Fifteen micrograms of CsCl purified total cellular RNA from each clonal cell line was analyzed for the presence of PyV MT-specific transcript using riboprobe MTR described above (A). Also analyzed for PyV MT transcript are pooled G418 resistant colonies harboring either MT Y250F (S pool) or wild-type MT (M pool) as well as primary breast tumor cell lines MT1A2 and MT2E2 derived from MMTV/wild-type PyV MT transgenic mice.

A.

B.

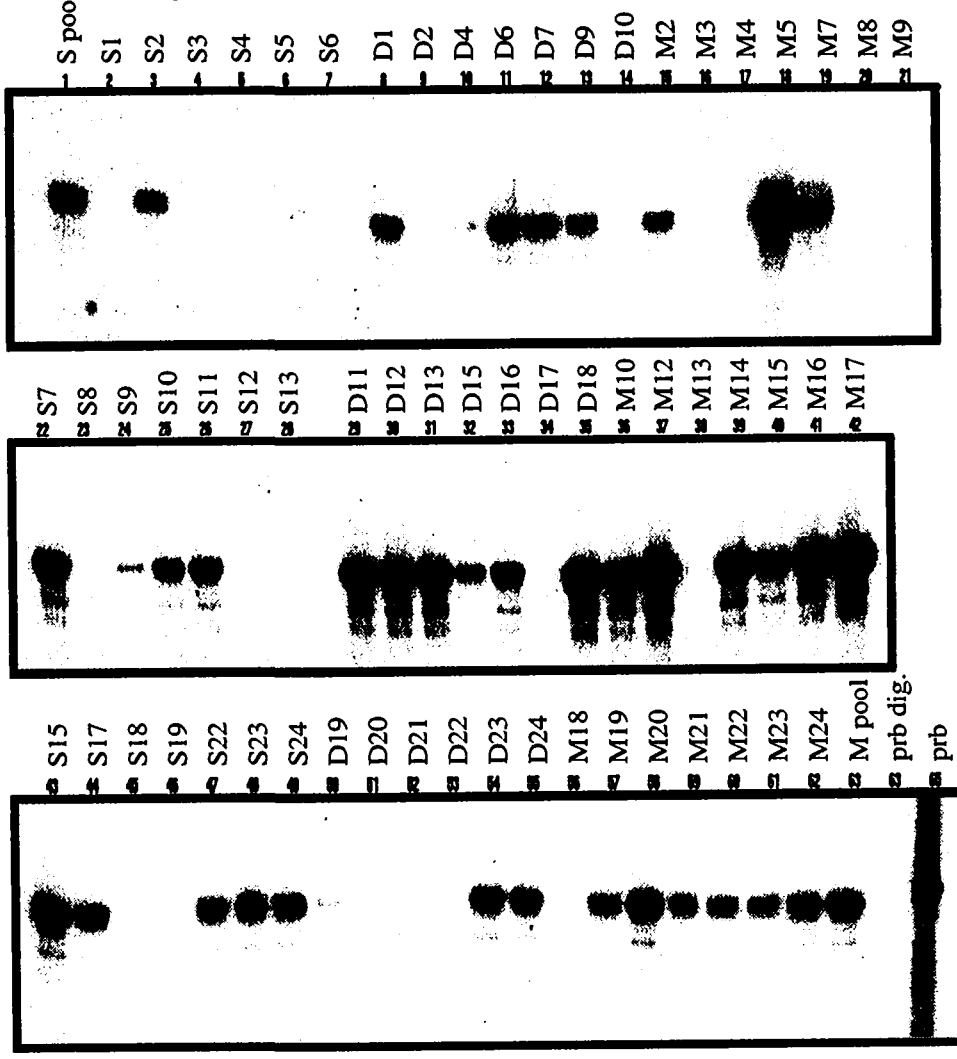

S = MT Y250F
D = MT Y315/22F
M = MT

ESTABLISHED
1° MT CELLS

Figure 5.3 Established Rat-1 cell lines harboring PyV MT, PyV MT Y250F or PyV MT Y315/22F express full-length MT protein with equivalent associated tyrosine kinase activities.

A. Immunoblot analyses of Rat-1 cell lines expressing PyV MT or PyV MT mutants using a rat monoclonal antisera specific for PyV MT. One hundred and fifty micrograms of total protein extract from each cell line was immunoprecipitated with a PyV MT-specific mouse monoclonal antibody.

B. Associated *in vitro* kinase activity with PyV MT and PyV MT mutants derived from Rat-1 expressing cell lines. One hundred and fifty micrograms of total protein extract from each cell line was immunoprecipitated with a PyV MT-specific mouse monoclonal antibody.

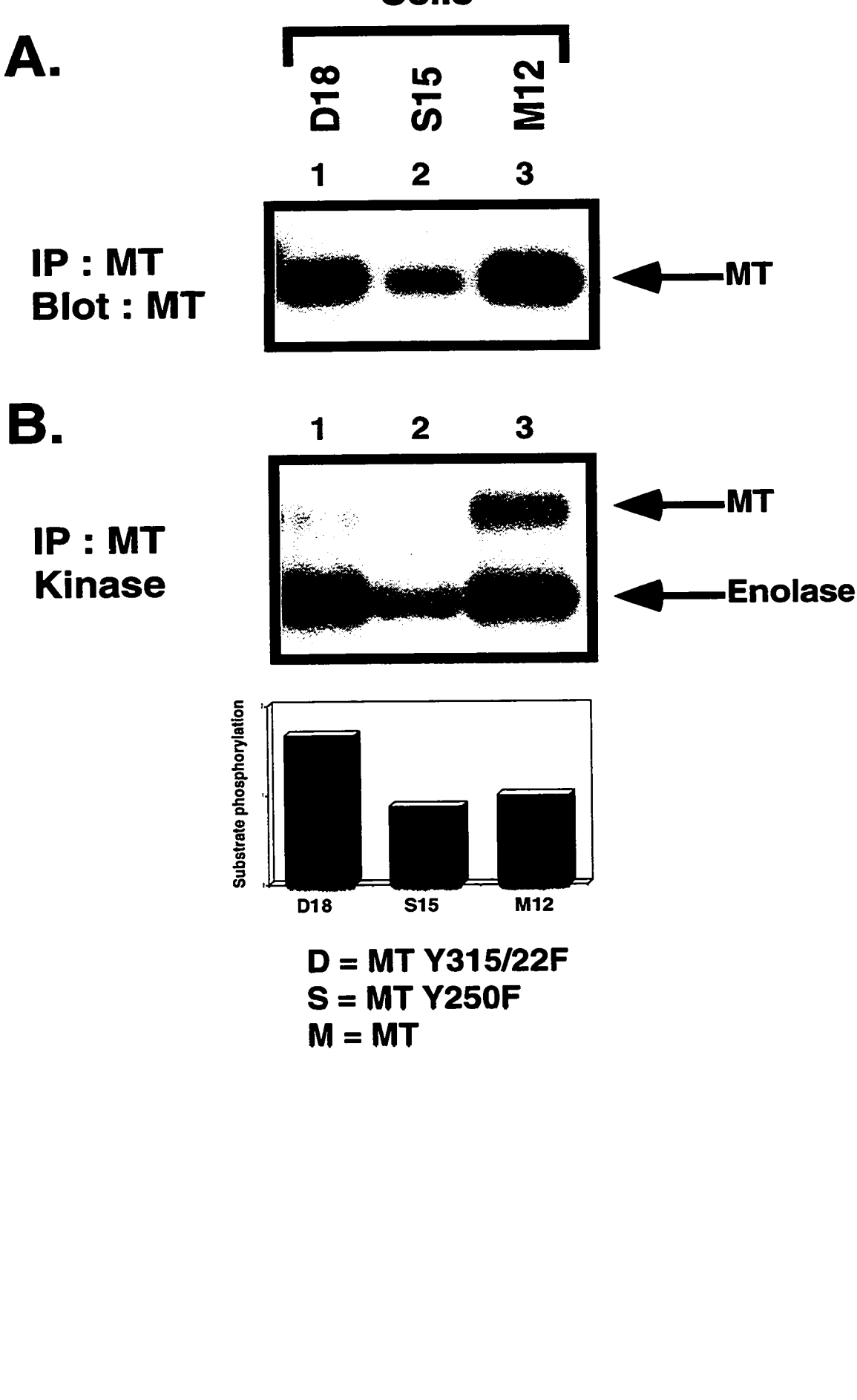
A.
D18
S15
M12
1
2
3
IP : MT
Blot : MT
MT
B.
1
2
3
IP : MT
Kinase
MT
Enolase
Substrate phosphorylation
D18
S15
M12
D = MT Y315/22F
S = MT Y250F
M = MT

SHC association and MT Y315/22F failing to bind the p85 subunit of PI3'K) co-immunoprecipitation studies were performed with SHC, p85 and PyV MT-specific antibodies. To examine the ability of SHC to bind either MT mutant, protein lysates from cell lines expressing either MT mutant or wild-type MT were immunoprecipitated with antisera specific for MT and immunoblotted for SHC. As evident in Figure 5.4A, SHC is isolated in a complex with wild-type MT and MT Y315/22F (lanes 1,3) but not with MT Y250F immunoprecipitates (lane 2). Employing a similar strategy, I examined whether PI3'K association was impaired in PyV MT immunoprecipitates from the MT Y315/22F expressing Rat-1 cells. PyV MT-specific antisera was used to immunoprecipitate MT protein complexes followed by immunoblot analyses with an antibody specific to the p85 subunit of PI3'K. As expected, p85 was detected in wild-type PyV MT immunoprecipitates (Figure 5.4B, lane 3), but could not be detected in MT Y315/22F immunoprecipitates (Figure 5.4B, lane 1). Unexpectedly, p85 association in MT Y250F immunoprecipitations was impaired when compared to immunoprecipitates from wild-type MT expressing cells (Figure 5.4B, lane 2). To further characterize the binding of the PI3'K p85 subunit to MT or MT mutants, a direct binding assay using a radiolabeled recombinant GST-p85 SH2 domain fusion protein was employed. To accomplish this, MT-specific antisera was used to immunoprecipitate MT from either parental MT, MT Y315/22F or MT Y250F Rat-1 expressing cell lines. Following size separation on SDS PAGE and transfer onto a polyvinyl membrane, P^{32}-labeled recombinant GST-p85 fusion protein was incubated with the membrane. Consistent with the co-immunoprecipitation analyses, the radiolabeled recombinant protein bound efficiently to wild-type MT, less well to MT Y250F and was even further reduced in the ability bind to MT Y315/22F (Figure 5.5B). To examine whether the reduced p85 binding seen in MT Y250F and MT Y315/22F correspondingly results in reduced PI3'K activity, MT immunoprecipitated complexes were prepared from various MT or MT mutant expressing cell lines. Immunoprecipitates were incubated with bovine phosphoinositol and γ-ATP-P^{32}, following which lipids were extracted and analyzed by thin layer chromatography (TLC) as shown in Figure 5.6A.

Figure 5.4 PyV MT Y250F and PyV MT Y315/22F demonstrate altered *in vitro* binding affinities for PyV MT associated cellular proteins p85 and SHC respectively.

A. Immunoprecipitation of total protein extracts derived from MT and MT mutant expressing Rat-1 cell lines with mouse monoclonal PyV MT-specific antibody followed by immunoblot analyses with polyclonal SHC-specific antibody.

B. Immunoprecipitation of total protein extracts derived from MT and MT mutant expressing Rat-1 cell lines with mouse monoclonal PyV MT-specific antibody followed by immunoblot analyses with polyclonal p85-specific antibody.

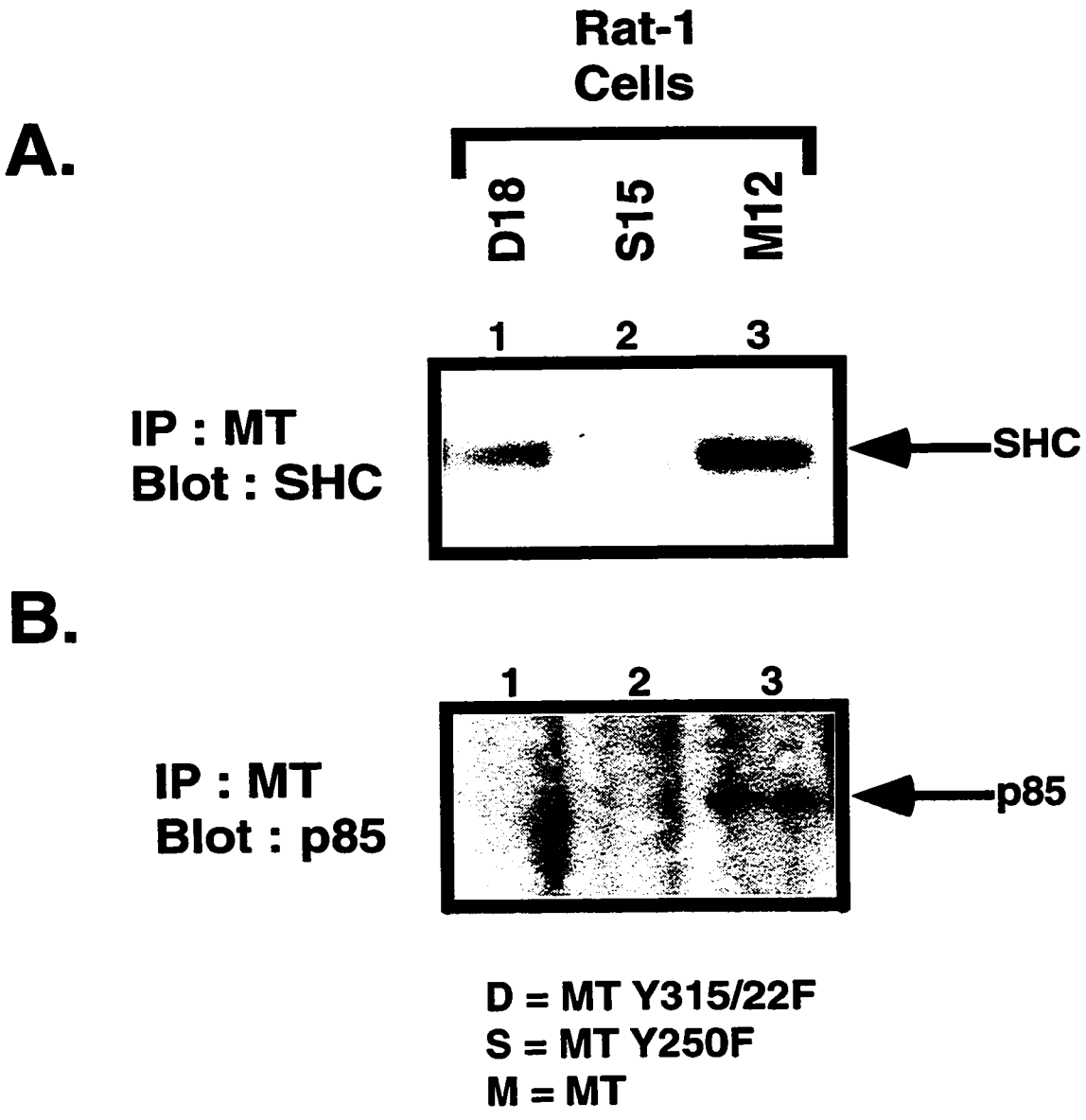
A.
Rat-1
Cells
D18
S15
M12
1
2
3
IP : MT
Blot : SHC
SHC
B.
1
2
3
IP : MT
Blot : p85
p85
D = MT Y315/22F
S = MT Y250F
M = MT

Figure 5.5 PyV MT mutants MT Y250F and, to a greater extent MT Y315/22F, demonstrate debilitated binding of p85 in a direct binding assay.

A. Immunoprecipitation of total protein extracts derived from MT and MT mutant expressing Rat-1 cell lines followed by immunoblot analyses using antibodies specific for PyV MT.

B. Immunoprecipitation of total protein extracts derived from MT and MT mutant expressing Rat-1 cell lines followed by protein blotting using P^{32} labeled recombinant GST-p85 fusion protein.

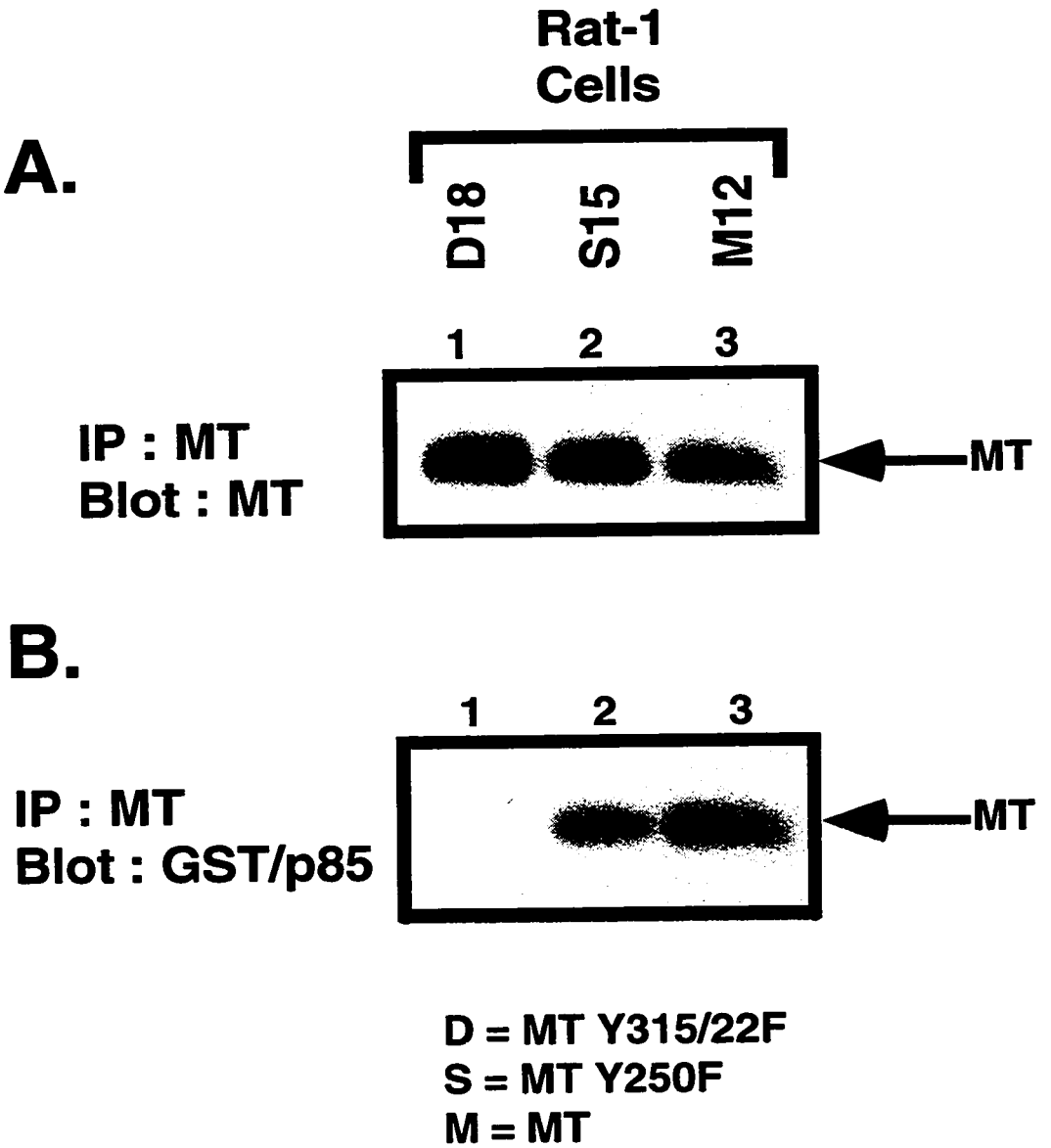
Rat-1
Cells
A.
D18
S15
M12
1
2
3
IP : MT
Blot : MT
MT
B.
1
2
3
IP : MT
Blot : GST/p85
MT
D = MT Y315/22F
S = MT Y250F
M = MT

Figure 5.6 ***In vitro*** **PyV MT associated lipid kinase activities are reduced in both PyV MT mutant proteins.**

A. Associated *in vitro* lipid kinase activity with PyV MT and PyV MT mutants derived from Rat-1 expressing cell lines. PyV MT complexes were immunoprecipitated from MT-expressing Rat-1 cell lines using PyV MT-specific mouse monoclonal antibody followed which *in vitro* lipid kinase products were extracted and analyzed by thin layer chromatography. The lower panel represents PhosphorImager quantitation of results obtained from this particular analysis normalized to levels of immunoprecipitated PyV MT protein (as determined by ^{125}I PyV MT immunoblotting) .

B. Immunoprecipitation of total protein extracts derived from MT and MT mutant expressing Rat-1 cell lines followed by immunoblot analyses using antibodies specific for PyV MT.

A.

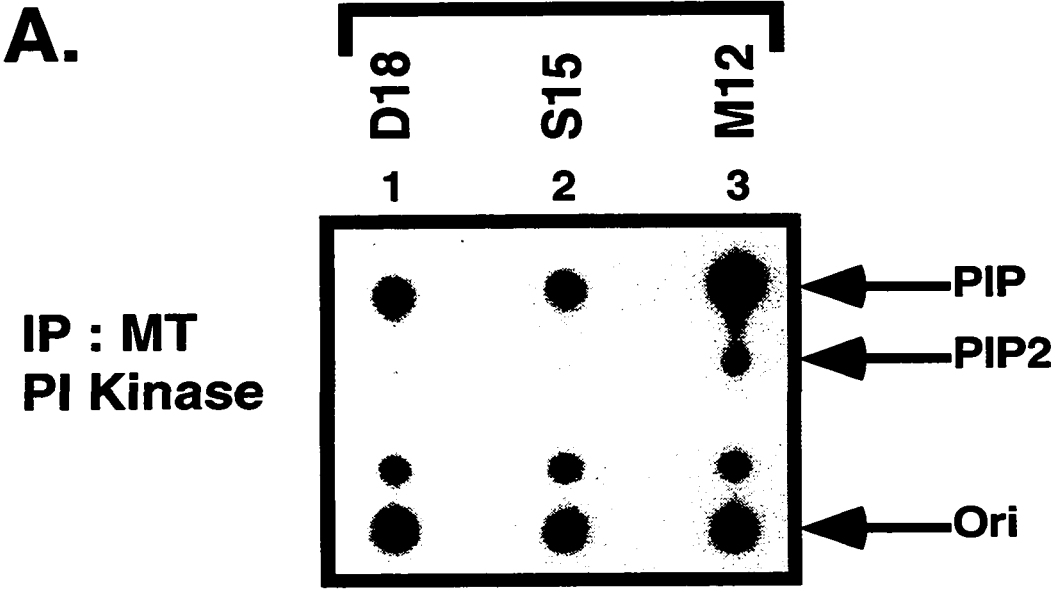

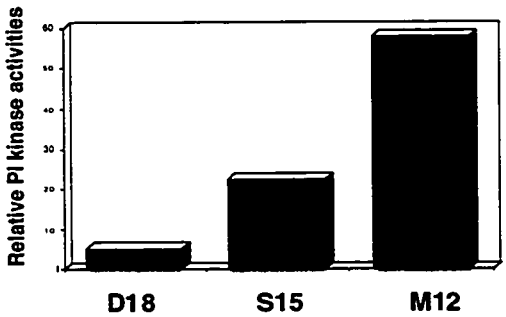

B.

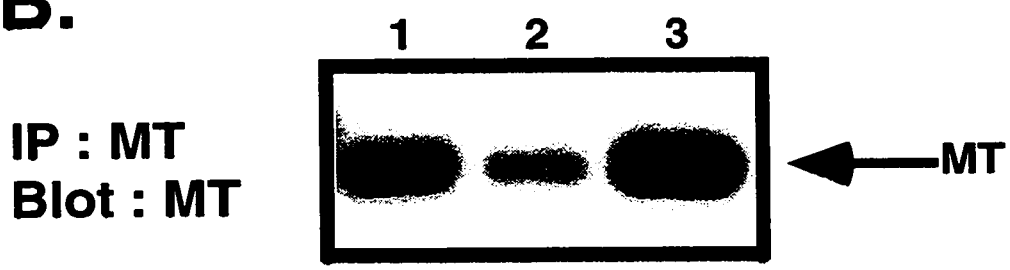

D = MT Y315/22F
S = MT Y250F
M = MT

protein, the MT Y315/22F mutant was more debilitated than the MT Y250F mutant. Taken together, these observations suggest that mutation of tyrosines 315/22 or 250 can interfere with the ability of PyV MT to complex and activate PI3'K *in vitro* , albeit, to different extents.

5.2.3. Generation and tissue site expression of MT mutant transgenic mouse strains

Although these studies suggested that the association of either PI-3'K or SHC proteins with PyV MT was crucial in inducing cellular transformation in established fibroblasts, it was important to assess the transforming properties of these mutant PyV MT proteins in the primary mammary epithelium of transgenic mice. To accomplish this objective, the MT Y250F and MT Y315/322F mutant MT cDNAs were placed under the transcriptional control of the MMTV promoter/enhancer and microinjected in one-cell mouse embryos. To this end, both mutant MT cDNAs were subcloned directionally (by virtue of unique HindIII and EcoRI restriction sites flanking the MT cDNA) into the corresponding sites of MMTV LTR expression vector p206 (Figure 5.7A and 5.8A). The MMTV sequences were derived from plasmid PA9 (Huang et al., 1981), while the SV40 small T intron (with corresponding splicing signals) and polyadenylation signal were derived from plasmid CDM8 (Seed & Aruffo, 1987). The entire expression cassette was released from plasmid sequences by restriction of the plasmids with SalI and SpeI. Microinjection of each purified expression cassette into one-cell mouse embryos resulted in the generation of seven MT Y315/22F transgenic strains and eight MT Y250F transgenic strains.

To examine the tissue specific expression of the transgene in these strains, 20 ug of total cellular RNA isolated from a variety of tissues was analyzed by RNase protection utilizing an antisense riboprobe spanning the first 203 nucleotides of the PyV early region (Figure 5.2A). Results from these analyses are summarized in Table 5.2 (Table 5.2) for MT Y250F strains and in Table 5.3 for MT Y315/22F strains (Table 5.3). Two independent strains were selected for further

Figure 5.7 Tissue specificity of transgene expression in MMTV / MT Y250F transgenic mice.

(A) Structure of the MMTV / MT Y250F transgene. The Bluescript vector backbone is represented by a thin line on either side of the expression cassette with the cross-hatched region corresponding to the MMTV LTR derived from plasmid pA9 (Sinn et al., 1987), the stippled portion to the MT Y250F cDNA with a phenylalanine substitution at amino acid position 250, and the solid region specifies the transcriptional processing sequences derived from the SV40 early transcription unit. Transcription start site is indicated by the arrow.

(B) RNA transcripts corresponding to the MMTV / MT Y250F transgene in various organs of the MT Y250F-5a transgenic strain as assessed by RNase protection. Tissues were derived from: a virgin tumor bearing female (#7398), a virgin female (#7952) and a male (#6882). The antisense probe used in this RNase protection analysis (MTR) protects a 203 nucleotide fragment corresponding to the amino terminus of PyV MT and is marked by MT250F and an arrow. Also shown is an RNase protection analyses on identical RNA samples with an antisense probe directed against phosphoglycerate kinase which protects a 124 nucleotide fragment indicated by PGK and an arrow.

A.

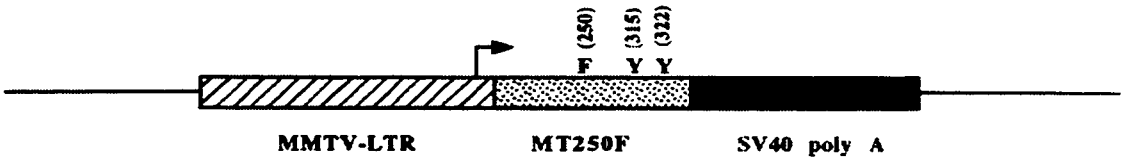
(250)
F
(315)
Y
(322)
Y
MMTV-LTR
MT250F
SV40 poly A

B.

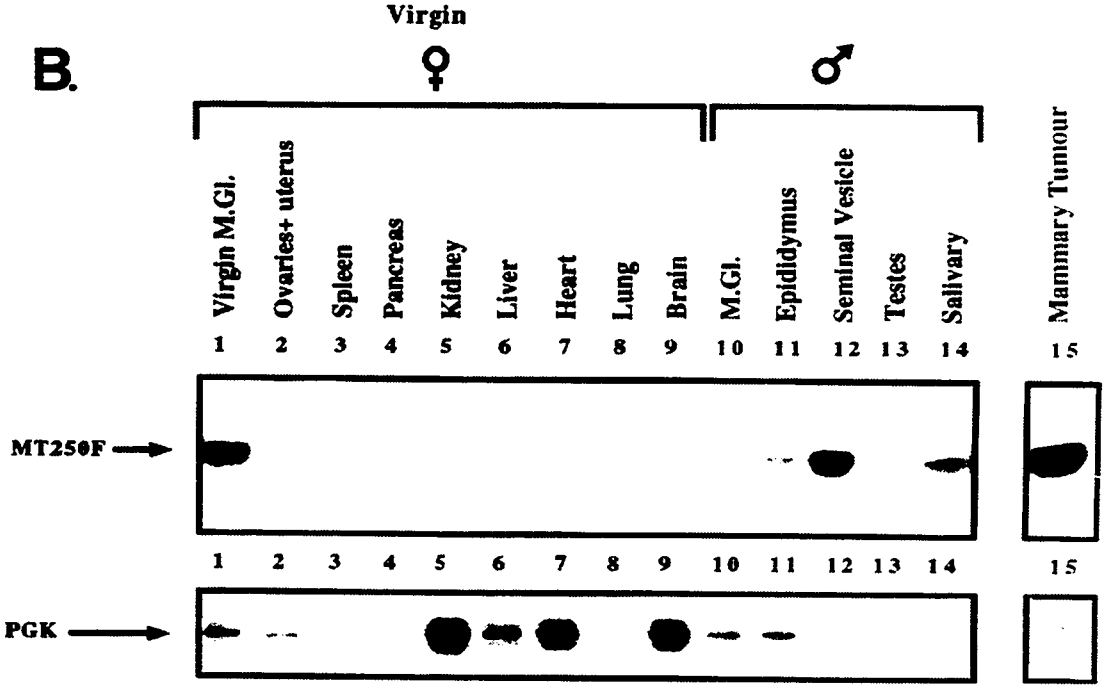
Virgin
♀
♂
Virgin M.Gl.
Ovaries+ uterus
Spleen
Pancreas
Kidney
Liver
Heart
Lung
Brain
M.Gl.
Epididymus
Seminal Vesicle
Testes
Salivary
Mammary Tumour
1 2 3 4 5 6 7 8 9 10 11 12 13 14 15
MT250F
1 2 3 4 5 6 7 8 9 10 11 12 13 14 15
PGK

Figure 5.8 Tissue specificity of transgene expression in MMTV / MT Y315/22F transgenic mice

(A) Structure of the MMTV / MT Y315/22F transgene. The Bluescript vector backbone is represented by a thin line on either side of the expression cassette with the cross-hatched region corresponding to the MMTV LTR derived from plasmid pA9 (Sinn et al., 1987), the stippled portion to the MT Y250F cDNA with a phenylalanine substitutions at amino acid positions 315 and 322, and the solid region specifies the transcriptional processing sequences derived from the SV40 early transcription unit. Transcription start site is indicated by the arrow.

(B) RNA transcripts corresponding to the MMTV / MT Y250F transgene in various organs of the MT Y315/22F-4 transgenic strain as assessed by RNase protection. Tissues were derived from: a virgin tumor bearing female (#5620), a virgin female (#6133) and a male (#5622). The antisense probe used in this RNase protection analysis (MTR) protects a 203 nucleotide fragment corresponding to the amino terminus of PyV MT and is marked by MT315/22F and an arrow. Also shown is an RNase protection analyses on identical RNA samples with an antisense probe directed against phosphoglycerate kinase which protects a 124 nucleotide fragment indicated by PGK and an arrow.

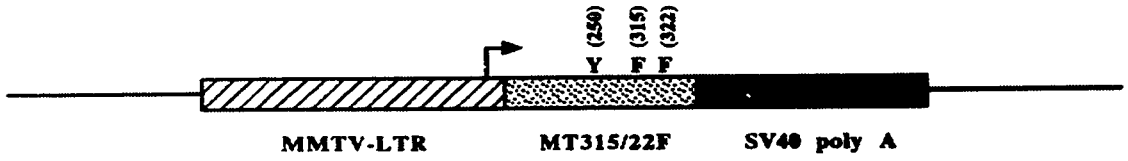
(250) Y
(315) F
(322) F
MMTV-LTR
MT315/22F
SV40 poly A

B.

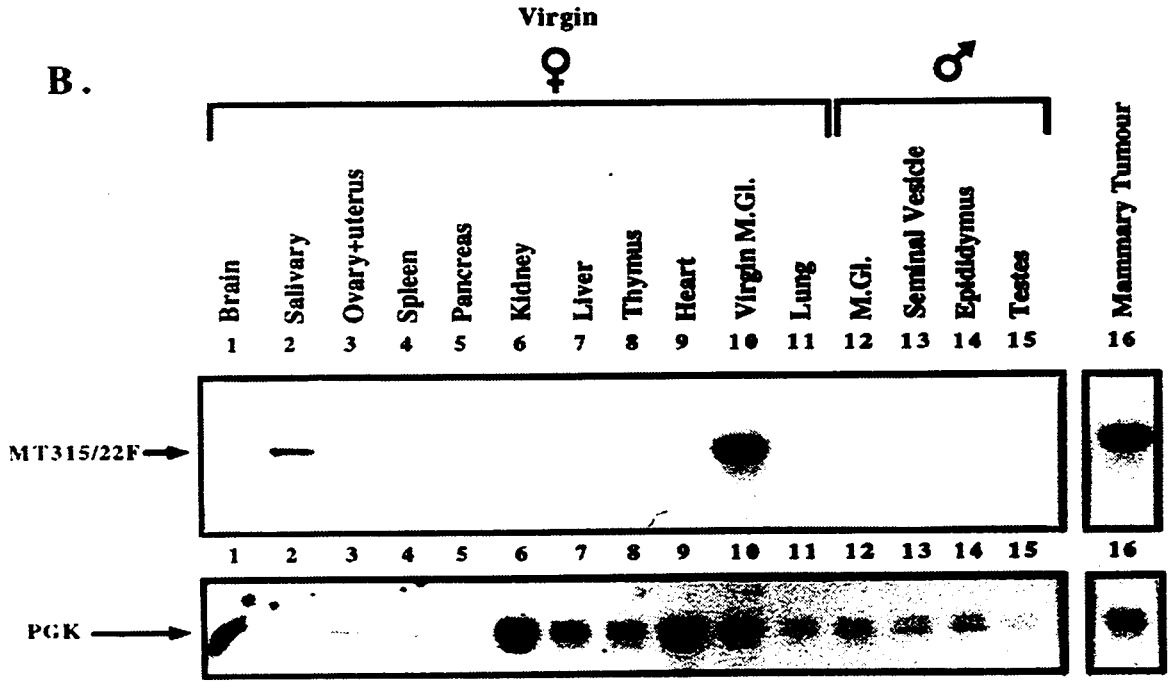
Virgin
♀
♂
Brain
Salivary
Ovary+uterus
Spleen
Pancreas
Kidney
Liver
Thymus
Heart
Virgin M.Gl.
Lung
M.Gl.
Seminal Vesicle
Epididymus
Testes
Mammary Tumour
1 2 3 4 5 6 7 8 9 10 11 12 13 14 15 16
MT315/22F
1 2 3 4 5 6 7 8 9 10 11 12 13 14 15 16
PGK

Table 5.2 Transgene expression and tumor onset in MMTV / MT Y250F mice.

Thirty micrograms of total cellular RNA isolated from a variety of tissues from male and female transgenic mice were analyzed for expression of PyV MT-specific transcript by RNase protection analyses. The riboprobe used in these analyses (MTR, figure 5.2A) recognizes the first 203 coding nucleotides of PyV MT. All normal tissues were derived from 8-10 week old mice while tumorous tissue derives from animals whose age was greater than the average onset at which respective neoplasias were first detected.

TABLE 5.2. Transgene expression and onset of tumors in MMTV / MT250F mice *

Expression of transgene							Average onset of mammary tumors in days (# animals)	Tumor types & Hyperplasias (# animals)
M.Gl.T (female)	M.GL. N (female)	M.Gl. N (male)	Sal.	Epidid.	Sem. Ves.	Testes		
NA	-	-	-	-	-	-	none	none
+++	+++	ND	+++	ND	ND	ND	136 days (n=26)	M.Gl. Adenocarcinomas Male reproductive abnormalities (Vas Deferens?) Hypersensitivity to parasitic infections
-	-	-	-	-	-	-	none	none
-	-	-	-	-	-	-	none	none
+++	+++	-	++	+	++	-	142 days (n=74)	M.Gl. Adenocarcinomas
+++	ND	ND	ND	ND	ND	ND	211 days (n=23)	M.Gl. Adenocarcinomas
NA	-	-	-	-	-	-	none	none
NA	-	-	-	-	-	-	none	none
NA	+/-	-	-	-	-	-	none	none

protection analysis was performed on 20 µg of total RNA isolated from a variety of organs in the MMTV / MT250F strains as described
rials and Methods. Relative levels of transgene expression (as determined by quantitative phosphorimager analysis) are indicated by - (not
l) + (low) ++ (intermediate) +++ (high). M.GL.N, normal mammary gland; M.GL.T, mammary gland tumor; Sal., salivary gland;
epididymus; Sem. Ves.; seminal vesicles; NA, not applicable; ND, not determined; n, number of animals analyzed.

Table 5.3 Transgene expression and tumor onset in MMTV / MT Y315/22F mice.

Thirty micrograms of total cellular RNA isolated from a variety of tissues from male and female transgenic mice were analyzed for expression of PyV MT-specific transcript by RNase protection analyses. The riboprobe used in these analyses (MTR, figure 5.2A) recognizes the first 203 coding nucleotides of PyV MT. All normal tissues were derived from 8-10 week old mice while tumorous tissue derives from animals whose age was greater than the average onset at which respective neoplasias were first detected.

TABLE 5.3. Transgene expression and onset of tumors in MMTV / MT315/22F mice*

Expression of transgene							Average onset of mammary tumors in days (# animals)	Tumor types & Hyperplasias (# animals)
M.Gl.T (female)	M.GL. N (female)	M.Gl. N (male)	Sal.	Epidid.	Sem. Ves.	Testes		
+++	+/-	-	-	-	-	-	255 (n=17)	M.Gl. Adenocarcinomas
NA	ND	ND	ND	ND	ND	ND	none	none
+++	+/-	-	ND	ND	ND	ND	253 (n=15)	M.Gl. Adenocarcinomas
+++	+++	-	++	-	-	-	120 (n=70)	M.Gl. Adenocarcinomas Salivary/Parotid neoplasms? Early develomental failure to arborize fat pad.
+++	+++	+	+++	+++	+++	-	107 (n=55)	M.Gl. Adenocarcinomas Salivary/Parotid neoplasms? Early develomental failure to arborize fat pad.
+++	+/-	-	-	-	-	-	~200 days	M.Gl. Adencarcinomas
+++	NA	NA	ND	NA	NA	NA	65 days (n=1)	M.Gl. Adencarcinomas

se protection analysis was performed on 20 µg of total RNA isolated from a variety of organs in the MMTV / MT315/22F strains as
ped in Materials and Methods. Relative levels of transgene expression (as determined by quantitative phosphorimager analysis) are indicated
not detected) + (low) ++ (intermediate) +++ (high). M.GL.N, normal mammary gland; M.GL.T, mammary gland tumor; Sal., salivary
Epidid., epididymus; Sem. Ves.; seminal vesicles; NA, not applicable; ND, not determined; n, number of animals analyzed.

each of the mutant PyV MT cDNAs. Representative RNase protections assays from the best characterized lines from MT Y250F (250-5) and MT Y315/22F (DB-4) are shown in Figures 5.7B and 5.8B respectively. Consistent with previous studies utilizing MMTV-driven transgenes, the highest levels of transgene transcript were detected in the mammary glands (Figures 5.7B and 5.8B, lanes 1 and 10 respectively). Lower levels of transgene expression could be detected in the salivary glands, and male reproductive organs - particularly in the epididymis and seminal vesicles (Figure 5.7B lanes 14, 11, 12 for MT Y250F strain 5a and Table 5.3 for MT Y315/22 strain DB-5).

5.2.4. Mammary gland-specific expression of mutant PyV MT cDNAs results in the development of global mammary epithelial hyperplasias and induction of focal mammary tumors.

Female transgenic mice expressing detectable levels of either mutant PyV MT proteins (MT Y250F or MT Y315/322F) in the mammary epithelium were incapable of nursing their young. To examine whether this lactation defect was due to aberrant epithelial development, wholemount analyses was conducted on 8 week old virgin mammary fat pads derived from FVB, MMTV/wild-type MT, MMTV/MT Y315/322F and MMTV/MT Y250F strains (Figure 5.9). By contrast to the multifocal mammary tumors arising in the MMTV/wild type MT strains (Figure 5.9D), mammary gland expression of either the MT Y315/322F or MT Y250F transgenes (Figures 5.9B and 5.9C respectively) resulted in the induction of global mammary epithelial hyperplasias. However, the mammary epithelial hyperplasias present in the MT Y315/322F strain differed in several aspects from those exhibited by the MT Y250F strain. For example, the MT Y250F strains had well defined alveolar hyperplasias which closely resembled those exhibited by MMTV/TGFα strains (Matsui et al., 1990). In contrast, the hyperplasia in the MT Y315/322F strains were extremely cystic and dilated without defined alveolar structures (compare Figures 5.10B and 4.10C).

Figure 5.9 Wholemount analyses of mammary glands from eight week-old FVB/n, MMTV/wild-type MT, MMTV/MT Y250F and MMTV/MT Y315/22F transgenic animals.

A panel of slide-mounted, wholemount preparations of hematoxylin stained mammary glands comparing the subgross morphology of a **(A)** nontransgenic virgin FVB female (8 weeks of age)(2.5X), **(B)** MMTV/MT Y250F transgenic virgin female (8 weeks of age)(2.5X), **(C)** MMTV/MT Y315/22F transgenic virgin female (8 weeks of age)(2.5X) and, **(D)** MMTV/wild-type MT transgenic virgin female (8 weeks of age)(2.5X). The mammary gland in (A) illustrates normal mammary morphology. Note the extensive hyperplasias in (B) and (C) and the conspicuous absence of hyperplasia in (D). Also note the absence of mammary tumor formation in either (B) or (C) and the multifocal mammary tumors arising stochastically in (D).

A
B
C
D

Figure 5.10 Histopathology of mammary glands derived from FVB/n, MMTV/MT, MMTV/MT Y250F and MMTV/MT Y315/22F transgenic animals.

(A) Photomicrograph of hematoxylin and eosin stained 7 μm thick section of a virgin female FVB non-transgenic animal (8 weeks of age). (100X)

(B) Photomicrograph of hematoxylin and eosin stained 7 μm thick section of a virgin female MMTV/MT Y250F transgenic animal. Note the dilated ductal lumen and the surrounding hyperproliferation of stromal tissues. (8 weeks of age). (100X)

(C) Photomicrograph of hematoxylin and eosin stained 7 μm thick section of a virgin female MMTV/MT Y315/22F transgenic animal. Note the extensive hyperplasia of the mammary ducts. (8 weeks of age). (100X)

(D) Photomicrograph of hematoxylin and eosin stained 7 μm thick section of a virgin female MMTV/wild-type MT transgenic animal. Note the formation of multiple sclerosing mammary adenocarinomas. (8 weeks of age). (100X)

B

further wholemount analyses was conducted on mice from the different strains at various time points (4, 8, 12, 16 weeks of age). All mammary epithelial tissues from both mutant MT animals appeared hyperplastic even at the earliest time point analyzed (4 weeks). In contrast, the mammary glands expressing wild-type PyV MT at the same 4 week time point revealed multiple focal occult tumors adjacent to apparently normal developing mammary gland (Figure 5.11). Consistent with the published observations of Guy et al. (Guy et al., 1992a), there appeared to be no evidence of precancerous hyperplastic lesions which normally preexists the formation of overt tumor. These observations suggest that malignant progression in MMTV/wild-type MT animals occurs very rapidly. Surprisingly, mammary glands from several MT Y315/22F mice at 4 weeks of age demonstrated an impairment in the ability of end buds to penetrate the surrounding fat pad (Figure 5.11C). Comparable mammary glands from wild-type MT or MT Y250F animals revealed no such migration defect (Figure 5.11D and 5.11B respectively). Examination of mammary glands from MT Y315/22F mice at later time points displayed no evidence of an equivalent developmental abnormality. These observations suggest that the migration defect can be overcome by as yet ill-defined mechanism(s).

Although the initial phenotype displayed by these mutant PyV MT transgenic mice was mammary epithelial hyperplasias, both strains eventually developed mammary tumors with 100% penetrance. The average age of mammary tumor incidence in addition to the age at which mammary tumors are first palpable is shown in Table 5.2 for characterized MT Y250F strains and Table 5.3 for all characterized MT Y315/22F strains. Comparison of the tumor kinetics between wild-type MT and those of the MT mutants (Figure 5.12), revealed that there is a significant delay in the ability of the MT mutants to form tumors *in vivo*. The MT Y250F bearing mice demonstrated the largest delay in tumor formation (T_{50}=145 days) while MT Y315/22F mice developed mammary tumors at a slightly earlier age (T_{50}=123 days). This represents a 3 fold and 2.6 fold respective increase in the latency period required to form mammary tumors compared to wild-type MT tumor kinetics. In addition, the tumors which arose in these strains were focal in origin

Figure 5.11 Wholemount analyses of mammary glands from four week-old FVB/n, MMTV/wild-type MT, MMTV/MT Y250F and MMTV/MT Y315/22F transgenic animals.

A panel of slide-mounted, wholemount preparations of hematoxylin stained mammary glands comparing the subgross morphology of a **(A)** nontransgenic virgin FVB female (4 weeks of age)(2.5X), **(B)** MMTV/MT Y250F transgenic virgin female (4 weeks of age)(2.5X), **(C)** MMTV/MT Y315/22F transgenic virgin female (4 weeks of age)(2.5X) and, **(D)** MMTV/wild-type MT transgenic virgin female (4 weeks of age)(2.5X). The mammary glands in (A), (B) and (D) illustrates normal ductal invasion of the surrounding fat pad. Note the retarded growth progression of ducts from the nipple. Also evident in (D) are two focal mammary tumors surrounded by morphologically normal mammary ducts. (B) and (C) panels reveal uniform epithelial hyperplasia of all ductal tissues in the absence of mammary tumor formation.

C
A
D
B

Figure 5.12 Mammary tumor onset in MMTV/MT#634, MMTV/MT Y250F-5a and MMTV/MT Y315/22F-4 transgenic strains.

The age at which mammary tumor is first palpable in each transgenic strain indicated. Also shown is the number of animals analyzed in each strain (n) in addition to the median (T_{50}) age at which tumors are palpable.

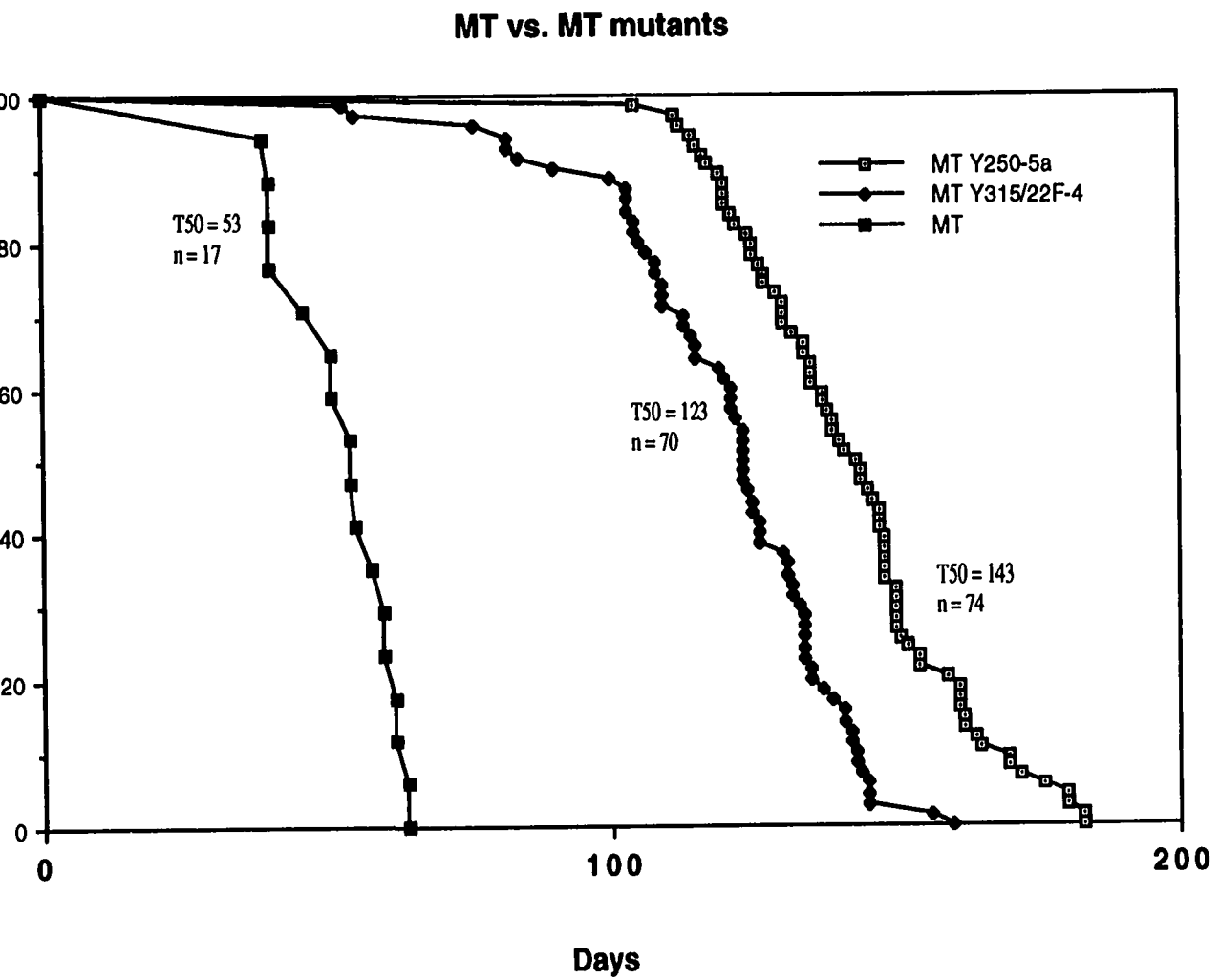
MT vs. MT mutants
MT Y250-5a
MT Y315/22F-4
MT
T50 = 53
n = 17
T50 = 123
n = 70
T50 = 143
n = 74
0
20
40
60
80
00
0
100
200
Days

both the cellular architecture and differentiation status of the tumors. Of note, tumors derived from MMTV/MT Y315/22F strains were the least well-differentiated in contrast to the well-differentiated MMTV/MT-derived tumors. Tumors from MMTV/MT Y250F strains were distinguished from other MT-derived tumors by virtue of a significant stromal component to the tumors. Interestingly, these tumors most resembled primary malignant lesions associated with MMTV/Src527F transgenic strains - namely schirrous carcinomas (Webster et al., 1995, Chapter 4).

In addition to the rapid and uniform formation of mammary tumors in MMTV/wild-type MT transgenic mice, these animals frequently develop pulmonary metastases. To establish whether similar rates of metastases occur in tumor-bearing mutant MT transgenic mice, lungs of all animals were examined at necropsy. In wild-type MT transgenic mice, 67% (n=9) of animals bearing tumors for greater than 31 days following initial palpation of a mammary tumor had developed overt lung metastases. When compared to MT Y315/22F and MT Y250F mice bearing tumors for the same period of time, only 36% (n=42) and 29%(n=24) respectively displayed obvious lung metastases. Although meaningful comparisons of metastatic rates is complicated by different tumor kinetic profiles in these strains (Figure 5.12), these data suggest that metastases may also be affected by inactivation of these PyV MT-associated signaling pathways.

5.2.5. Hyperplasias from MT Y315/22F transgenics are associated with an elevated apoptotic index

Recent observations have suggested that activation of the PI-3' kinase pathway plays an important role in preventing apoptotic cell death in P19 cells (Yao et al., 1995). Furthermore, several members of the PI3'K family have similar reported anti-apoptotic influences in several cell types (McConnell et al., 1996, Savitsky et al., 1995, Scheid et al., 1995). Given these observations and the unusual histological characteristics of the epithelial hyperplasias in MT Y315/22F mice (Figure 5.9 and 5.10), we were interested to assess whether these epithelial

Figure 5.13 Histopathology of mammary tumors derived from MMTV/MT, MMTV/MT Y250F and MMTV/MT Y315/22F transgenic animals.

A panel of slide-mounted, hematoxylin and eosin stained sections showing typical tumor morphologies.

(A) MMTV/MT Y250F transgenic virgin female. Note the extensive fibrosis associated with this mixed mammary adenocarcinoma. (X100)

(B) MMTV/MT Y315/22F transgenic virgin female. Note the pleomorphic cells with a solid growth pattern without glandular differentiation and the large number of mitotic figures. (X100)

(C) MMTV/wild-type MT transgenic virgin female. Note the papillary growth pattern with small glands within the epithelium. The luminal space is filled with an acellular pink fluid and apical blebs appear above the cell surface. (100X)

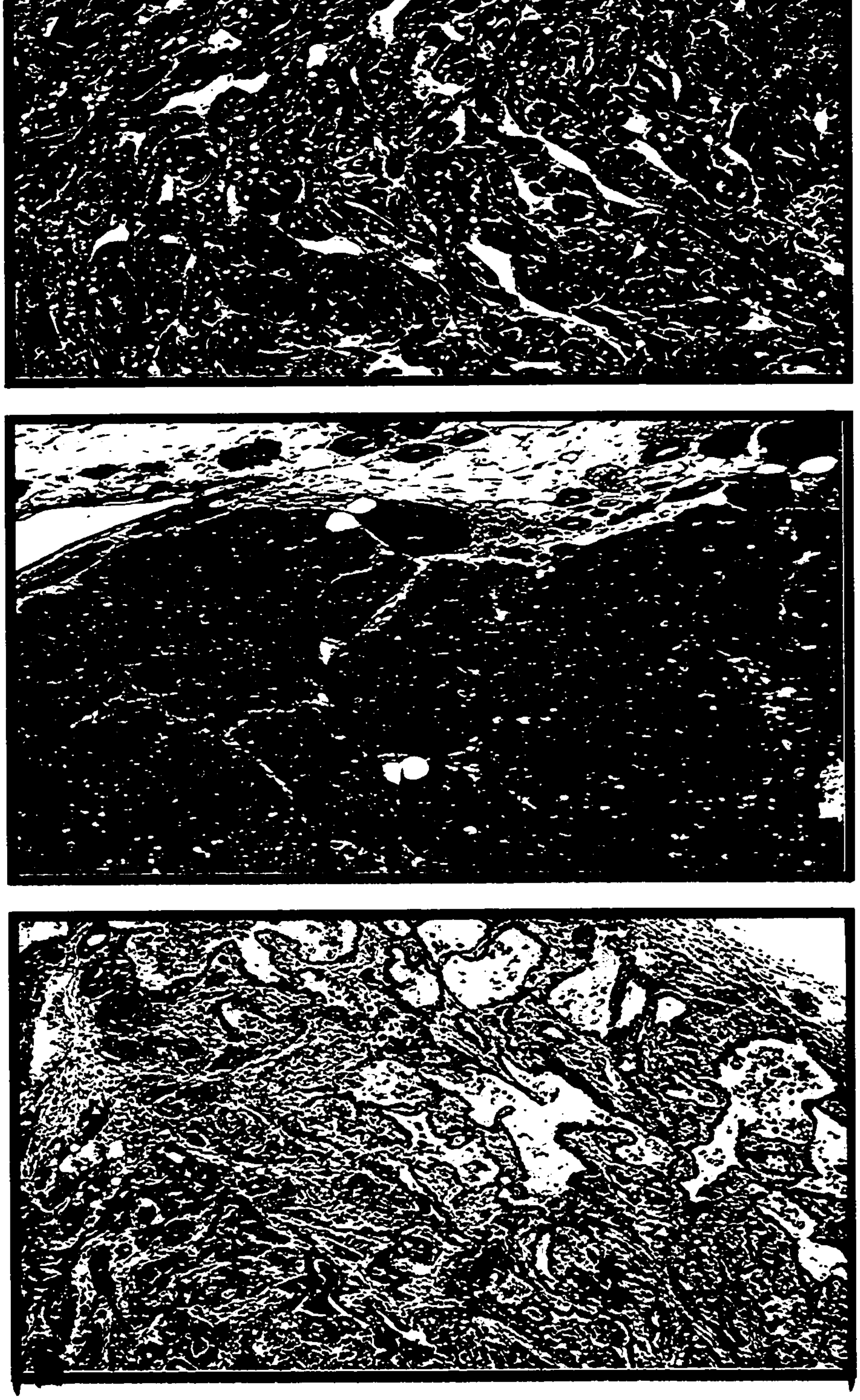

PyV MT antigen was involved in preventing apoptosis in the mammary glands of these various transgenic strains, histological samples from age-matched 8 week-old transgenic animals expressing either wild-type MT or MT mutants were subjected to TUNEL analyses (Figure 5.14). This *in situ* method allows one to score for cells displaying extensive DNA fragmentation which is a hallmark feature of apoptotic cell death (Surh et al., 1994). Although few apoptotic cells were observed in tumor tissue derived from wild-type PyV MT transgenics (Figure 5.14A) or from hyperplastic mammary epithelium derived from MT Y250F mice (Figure 5.14B), extensive apoptosis was noted in age-matched mammary epithelium from MT Y315/322F strains (Figure 5.14C). Extensive cell death was noted in histological samples from two independently derived MT Y315/22F transgenic lines (MMTV/MT Y315/22F-4 (DB-4) and MMTV/MT Y315/22F-5 (DB-5)). These data suggest that the capacity of PyV MT to activate PI-3'K may play a critical role in preventing apoptosis.

5.2.6. Biochemical characterization of mammary tumors expressing the mutant PyV MT antigens.

To ensure that PyV MT transcripts detected in these tumors encoded authentic PyV MT protein, 200 ug of total protein lysate from MT Y315/22F , MT Y250F or wild-type MT tumor tissue was subjected to immunoblot analyses with PyV MT-specific antisera (Figure 5.15). As expected, these analyses revealed the presence of both a 56 kDa and 58 kDa MT species in tumor extracts from all tumors analyzed (Figure 4.15). To control for the specificity of the antisera, a non-specific mammary tumor from a MMTV/Neu mouse was also included (Figure 5.15, lane 7). Because association of MT with Src family members is critical in effecting transformation (Schaffhausen et al., 1981), it was important to assess whether either MT mutant was impaired in its associated kinase activity. To this end, tumor extracts from both MT and MT mutants were immunoprecipitated with PyV MT-specific antisera and *in vitro* kinase activity assessed utilizing acid denatured enolase as an exogenous phosphorylatable substrate (Figure 5.16A). Although

Figure 5.14 Elevated levels of apoptosis in MMTV/MT Y315/22F transgenic strains as assessed *in situ* by TUNEL analyses.

A panel of slide-mounted Mayer's hematoxylin stained mammary tissue sections from age-matched mice from non-transgenic FVB **(A)**, or transgenic MMTV Y250F **(B)**, MMTV/MT Y315/22F **(C)**, and MMTV/wild-type MT **(D)** strains. Cells were analyzed for apoptotic DNA degradation by the method of Surh et al. (Surh et al., 1994). Digoxigenin labeled DNA ends were detected with horseradish peroxidase conjugated anti-digoxigenin antibodies. Note the multiple apoptotic cells in (C) and the conspicuous absence of apoptosis-specific staining in panels (A), (B), and (D).

A
B

Figure 5.15 Mammary tumors derived from MMTV/MT, MMTV/MT Y250F and MMTV/MT Y315/22F transgenic animals express full-length MT protein.

Immunoblot analyses of control and PyV MT mammary tumors derived from MMTV/MT, MMTV/MT Y250F and MMTV/MT Y315/22F transgenic animals with a rat monoclonal PyV MT-specific antibody. Mammary tumor extracts derived from virgin MMTV/MT Y315/22F (#7888, #8672 BT-2), MMTV/MT Y250F (#8139, #8442) and MMTV/MT (#170, #171) were immunoprecipitated with a mouse monoclonal PyV MT-specific antibody. As a non-specific control, a MMTV/Neu-derived mammary tumor (#9573) was included. The 56 and 58 kDa PyV MT proteins are indicated by MT and the arrows. The asterisk denotes that a reversion event was detected in the transgene originating from this particular tumor (section 4.2.6.).

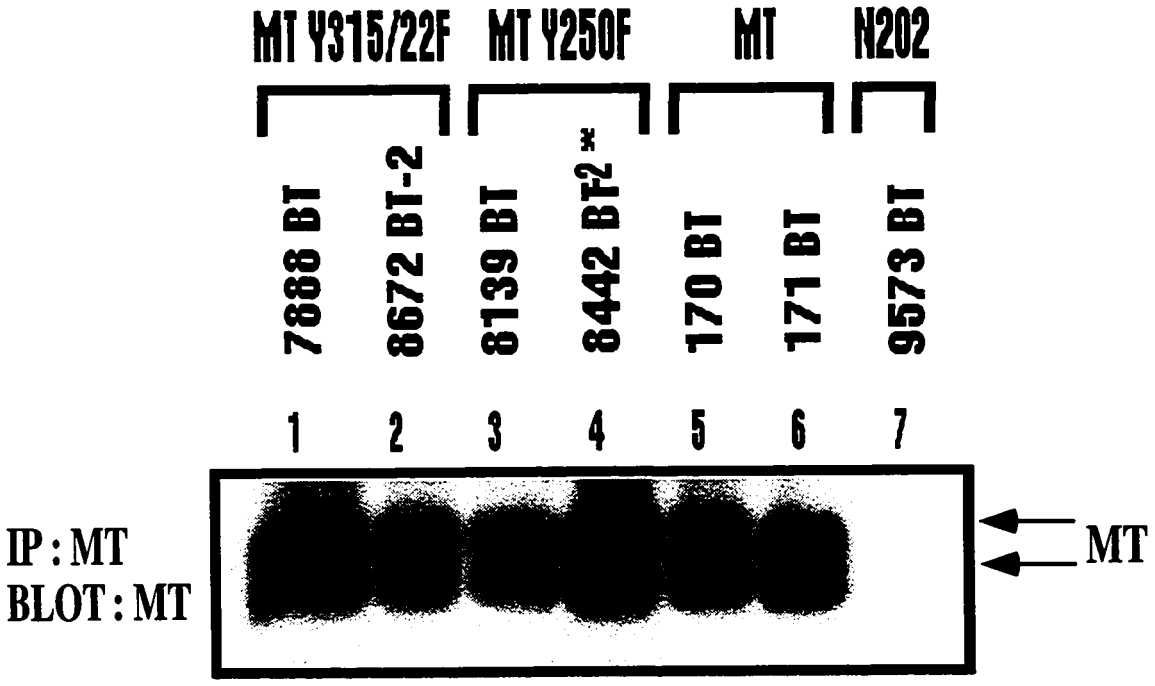
MT Y315/22F
MT Y250F
MT
N202
7888 BT
8672 BT-2
8139 BT
8442 BT2 **
170 BT
171 BT
9573 BT
1
2
3
4
5
6
7
IP : MT
BLOT : MT
MT

Figure 5.16 In vitro kinase activities of MT, MT Y250F and MT Y315/22F

(A) PyV MT-associated tyrosine kinase activity. Mammary tumors lysates derived from MMTV/MT (#170, #171), MMTV/MT Y250F (#8139, #8442) or MMTV/MT Y315/22F (#7888, #8672) transgenic animals were subject to immunoprecipitation with PyV MT-specific antisera. Immunoprecipitated complexes were incubated with [γ-P32] ATP in the presence of exogenous kinase substrate.- acid denatured enolase. Shown are phosphorylated enolase product (indicated by enolase and arrow) as well as phosphorylated PyV MT product (indicated by MT and arrow). Also included is MMTV/Neu-derived mammary tumor (#9573) as a non-specific control

(B) Src tyrosine kinase activity. Mammary tumors lysates derived from MMTV/MT (#170, #171), MMTV/MT Y250F (#8139, #8442), MMTV/MT Y315/22F (#7888, #8672) or MMTV/Neu (#9573) transgenic animals were subject to immunoprecipitation with Src-specific antisera. Immunoprecipitated complexes were incubated with [γ-P32] ATP in the presence of exogenous kinase substrate.- acid denatured enolase. Shown is the phosphorylated enolase product (indicated by enolase and arrow). PhosphorImager quantitation of enolase phosphorylation for this particular experiment is represented in bar graph form next to the image.

Note that protein lysate MMTV/MT Y250F #8442 BT-2 (indicated by *) was subsequently shown to encode a somatic mutational event which reverts the phenylalanine residue at site 250 to the wild-type tyrosine residue.

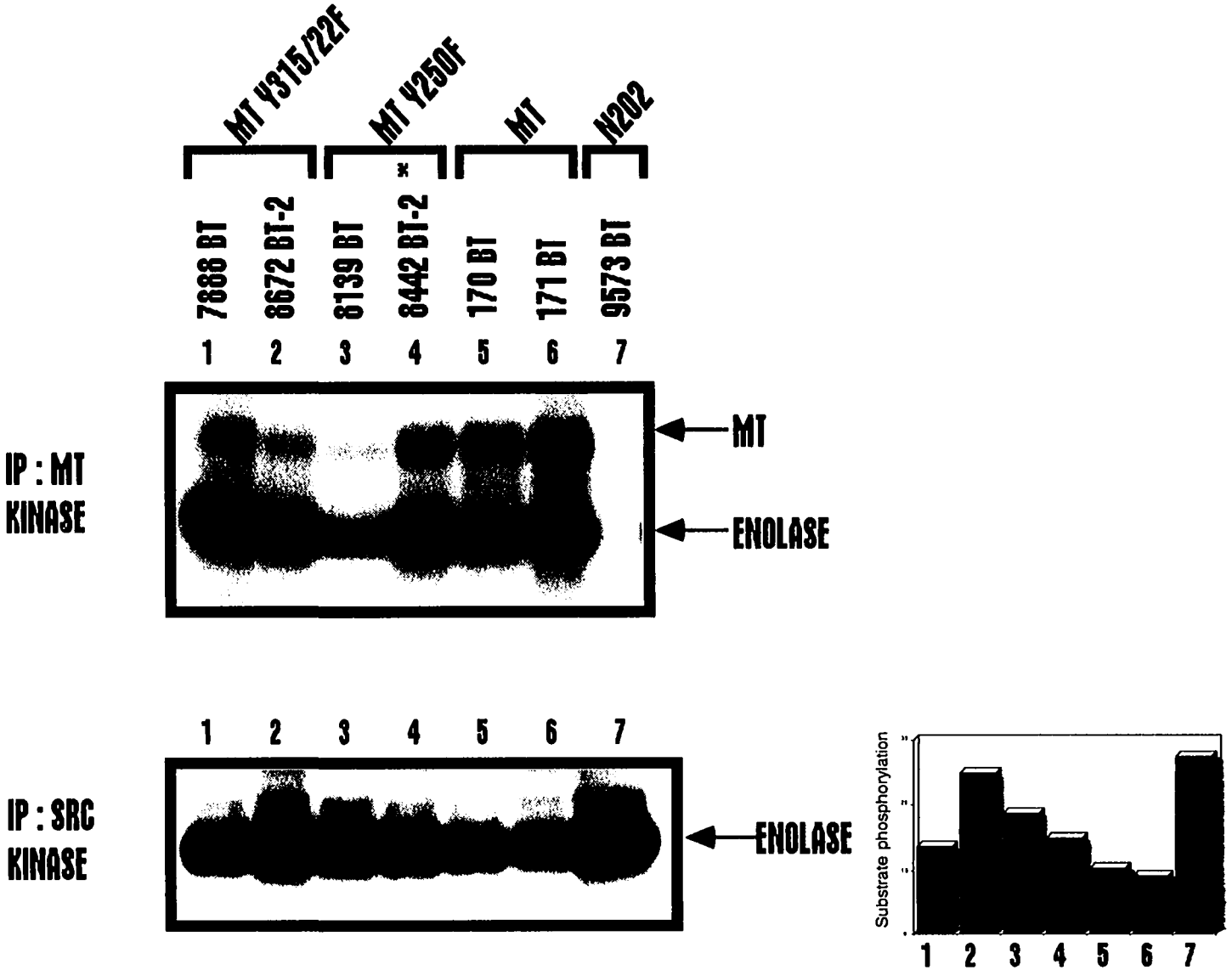
MT Y315/22F
MT Y250F
MT
N202
7888 BT
8672 BT-2
8139 BT
8442 BT-2
170 BT
171 BT
9573 BT
1 2 3 4 5 6 7
IP : MT KINASE
MT
ENOLASE
1 2 3 4 5 6 7
IP : SRC KINASE
ENOLASE
Substrate phosphorylation
1 2 3 4 5 6 7

immunoblot analysis), careful quantitation of the data indicate that associated kinase activities of the mutant PyV MT proteins were comparable to wild-type MT (Figure 5.17). Furthermore, *in vitro* measurement of Src kinase activity from Src immunoprecipitations isolated from MT mutant derived tumors revealed, on average, slightly higher kinase activity compared to Src kinase activity from wild-type MT tumors (Figure 5.16B). Taken together, these observations strongly argue that the delay in tumor formation in both mutant MT transgenics is not a consequence of the inability to complex and functionally activate c-Src tyrosine kinase family members.

5.2.7. The association of SHC with PyV MT plays an important role in PyV MT mediated tumorigenesis and metastases.

Tyrosine phosphorylation of MT residue 250 along with residues immediately upstream, creates a high affinity binding site for the PTB domain of SHC (Trub et al., 1995). Deletion or substitution within the core 'NPTY' sequence of MT desatibilizes this interaction and as a consequence severely impairs the ability of MT to transform (Druker et al., 1992). To directly test the ability of MT mutants to bind SHC, co-immunoprecipitation studies were undertaken. To confirm that SHC binding was ablated in tumors induced by the MT Y250F transgene, reciprocal immunoprecipitation/immunoblot analyses with either SHC or MT-specific antisera were conducted on tumor lysates derived from both mutant and wild-type MT strains. As expected, complexes of SHC and PyV MT were detected in tumor lysates derived from either mutant MT Y315/22F or wild-type MT protein lysates (Figure 5.18 A and B, lanes 5, 6, 9 and 7, 8, 11 respectively). However, no detectable complexes between PyV MT and SHC were observed in tumor lysates from MT Y250F strains (Figure 5.18 A and B, lanes 2-4 and 10).

To further corroborate the association of SHC with both wild-type MT and MT Y315/22F but not with MT Y250F induced mammary tumors, a direct blot assay similar to that described for p85 binding in Section 5.2.2. was employed. To this end, recombinant GST-SHCY317F (full-length SHC containing a tyrosine to phenylalanine substitution at position 317 (the site implicated

Figure 5.17 Graphic representation of wild-type and mutant MT-associated kinase activities in mammary tumors.

This bar graph represents the mean relative associated tyrosine kinase activity (measured through enolase phosphorylation) of MMTV/MT Y250F and MMTV/MT Y315/22F tumors with respect to MMTV/MT-induced mammary tumors (± mean of standard error (error bars)) averaged over five independent experiments analyzing a total of ten independently arising tumors from each strain. Results are normalized for PyV MT protein levels for each analyses.

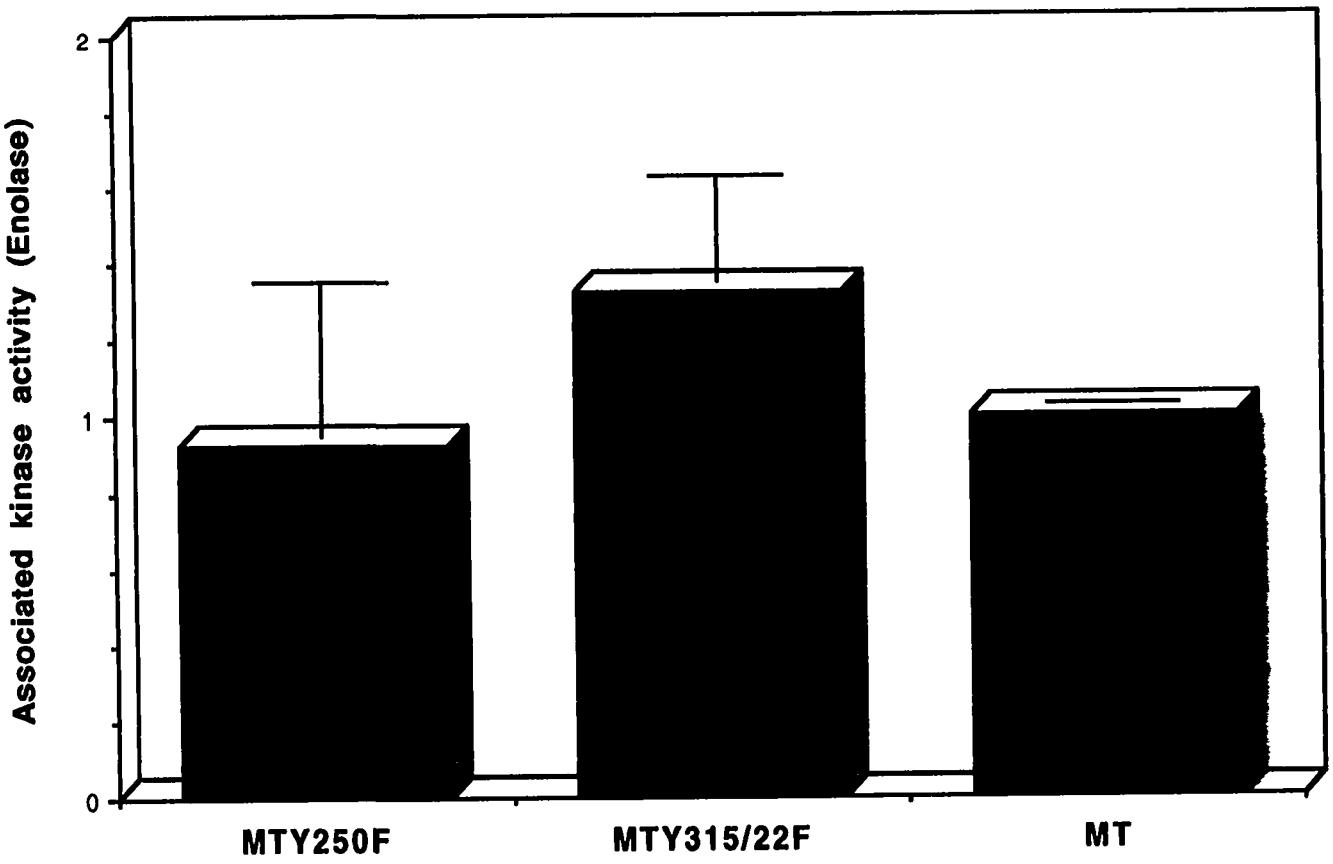
Associated kinase activity (Enolase)
2
1
0
MTY250F
MTY315/22F
MT

Figure 5.18 Reciprocal co-immunoprecipitation studies demonstrate the failure of MMTV/MT Y250F to bind to cellular SHC.

(A) SHC immunoblot analysis of MT-specific immunoprecipitates isolated from MMTV/MT (#702, #705), MMTV/MT Y250F (#1759, #8136, #8566), or MMTV/MT Y315/22F (#9591, #8672) mammary tumors. As a non-specific control, protein lysate derived from MMTV/Neu (#9560) mammary tumor was included. Shown is MT-associated 52 kDa SHC protein indicated by the arrow and SHC.

(B) PyV MT immunoblot analysis of SHC-specific immunoprecipitates isolated from MMTV/MT (#702, #705), MMTV/MT Y250F (#1759, #8136, #8566), or MMTV/MT Y315/22F (#9591, #8672) mammary tumors. As a non-specific control, mammary tumor protein lysate derived from mouse MMTV/Neu (#9560) was included. Shown is SHC-associated 56 kDa PyV MT protein indicated by the arrow and MT.

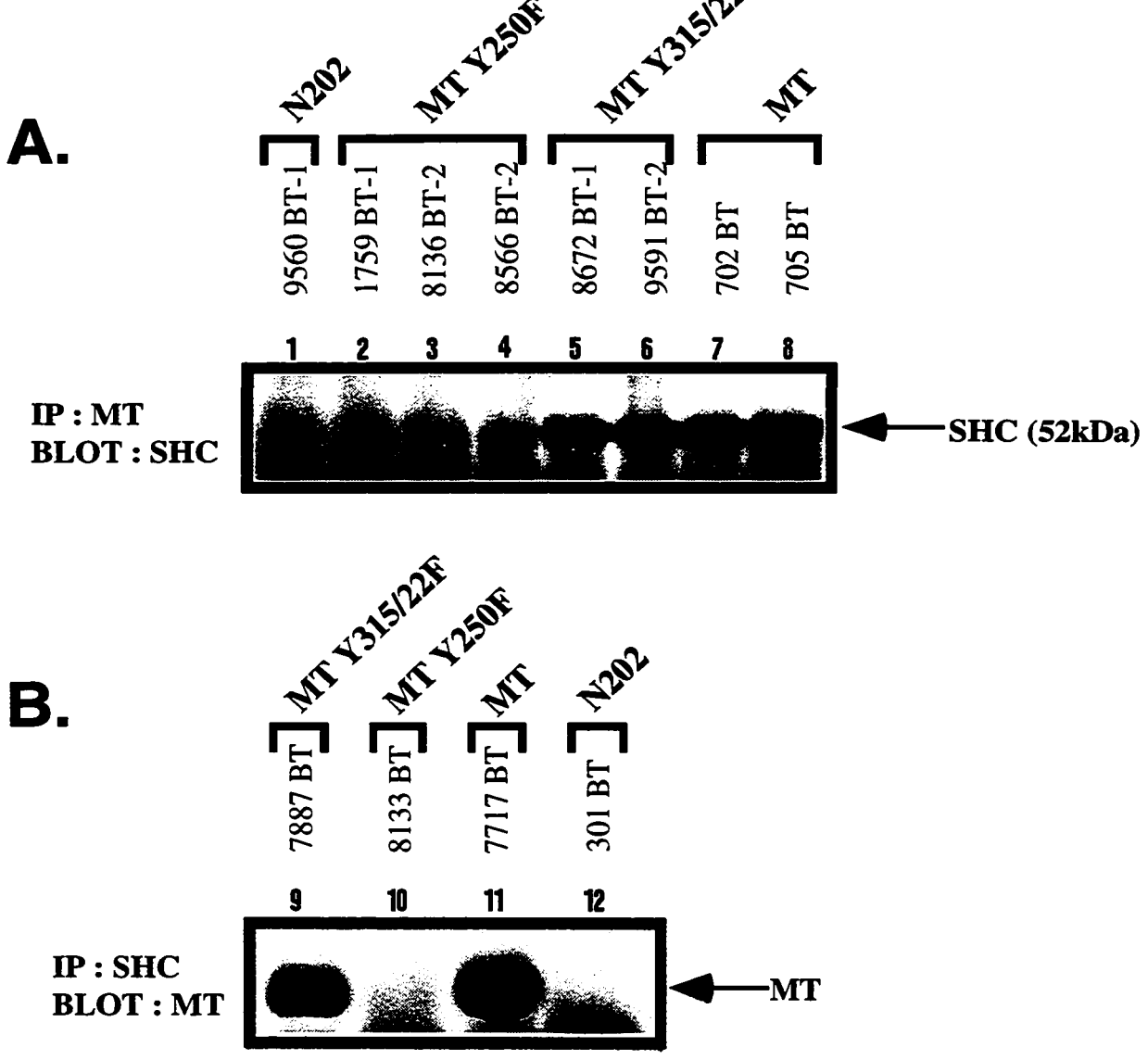
A.
N202
MT Y250F
MT Y315/22
MT
9560 BT-1
1759 BT-1
8136 BT-2
8566 BT-2
8672 BT-1
9591 BT-2
702 BT
705 BT
1 2 3 4 5 6 7 8
IP : MT
BLOT : SHC
SHC (52kDa)
B.
MT Y315/22F
MT Y250F
MT
N202
7887 BT
8133 BT
7717 BT
301 BT
9 10 11 12
IP : SHC
BLOT : MT
MT

from mammary tumors originating from wild-type MT or MT mutant mice. As seen in Figure 5.19 the PTB domain from SHC binds to MT Y315/22F (lanes 1 and 2) and wild-type MT (lanes 5 and 6) but failed to bind MT Y250F (lane3) or a non-specific immunoprecipitate from a Neu-induced mammary tumor (lane1). Re-probing of the same blot with MT-specific antibody pAB701 revealed that SHC association with MT occurs exclusively with the 56 kDa species (Figure 5.19B). In the course of these analyses, one of the MT Y250F tumor immunoprecipitates was observed to bind strongly to the GST SHC constructs (Figure 5.19, lane4). Because reversion to wild-type MT requires a single nucleotide substitution at site 250, we were interested to determine whether this particular tumor resulted from such an event. RNA isolated from this tumor in addition to other tumors from strain MT Y250F, MT Y315/22F and the parental MT strain, were reverse transcribed and the region of interest PCR amplified. Sequencing of the desired product revealed that mammary tumor #8442 BT-2 from strain MT Y250F (Figure 5.19, lane 4) had indeed reverted to its parental sequence, whereas, all other analyzed MT transcripts revealed no further somatic mutations.

Because somatic mutation and consequent reversion of the transgene was detected in at least one mammary tumor, we sought to design a method with which to screen large numbers of mammary tumors or lung metastases for potential reversion of the transgene to its parental isoform. To accomplish this, an RNase protection probe from wild-type MT spanning the region containing the mutations was created. RNase protection conditions were modified so as to allow the detection of single pyrimidine base pair mismatches or deletions (see Chapter 2). As shown in Figure 5.20, incubation of tumor RNA derived from the various mutants under these stringent RNase digestion conditions exhibited characteristic protected fragments reflective of cleavage at the mutated residues. Analyses of MT Y250F mammary tumors (n=56) demonstrated a low rate of reversion (n=2). In addition to the mammary tumor previously identified, one more of 56 tumors analyzed revealed the reversion to wild-type MT sequence. Interestingly, both of these mice had

Figure 5.19 Direct binding assay measuring the association of the SHC PTB domain with MT and MT mutants.

(A) Radiolabeled GSTag-PTB was used as a probe to detect MT-specific immunoprecipitates isolated from MMTV/MT (#170, #171), MMTV/MT Y250F (#8442, #8139), or MMTV/MT Y315/22F (#7881, #8672) mammary tumors. Twice as much protein lysate from MMTV/MT Y250F tumors was analyzed in this particular experiment to normalize the total levels of PyV MT. Shown is bound probe to a protein corresponding to the correct size of PyV MT indicated by the arrow and 56 kDa.

(B) Immunoblot analyses of control and PyV MT mammary tumors derived from MMTV/MT, MMTV/MT Y250F and MMTV/MT Y315/22F transgenic animals with a rat monoclonal PyV MT-specific antibody. Mammary tumor extracts derived from virgin MMTV/MT Y315/22F (#7888, #8672 BT-2), MMTV/MT Y250F (#8139, #8442) and MMTV/MT (#170, #171) were immunoprecipitated with a mouse monoclonal PyV MT-specific antibody. As a non-specific control, a MMTV/Neu-derived mammary tumor (#9573) was included. The 56 and 58 kDa PyV MT proteins are indicated by MT and the arrows.

Note that protein lysate MMTV/MT Y250F #8442 BT-2 (indicated by *) was subsequently shown to encode a somatic mutational event which reverts the phenylalanine residue at site 250 to the wild-type tyrosine residue.

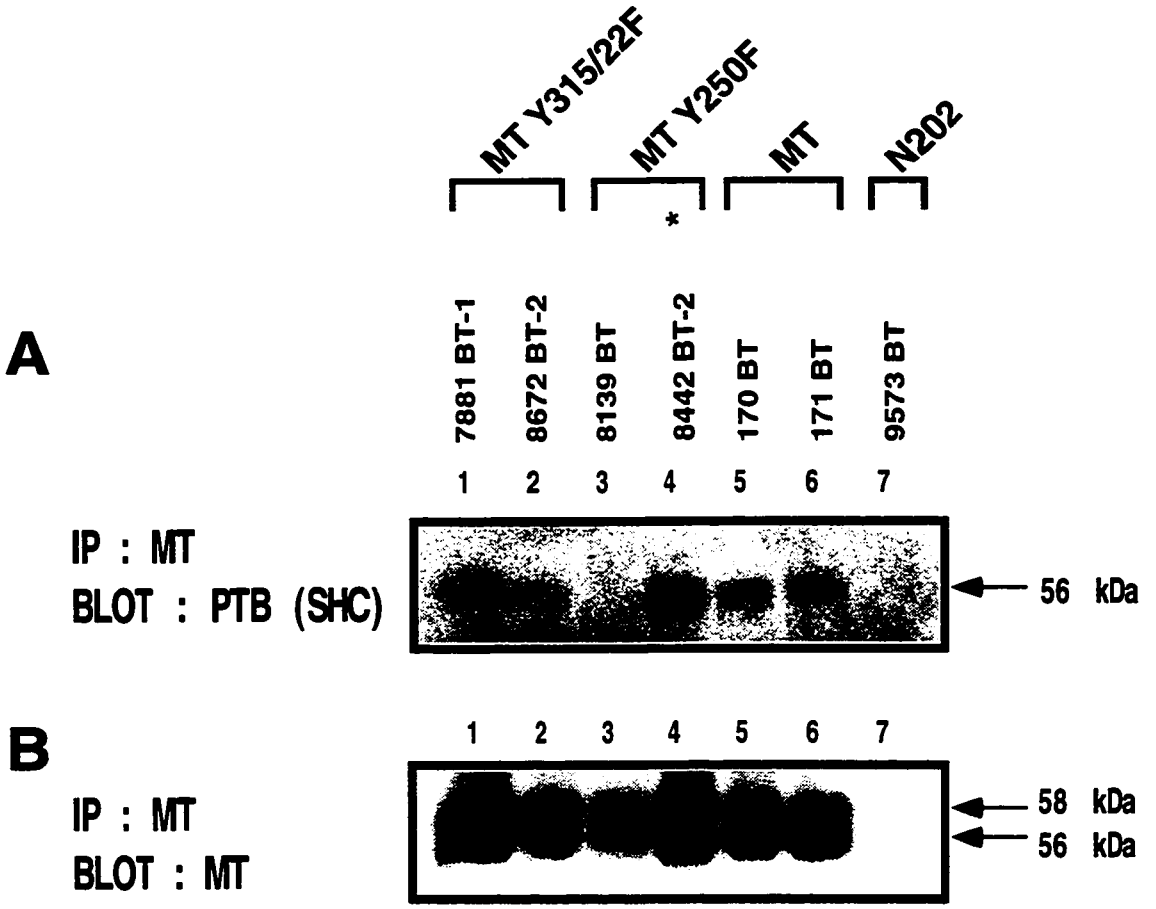
MT Y315/22F
MT Y250F
MT
N202
*
A
7881 BT-1
8672 BT-2
8139 BT
8442 BT-2
170 BT
171 BT
9573 BT
1 2 3 4 5 6 7
IP : MT
BLOT : PTB (SHC)
56 kDa
B
1 2 3 4 5 6 7
IP : MT
BLOT : MT
58 kDa
56 kDa

Figure 5.20 RNase protection analyses designed to detect single nucleotide differences between PyV MT transgenes.

(A) Representative results from RNase protection analyses using conditions to detect single nucleotide differences between PyV MT transgenes. Equal amounts of total cellular RNA isolated from MMTV/MT (#171), MMTV/MT Y250F (#8133), or MMTV/MT Y315/22F (#7888) mammary tumors were analyzed for PyV MT-specific transcript with riboprobe MTsn301 which recognizes nucleotides #529-#1036 of MT coding sequences. RNase protection pattern results correspond to individual transgenes as indicated by the arrows and corresponding transgene cDNA. Also included as controls are undigested full-length probe (lane 5) in addition to digested probe in the presence of non-specific tRNA (lane 4).

(B) Schematic representation of riboprobe protected fragments in various PyV MT transgenes. Mismatches are identified by a bend in the dashed line in addition to the arrows highlighting RNase sensitive sites.

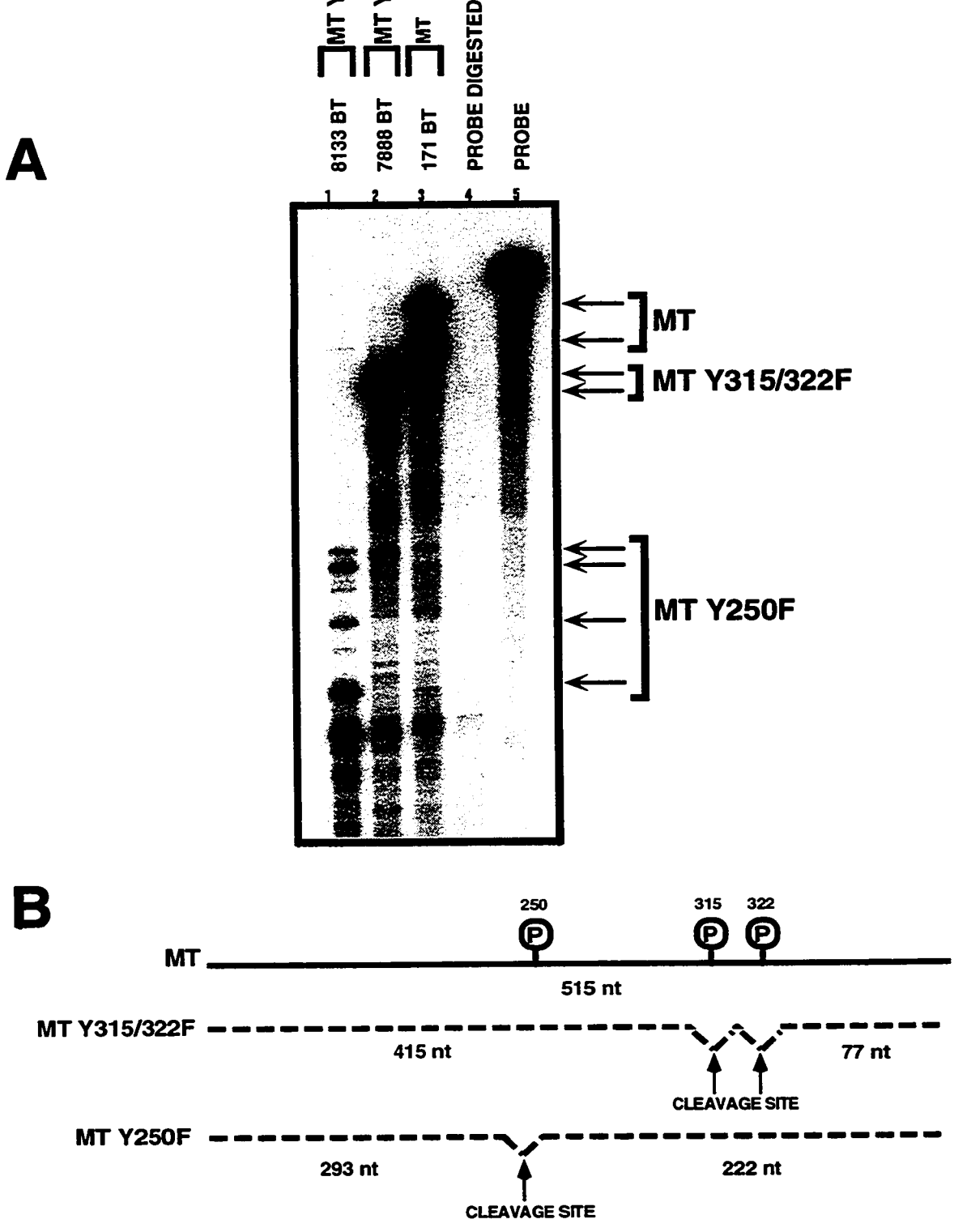
A
MT Y315/322F
MT
8133 BT
7888 BT
171 BT
PROBE DIGESTED
PROBE
1
2
3
4
5
MT
MT Y315/322F
MT Y250F
B
250
315
322
P
MT
515 nt
MT Y315/322F
415 nt
77 nt
CLEAVAGE SITE
MT Y250F
293 nt
222 nt
CLEAVAGE SITE

reversion event (Figure 5.21, lane 15, 16). The presence of reversion mutations in both lung metastases and mammary tumors was confirmed by sequencing reverse transcribed and PCR amplified product. Curiously, two mammary tumors from different animals gave identical patterns of protection which differed from the expected protected sizes (ie. Figure 5.21, lane 5). Furthermore, in one of these animals, lung metastases were evident and the RNase protection pattern of MT transcripts isolated from these metastases showed the same altered protection pattern (Figure 5.21, lane 13). Sequencing of RT PCR material from these malignancies revealed the presence of a small 18 nucleotide in frame deletion. The deletion removed the phenylalanine residue at position 250 in addition to 5 amino acids immediately downstream. The union of DNA following the deletion creates a tyrosine residue, and in so doing, regenerates the SHC binding core sequence 'NPTY' (Figure 5.22).

To test the possibility that this deletion facilitates SHC association, protein lysates from tumors expressing these altered MT proteins were immunoprecipitated with MT-specific antisera and immunoblotted for SHC. As is evident in Figure 5.23A (lanes 5 and 6), the MT deletion products were capable of associating with comparable levels of SHC as seen with wild-type MT from mammary tumors (compare lanes 5 and 6 with lanes 9 and 10). Moreover, immunoblot analyses of these extracts with PyV MT antisera revealed that the deletion resulted in a significant alteration of the electrophoretic mobility of the mutant PyV MT (Figure 5.23B, lanes 5 and 6). To further test the possibility that the MT deletion was responsible for the induction of the mammary tumor and subsequent pulmonary metastases *in vivo*, the corresponding deletion (dlMT) was engineered into a wild-type MT cDNA in mammalian expression cassette J4-Ω and assessed for its capacity to induce transformed foci in Rat-1 cells. To control for efficiency of transfection and possible lethality associated with expression of any cDNA, plasmid pSV2neo was co-transfected and cells selected for G418 resistance. Representative results from these analyses are shown in Table 5.4. The results revealed that dlMT mutant displayed a comparable transforming activity to

transgene.

(A) Various mammary tumors derived from strain MMTV/MT Y250F-5a screened for mismatches in the transgene. All tumors are derived from virgin tumor-bearing animals. Thirty micrograms of total cellular RNA was analyzed for MT-specific transcript utilizing riboprobe MTsn301. Indicated with arrows are expected protected sizes for wild-type MT (MT). and MT Y250F (MT Y250F) transgenes. Also indicated by arrows and dlMT are aberrant migrating species presumably resulting from a deletion in the transcript.

(B) RNase protection analyses demonstrating high somatic mutation frequency in lung metastases solely in MMTV/MT Y250F strains. Thirty micrograms of total cellular RNA derived from MMTV/MT Y250F (lanes 13-18) or MMTV/MT Y315/22F (lanes 19-22) animals demonstrating overt pulmonary metastases upon necropsy were analyzed for MT-specific transcript utilizing riboprobe MTsn301.Indicated with arrows are expected protected sizes for wild-type MT (MT). and MT Y250F (MT Y250F) transgenes. Also indicated by arrows and dlMT are aberrant migrating species presumably resulting from a deletion in the transcript.

Note reversion event resulting in wild-type MT RNase protection pattern (lanes 7, 15, 16). Sequence analysis of transcript from these tumors confirmed the presence of a phenylalanine to tyrosine residue substitution at site 250. Also note aberrant protected species in lanes 5 and 13. Sequence analyses revealed the presence of an 18 nucleotide in-frame deletion spanning site 250.

A

MAMMARY TUMORS

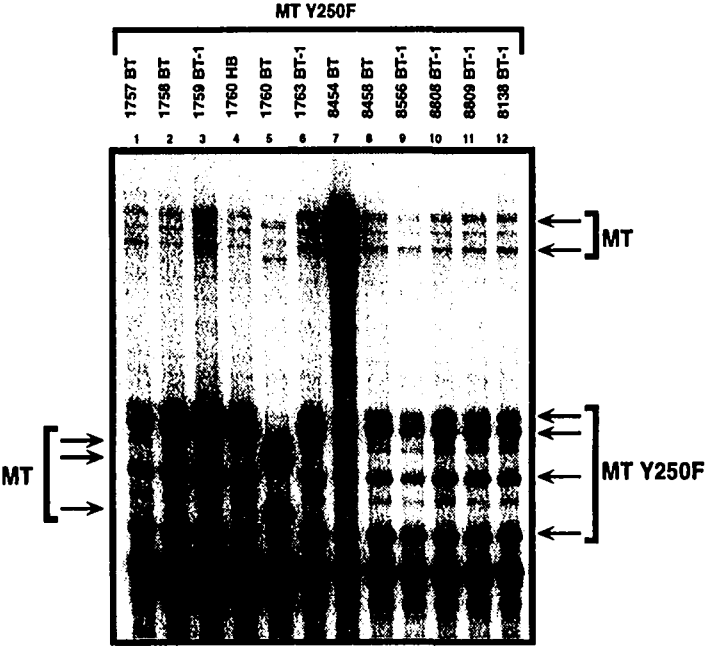

B

LUNG METASTASES

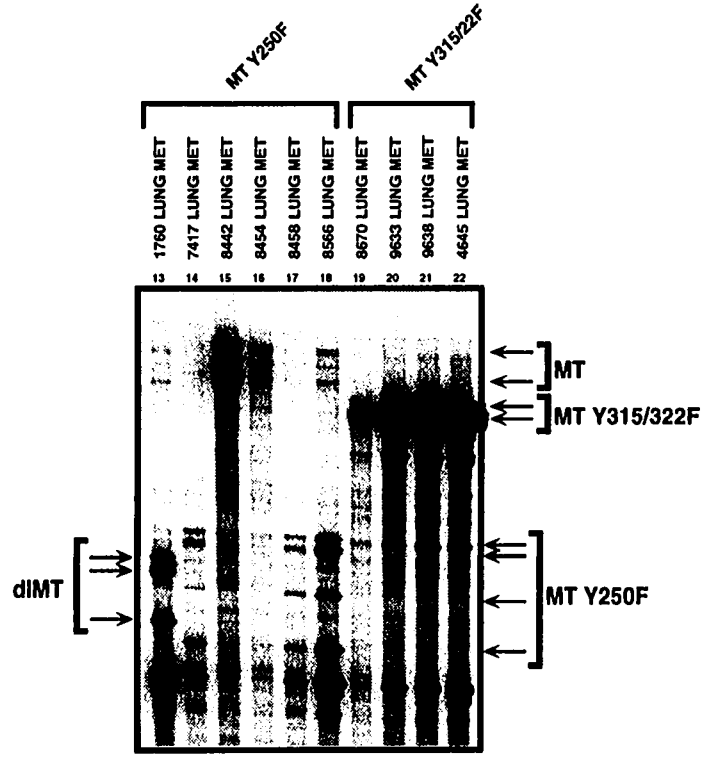

Figure 5.22 Lung metastases derived from MMTV/MT Y250F strains demonstrate a high frequency of somatic mutation within the transgene.

Sequence alignment showing nucleotides (730-783) of wild-type MT (WT MT) MT Y250F (MT Y250F) and a deletion mutant (7160 BT/LM) isolated from both a lung metastases and a mammary tumor. Also indicated are critical amino acid residues implicated in SHC and 14-3-3 binding. Destruction of the core binding sequence for either SHC or 14-3-3 is indicated by a strike out through the corresponding label. Intact core binding sequences which presumably mediate protein interaction are indicated without a strike through label. Also shown is the frequency with which the corresponding sequences are detected in mammary (BT) tumors or lung metastases (LM) derived from MMTV/MT Y250F strains.

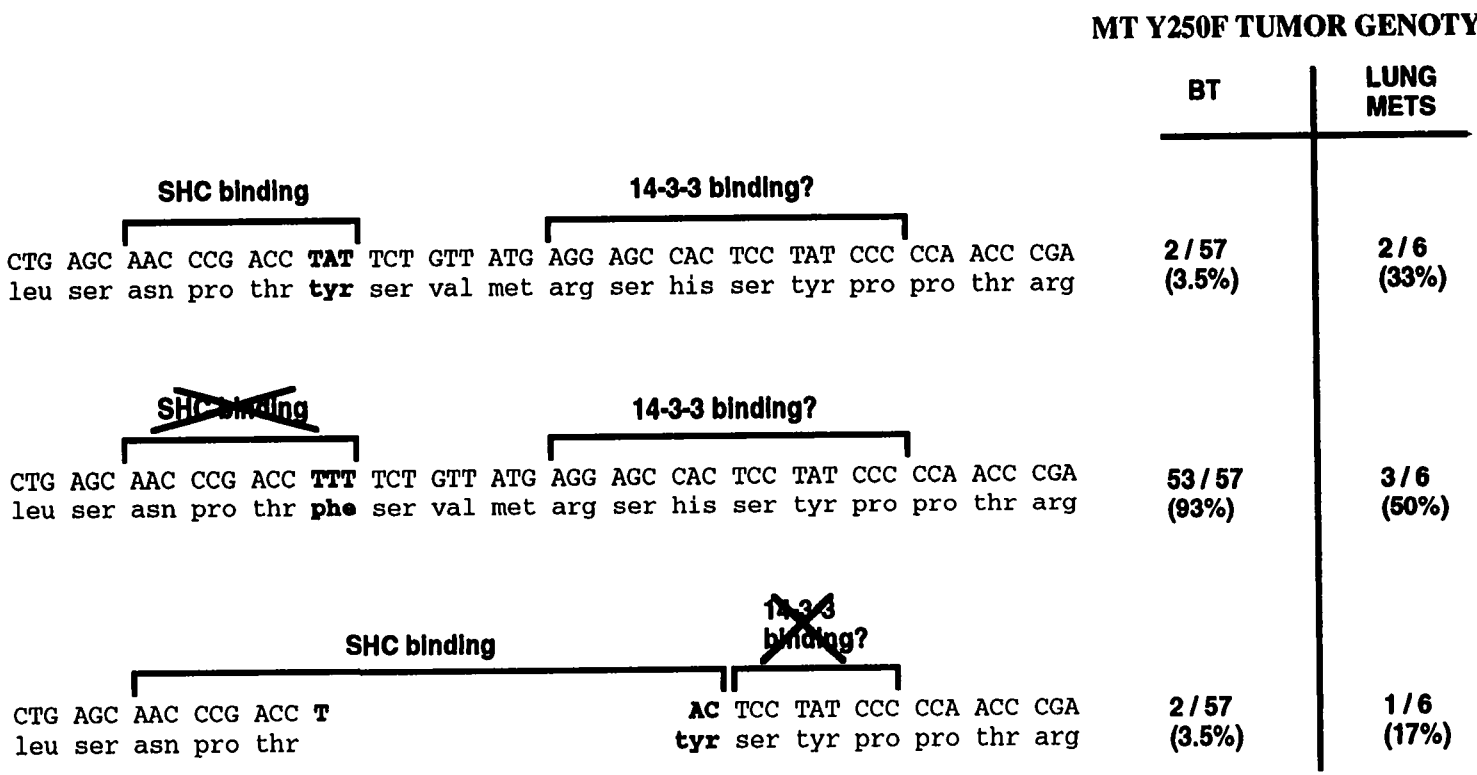
MT Y250F TUMOR GENOTYPES
BT
LUNG METS
SHC binding
14-3-3 binding?
CTG AGC AAC CCG ACC TAT TCT GTT ATG AGG AGC CAC TCC TAT CCC CCA ACC CGA
leu ser asn pro thr tyr ser val met arg ser his ser tyr pro pro thr arg
2 / 57 (3.5%)
2 / 6 (33%)
SHC binding
14-3-3 binding?
CTG AGC AAC CCG ACC TTT TCT GTT ATG AGG AGC CAC TCC TAT CCC CCA ACC CGA
leu ser asn pro thr phe ser val met arg ser his ser tyr pro pro thr arg
53 / 57 (93%)
3 / 6 (50%)
SHC binding
14-3-3 binding?
CTG AGC AAC CCG ACC T
leu ser asn pro thr
AC TCC TAT CCC CCA ACC CGA
tyr ser tyr pro pro thr arg
2 / 57 (3.5%)
1 / 6 (17%)

Figure 5.23 Deletion of nucleotides 746-763 in the MT Y250F cDNA restores SHC binding.

(A) SHC immunoblot analyses of MT immunoprecipitates derived from MMTV/MT (#702, #705), MMTV/MT Y250F (#1759, #8136 BT-2, #8566), or MMTV/MT Y315/22F (#8672, #9591) mammary tumors. Also analyzed are two MMTV/MT Y250F mammary tumors (#1760, #8136 BT-1) which reveal a deletion within the transgene. Non-specific protein lysate derived from a MMTV/Neu derived mammary tumor was also included. Indicated is the 52 kDa SHC species which interacts with immunoprecipitated MT/MT Y315/22/dlMT (lanes5-10) but not MT Y250F (lanes 2-3).

(B) MT immunoblot analyses of MT immunoprecipitates derived from MMTV/MT (#702, #705), MMTV/MT Y250F (#1759, #8136 BT-2, #8566), or MMTV/MT Y315/22F (#8672, #9591) mammary tumors. Non-specific protein lysate derived from a MMTV/Neu derived mammary tumor was also included. Indicated with arrows and MT or dlMT are PyV MT protein products.

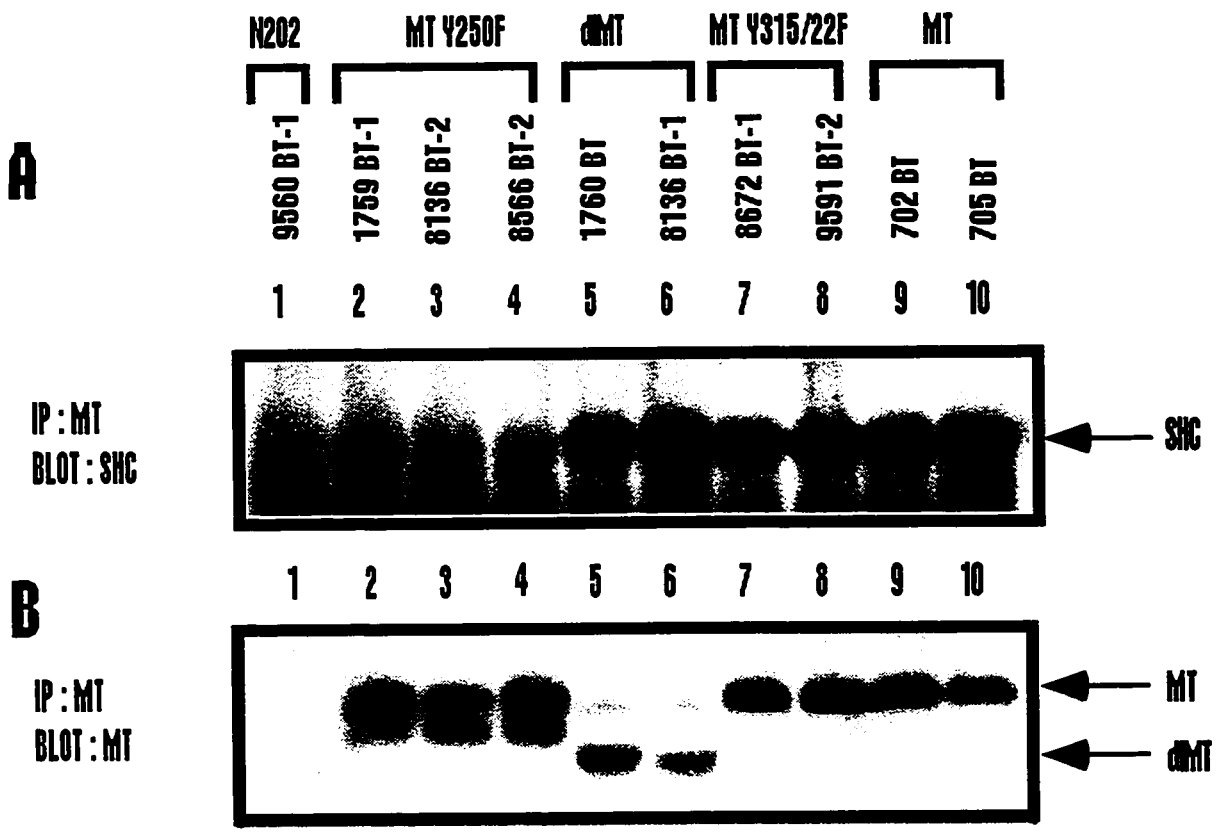
N202
MT Y250F
dMT
MT Y315/22F
MT
9560 BT-1
1759 BT-1
8136 BT-2
8566 BT-2
1760 BT
8136 BT-1
8672 BT-1
9591 BT-2
702 BT
705 BT
1 2 3 4 5 6 7 8 9 10
A
IP : MT
BLOT : SHC
SHC
1 2 3 4 5 6 7 8 9 10
B
IP : MT
BLOT : MT
MT
dMT

Table 5.4 Transformation potential of dlMT, wild-type PyV MT, and PyV MT mutants in Rat-1 cells.

Established fibroblast cell line Rat-1 was used to assess the *in vitro* transforming properties of PyV MT and PyV MT mutants. MoMLV expression cassettes harboring the MT cDNAs (or empty vector alone) were electroporated into Rat-1 cells following which monolayers were analyzed for focus formation after 14 days.

TABLE 5.4. Transformation of Rat-1 cells [a]

ession id	Focus assay 1 [b] Average no. of foci [f]	Average no. of G418 colonies [g]	% Transformation of pJ4ΩMT [h]	Focus assay 2 [c] Average no. of foci [f]	Average no. of G418 colonies [g]	% Transformation of pJ4ΩMT [h]
	0	85±6	0	0	85±6	0
MT Y250F	3±1	85±9	2.8	2±1	85±9	5
MT Y315/22F	8±4	89±15	6.7	3±1	89±15	8.1
dlMT	77±6	71±4	78.1	32±4	71±4	106.1
MT	106±7	77±6	100	32±3	77±6	100

ession id	Focus assay 3 [d] Average no. of foci [f]	Average no. of G418 colonies [g]	% Transformation of pJ4Ω MT [h]	Focus assay 4 [e] Average no. of foci [f]	Average no. of G418 colonies [g]	% Transformation of pJ4ΩMT [h]
	0	347±11	0	0	347±11	0
MT Y250F	22±4	157±1	6.9	34±2	157±1	8.1
MT Y315/22F	43±5	182±9	11.6	47±2	182±9	9.8
dlMT	471±14	244±10	95.9	822±19	244±10	119
MT	487±22	242±8	100	825±44	242±8	100

tive transforming ability [i]	
Ω	0.0
ΩMT Y250F	5.7
ΩMT Y315/22F	9.1
ΩdlMT	99.7
ΩMT	100.0

Four independent focus assays were performed with Rat-1 fibroblasts. All transfections performed with CsCl purified DNA preparations. MT and all mutant MT cDNAs inserted into plasmid pJ4Ω under transcriptional control of the Moloney murine leukemia virus s long terminal repeat. pJ4Ω represents parent empty vector used for mock transfections. Two plates from each transfection were treated with 40 ug/ml G418. All plates fixed in 10% phosphate buffered formalin and stained with Giemsa 14 days following transfection.

[b] pJ4Ω plasmid concentration per 100 mm plate is 500ng. pSV2neo plasmid concentration is 50ng per 100 mm plate. 20 ug salmon sperm per 100mm plate

[c] pJ4Ω plasmid concentration per 100 mm plate is 100ng. pSV2neo plasmid concentration is 50ng per 100 mm plate. 20 ug salmon sperm per 100mm plate

[d] pJ4Ω plasmid concentration per 100 mm plate is 500ng. pSV2neo plasmid concentration is 50ng per 100 mm plate.

[e] pJ4Ω plasmid concentration per 100 mm plate is 750ng. pSV2neo plasmid concentration is 50ng per 100 mm plate.

[f] Values are the mean numbers of foci counted on four plates ± the standard error

[g] Values are the mean number of G418 resistant colonies counted from 2 plates ± the standard error.

[h] Values represent the ratio of foci obtained for each construct with respect to wild-type MT (pJ4Ω MT) normalized to the number of G418 resistant colonies obtained per transfection ± the standard error.

[i] Values represent the mean transforming efficiencies over four transfections normalized to the number of G418 resistant colonies obtained per transfection ± the standard error.

were able to efficiently transform Rat-1 cells. Taken together, these data argue that the deletion has restored both SHC binding and further suggests that recruitment of SHC is strongly selected for in the induction of metastases. This is underscored by the observation that 50% of the metastatic tumors analyzed from MT Y250F animals contain somatic mutations which restore the NPTY motif facilitating SHC interaction (Figure 5.22).

5.2.8. Analyses of PyV MT associated PI-3' kinase activity in tissues expressing the middle T mutants.

Because analyses of stable Rat-1 cell lines expressing the PyV MT mutants suggested that binding of the 85 kDa subunit of PI3'K was affected in both PyV MT mutants, we measured the levels of PyV MT associated PI-3' kinase activities from tumor tissues derived from transgenic mice expressing either mutant PyV MT antigen. To accomplish this, PyV MT immunoprecipitates were incubated with bovine PI in the presence of γ-^{32}P-ATP, following which lipids were extracted and levels of PI-P were measured by TLC (Figure 5.24A). To control for the variable levels of PyV MT, parallel MT-specific ^{125}I immunoblots were conducted on these samples (Figure 5.24B). and PI3'K activities were normalized to the levels of PyV MT protein. As expected the levels of PyV MT-associated PI3'K from MT Y315/22F tissues was significantly reduced compared to levels exhibited by wild type MT tumors (30%±10%, Figure 5.25). However, measurement of the levels of PI-3' kinase activity in MT Y250F tumors revealed that these tumors also possessed reduced levels compared to tumors expressing wild-type PyV MT antigen (63% ±26%, Figure 5.25). Nonetheless, phosphoinositol 3-kinase levels exhibited by the MT Y250F tumors were elevated in comparison to those exhibited by the MT Y315/322F tumors. Taken together, these data argue that mutation of tyrosines 250 or 315/22 affects PyV MT PI3'K activity *in vitro*, albeit, to different extents.

To assess whether the levels of PI-3' kinase activity in these tumors correlates with the capacity of PyV MT to complex the p85 subunit of PI3'K, tumor extracts were subjected to

Figure 5.24 Phosphatidylinositol 3-kinase activities associated with wild-type MT, MT Y250F or MT Y315/22F protein complexes.

Thin layer chromatography of P^{32} phosphorylated lipid products. Equal amounts of protein lysate from MMTV/MT (#7717, #8159), MMTV/MT Y250F (#7698, #8133), or MMTV/MT Y315/22F (#7890, #7887) mammary tumors were immunoprecipitated for MT using antisera specific for PyV MT. Immune complexes were incubated with bovine phosphoinositol following which, lipid product were extracted and analyzed as shown. Indicated is the origin (ORI), and positions corresponding to migration of mono- (PIP) or dual phosphorylated lipid products (PIP2). Non-specific protein lysate derived from a MMTV/Neu derived mammary tumor (#301) was also included.

Note: the phosphorylated lipid product in the non-specific control lane (lane 7) was seen repeatedly in different control lysates. When phosphatidylinositol 3-kinase activities of MT and MT mutants was quantitated, control lipid kinase levels were subtracted from the obtained MT values.

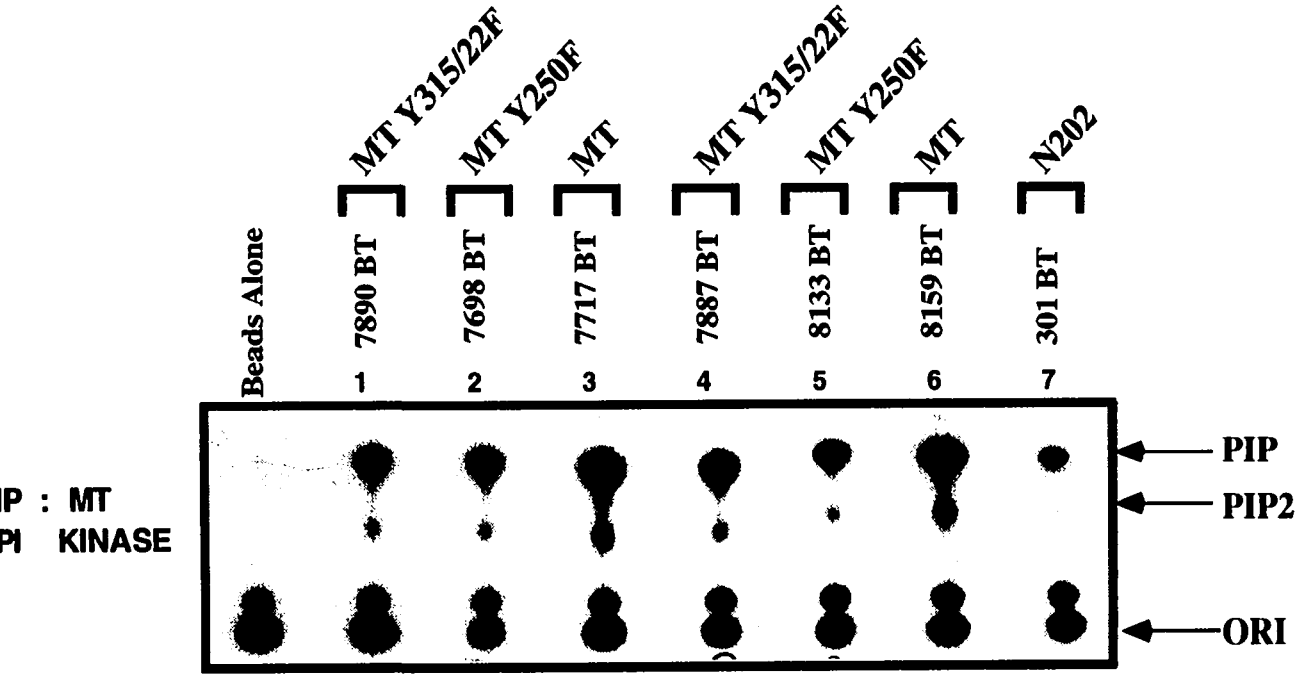
MT Y315/22F
MT Y250F
MT
MT Y315/22F
MT Y250F
MT
N202
Beads Alone
7890 BT
7698 BT
7717 BT
7887 BT
8133 BT
8159 BT
301 BT
1
2
3
4
5
6
7
PIP
PIP2
ORI
IP : MT
PI KINASE

Figure 5.25 MT mutant associated phosphatidylinositol 3-kinase activities are reduced in comparison to wild-type MT

This bar graph represents the mean relative associated lipid kinase activity (measured through phosphoinositol phosphorylation) of MMTV/MT Y250F and MMTV/MT Y315/22F tumors with respect to MMTV/MT-induced mammary tumors (± mean of standard error (error bars)) averaged over five independent experiments analyzing a total of ten independently arising tumors from each strain.

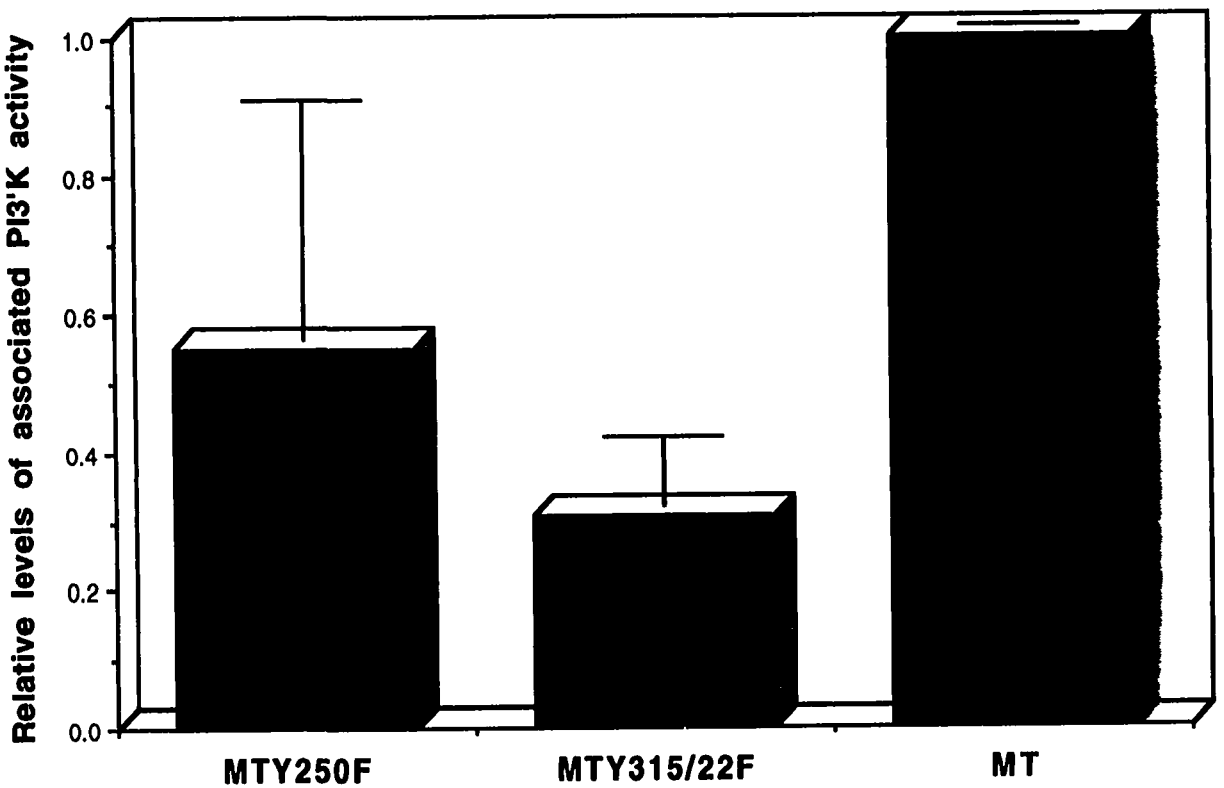
Relative levels of associated PI3'K activity
1.0
0.8
0.6
0.4
0.2
0.0
MTY250F
MTY315/22F
MT

antibodies specific to the PI-3' kinase p85 regulatory subunit. Results of these analyses revealed that the 85 kDa PI-3' kinase subunit could be detected in PyV MT immunoprecipitates (Figure 5.26A lanes 7 and 8). The converse experiment (immunoprecipitation of p85 followed by a MT immunoblot) revealed the presence of the 56 kDa MT protein (Figure 5.26B, lane 11). By contrast, similar analyses on MT Y315/322F tumor lysates demonstrated greatly reduced levels of PyV MT/p85 kDa complexes (Figure 5.26 A and B lanes 5, 6 and 9). Analyses of tumor lysates derived from MT Y250F animals revealed weak binding of the p85 subunit with the mutant PyV MT protein (Figure 5.26 A and B lanes 2-4 and 10).

Given that the reported p85 binding site (Y315 and Y322) is unaltered in MT Y250F, it seems paradoxical that the associated p85 subunit and corresponding PI3'K activity should be affected. To further examine the ability of the p85 subunit to bind these mutant PyV MT proteins, we tested the ability of recombinant GST-p85 to bind MT isolated from various MT and MT mutant tumor lysates in a direct blot assay as described in section 5.2.2. As expected, recombinant GST-p85 failed to bind to any appreciable extent with MT Y315/22F, while binding was readily detected in MT isolated from wild-type MT induced tumors. Lower levels of binding was seen in MT Y250F immunoprecipitates (with noted exception of tumor #8442 BT-2 which revealed equivalent binding when compared to wild-type MT immunoprecipitates (Figure 5.27, lane 4)(see below for further discussion)). PhosphorImager quantitation of bound probe when normalized to levels of MT (as determined by ^{125}I MT immunoblotting) demonstrated, on average, a 54.7% reduction in the amount of p85 bound to MT Y250F as compared to parental MT (excluding the reversion mutant #8442 BT-2). Similar analyses with MT Y315/22F immunoprecipitates exhibited a 95.4% decrease in the ability of GST-p85 to bind. Taken together, these data suggest that the *in vitro* levels of PyV MT associated PI-3' kinase activity in tumor lysates correlates with the capacity of MT molecules to associate with the p85 regulatory subunit of PI3'K.

While MT Y250F appears less able to bind p85 *in vitro*, one particular mammary tumor from this strain (#8442 BT-2) appears to have comparable associated *in vitro* lipid kinase activity

Figure 5.26 Reciprocal co-immunoprecipitation studies demonstrate altered binding affinities of MT mutants for the regulatory subunit of phosphatidylinositol 3-kinase

(A) p85 immunoblot analysis of MT-specific immunoprecipitates isolated from MMTV/MT (#702, #705), MMTV/MT Y250F (#1759, #8136, #8566), or MMTV/MT Y315/22F (#9591, #8672) mammary tumors. As a non-specific control, protein lysate derived from MMTV/Neu (#9560) mammary tumor was included. Shown is the MT-associated p85 protein of PI3'K indicated by the arrow and p85.

(B) PyV MT immunoblot analysis of p85-specific immunoprecipitates isolated from MMTV/MT (#7717), MMTV/MT Y250F (#8133), or MMTV/MT Y315/22F (#7887) mammary tumors. As a non-specific control, mammary tumor protein lysate derived from mouse MMTV/Neu (#301) was included. Shown is p85-associated 56 kDa PyV MT protein indicated by the arrow and MT.

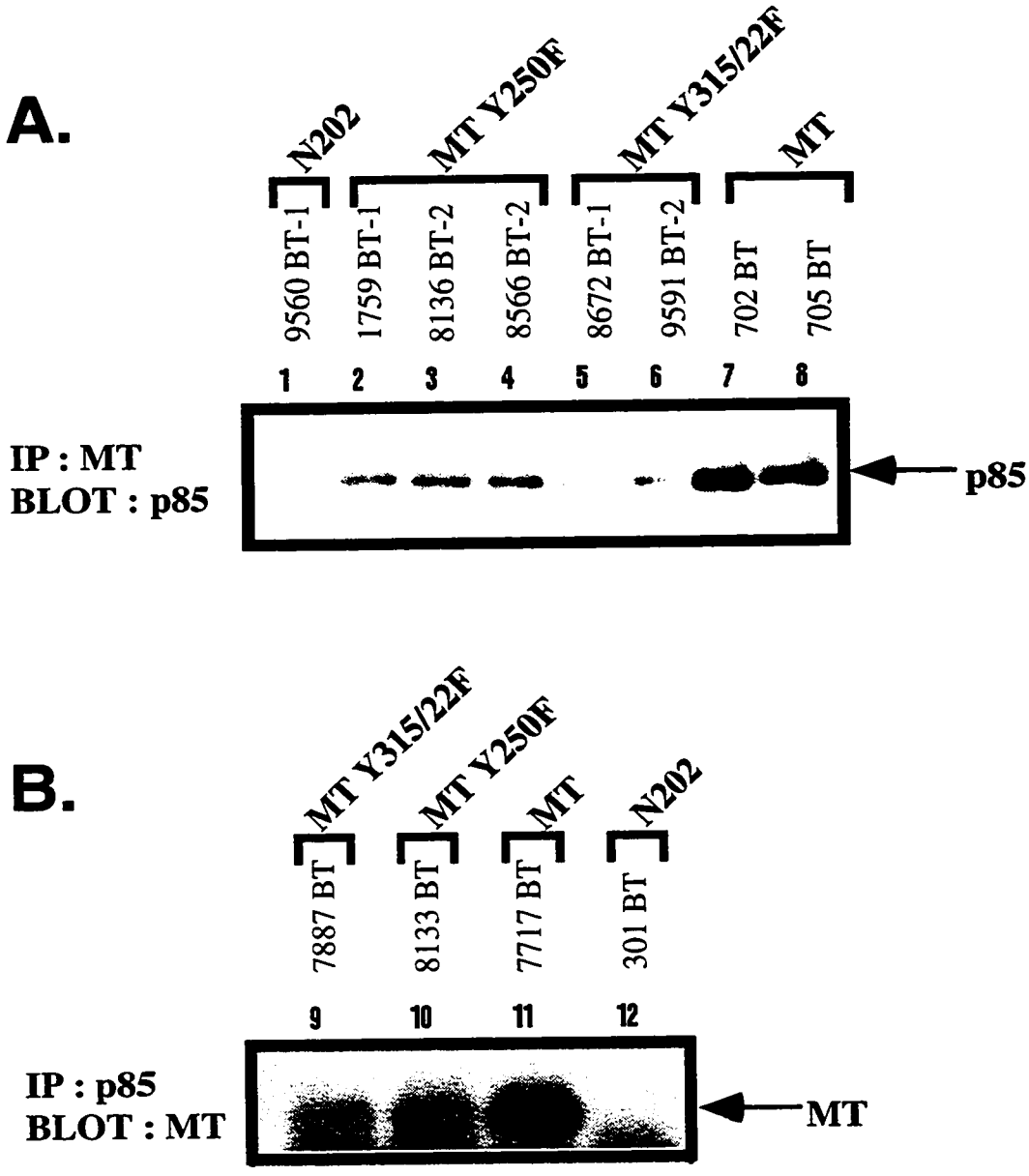
A.
N202
MT Y250F
MT Y315/22F
MT
9560 BT-1
1759 BT-1
8136 BT-2
8566 BT-2
8672 BT-1
9591 BT-2
702 BT
705 BT
1
2
3
4
5
6
7
8
IP : MT
BLOT : p85
p85
B.
MT Y315/22F
MT Y250F
MT
N202
7887 BT
8133 BT
7717 BT
301 BT
9
10
11
12
IP : p85
BLOT : MT
MT

Figure 5.27 MT Y315/22F and MT Y250F mutants demonstrate weakened affinity for p85 SH2 domains in comparison to wild-type MT in a direct binding assay

(A) Recombinant P32 labeled GSTag/p85 protein was used to probe MT-specific immunoprecipitates MMTV/MT (lanes 13-18), MMTV/MT Y250F (lanes 1-6), or MMTV/MT Y315/22F (lanes 7-12) mammary tumors. Bound probe corresponded to the 56 kDa MT protein as indicated by the arrow and 56kDa MT.

(B) Levels of immunoprecipitated MT protein. MT-specific antibody was used to immunoprecipitate MT from MMTV/MT (lanes 13-18), MMTV/MT Y250F (lanes 1-6), or MMTV/MT Y315/22F (lanes 7-12) mammary tumors. Shown are the 56 and 58 kDa MT species.

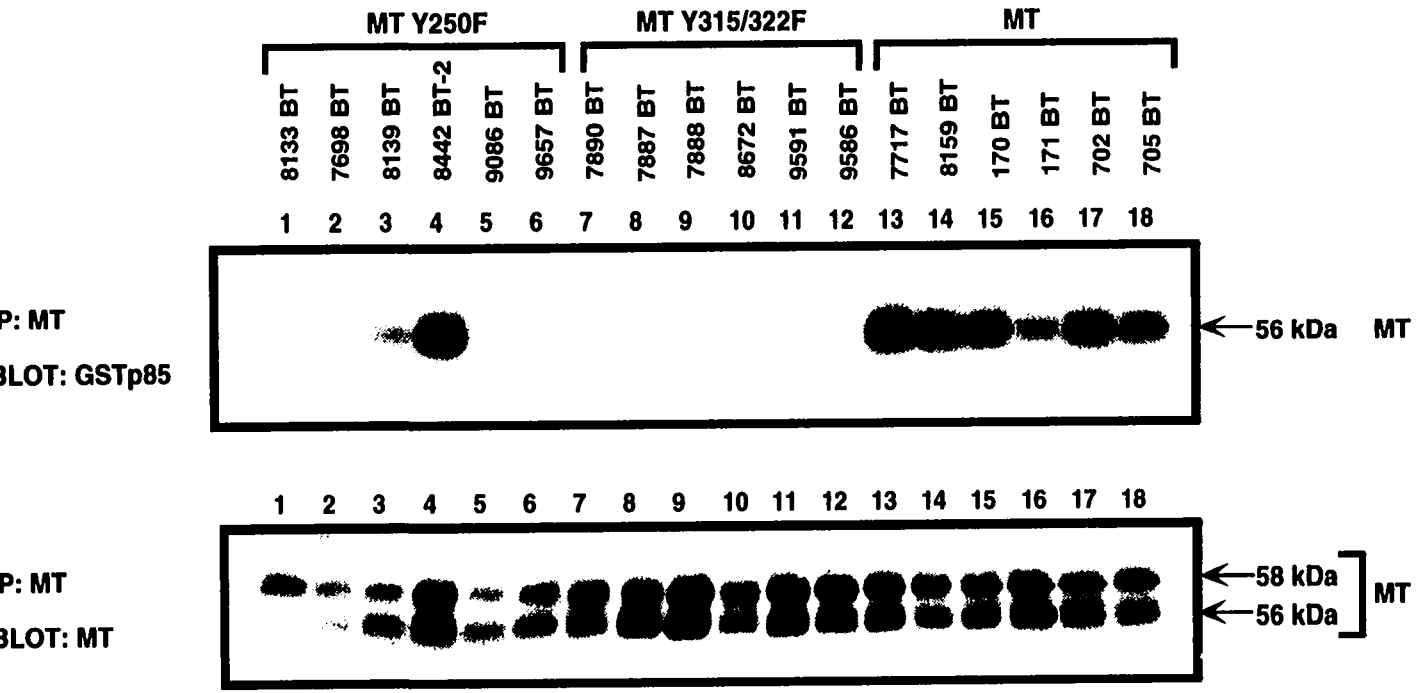
MT Y250F
MT Y315/322F
MT
8133 BT
7698 BT
8139 BT
8442 BT-2
9086 BT
9657 BT
7890 BT
7887 BT
7888 BT
8672 BT
9591 BT
9586 BT
7717 BT
8159 BT
170 BT
171 BT
702 BT
705 BT
1 2 3 4 5 6 7 8 9 10 11 12 13 14 15 16 17 18
P: MT
BLOT: GSTp85
56 kDa
MT
1 2 3 4 5 6 7 8 9 10 11 12 13 14 15 16 17 18
P: MT
BLOT: MT
58 kDa
56 kDa
MT

PI3'K. Indeed this tumor appears to contain the reversion event at tyrosine 250 (see Section 5.2.7.). To ascertain whether SHC binding facilitated p85 association, I also tested the dlMT mutation for its capacity to associate with p85 (Figure 5.28). Consistent with the reversion point mutant, the deletion MT mutant also demonstrated enhanced binding of p85. Therefore, these data argue that SHC binding influences the capacity of p85 to bind the mutant PyV MT molecule at least *in vitro*.

5.2.9. PLC-γ is not detected in PyV MT complexes

Although the data generated thus far suggest that the phenotype exhibited by MT Y315/22F is due to the decoupling of PI3'K from PyV MT, it is also conceivable that other SH2-containing signaling molecules may be affected by mutation at these sites. Indeed, it has recently been demonstrated that tyrosine residue 322 may be involved in binding PLC-γ *in vitro* (Su et al., 1995). However, other laboratories have been unable to reproduce this observation (Brizuela et al., 1995). Given these conflicting observations, I attempted to assess whether complexes of PLC-γ and PyV MT could be detected in tumor extracts from either mutant or wild-type PyV MT mice. Immunoprecipitation analyses with PLC-γ antisera failed to reveal co-immunoprecipitated PyV MT in tumors derived from either mutant or wild-type MT mice (Figure 5.29). Although I cannot formally preclude weak interaction between PyV MT and PLC-γ, these results argue that the observed mammary phenotype is primarily due to inactivation of the PI3'K pathway.

5.2.10. Expression and activation of ERK related kinases in tumor tissues derived from the mutant PyV MT strains

Because PyV MT is known to signal through the Ras pathway (Jelinek & Hassell, 1992), it was of interest to examine the expression of potential downstream Ras targets including members of the MAP kinase pathway in mammary tissues derived from the various mutant MT

Figure 5.28 Deletion of nucleotides 746-763 in the MT Y250F cDNA restores wild--type levels of p85 binding.

(A) p85 immunoblot analyses of MT immunoprecipitates derived from MMTV/MT (#702, #705), MMTV/MT Y250F (#1759, #8136 BT-2, #8566), or MMTV/MT Y315/22F (#8672, #9591) mammary tumors. Also analyzed are two MMTV/MT Y250F mammary tumors (#1760, #8136 BT-1) which reveal a deletion within the transgene. Non-specific protein lysate derived from a MMTV/Neu derived mammary tumor was also included. Indicated is the p85 PI3'K regulatory subunit

(B) MT immunoblot analyses of MT immunoprecipitates derived from MMTV/MT (#702, #705), MMTV/MT Y250F (#1759, #8136 BT-2, #8566), or MMTV/MT Y315/22F (#8672, #9591) mammary tumors. Non-specific protein lysate derived from a MMTV/Neu derived mammary tumor was also included. Indicated with arrows and MT or dlMT are PyV MT protein products.

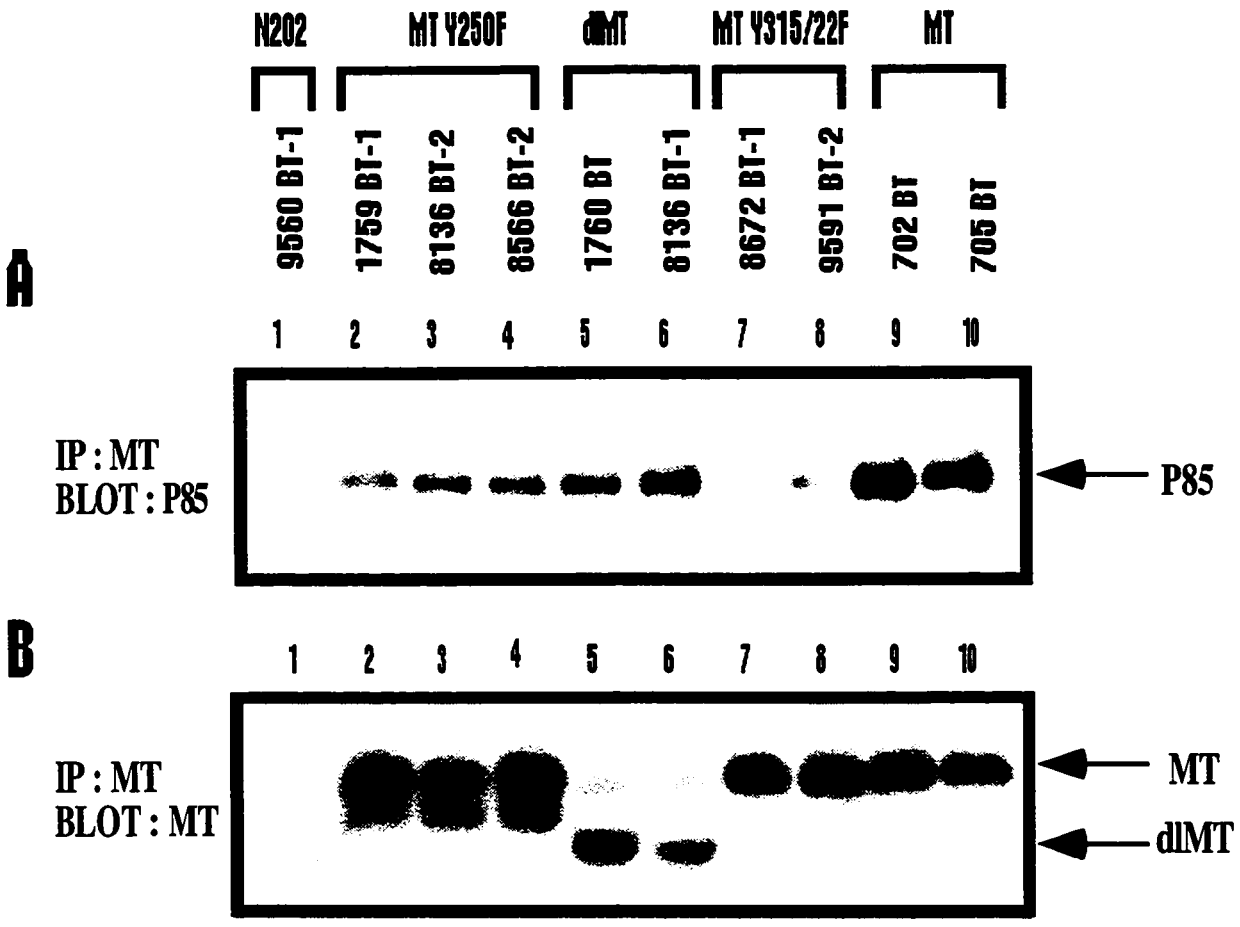
N202
MT Y250F
dlMT
MT Y315/22F
MT
9560 BT-1
1759 BT-1
8136 BT-2
8566 BT-2
1760 BT
8136 BT-1
8672 BT-1
9591 BT-2
702 BT
705 BT
A
1 2 3 4 5 6 7 8 9 10
IP : MT
BLOT : P85
P85
B
1 2 3 4 5 6 7 8 9 10
IP : MT
BLOT : MT
MT
dlMT

Figure 5.29 Co-immunoprecipitation analyses fail to detect MT: PLC-γ complexes.

Immunoblot analyses of PLC-γ immunoprecipitates derived from MMTV/MT (#7717), MMTV/MT Y250F (#8133), or MMTV/MT Y315/22F (#7887) mammary tumors. Non-specific protein lysate derived from a MMTV/Neu derived mammary tumor (#301) was also included. Indicated with the arrow and 56 kDa T is the expected size PyV MT protein products should migrate.

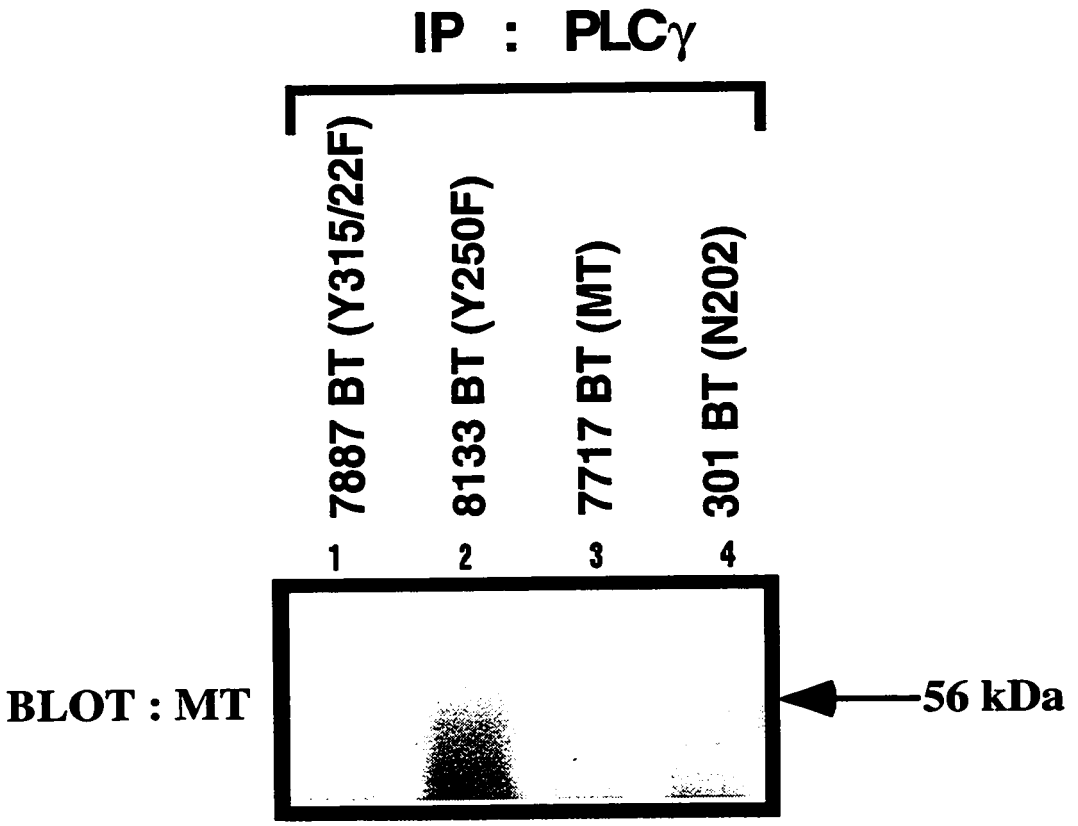
IP : PLCγ
7887 BT (Y315/22F)
8133 BT (Y250F)
7717 BT (MT)
301 BT (N202)
1
2
3
4
BLOT : MT
56 kDa

Figure 5.30 Mitogen activated protein kinases in mammary hyperplasias and tumors derived from MMTV/MT, MMTV/MT Y250F and MMTV/MT Y315/22F transgenic mice.

(A) Immunoblot analyses of Erk1 and ERK 2 from total protein lysate derived from: eight week-old mammary glands (MMTV/MT (lanes 8, 16), MMTV/MT Y250F (lanes 2,10), or MMTV/MT Y315/22F (lanes 5, 13)); day 1 post-parturition mammary glands (MMTV/MT Y250F (lanes 3,11), or MMTV/MT Y315/22F (lanes 6,14)) ; and mammary tumors (MMTV/MT (lanes 9,17), MMTV/MT Y250F (lanes 4,12), or MMTV/MT Y315/22F (lanes 7,15)). Also included was a mammary tumor derived from a MMTV/Neu animal (lane 1) for comparison. Indicated by the arrows are the products of Erk1 and Erk2.

(B) Identical lysates immunoblotted with antisera specific for tyrosine phosphorylated Erk1 and ERK-2. Indicated by the arrows are the products of Erk1 and Erk2.

(C) Immunoblot analyses identical to (A) revealed the presence of an ERK-related 85 kDa species which correlates with mammary tumor formation and aggressive hyperplasias in MMTV/MT Y250F strains. Indicated by the arrow is the 85 kDa ERK-related protein.

(D) Immunoblot analyses of MT-immunoprecipitates from identical protein lysates. Indicated by the arrows and size designations (56kDa, 58kDa) are the products of the MT protein.

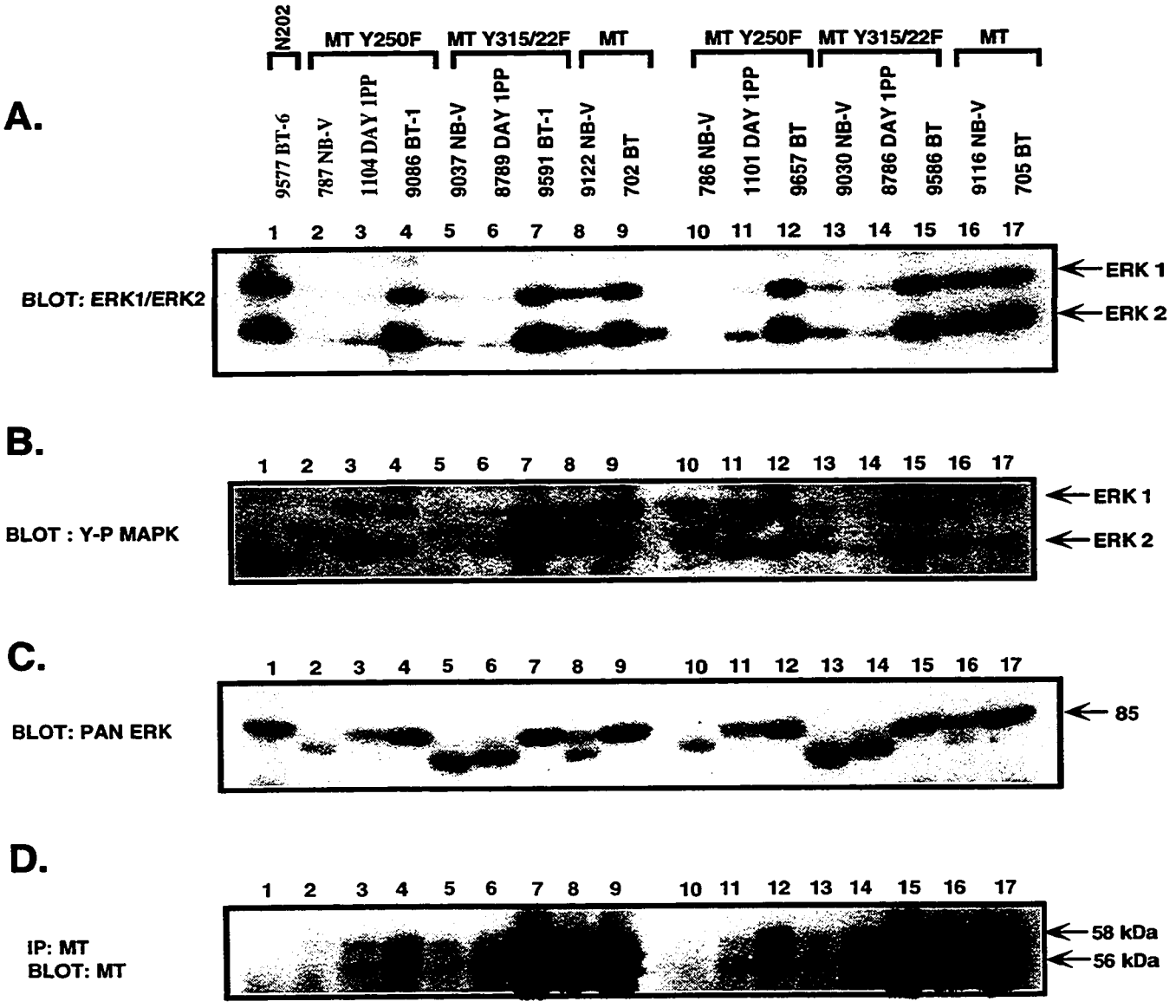
A.
N202
MT Y250F
MT Y315/22F
MT
MT Y250F
MT Y315/22F
MT
9577 BT-6
787 NB-V
1104 DAY 1PP
9086 BT-1
9037 NB-V
8789 DAY 1PP
9591 BT-1
9122 NB-V
702 BT
786 NB-V
1101 DAY 1PP
9657 BT
9030 NB-V
8786 DAY 1PP
9586 BT
9116 NB-V
705 BT
1 2 3 4 5 6 7 8 9 10 11 12 13 14 15 16 17
BLOT: ERK1/ERK2
ERK 1
ERK 2
B.
1 2 3 4 5 6 7 8 9 10 11 12 13 14 15 16 17
BLOT : Y-P MAPK
ERK 1
ERK 2
C.
1 2 3 4 5 6 7 8 9 10 11 12 13 14 15 16 17
BLOT: PAN ERK
85
D.
1 2 3 4 5 6 7 8 9 10 11 12 13 14 15 16 17
IP: MT
BLOT: MT
58 kDa
56 kDa

tumor tissue by immunoblot analyses utilizing a pan-ERK antibody (Figure 5.30A). Because tyrosine phosphorylation of ERK family members is essential for activation (Waskiewicz & Cooper, 1995), I also measured their state of tyrosine phosphorylation by employing an antibody that specifically recognizes tyrosine phosphorylated forms of Erk1/2 (Figure 5.30B). The results showed that the levels and activity of ERK expression were elevated in tumor tissues from all MT and mutant MT strains by comparison to hyperplastic mammary tissues derived from either MT mutant (compare Figure 5.30 A and B lanes 4, 7, 9, 12, 15, 17 with lanes 2, 5, 10, 13). Because tumor and hyperplastic tissues likely differ in epithelial content, I also measured the levels of PyV MT expressed in each sample by immunoblot analyses (Figure 5.30D). All tumor tissues examined contain elevated levels of PyV MT antigen suggesting that, in part, the elevated levels of activity may reflect differences in epithelial content between tumor and hyperplastic mammary epithelium. In the course of these observations, an Erk antibody cross-reacting protein of approximately 85 kDa in size was noted in tumor epithelium but was absent in age-matched eight week old virgin hyperplastic tissue from both MT mutant-bearing transgenic strains (Figure 5.30C). Interestingly, two distinct lower molecular weight species were readily detected in these hyperplastic samples. However, whether these represent hypophosphorylated p85 kDa isoforms or novel related proteins is at present unclear.

5.2.11. Co-expression of MT Y315/22F and MT Y250F within mammary glands of bigenic animals fails to recapitulate wild-type MT tumorigenic potential

Because the mutant MT proteins used thus far lack association with distinct cellular signaling molecules, co-expression of both mutants within a cell should, in theory, regenerate wild-type MT signaling. In other words, wild-type levels of PI3'K products should be delivered from the MT Y250F mutant while Ras activation through concerted binding of SHC and GRB2:SOS complexes are effected through the MT Y315/22F mutant. To test this possibility, mice from strain MT Y250F-5a and MT Y315/22F-4 were interbred. Because female transgenic carriers from both

with lactation-competent females. Bigenic carriers were identified by Southern blot analyses (as described in Chapter 2) with minor modifications to distinguish between individual transgenes. Briefly, modifications include restriction of tail-derived DNA with PstI in addition to the use of a DNA probe derived from SV40 polyadenylation signals of plasmid p206 used in the generation of both MT mutant expression cassettes. PstI restricted DNA will cut once within the SV40 P/A cassette of the transgene and once in adjacent host DNA sequences. Due to the random nature with which transgene constructs integrate into host genomes, the band pattern obtained through these modifications allowed identification of dual transgene carriers (Figure 5.31). To date 21 bigenic animals have been generated. Surprisingly, dual transgene carriers do not develop multifocal mammary tumors with apparent one-step kinetics similar to MMTV/wild-type MT strains. Indeed, global mammary epithelial hyperplasia preceded the eventual formation of focal mammary tumors in these animals(Figure 5.32A). The average latency with which mammary tumors arose in bigenic carriers did not differ significantly from MT Y315/322F transgenics (111.1 ±13.6 days compared to 120.4±20.7 days respectively (Figure 5.33)). Further, the tumors arising from these mice were histologically distinct to tumors arising from wild-type MT, MT Y315/22F or MT Y250F transgenics. Tumors were characterized as having a mixed nodular and sclerosing cellular morphology (Figure 5.32B).

To examine whether the failure to recapitulate wild-type MT tumor kinetics was the consequence of a failure to co-express both transgenes, hyperplastic tissue in addition to mammary tumors derived from bigenic animals were analyzed for MT transcripts using the modified RNase protection procedure as outlined above (section 5.2.7.). Although epithelial hyperplasias from both 11 week old bigenic animals revealed co-expression of both transgenes (Figure 5.34, lanes 5 and 6), analyses of the tumor RNA's gave somewhat different results. In one mammary tumor analyzed, there was a failure to detect transcript from MT Y250F (Figure 5.34, lane 10). Another breast tumor demonstrated sharply reduced levels of MT Y250F transcript (Figure 5.34 lane 7) while yet another tumor showed the converse - i.e. reduction in levels of MT

Figure 5.31 Southern blot analyses used to distinguish between MT mutant transgene carriers.

Representative Southern blot analyses used in the identification of dual MT mutant transgene carriers. Tail biopsied tissue DNA was restricted with PstI and DNA probe 206SPA was used to identify individual transgenes. Indicated by the arrows and strain designations (MT Y315/22F, MT Y250F) are bands characteristic for MMTV/MT Y315/22F-4 and MMTV/MT Y250F-5a strains.

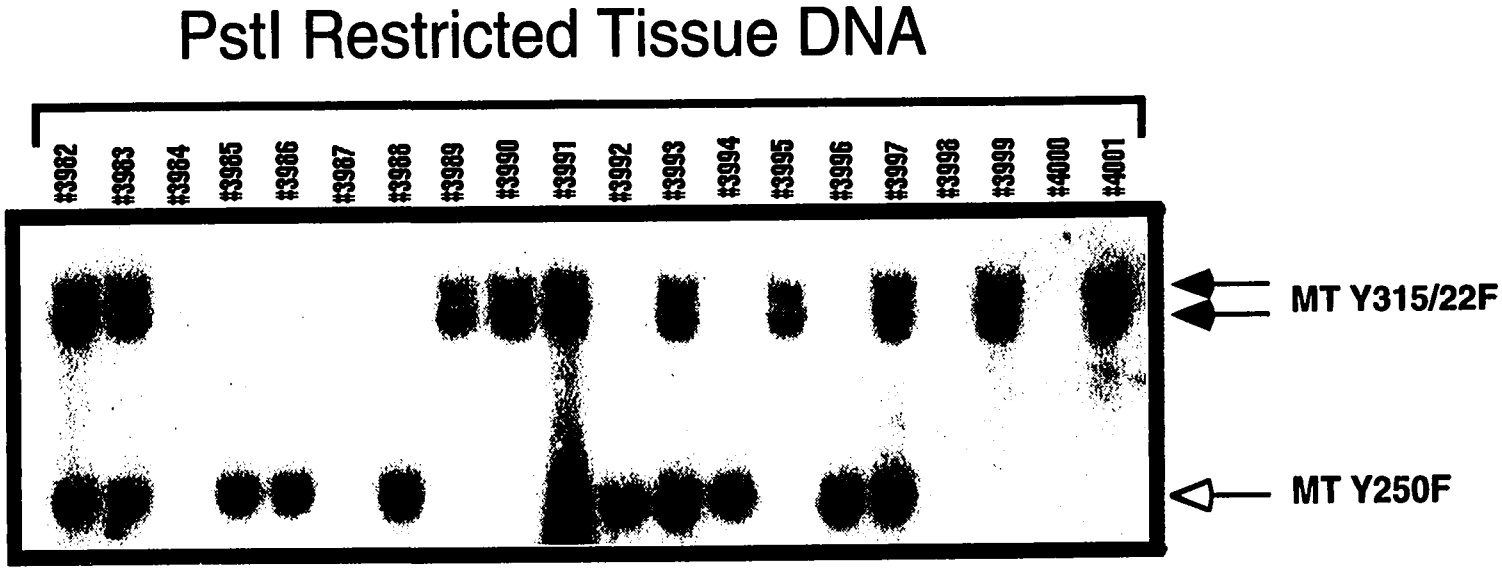
PstI Restricted Tissue DNA
#3982
#3983
#3984
#3985
#3986
#3987
#3988
#3989
#3990
#3991
#3992
#3993
#3994
#3995
#3996
#3997
#3998
#3999
#4000
#4001
MT Y315/22F
MT Y250F

Figure 5.32 Mammary gland histopathology of dual transgene carriers.

(A) Slide-mounted hematoxylin and eosin stained section of a virgin (11 week old) female bigenic (MMTV/MT Y250F & MMTV/MT Y315/22F) mammary gland. Note the distended epithelial lumen of mammary ducts. (100X)

(B) Slide-mounted hematoxylin and eosin stained section of a female bigenic (MMTV/MT Y250F & MMTV/MT Y315/22F) mammary tumor. Note the mixed sclerosing and nodular morphologies and the lack of glandular differentiation.

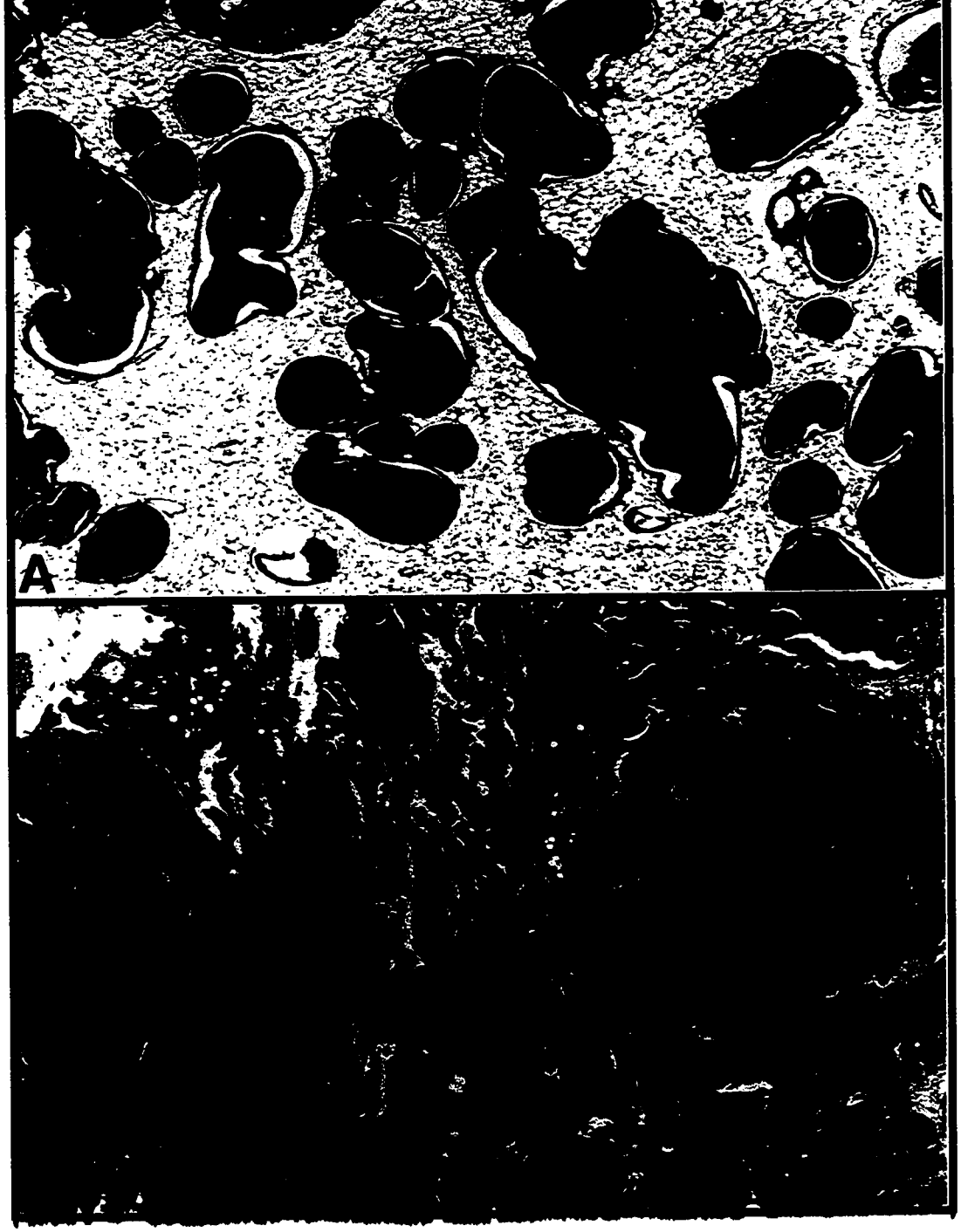
A

Figure 5.33 Mammary tumor onset in MMTV/MT#634, MMTV/MT Y250F-5a, MMTV/MT Y315/22F-4 and dual transgene carrier (MMTV/MT Y250F-5a + MMTV/MT Y315/22F-4) transgenic strains.

The age at which mammary tumor is first palpable in each transgenic strain indicated. Also shown is the number of animals analyzed in each strain (n) in addition to the median (T_{50}) age at which tumors are palpable.

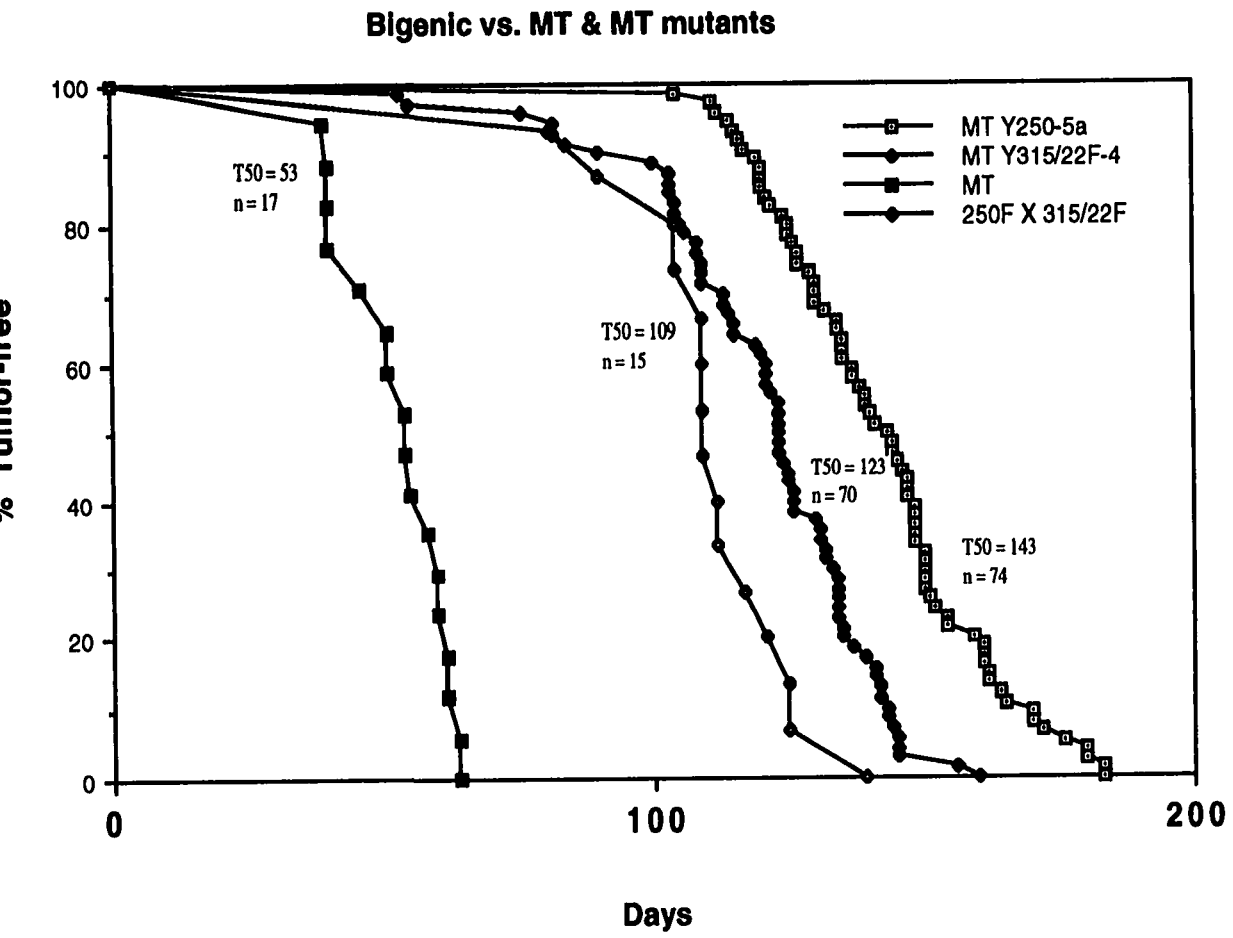
Bigenic vs. MT & MT mutants
% Tumor-free
100
80
60
40
20
0
0
100
200
Days
MT Y250-5a
MT Y315/22F-4
MT
250F X 315/22F
T50 = 53
n = 17
T50 = 109
n = 15
T50 = 123
n = 70
T50 = 143
n = 74

Figure 5.34 Mammary hyperplasias and tumors derived from dual transgenic mice (MMTV/MT Y250F-5a + MMTV/MT Y315/22F-4) co-express both transgenes

(A) Mammary hyperplasias derived from eight week old MMTV/MT Y250F-5a (lanes 1,2), MMTV/MT Y315/22F-4 (lanes 3,4) and bigenic animals (MMTV/MT Y250F-5a + MMTV/MT Y315/22F-4 (lanes 5,6)) were analyzed for MT-specific transcript utilizing riboprobe MTsn301. Indicated with arrows are expected protected sizes for MT Y315/22F. and MT Y250F transgenes. **(B)** Mammary tumors derived from virgin tumor-bearing bigenic animals were analyzed for MT-specific transcript utilizing riboprobe MTsn301. Indicated with arrows are expected protected sizes for MT Y315/22F. and MT Y250F transgenes.

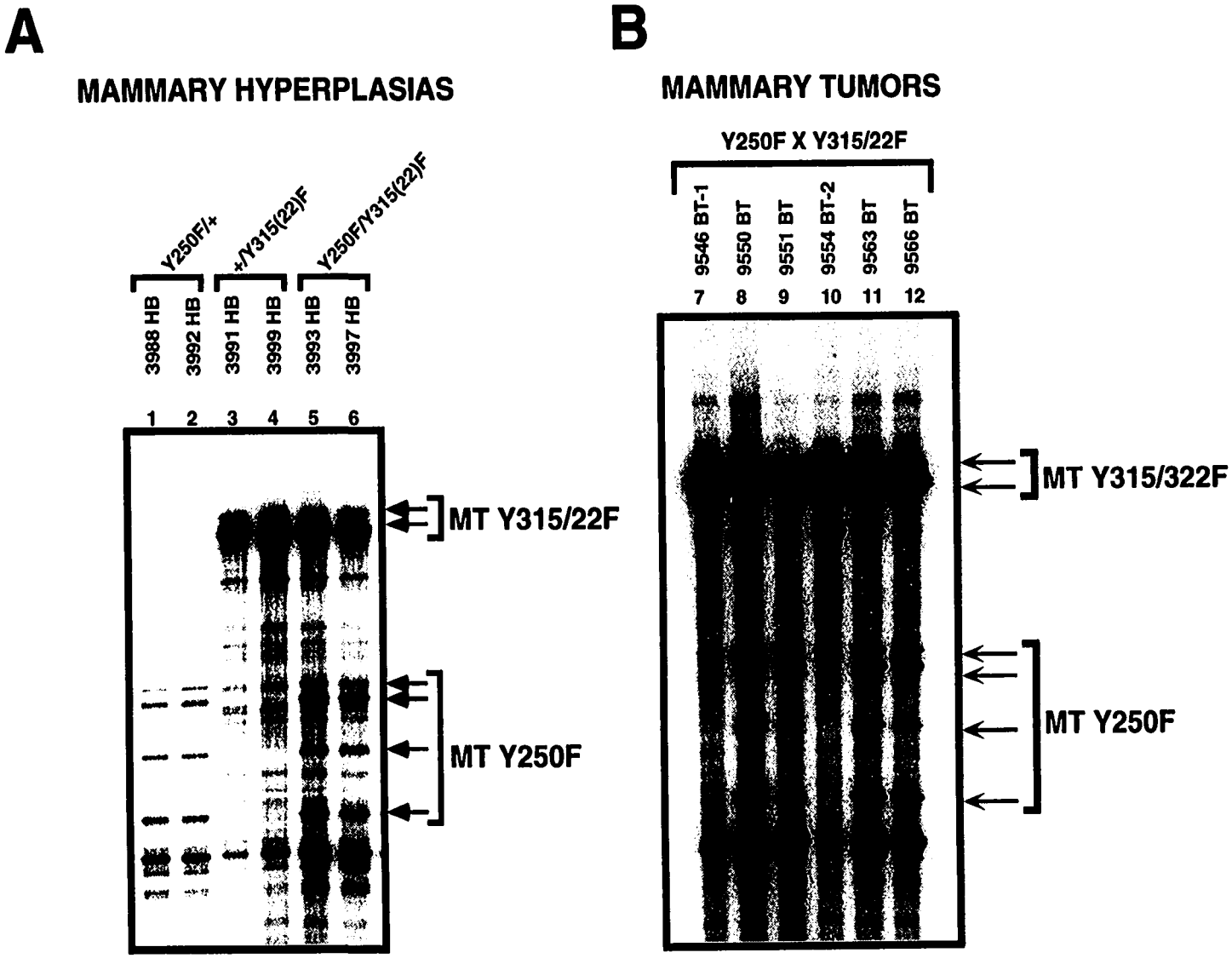
A
MAMMARY HYPERPLASIAS
Y250F/+
+/Y315(22)F
Y250F/Y315(22)F
3988 HB
3992 HB
3991 HB
3999 HB
3993 HB
3997 HB
1 2 3 4 5 6
MT Y315/22F
MT Y250F
B
MAMMARY TUMORS
Y250F X Y315/22F
9546 BT-1
9550 BT
9551 BT
9554 BT-2
9563 BT
9566 BT
7 8 9 10 11 12
MT Y315/322F
MT Y250F

tumors co-expressed both mutant transcripts to similar relative levels. Whether these observations reflect differences in the selective pressures that gave rise to these tumors is unclear at present.

5.3. DISCUSSION

The PyV MT oncogene provides an excellent model to allow identification of the important signaling pathways involved in mammary tumorigenesis. Given the potent transforming activity of PyV MT oncogene in the mammary epithelium of transgenic mice and the well defined signaling pathways utilized by PyV MT oncogene (Guy et al., 1992a), I sought to exploit this system to elucidate the importance of individual signal transduction pathways in PyV MT-mediated mammary tumorigenesis. In this chapter, the role of SHC and PI3'K signaling pathways in PyV MT-mediated tumorigenesis was explored by deriving transgenic mice that express mutant PyV MT oncogenes debilitated in their capacity to bind and activate these signaling proteins.

Consistent with previous studies of MMTV-driven transgenes, analyses of the tissue-specific pattern of both PyV mutant MT cDNAs revealed that the primary site of expression was the mammary gland with secondary sites noted in the male reproductive tissues and salivary glands (Figure 5.7, 5.8 and Tables 5.2, 5.3). In both sets of transgenic strains the initial phenotype exhibited by female mice was the inability to lactate. Wholemount analyses of the mammary epithelium of virgin females from either MT Y250F or MT Y315/322F strains revealed extensive epithelial hyperplasias (Figure 5.9) that were histologically distinct (Figure 5.10). In contrast to the well-defined alveolar hyperplasias observed in the MT Y250F strain, the MT Y315/322F strain exhibited cystic hyperplasias that possessed extensively dilated ducts (Figure 5.10). The molecular basis for these different morphologies is unclear.

Although the initial phenotypes observed with these mutant strains was mammary epithelial hyperplasias, females derived from both mutant PyV MT strains developed mammary tumors with 100% penetrance. However, in contrast to parental wild-type PyV MT strains which

strains were focal in origin arising adjacent to hyperplastic mammary tissue (Figure 5.15). Moreover, the tumors arose with delayed onset by comparison to wild-type MT strains. In general, the MT Y250F strains developed tumors with later onset compared to MT Y315/22F strains. Interestingly, the *in vivo* oncogenic potential of these mutant PyV MT strains closely correlates with their *in vitro* transforming capacities in Rat-1 cells. Taken together, these observations suggest that mutation of either of these tyrosine phosphorylation sites in PyV MT can severely interfere with the ability of PyV MT to induce mammary tumors.

Measurement of associated kinase activity of mutant MT species isolated from mammary hyperplasias or tumors revealed that association and consequent activation of Src or Yes was, by in large, unaffected compared to wild-type MT. The variation observed between different tumor extracts may reflect relative levels of MT complex analyzed between experiments or the clonal origin of individual tumors. The fact that Src kinase levels between tumors were equivalent argues that this association is unaffected in MT mutant proteins. These results correlate with published observations by others using identical MT mutants *in vitro* (reviewed in Markland & Smith, 1987). Thus the increased latency with which mammary tumors arise in both MT mutant transgenic strains is not due to an inability to complex and activate the Src family of tyrosine kinases. Rather, the failure of PyV MT to bind the corresponding associated cellular protein (i.e. SHC in MT Y250F mice and PI3K/PLC–γ in MT Y315/22F transgenics) is likely responsible for the reduced oncogenic potential observed in these mutant PyV MT strains.

A clue to the *in vivo* function of PI3K in the genesis of mammary tumors comes from the observation that significantly elevated levels of apoptosis are present in hyperplasias from MT Y315/22F animals when compared to hyperplasias from MT Y250F transgenic mice or tumors from wild-type MT animals. It is conceivable that activation of PI3'K provides a survival signal while activation of Ras (through SHC association) results in a proliferative signal. Dissociation of these integrated processes would result in the impairment of MT-mediated transformation. Indeed, the ability to deliver both proliferative and anti-apoptotic signals simultaneously may

transgenic animals. If this were true then MT Y315/22F expressing mammary glands should display high proliferative levels in addition to a corresponding increase in apoptosis. Although MT Y250F strains show reduced PI3'K activities *in vitro*, levels of PI3' metabolites in tumors and hyperplasias may be sufficient to extend a survival signal in the absence of the SHC proliferative signal. Indeed, the *in vivo* lipid kinase activities associated with this mutant have been reported to be comparable to wild-type MT levels (Dahl et al., 1996, Druker et al., 1992). Several recent reports have demonstrated similar survival signals associated with activation of PI3'K (McConnell & Dynan, 1996, Savitsky et al., 1995, Scheid et al., 1995, Yao & Cooper, 1995).

How PI3'K delivers this anti-apoptotic response is presently unknown. However, several proteins are known to be activated in response to elevated PI3'K products including Rac and PKB/Akt. PKB/Akt is a ubiquitously expressed serine/threonine protein kinase whose gene product is found amplified in human gastric adenocarcinomas (Bos, 1995) and transduced in retrovirus Akt. Because Akt/PKB is implicated in genesis of neoplasias, it is conceivable that it is also involved in MT-mediated mammary tumorigenesis. Indeed, Akt/PKB substrate pp70^{S6K} (Bos, 1995, Burgering et al., 1995, Franke et al., 1995, Kohn et al., 1995) is thought to serve a role in normal mitogenesis mediating G1 cell cycle progression (Lane et al., 1993) and is activated by virtually all mitogenic stimuli (Chou et al., 1992, Ferrari et al., 1994). Support for PI3'K in pp70S6K activation derives from the observation that the PyV MT Y315F mutant has been shown defective in pp70^{S6K} activation, while the MT Y250F mutant which couples the PI3'K pathway, can fully activate this enzyme (Dahl et al., 1996).

Another regulator of pp70^{S6K} activity is the Rho family of G proteins. GTP-bound CDC42 and Rac1 (but not RhoA) stimulates pp70^{S6K} activity (Dahl et al., 1996). Moreover, Rac1 has been shown to be activated in response to elevated PI3' lipid products (Hawkins et al., 1995,Parker, 1995). Taken together these data argue that activation of pp70^{S6K} is an important event in PI3'K signaling. It is important to note that pp70^{S6K} is not the only substrate for Rac. Indeed, Rac binds and activates members of the Ste20-like protein family - the p21 activated

distinct MAPK pathways (Coso et al., 1995, Minden et al., 1995). Because differential activation of MAPK pathways has been shown to mediate distinct cellular fates in various cell lines (i.e. proliferation versus apoptosis (Marshall, 1995, Xia et al., 1995)), it is intriguing to speculate that PyV MT may similarly influence MAPK pathways in such a way as to effect proliferation in the mammary epithelial cell.

Activation of Ras appears to be a common component of many receptor signaling cascades. It was therefore not surprising that MT mutant Y250F which fails to complex SHC and the Ras activating complex GRB2/SOS, would be severely impaired in transformation. The fact that hyperplasias are evident very early in mammary gland development is consistent with Ras-independent signaling and/or alternatively indirect weak activation of Ras. It is also conceivable that sufficient activation of Ras in tumors may occur through the interaction of Ras with the catalytic subunit of PI3'K bound to this particular mutant *in vivo* (Hu et al., 1995, Kodaki et al., 1994, Rodriguez-Viciana et al., 1994, Rodriguez-Viciana et al., 1996).

Further evidence supporting a role for the Ras pathway in tumorigenesis in these PyV MT mutant strains derives from the observation that mammary tumorigenesis appears to rely on the activation of ERK proteins. Even tumors derived from MT Y250F strains demonstrate tyrosine phosphorylated Erk1 and Erk2 to levels comparable with wild-type MT or MT Y315/22F tumors. This suggests that activation of members of the ERK family are intimately associated with the induction of mammary tumors. Interestingly, in the course of these analyses we detected the presence of a higher molecular weight ERK cross-reacting protein. The correlation of a novel 80/85 kDa isoform with transformation in the mammary gland raises the possibility that this protein may be integrally linked to the transformation process. Identification of this protein may yield significant information regarding MAPK family member activation in mammary carcinogenesis. Recently an ERK family member (Erk5) of 85 kDa in size was recently isolated (Zhou et al., 1995). It is interesting to speculate that this protein may in fact represent the related species evident in all mammary tumors analyzed.

events. One important clue to the nature of these additional events derives from observations made with MT Y250F strains. In 7% of the tumors arising in the MT Y250F strains, the mutant PyV MT antigen had reacquired the capacity to bind SHC through the occurrence of somatic mutations in the MT transgene. Sequence analyses of these alterations revealed that restoration of SHC binding can occur either through simple point mutation at the substituted phenylalanine codon or through an in frame deletion of 18 nucleotides occurring immediately downstream of the phenylalanine codon. Union of the DNA ends results in the generation of a tyrosine residue (Figure 5.23). Because SHC recognizes this tyrosine residue in the context of amino terminal sequences through its PTB domain, the amino acids deleted immediately downstream of this tyrosine residue in this mutant are obviously dispensable for SHC binding to MT. Indeed, this mutant PyV MT harboring the in frame deletion possessed wild-type transforming properties in Rat-1 fibroblasts (Table 5.4). It is worth noting that critical residues at the putative 14-3-3 binding site in MT are deleted in this particular mutant (see Figure 5.22, (Muslin et al., 1996)). It is possible that 14-3-3 is dispensable for MT-mediated transformation, although the remaining residues may constitute a low affinity binding site for 14-3-3 thereby obscuring interpretation. Further investigation of this deletion mutant with respect to its ability to bind 14-3-3 proteins should provide important insight into the function of 14-3-3 in PyV MT-mediated mammary tumorigenesis.

Another interesting aspect of these reversion events is that they occurred at a much higher frequency in lung metastases (Figure 5.22). Indeed, of the six metastatic lesions examined, 50% possessed either reversion event. Although the sample size is relatively small, these observations suggest that there is a selective pressure for restoration of SHC binding during PyV MT-mediated metastatic progression. Because SHC can recruit the GRB2/SOS/Ras complex to PyV MT, it is conceivable that activation of the Ras pathway is critical for PyV MT-mediated metastases. Alternatively, the requirement for SHC binding may reflect its ability to

complex with a PI5' phosphatase (Loubin et al., 1996). Determination of the prevalent signaling pathways involved in this phenotype will provide important insight into the molecular basis of metastatic progression.

Another interesting aspect of the MT Y250F strains, is the observation that they are also impaired in their capacity to bind and activate PI3'K *in vitro*. In both established Rat-1 cell lines and tumors derived from MT Y250F mice, the ability of the p85 subunit of PI3'K to bind MT Y250F is impaired despite the presence of intact tyrosine residues 315 and 322. Consistent with these biochemical studies, the ability of the MT Y250F mutant to activate PI3'K is also affected in both fibroblast cell lines and primary tumors (Figure 5.6 and 5.24, 5.25 respectively). Moreover, in reversion mutants that have restored SHC binding, the p85 PI3'K subunit is now capable of efficiently binding PyV MT (Figure 5.28). One explanation for these observations is that the binding of the SHC adapter protein stabilizes the binding of the p85 subunit of PI3'K to PyV MT through direct interaction. In this regard it is interesting to note that SHC possesses a polyproline tract that might serve as a potential binding site for the p85 SH3 domain (Rozakis-Adcock et al., 1992). Alternatively, the absence of tyrosine site 250 may indirectly affect the ability of tyrosine sites 315 and 322 to be efficiently phosphorylated by affecting the conformation of the protein. Whatever the mechanism, these observations argue that these tyrosine phosphorylation sites may not function independently.

In contrast to MT Y250F transgenic animals, mammary tumors and particularly lung metastases derived from the MT Y315/22F strains, fail to demonstrate reversion at either tyrosine site in the transgene responsible for p85 binding . It is conceivable that tumorigenesis in these mutant MT strains requires activation of PI3'K but that this occurs in an indirect manner. For example, activation of growth factor receptors in an autocrine or paracrine manner can result in the indirect recruitment of the PI3'K signaling pathway through receptor heterodimerization (Alimandi et al., 1995, Pinkas-Kramarski et al., 1996).

proliferative signal) that I propose were correct, then one might anticipate that the combination of the two MT mutants should result in tumor formation. The fact that co-expression of these transgenes within mammary glands of bigenic animals does not recapitulate wild-type MT expression in transgenic animals suggests that these mutants cannot complement in trans. Furthermore, tumors that did arise failed to demonstrate the high rate of metastases observed in wild-type MT transgenic mice (compare 25% (n=12) bigenic mice bearing tumors greater than 31 days which developed lung metastases compared to 67% (n=9) of equivalent wild-type MT tumor-bearing animals which progressed to metastases in the same time frame). These data argue that PyV MT signaling complexes must be assembled on the same molecule to effectively deliver a proliferative signal. Indeed, the observation that the MT Y250F mutant is impaired in its capacity to associate with the p85 regulatory subunit of PI3'K is suggestive of a cis acting macromolecular signaling complex. Alternatively, squelching of MT-associated products associated with the overexpression of one particular mutant over the other may result in this failure to deliver effective transforming signals. In this regard it has recently been demonstrated that PyV MT functions as a dimer (K. Ballmer-Hofer personal communication). Thus overexpression of one of the mutant transgenes would result in formation of an excess of nonfunctional signaling dimers.

Similarly, it is interesting to note that in tumors from bigenic animals there appears to be a selective advantage for fluctuation of individual MT mutant transgene levels. In 3/6 tumors analyzed by RNase protection, approximately equal levels of both transgenes were detected. In 1 of 6 tumors analyzed, lower levels of MT Y315/22F transcript was seen in comparison to MT Y250F transcript levels while in the remaining 2 of 6 mammary tumors studied, the converse was true. Importantly, no tumors demonstrated reversion of any tyrosine site to wild-type MT sequence suggesting that, given the proper ratio of MT mutants, transformation may indeed result. In this regard, it will be of interest to examine whether reversions are selected for in lung metastases originating from these animals. Finally, it is possible that assembly of SHC and PI3'K on the same MT molecule creates a scaffold onto which other critical signaling protein(s) may

arise in bigenic animals, a third compensating signal is absent which would normally be delivered from the full complement of MT associated proteins.

The terminal and most devastating phase in tumorigenesis is the progression of carcinoma *in situ* to its malignant counterpart. MT-mediated transformation of the mouse mammary gland is often associated with this malignant conversion. Metastases in wild-type MT transgenics in addition to metastases in MT mutant transgenic mice appeared to directly correlate with the period of time animals harbored palpable mammary tumors. Strikingly, however, there was a significant reduction (>50% reduction in both strains analyzed) in the number of MT mutant transgenic mice which developed lung metastases despite equivalent tumor-bearing times. This suggests that although capable of forming mammary tumors *in vivo*, both MT mutants were impaired in their ability to progress to metastases. Further, primary cell lines derived from MT Y315/22F tumors show an equivalent reduction in their ability to metastasize as compared to wild-type MT primary mammary tumor cell lines (R. Cardiff, unpublished observations). Interestingly, the MT Y315/22F mammary glands display an early developmental migratory defect possibly owing to a failure to produce sufficient levels of tissue-specific proteases or alternatively an intrinsic cell-specific morphogenic defect. Indeed, it has been demonstrated that Rac, a putative PI3'K substrate, is involved in organization of cytoskeletal elements mediating membrane ruffling and stress fiber formation (reviewed in Chant et al., 1995). This failure to fully arborize the entire fat pad early in development is most likely compensated for by hormonal influences associated with the advent of puberty.

The studies which I have described here provide further insight into the mechanism by which MT transforms mammary epithelial tissues. By extension of these observations, one can draw similarities between the events necessary to effect MT-mediated transformation and those that are important in receptor-mediated cell growth and/or transformation. A common theme in oncogenesis is the ability to tilt the balance of cell-death versus cell-growth in favor of proliferation. MT and the activated Neu receptor tyrosine kinase share the ability to transform the

manipulating simultaneously both apoptotic and proliferative responses. Neu-mediated transformation, on the other hand, likely requires heterodimerization with family members to achieve identical results (Alimandi et al., 1995, Pinkas-Kramarski et al., 1996). These data argue that, similar to PyV MT, the potent transforming activity of Neu in the mammary epithelium is due to its capacity to stimulate both proliferative and anti-apoptotic signaling pathways. The identification of these pathways may have important therapeutic implications in the treatment of human breast cancer.

6.1. Conclusions

Cancer progression is generally viewed as a multistep process by which several independent somatic mutational events culminate in the loss of responsiveness to normal regulatory controls. Transformation *in vitro* generally requires the concerted action of at least two oncogenes- one cytoplasmic and the other nuclear- although several exceptions are known to occur (Weinberg, 1985). *In vivo*, however, this simple model of malignant progression breaks down. While co-expression of *myc* and *ras* oncogenes in Rat1 cells in culture results in a synergistic elevation of transforming ability over either oncogene alone (Land et al., 1983), similar co-expression of these oncogenes within mammary glands of transgenic mice results in only a marginal decrease in tumor latency (Andres et al., 1988, Sinn et al., 1987) suggesting that additional factors are necessary to incur full tumorigenic potential. The fact that transgenic mice harboring either activated Neu or wild-type MT develop multifocal mammary tumors with minimal latency suggests that expression of these oncogenes alone appears sufficient for tumor formation. This apparent paradox may be reconciled by the observation that both oncogenes activate a number of distinct signaling pathways in the resident expressing cell. Indeed, both oncogenes activate cellular signaling proteins PI3'K, Ras, and PLC-γ. These inherent similarities identify signaling pathways which are critical for malignant conversion of the primary mammary epithelial cell.

In the work which I have summarized in the previous three chapters, I have dissected the role which certain signaling proteins or tumor suppressor genes play in tumorigenesis of the mouse mammary gland. To accomplish this I have made use of the potent transforming nature of Polyomavirus. Because Polyomavirus infection transforms a number of tissues including the mammary gland of newborn rodents (Dawe et al., 1987), I sought to determine which of the three virally expressed 'T' antigens is responsible for mammary tumor formation.

transforming capacity. Tumors that arose were focal in origin with extended latency. This suggests that further genetic mutation was necessary to incur a neoplastic state. Interestingly, there appeared to be a predominance of tumors in MMTV/LT animals which had undergone multiple rounds of pregnancy. Because transgene expression is known to increase with the onset of pregnancy and the differentiation status of the mammary epithelium, the absolute level of PyV LT within any given cell may define a threshold above which transformation ensues. Indeed, high level of PyV LT associated with hormonal differentiation of the mammary gland may be required to sequester all available RB or RB family members to relieve negative growth suppression. This is supported by the observation that PyV LT levels are elevated in mammary tumors that do arise. The simultaneous delivery of growth supportive signals incurred upon conception coupled with the functional inactivation of RB or its relatives may provide a fertile environment for tumorous growth. Alternatively, the differentiation state of the mammary epithelial cell may govern the susceptibility to PyV LT transformation. In this case elevated expression within a subset of differentiated mammary cells would yield a population of cells prone to transformation.

Another means by which PyV LT might influence transformation is through its ability to affect the functional activity of Cut. In this regard it is interesting to note that Cut can repress *myc* expression and that elevated Myc levels positively regulate proliferation in response to growth signals (Dufort & Nepveu, 1994). While *myc* levels do not appear greatly elevated in mammary tumors (when normalized to PGK levels), adjacent hyperplastic tissue does show a marginal 1.2 fold elevation. This may represent an early event in the transformation process. Indeed, overexpression of Myc has been demonstrated to lead to transformation of the mouse mammary gland (Andres et al., 1987, Andres et al., 1988, Schonenberger, 1988). Regardless of the means by which PyV LT sensitizes the mammary gland to transformation, the lack of mammary tumor formation despite detectable levels of transgene suggests that PyV LT may serve primarily an initiating function in transformation rather than in the maintenance or progression of the neoplastic state. This contention is supported by studies utilizing Polyomavirus ts-A mutants. These

impaired in initiating viral DNA synthesis and cell transformation at the non-permissive temperature (Fluck & Benjamin, 1979). If, however, cells are first transformed at the permissive temperature and subsequently shifted to the non-permissive temperature, cells remain transformed. Furthermore, the observation that cells stably transformed by Polyomavirus often fail to express intact PyV LT, suggests that the role of PyV LT in the transformation process is one of initiation and not in the maintenance of transformation (Fluck & Benjamin, 1979).

The transforming nature of Polyomavirus infection - at least in the mammary gland - appears dependent on the presence of PyV MT. This is supported by several observations. The rapid apparently synchronous development of multifocal mammary tumors in transgenic mice expressing MT suggests that MT alone may be sufficient to transform the mouse mammary gland. Moreover, Polyomavirus stocks which harbor debilitating MT mutations, dramatically affect the transforming potential of the virus (Laing et al., 1984). Because detection of MT transcript in the mammary gland is coincident with transformation, and given the fact that there appears no intermediate hyperplasia evident in this transformation process (Guy et al., 1992a), it is likely that MT expression alone is sufficient to induce transformation of the mammary epithelial cell.

Indeed, MT transformation of the mouse mammary gland is reminiscent of the single-step manner by which activated Neu expression transforms this tissue (Muller et al., 1988). Many of the signaling pathways activated by Neu are additionally activated by MT, suggesting a common underlying mechanism of transformation. One such molecule activated by both Neu and MT is the cytoplasmic tyrosine kinase Src (Courtneidge & Smith, 1983,Muthuswamy et al., 1994). Transformation of the mouse mammary gland by either oncogene results in a corresponding increase in the specific activity of Src. Both proteins are known to physically associate and (presumably in the case with Neu) activate Src. The importance of Src activation in MT-mediated tumorigenesis is underscored by the failure of MT to induce efficient transformation of mammary glands in mice bearing homozygous deletion of both *c-src* alleles (Guy et al., 1994).

constitutively activated c-*src* gene was placed under control of the MMTV promoter and used in the generation of transgenic mice. While kinase active Src was detected in the mammary gland, expression did not lead to global transformation akin to wild-type MT. Indeed, expression of the transgene was detected in histologically normal epithelium from virgin animals at all ages. Expression of kinase active Src, however, was incompatible with normal mammary gland differentiation in response to lactogenic hormone stimulation. Similar to that observed with the PyV LT transgenics, tumor formation occurred only after a long latency and was evident almost exclusively in multiparous animals. In contrast to PyV LT, however, tumor occurrence was more prevalent and the tumor histotype was distinct with greater than 50% of the tumors resembling schirrous carcinoma *in situ*- the most common mammary neoplasm in women (Bartow et al., 1988). In almost all multiparous animals, clear signs of hyperplasia resembling the preneoplastic lesions HANS in MMTV infected mice (Morris & Cardiff, 1987) were evident, suggesting that these hyperplasias may represent an early progression in the transformation process. Because tumor formation was clonal in nature and given that the tumors occurred after a long latency suggests that kinase activation of Src alone is not sufficient for tumorigenesis. Further, the fact that several distinct tumor types were observed coupled with the observation that tumors had distinct phosphotyrosine profiles suggests that tumor progression in each circumstance likely arose via distinct routes.

The mechanism by which Src induces transformation is unclear. Perhaps expression of kinase active Src predisposes cells to formation of a neoplasm similar to the model proposed for PyV LT. In contrast to the ability of PyV LT to interfere with negative growth regulatory molecules, Src likely predisposes cells to transformation through the delivery of a continuous proliferative signal. In the absence of inhibition of negative regulatory checks, however, this hyperproliferative signal may result in abortive apoptosis. Preliminary studies have indicated that some hyperplastic lesions and schirrous carcinomas - but not papillary or acinar carcinomas- do indeed demonstrate elevated levels of apoptosis as judged by TUNEL analyses (M.Webster and J.Hutchinson

homozygous constitutive deletion of both p53 alleles demonstrates a significant acceleration of dysplasia. This implies that p53 inactivation may be a key event in Src-mediated tumorigenesis. Future analysis of p53 from tumor tissue derived from SRC527 animals should provide valuable insight into the molecular mechanism by which Src transforms the mammary epithelial cell.

While Src activation is clearly required for MT and perhaps Neu-mediated mammary tumorigenesis, expression of kinase active Src alone is not sufficient to transform the mammary epithelium of transgenic mice. Indeed this process likely requires activation of additional signaling pathways. Ras activation appears to be central in the formation of many cancers. Indeed, both Neu and MT-mediated mammary tumorigenesis activate Ras through similar mechanisms. Neu receptor kinase activation effects redundant but equally effective means to activate this GDP/GTP-binding protein. Phosphorylated tyrosines residues #1144 and #1226/7 in the activated Neu receptor tyrosine kinase (RTK) form binding sites for SHC and GRB2 respectively, both of which effectively couple proteins responsible for Ras localization and activation (Dankort, unpublished observations). Similar to Neu and many other RTKs, MT interfaces with the Ras signaling apparatus through its ability to bind SHC which in turn recruits the Ras activating complex GRB2:SOS (Egan et al., 1993,Rozakis-Adcock et al., 1992). The universality through which RTKs activate Ras suggests that this process is paramount in transducing proliferative signals to the nucleus.

Deletion of tyrosine residue 250 in MT (which recruits SHC binding) interferes with the ability of MT to transform mammary epithelial tissues in transgenic mice. In contrast to the rapid multifocal nature by which MT transforms, MT Y250F induces focal mammary tumors over an extended period of time. The observation that MT Y250F transgenic mice develop global hyperplasias of the mammary gland at a very early age coupled with the fact that high levels of transgene are seen in these tissues, argues that lack of transgene expression is not the reason for the tumor kinetic discrepancies observed between these transgenic animals. The fact that tumors arise in MT Y250F animals suggests either an indirect activation of Ras or alternatively

date does not exclude either possibility, the fact that reversion to wild-type MT was rare in breast tumor formation (7%), suggests that a compensatory activation mechanism is selected over somatic reversion. A closer examination of Ras activation or Ras activated substrates in tumors or equivalent established primary cell lines may shed some information on this issue.

Regardless of the means by which MT Y250F transforms the mammary epithelium, metastatic progression in these animals appears heavily dependent on Ras activation. Indeed, 50% of lung metastases analyzed demonstrate that the MT protein has reacquired SHC binding through somatic mutation of the transgene. This suggests that mammary tumors which fail to progress to metastases in these animals may be due to an inadequacy in the ability to recruit Ras activating proteins to the MT signaling complex. To examine whether Ras activation in MT Y250F animals is sufficient for tumorigenesis or whether additional factors are necessary, bigenic animals carrying an activated *ras* allele together with MT Y250F would provide some useful insight. In theory, introduction of an activated *ras* allele in a MT Y250F background should compensate for the tumor delay and mimic wild-type MT tumor formation and, presumably, increase the metastatic potential of the primary tumor. It is also conceivable that SHC activates other signaling proteins in addition to Ras. Indeed, the recent identification of inositol polyphosphate-5-phosphatase Ship as a SHC-associating protein suggests that further elucidation of SHC signaling is necessary to fully understand its role in tumorigenesis.

Another pathway thought to be critical in the transformation process of MT is the 3' phospholipid generating enzyme PI3'K. Evaluation of almost all MT mutant molecules to date have correlated the inability to elevate intracellular PI 3,4,5P levels with their lack of transforming potential (Kaplan et al., 1988). This tight correlation is particularly evident in both the spectrum of tumors and the kinetics with which they arise in newborn rodents infected with viruses harboring a MT mutant incapable of complexing PI3'K (Freund et al., 1992). These studies, however, are marred by the fact that both PyV LT and PyV ST are present during viral infection obscuring interpretation of the results. To observe the effect of this mutant in isolation, I have generated

complexing PI3'K. Similar to MT Y250F strains, the phenotypic consequence of high mammary gland-specific levels of MT Y315/22F is global mammary gland hyperplasias. Examination of hyperplasias derived from age-matched MT Y250F and MT Y315/22F animals reveal distinct histological differences which suggest that the proliferative response generated by these two MT mutants may be functionally distinct and/or only partially overlapping. In further support of this contention, tumors which eventually supervened the hyperplasias were histologically distinct.

Histological signs of apoptosis were particularly evident in hyperplasias analyzed from MT Y315/22F transgenics. The fact that similar signs of apoptosis were lacking or much less severe in wild-type MT or MT Y250F strains , indicated that rapid apoptotic elimination of MT Y315/22F expressing tissues was occurring. TUNEL analyses on age-matched histological sections derived from FVB, MT Y250F, MT Y315/22F or MT animals corroborated these initial observations. It is intriguing to speculate that perhaps the *in vivo* function of PI3'K may be to deliver a survival signal. Because MT Y315/22F is able to complex SHC and therefore, activate the Ras pathway, a corresponding inhibition of apoptosis may render these cells tumorigenic. It would be interesting to intercross these MT mutant bearing transgenic animals with transgenic mice expressing elevated mammary-specific levels of Bcl2 or with animals which are homozygous null for p53 (Donehower et al., 1992). Both molecules are thought to play central roles in the apoptotic process (Harrington et al., 1994, Shen et al., 1995). One might anticipate from such crosses, a significant acceleration in the tumor latency compared to MT Y315/22F transgenics alone.

Unlike the somatic transgene mutations which occurred at low frequencies in mammary tumors and at comparatively higher frequencies in pulmonary metastases from MT Y250F transgenics, no comparable mutations have been detected in MT Y315/22F transgenes derived from tumors or lung metastases. This suggests that reversion of either site 315 or 322 is not selected for in the progression from hyperplasia to malignancy. In this regard it would be interesting to examine intracellular PI3'K levels in established primary tumor cell lines and/or the

It is unclear whether tumor formation and subsequent metastases is a function of MT-independent PI3'K activation or alternative use of parallel/downstream compensatory signals. To address this concern in more detail, I interbred both MT mutant transgenics in hopes of recapitulating the wild-type MT signal. Because both MT mutants when co-expressed should carry non-overlapping complementing signaling complexes, tumors and ensuing metastases should in theory mimic wild-type MT transformation. The fact that this was not observed suggests that these PyV MT signaling pathways cannot complement each other in trans. It is also interesting to note that no apparent somatic mutations of either transgene was selected for in the transformation process. Tumors which did arise, demonstrated clonal variations in relative transgene expression levels. Perhaps the ratio of mutant MT signaling complexes is important in generating a sufficient proliferative response. Further numbers of bigenic animals and analyses of transgenes from mammary tumors and lung metastases from these animals should provide considerable insight into the MT-mediated transformation process. In particular, it would be of interest to examine whether similar frequencies of somatic mutation occur specifically on the MT Y250F transgene in lung metastases arising in these doubly transgenic animals.

Tumorigenesis is largely believed to originate from an imbalance in diametrically opposed actions of tumor suppressor genes and their proliferative counterparts - proto-oncogenes. The animal models which I have generated should prove invaluable in further elucidating the molecular machinery and the mechanisms by which carcinogenesis originates in the mammary gland. While PyV LT transgenic mice demonstrate susceptibility to transformation through functional inactivation of tumor suppressor gene(s), Src-mediated tumorigenesis relies in its ability to deliver a strong proliferative signal. MT tumorigenesis, on the other hand, likely embraces both strategies in effecting the rapid single-step transformation of mammary epithelial tissues (Figure 6.1A). Indeed, emerging evidence suggests that proliferation signals are intimately linked to the apoptotic machinery (Harrington et al., 1994). Thus, a coordinated inactivation of negative regulatory signals (including disarming the apoptotic system) coupled to a constitutive proliferative

Figure 6.1 A model for PyV MT in mammary tumorigenesis.

(A) Schematic representation of PyV MT (waved lines) and cellular associating proteins SHC and p85 with their hypothetical biological effect.

(B) Schematic representation of MT Y315/22F (waved lines) and signaling proteins with their hypothetical biological effect.

(C) Schematic representation of MT Y250F (waved lines) and signaling proteins with their hypothetical biological effect.

Hypothetical signal effects emanating from each associated protein complex is represented as an arrow. Thick arrows denote a strong response while thin arrows represent weak to non-existent responses. The cellular fate of cells expressing the indicated MT molecule is shown below arrows. (Note that other associating cellular proteins are left out for clarity).

MT
TRANSFORMATION
MT Y315/22F
HYPERPLASIA
MT Y250F
HYPERPLASIA
MT
MT Y315/22F
MT Y250F
SHC
GRB2
SOS
RAS
RAF
MEK
ERK
PI3K
p85
PROLIFERATIVE RESPONSE
ANTI-APOPTOTIC RESPONSE

uncouple the default apoptotic machinery in response to a proliferative signal would yield incomplete transformation or hyperplasia (Figure 6.1B). A similar outcome would result from the delivery of a weak proliferative response in the presence of a strong survival signal (Figure 6.1C).

Not only do these transgenic models present workable *in vivo* models to test these tumorigenesis hypotheses, however, they also represent a biological model underlying the fundamental mechanisms by which receptor-mediated proliferation is effected during normal mammary gland differentiation. The identification of key signaling molecules, in addition to normal negative regulatory proteins which keep proliferation in check, provides a framework upon which potential therapeutic interventions may be designed.

Aitken, A., Howell, S., Jones, D., Madrazo, J., Martin, H., Patel, Y., & Robinson, K. (1995). Post-translationally modified 14-3-3 isoforms and inhibition of protein kinase C.

Alimandi, M., Romano, A., Curia, M. C., Muraro, R., Fedi, P., Aaronson, S. A., Di Fiore, P. P., & Kraus, M. H. (1995). Cooperative signaling of ErbB3 and ErbB2 in neoplastic transformation and human mammary carcinomas. Oncogene, 10, 1813-1821.

Andres, A. C., Schonenberger, B., Groner, B., Hennighausen, L., LeMeur, M., & P., G. (1987). Ha-ras oncogene expression directed by a milk protein gene promotor: Tissue specificity, hormonal regulation, and tumor induction in transgenic mice. Proc. Natl. Acad. Sci., 84, 1299-1303.

Andres, A. C., van der Valk, M. A., Schonenbereger, C. A., Fluckiger, F., Lemeur, M., Gerlinger, P., & Groner, P. (1988). Ha-ras and c-myc oncogene expression interferes with morphological and functional differentiation of mammary epithelial cells in single and double transgenic mices. Genes and Dev., 2, 1486-1495.

Asselin, C., Vass-Marengo, J., & Bastin, M. (1986). Mutation of the Polyomavirus genome that activates the properties of large T associated with neoplastic transformation. J. Virol., 57, 165-172.

Bartow, S. A., & Fenoglio-Preiser, C. (1988). The breast. *In*: Pathology, Rubin, E., Farber, J.L., J.B. Lippincott Co., New York. , 992-1013.

Benjamin, T., & Vogt, P. K. (1990). Cell transformation by viruses. In Virology, Second Edition, Ed. B.N. Fields, D.M. Knipe et al., Raven Press Ltd., New York. , 317-367.

Berger, H., & Wintersberger, E. (1986). Polyomavirus small T antigen enhances replication of viral genomes in 3T6 mouse fibroblasts. J. Virol., 60, 768-770.

Bolen, J. (1993). Nonreceptor tyrosine protein kinases. Oncogene, 8, 2025-2031.

Borellini, R. F., & Oka, T. (1989). Growth control and differentiation in mammary epithelial cells. Environ. Health Persp., 80, 85-99.

Bos, J. L. (1995). A target for phosphoinositide 3-kinase: Akt/PKB. TIBS, 20, 441-442.

Boston, P., & Jackson, P. (1980). Purification and properties of a brain-specific protein, human 14-3-3 protein. Biochem. Soc. Trans., 8, 617-618.

Bouchard, L., Lamarre, L., Tremblay, P. J., & Jolicoeur, P. (1989). Stochastic appearence of mammary tumors in transgenic mice carrying the activated c-*neu* oncogene. Cell, 57, 931-936.

Braselmann, S., & McCormick, F. (1995). Bcr and Raf form a complex *in vivo* via 14-3-3 proteins. EMBO J., 14, 4839-4848.

Brizuela, L., Ulug, E. T., Jones, M. A., & Courtneidge, S. A. (1995). Induction of interleukin-2 transcription by the hamster polyomavirus middle T antigen: a role for Fyn in T cell signal transduction. Eur. J. Immunol., 25, 385-393.

Burgering, B. M. T., & Coffer, P. J. (1995). Protein kinase B (c-Akt) in phosphatidylinositol-3-OH kinase signal transduction. Nature, 376, 599-602.

Campbell, K. S., Auger, K. R., Hemmings, B. A., Roberts, T. M., & Pallas, D. C. (1995). Identification of regions in Polyomavirus middle T and small T antigens important for association with protein phosphatase 2A. J. Virol., 69, 3721-3728.

Campbell, K. S., Orgis, E., Burke, B., Su, W., Auger, K. R., Druker, B. J., Schaffhausen, B. S., Roberts, T. M., & Pallas, D. C. (1994). Polyoma middle tumor antigen interacts with SHC protein via the NPTY (Asn-Pro-Thr-Tyr) motif in middle tumor antigen. Proc. Natl. Acad. Sci. USA, 91, 6344-6348.

Cardiff, R. D. (1984). Protoneoplasia: the molecular biology of mouse mammary hyperplasia. Advances in Cancer Res., 42, 167-190.

Cardiff, R. D., & Muller, W. J. (1993). Transgenic mouse models of mammary tumorigenesis. Cancer Surv., 16, 97-113.

Carpenter, C. L., Auger, K. R., Chanudhuri, M., Yoakim, M., Schaffhausen, B., Shoelson, S., & Cantley, L. C. (1993). Phosphoinositide 3-kinase is activated by phosphopeptides that bind to the SH2 domains of the 85-kDa subunit. J. Biol. Chem., 13, 9478-9483.

Cartwright, C. A., Eckhart, W., Simon, S., & Kaplan, P. L. (1987). Cell transformation by pp60c-src mutated in the carboxy-terminal regulatory region. Cell, 49, 83-91.

Chant, J., & Stowers, L. (1995). GTPase cascades choreographing cellular behavior: movement, morphogenesis, and more. Cell, 81, 1-4.

Cheng, S. H., Harvey, R., Espino, P. C., Semba, K., Yamamoto, T., Toyoshima, K., & Smith, A. E. (1988). Peptide antibodies to the human c-fyn gene product demonstrate pp59 c-fyn is capable of complex formation with the middle-T antigen of polyomavirus. EMBO J., 7, 3845-3855.

Cherington, M. V., Morgan, B., Spiegelman, B. M., & Roberts, T. M. (1986). Recombinant retroviruses that transduce individual polyoma tumor antigens: effects on growth and differentiation. Proc. Natl. Acad. Sci., 83, 4307-4311.

Chirgwin, J. M., Przybyla, A. E., MacDonald, R. J., & Rutter, W. J. (1979). Isolation of biologically active ribonucleic acid from sources enriched in ribonuclease. Biochemistry, 18, 5294-5299.

Chou, M. M., & Blenis, J. (1992). The 70 kD S6 kinase: a kinase with multiple roles in mitogenic signaling. Curr. Opin. Cell Biol., 7, 806-814.

Chow, L. M., Jarvis, C., Hu, Q., Nye, S. H., Gervais, F. G., Veillette, A., & Matis, L. A. (1994). Ntk: A Csk related protein-tyrosine kinase expressed in brain and T lymphocytes. Proc. Natl. Acad. Sci., 91, 4975-4979.

Conklin, D. S., Galaktionov, K., & Beach, D. (1995). 14-3-3 proteins associate with cdc25 phosphatases. Proc. Natl. Acad. Sci., 92, 7892-7896.

Cooper, J. A., & Howell, B. (1993). The when and how of Src regulation. Cell, 73, 1051-1054.

Coso, O. A., Chiariello, M., Yu, J., Teramoto, H., Crespo, P., Xu, N., Miki, T., & Gutkind, J. S. (1995). The small GTP-binding proteins Rac1 and CDC42 regulate the activity of the JNK/SAPK signaling pathway. Cell, 81, 1137-1146.

65, 3301-3308.

Courtneidge, S. A., & Smith, A. E. (1983). Polyoma virus transforming protein associates with the product of the *c-src* cellular gene. Nature (London), 303, 435-439.

Coussens, L., Yang-Feng, T. L., Liao, Y., Chen, E., Gray, A., McGrath, J., Seeburg, P. H., Liberman, T. A., Schlessinger, J., Francke, U., Levinson, A., & Ullrich, A. (1985). Tyrosine kinase receptor with extensive homology to EGF receptor shares chromosomal location with *neu* oncogene. Science, 230, 1132-1139.

Dahl, J., Freund, R., Blenis, J., & Benjamin, T. J. (1996). Studies of partially transforming Polyomavirus mutants establish a role for phosphatidylinositol 3-kinase in activation of pp70 S6 kinase. Mol. Cell. Biol., 16, 2728-2735.

Dawe, C. J., Freund, R., Mandel, G., Ballmer-Hoffer, K., Talmage, D.A. and Benjamin, T.L. (1987). Variations in polyoma virus genotype in relation to tumor induction in mice. Am. J. of Pathology, 127(2), 243-261.

DePamphilis, M. L., & Bradley, M. K. (1986). Replication of SV40 and polyoma virus chromosomes. In N.P. Salzman (ed.), The papovaviridae, vol . 1. Plenum Publishing Corp., New York. , 99-244.

Devoto, S. H., Mudryj, M., Pines, J., Hunter, T. and Nevins, J. (1992). A cyclin A-protein kinase complex possesses sequence-specific DNA binding activity: p33cdk2 is a component of the E2F-cyclin A complex. Cell, 68, 167-176.

Dickson, R. B., Gottardis, M. M., & Merlino, G. T. (1991). Molecular insights into breast cancer from transgenic mouse models. Bioessays, 13, 591-596.

Dilworth, S. M., Brewster, C. E. P., Jones, M. D., Lanfrancone, L., Pelicci, G., & Pelicci, P. G. (1994). Tranformation by polyoma virus middle T-antigen involves the binding and tyrosine phosphorylation of Shc. Nature (London), 367, 87-90.

Dilworth, S. M., & Horner, V. P. (1993). Novel monoclonal antibodies that differentiate between the binding of pp60 c-src or protein phosphatase 2A by polyomavirus middle T antigen. J. Virol., 67, 2235-2244.

Donehower, L. A., Harvey, M., Slagle, B. L., McArthur, M. J., Montgomery Jr., C. A., Brutel, J. S., & Bradley, A. (1992). Mice deficient for p53 are developmentally normal but susceptible to spontaneous tumors. Nature (London), 356, 215-221.

Dotto, G. P., Weinberg, R. A., & Ariza, A. (1988). Malignant transformation of mouse primary keratinocytes by HaSV and its modulation by surrounding normal cells. Proc. Natl. Acad. Sci., 85, 6389-6393.

Druker, B. J., Sibert, L., & Roberts, T. M. (1992). Polyomavirus middle T-antigen NPTY mutants. J. Virol., 66, 5770-5776.

Dubensky, T. W., Freund, R., Dawe, C. J., & Benjamin, T. L. (1991). Polyomavirus replication in mice: Influences of VP1 type and route of inoculation. J. Virol., 65, 342-349.

Dufort, D., & Nepveu, A. (1994). The human Cut homeodomain protein represses transcription from the *c-myc* promotor. Mol. Cell. Biol., 14, 4251-4257.

complexes with the retinoblastoma protein. J. Virology, 64, 1353-1356.

Dyson, N. B. K., Whyte, P., & Harlow, E. (1989). The cellular 107K protein that binds to adenovirus E1A also associates with the large T antigens of SV40 and JC virus. Cell, 58, 249-255.

Eddy, B. E. (1969). Polyoma virus. Virology monograghs 7. Edited by S.Gard, C. Hallauer, K.F. Meyer. New York, Springer-Verlag, 1-114.

Egan, S. E., Giddings, B. W., Brooks, M. W., Buday, L., Sizeland, A. M., & Weinberg, R. A. (1993). Association of Sos Ras exchange protein with Grb2 is implicated in tyrosine kinase signal transduction and transformation. Nature (London), 363, 45-51.

Escobedo, J. A., Kaplan, D. R., Kavanaugh, W. M., Turck, C. W., & Williams, L. T. (1991). Mol. Cell. Biol., 11, 1125-1132.

Ewen, M. E., B., F., Harlow, E., & Livingston, D. M. (1992). Interaction of p107 with cyclin A independent of complex formation with viral oncoproteins. Science, 255, 65-86.

Feinberg, A. P., & Vogelstein, B. (1983). A technique for radiolabeling DNA restriction endonuclease fragments to high specific activity. Anal. Biochem., 132, 6-13.

Ferrari, S., & Thomas, G. (1994). S6 phosphorylation and the p70S6K/p85S6K. Crit. Rev. Biochem. Mol. Biol., 29, 385-413.

Fluck, M., & Benjamin, T. L. (1979). Comparison of two early gene functions essential for transformation in polyoma virus and SV40. Virology, 96, 205-228.

Franke, T. F., Yang, S., T.O., C., Datta, K., Kazlauskas, A., Morrison, D. K., Kaplan, D. R., & Tsichlis, P. (1995). The protein kinase encoded by the Akt proto-oncogene is a target of the PDGF-activated phosphatidylinositol 3-kinase. Cell, 81, 727-736.

Freed, E., McCormick, F., & Ruggieri, R. (1994). Proteins of the 14-3-3 family associate with Raf and contribute to its activation. Cold Spring Harbour Symp. Quat. Biol., 59, 187-193.

Freund, R., Dawe, C. J., Carroll, J. P., & Benjamin, T. L. (1992). Changes in frequency, morphology, and behavior of tumors induced in mice by a polyoma virus mutant with a specifically altered oncogene. Am. J. Path., 141, 1409-1425.

Friend, S. H., Bernards, R., Rogelj, S., Weinberg, R. A., Rapaport, J. M., Albert, D. M., & Dryja, T. P. (1986). A human DNA segment with properties of the gene that predisposes to retinoblastoma and osteosarcoma. Nature (London), 323, 643-646.

Garcia, I., Dietrich, P.-Y., Aapro, M., Vauthier, G., Vadas, L. and Engel, E. (1989). Genetic alterations of *c-myc*, c-erbB-2, and *c-Ha-ras* protooncogenes and clinical associations in human breast carcinoomas. Cancer Res., 49, 6675-6679.

Glenn, G. M., & Eckhart, W. (1995). Amono-terminal regions of polyomavirus middle T antigen are required for interactions with protein phosphatase 2A. J. Virol., 69, 3729-3736.

Gross, L. (1970). The parotid tumor (Polyoma) virus. Oncogenic Viruses. Edited by L.Gross. Pergamon Press, Toronto, 651-750.

Guy, C. T., Cardiff, R. D., & Muller, W. J. (1992a). Induction of mammary tumors by expression of polyomavirus middle T oncogene: a transgenic mouse model for metastatic disease. Mol. Cell. Biol., 12, 954-961.

progression. J. Biol. Chem., 271, 7673-7678.

Guy, C. T., Muthuswamy, S. K., Cardiff, R. D., Soriano, P., & Muller, W. J. (1994). Activation of c-Src tyrosine kinase is required for the induction of mammary tumors in transgenic mice. Genes Dev., 8, 23-32.

Guy, C. T., Webster, M. A., Schaller, M., Parson, T. J., Cardiff, R. D., & Muller, W. J. (1992b). Expression of the *neu* proto-oncogene in the mammary epithelium of transgenic mice induces metastatic disease. Proc. Natl. Acad. Sci. USA, 89, 10578-10582.

Hagar, G. L. (1988). MMTV as a model for gene expression in mammary tissue. *In* M.E. Lippman and R. Dickson (ed.) Breast cancer: cellular and molecular biology. Kluwer Academic Publishers, Boston. , 267-281.

Harlow, E., Whyte, P., Franza, R., Jr., and Schely, C. (1986). Association of adenovirus early-region 1A proteins with cellular polypeptides. Mol. Cell. Bio., 6, 1579-1589.

Harrington, E. A., Fanidi, A., & Evan, G. I. (1994). Oncogenes and cell death. Curr. Opin. Gen. Dev., 4, 120-129.

Hawkins, P. T., Eguinoa, A., Rong-Guo, Q., Stokoe, D., Cooke, F. T., Walters, R., Wennstrom, S., Claesson-Welsh, L., & Symons, M. (1995). PDGF stimulates an increase in GTP-Rac via the activation of phosphoinositide 3-kinase. Current Biol., 5, 393-403.

Horak, I. D., Kawakami, T., Gregory, F., Robbins, K. C., & Bolen, J. B. (1989). Association of p60 fyn with middle tumor antigen in murine polyomavirus-transformed rat cells. J. Virol., 63, 2243-2247.

Hu, Q., Klippel, A., Muslin, A. J., Fantl, W. J., & Williams, L. T. (1995). Ras-dependant induction of cellular responses by consitiutively active phosphatidylinositol-3 kinase. Science, 268, 100-102.

Huang, H. G., Ostrowski, M. C., Berard, D., & Hager, G. (1981). Glucocorticoid regulation of the Ha-MuSV p21 gene conferred by sequences from mouse mammary tumor virus. Cell, 27, 245-255.

Hunter, T. (1991). Cooperation between oncogenes. Cell, 64, 249-270.

Ichimura, T., Uchiyama, J., Kunihiro, O., Horigome, T., Omata, S., Shinkai, F., Kaji, H., & Isobe, T. (1995). Identification of the site of interaction of the 14-3-3 protein with phosphorylated tryptophan hydroxylase. J. Biol. Chem., 270, 28515-28518.

Jacobs, C., & Rubsamen, H. (1983). Expression of pp60c-src protein kinase in adult and fetal human tissues: high activities in some sarcomas and mammary carcinomas. Cancer Res., 43, 1696-1702.

Jehn, B., Costello, E., Marti, A., Keon, N., Deane, R., Li, F., Friis, R. R., Burri, P. H., Martin, F., & Jaggi, R. (1992). Overexpression of Mos, Ras, Src, and Fos Inhibits Mouse Mammary Epithelial Cell Differentiation. Mol. Cell. Biol., 12, 3890-3902.

Jelinek, M. A., & Hassell, J. A. (1992). Reversion of middle T antigen-transformed Rat-2 cells by Krev-1: implications for the role of p21c-ras in polyomavirus-mediated transformation. Oncogene, 7, 1687-1698.

Oncogene, 4, 295-300.

Kaplan, D. R., Pallas, D. C., Morgan, W., Scaffhausen, B., & Roberts, T. M. (1988). Mechanisms of transformation by polyoma virus middle T antigen. Biochem. Biophys. Acta, 948, 345-364.

Kiefer, F., Courtneidge, S. A., & Wagner, E. F. (1994). Oncogenic properties of the middle T antigens of polyomaviruses. Adv. Cancer Res.

King, C. R., Kraus, M.H., and Aaronson, S.A. (1985). Amplification of a novel v-erbB-related gene in a human mammary carcinoma. Science, 229, 974-976.

Kmiecik, T. E., & Shalloway, D. (1987). Activation and suppression of pp60c-src transforming ability by mutation of its primary sites of tyrosine phosphorylation. Cell, 49, 65-73.

Kodaki, T., Woscholski, R., Hallberg, B., Rodriguez-Viciana, P., Downward, J., & Parker, P. (1994). The activation of phosphatidylinositol 3-kinase by Ras. Curr. Biol., 4, 798-806.

Kohn, A. D., Kovacina, K. S., & R.A., R. (1995). Insulin stimulates the kinase activity of RAC-PK, a pleckstrin homology domain containing ser/thr kinase. EMBO J., 14, 4288-4295.

Kornbluth, S., Sudol, M., & Hanafusa, H. (1987). Association of the polyomavirus middle-T antigen with c-yes protein. Nature (London), 325, 171-173.

Kratochwil, K. (1969). Organ specificity in mesenchymal induction demonstrated in the embryonic development of the mammary gland of the mouse. Dev. Biol., 20, 46-71.

Kypta, R. M., Hemming, A., & Courtneidge, S. A. (1988). Identification and characterization of p59 fyn (a src-like protein tyrosine kinase) in normal and ployoma virus transformed cells. EMBO J., 7, 3837-3844.

Laing, T. J., Carmichael, G. G., & Benjamin, T. L. (1984). A polyoma mutant that encodes small T antigen but not middle T antigen demonstrates uncoupling of cell surface and cytoskeletal changes associated with cell transformation. Mol. Cell. Biol., 4, 2774-2783.

Lam, E. W., & La Thangue, N. B. (1994). DP and E2F proteins: coordinating transcription with cell cycle progression. Curr. Opin. Cell Biol., 6, 859-866.

Land, H., Chen, A. C., Morgenstern, J. P., Parada, L. F., & Weinberg, R. A. (1986). Behavior of myc and ras oncogenes in transformation of rat embryo fibroblasts. Mol. Cell. Biol., 6, 1917-1925.

Land, H., Parada, L. F., & Weinberg, R. A. (1983). Tumorigenic conversion of primary embryo fibroblasts requires at least two cooperating oncogenes. Nature (London), 304, 596-602.

Lane, H. A., Fernandez, A., Lamb, N. J., & Thomas, G. (1993). p70S6K function is essential for G1 progression. Nature (London), 363, 170-172.

Larose, A., Dyson, N., Sullivan, M., Harlow, E., & Bastin, M. (1991). Polyomavirus large T mutants affected in retinoblastoma protein binding are defective in immortilization. J. Virol., 65, 2308-2313.

Leder, A., Pattengale, P.K., Kuo, A., Stewart, T. and Leder, P. (1986). Consequences of widespread deregulation of the *c-myc* gene in transgenic mice. Cell, 45, 485-495.

1394-1399.

Lemieux, N., Zhang, X.-X., Dufort, D., & Nepveu, A. (1994). Assignment of the human homologue of the Drosophila Cut homeobox gene (CutL1) to band 7q22 by fluorescence in situ hybridization. Genomics, 24, 191-193.

Linzer, D. I. H., & Levine, A. J. (1979). Characterization of a 54K dalton cellular SV40 tumor antigen present in SV40 transformed cells and uninfected embryonal carcinoma cells. Cell, 17, 43-52.

Lioubin, M. N., Algate, P. A., Tsai, S., Carlberg, K., Aebersold, R., & Rohrschneider, L. R. (1996). p150Ship, a signal transduction molecule with inositol polyphosphate-5-phosphatase activity. Genes and Dev., 10, 1084-1095.

Lundberg, C., Skoog, L., & Cavenee, W. K. (1987). Loss of heterozygosity in human ductal breast tumors indicates a recessive mutation on chromosome 13. Proc. Natl. Acad. Sci., 84, 2372-2376.

Luttrell, D. K., Lee, A., Lansing, T. J., Crosby, R. M., Jung, K. D., Willard, D., Luther, M., Rodriguez, M., & Gilmer, T. M. (1994). Involvement of pp60c-src with two major signalling pathways in human breast cancer. Proc. Natl. Acad. Sci. USA, 91, 83-87.

Mangues, R., Seidman, I., Pellicer, A., & Gordon, J. W. (1990). Tumorigenesis and male sterility in transgenic mice expressing MMTV/N-ras oncogene. Oncogene, 5, 1491-1497.

Manser, E., Leung, T., Salihuddin, H., Zhao, Z., & Lim, L. (1994). A brain serine/threonine protein kinase activated by Cdc42 and Rac1. Nature (London), 367, 40-46.

Markland, W., & Smith, A. E. (1987). Mutants of polyomavirus middle-T antigen. Biochem. Biophys. Acta, 907, 299-321.

Marshall, C. J. (1991). Tumor suppressor genes. Cell, 64, 313-326.

Marshall, C. J. (1995). Specificity of receptor tyrosine kinase signaling: transient versus sustained extracellular signal-regulated kinase activation. Cell, 80, 179-185.

Matsui, Y., Halter, S. A., Holt, J. T., Hogan, B. L., & Coffey, R. J. (1990). Development of mammary hyperplasia and neoplasia in MMTV-TGFa transgenic mice. Cell, 61, 1147-1155.

Matthews, J. T., & Benjamin, T. L. (1986). 12-O-Tetradecanoylphorbol-13-acetate stimulates phosphorylation of the 58,000-Mr form of Polyomavirus middle T antigen in vivo: implications for a possible role of protein kinase C in middle T function. J. Virol., 58, 239-246.

Mayol, X., Grana, X., Baldi, A., Sang, N., Hu, Q., & Giordano, A. (1993). Cloning of a new member of the retinoblastoma gene family (pRb2) which binds to the E1A transforming domain. Oncogene, 8, 2561-2566.

McConnell, K., & Dynan, W. S. (1996). The DNA-dependant protein kinase: a matter of life and (cell) death. Curr. Opin. in Cell Biol., 8, 325-330.

McVicar, D. W., Lal, B. K., Lloyd, A., Kawamura, M., Chen, Y. Q., Zhang, X., Staples, J. E., Ortaldo, J. R., & O'Shea, J. J. (1994). Molecular cloning of Isk, a carboxyl-terminal src kinase (csk) related gene expressed in leukocytes. Oncogene, 9, 2037-2044.

containing a bacteriophage SP6 promotor. Nucleic Acids Res., 12, 7035-7056.

Migliaccio, A., Pagano, M., & Auricchio, F. (1993). Immediate and transient stimulation of protein tyrosine phosphorylation by estradiol in MCF-7 cells. Oncogene, 8, 2183-2191.

Minden, A., Lin, A., Claret, F., Abo, A., & Karin, M. (1995). Selective activation of the JNK signaling cascade and c-Jun transcriptional activity by the small GTPases Rac and CDC42Hs. Cell, 81, 1147-1157.

Morris, D. W., Barry, P. A., Bradshaw, H. D., & Cardiff, R. D. (1990). Insertion mutagesis of the *int-1* and *int-2* loci by mouse mammary tumor virus in premalignant and malignant neoplasms from the GR mouse strain. J. Virol., 64, 1794-1802.

Morris, D. W., & Cardiff, R. D. (1987). The multistep model of mouse mammary tumor development. Advances in Viral Oncology, 7, 123-140.

Muller, W. J. (1991). Expression of activated oncogenes in the murine mammary gland: transgenic models for human breast cancer. Cancer Metast. Rev., 10, 217-227.

Muller, W. J., Lee, F. S., Dickson, C., Peters, G., Pattengale, P., & Leder, P. (1990). The *int-2* gene product acts as an epithelial growth factor in transgenic mice. EMBO J., 9, 907-913.

Muller, W. J., Sinn, E., Wallace, R., Pattengale, P. K., & Leder, P. (1988). Single-step induction of mammary adenocarcinoma in transgenic mice bearing the activated *c-neu* oncogene. Cell, 54, 105-115.

Muslin, A. J., Tanner, J. W., Allen, P. M., & Shaw, A. S. (1996). Interaction of 14-3-3 with signaling proteins is mediated by the recognition of phosphoserine. Cell, 84, 889-897.

Muthuswamy, S. K., & Muller, W. J. (1995). Activation of Src family kinases in Neu-induced mammary tumors correlates with their association with distinct sets of tyrosine phosphorylated proteins *in vivo*. Oncogene, 11, 1801-1810.

Muthuswamy, S. K., Siegel, P. M., Dankort, D. L., Webster, M. A., & Muller, W. J. (1994). Mammary tumors expressing the *neu* proto-oncogene possess elevated c-Src tyrosine kinase activity. Mol. Cell. Biol., 14(1), 735-743.

Nevins, J. R. (1994). Cell cycle targets of the DNA tumor viruses. Curr. Opin. Gen. Dev., 4, 130-134.

Noh, D. Y., Shin, S. H., & Rhee, S. G. (1995). Phosphoinositide-specific phopholipase C and mitogenic signaling. Biochim. Biophys. Acta., 1242, 99-113.

Okada, M., Nada, S., Yamanashi, Y., Yamamoto, T., & Nakagawa, H. (1991). CSK: a protein-tyrosine kinase involved in regulation of Src family kinases. J. Biol. Chem., 266, 24249-24252.

Ornitz, D., Moreadith, R. W., & Leder, P. (1991). Binary system for regulating transgene expression in mice: targeting *int-2* gene expression with yeast GAL4/UAS control elements. Proc. Natl. Acad. Sci., 88, 698-702.

Ottenhoff-Klaff, A. E., Rijksen, G., van Beurden, E. A. C. M., Hennipman, A., Michels, A. A., & Staal, G. E. J. (1992). Characterization of protein tyrosine kinases from human breast cancer: involvement of the *c-src* oncogene product. Cancer Res., 52, 4773-4778.

Ozisik, Y. Y., Meloni, A. M., Surti, U., & Sandberg, A. A. (1993). Deletion 7q22 in uterine leiomyoma. A cytogenetic review. Cancer Gen. Cytogen., 71, 1-6.

Pallas, D. C., Shahrik, L. K., Martin, B. L., Jaspers, S., Miller, T. B., Brautigan, D. L., & Roberts, T. M. (1990). Polyoma small and middle T antigens and SV40 small T antigen form stable complexes with protein phosphatase 2A. Cell, 60, 167-176.

Palmiter, R. D., Chen, H.Y., Messing, A. and Brinster, R.L. (1985). SV40 enhancer and large T antigen are instrumental in development of choroid plexus tumours in trangenic mice. Nature, 316, 457-460.

Parker, P. J. (1995). PI 3-kinase puts GTP on the Rac. Current Biol., 5(6), 577-579.

Peto, R., Lee, P., Levy, L., & Clack, J. (1975). Cancer and aging in mice and men. Br. J. Cancer, 32, 411-426.

Pinkas-Kramarski, R., Soussan, L., Waterman, H., Levkowitz, G., Alroy, I., Klapper, L., Lavi, S., Seger, R., Ratzkin, B. J., Sela, M., & Yarden, Y. (1996). Diversification of Neu differentiation factor and epidermal growth factor receptor signaling by combinatorial interactions. EMBO J., 15, 2452-2467.

Piwnica-Worms, H., Saunders, K. B., Robert, T. M., Smith, A. E., & Cheng, S. H. (1987). Tyrosine phosphorylation regulates the biochemical and biological properties of pp60c-src. Cell, 49, 75-82.

Rassoulzadegan, M., Naghashfar, Z., Cowie, A., Carr, A., Grisoni, M., Kamen, R. and Cuzin, F. (1983). Expression of the large T protein of polyomavirus promotes the establishment in culture of 'normal' rodent fibroblast cell lines. Proc. Natl. Acad. Sci., 80, 4354-4358.

Rassoulzadegan, M., Cowie, A., Carr, A., Glaichenhaus, N., Kamen, R., & Cuzin, F. (1982). The roles of individual polyoma virus early proteins in oncogenic transformation. Nature (London), 300, 713-718.

Roboy, S. J., Duggan, M. A., & Kurman, R. J. (1988). Gynecologic pathology. *In*: Pathology, Rubin, E., Farber, J.L., J.B. Lippincott Co., New York. , 944-989.

Rodriguez-Viciana, P., Warne, P. H., Dhand, R., Vanhaesebroeck, B., Gout, I., Fry, M. J., Waterfield, M. D., & Downward, J. (1994). Phosphatidylinositol-3-OH kinase as a direct target of Ras. Nature (London), 370, 527-532.

Rodriguez-Viciana, P., Warne, P. H., Vanhaesebroeck, B., Waterfield, M. D., & Downward, J. (1996). Activation of phosphatidylinositol 3-kinase by interaction with Ras and by point mutation. EMBO J., 15, 2442-2451.

Ron, D., & Dressler, H. (1992). pGSTag-a versatile bacterial expression plasmid for enzymatic labelling of recombinant proteins. Biotechniques, 13, 866-869.

Rosen, N., Bolen, J. B., Schwartz, A. M., Cohen, P., DeSeau, V., & Israel, M. A. (1986). Analysis of pp60 c-src protein kinase activity in human tumor cell lines and tissues. J. Biol. Chem., 261, 13754-13759.

Rozakis-Adcock, M., McGlade, J., Mbamalu, G., Pelicci, G., Daly, R., Thomas, S., Brugge, J., Pelicci, P. G., Schlessinger, J., & Pawson, T. (1992). Association of Shc and Grb2/Sem5 SH2-containing proteins is implicated in activation of the Ras pahway by tyrosine kinases. Nature (London), 360, 689-692.

Savitsky, K., Bar-Shira, A., Gilad, S., Rotman, G., Ziv, Y., Vanagaite, L., Tagle, D. A., Smith, S., Uziel, T., Sfez, S., Ashkenazi, M., Pecker, I., Frydman, M., Harnik, R., Patanjali, S. R., Simmons, A., Clines, G. A., Sartiel, A., Gatti, R. A., Chessa, L., Sanal, O., Lavin, M. F., Jaspers, N. G. J., Taylor, A. M. R., Arlett, C. F., Miki, T., Weissman, S. M., Lovett, M., Collins, F. S., & Shiloh, Y. (1995). A single ataxia telengiectasia gene with a product similar to PI-3 kinase. Science, 268, 1749-1753.

Schaffhausen, B., & Benjamin, T. L. (1981). Comparison of phosphorylation of two polyoma virus middle T antigens i*n vivo* and *in vitro*. J. Virol., 1, 184-196.

Scheid, M. P., Lauener, R. W., & Duronio, V. (1995). Role of phosphatidylinositol 3-OH-kinase activity in the inhibition of apoptosis in haemopoietic cells: phosphatidylinositol 3-OH-kinase inhibitors reveal a difference in signalling between interleukin-3 and granulocyte-macrophage colony stimulating factor. Biochem. J., 312, 159-162.

Schonenberger, C. A., Andres, C., Groner, B., van der Valk, M.A., LeMeur, M. and Gerlinger, P. (1988). Targetted *c-myc* gene expression in mammary glands of transgenic mice induces mammary tumors with constituitive milk protein gene transcription. EMBO J., 7, 169-175.

Schuuring, E., Verhoeven, E., Litvinov, S., & Michalides, R. J. A. M. (1993). The product of the EMS1 gene, amplified and overexpressed in human carcinomas, is homologous to a *v-src* substrate and is located in cell-substratum contact sites. Mol. Cell. Biol., 13, 2891-2898.

Seed, B., & Aruffo, A. (1987). Molecular cloning of the CD2 antigen, the T cell erythrocyte receptor, by rapid immunoselection procedure. Proc. Natl. Acad. Sci., 84, 3365-3369.

Sefton, B. M., & Taddie, J. A. (1994). Role of tyrsine kinases in lymphocyte activation. Curr. Opin. Immun., 6, 372-379.

Seger, R., & Krebs, E. G. (1995). The MAPK signaling cascade. FASEB J., 9, 726-735.

Shen, Y., & Shenk, T. E. (1995). Viruses and apoptosis. Curr. Opin. Gen. Dev., 5, 105-111.

Sherr, C. J. (1994). The ins and outs of RB: coupling gene expression to the cell cycle clock. Trends in Cell Biol., 4, 15-18.

Sinn, E., Muller, W., Pattengale, P., Tepler, I., Wallace, R., & Leder, P. (1987). Coexpression of MMTV/v-Ha-ras and MMTV/c-myc genes in transgenic mice: synergistic action of oncogenes *in vivo*. Cell, 49, 465-475.

Skalnik, D. G., Strauss, E. C., & Orkin, S. H. (1991). CCAAT displacement protein as a repressor of the myelomonocytic-specific gp91-phox gene promoter. J. Biol. Chem., 266, 16736-16744.

Skoinik, E. Y., Margolis, B., Mohammadi, M., Lowenstein, E., Fischer, R., Drepps, A., Ullrich, A., & Schlessinger, J. (1991). Cloning of PI3 kinase- associated p85 utilizing a novel method for expression/cloning of target proteins for receptor tyrosine kinases. Cell, 65, 83-90.

Slamon, D. J., Clark, G. M., Wong, S. G., Levin, W. J., Ullrich, A., & McGuire, W. L. (1987). Human breast cancer: Correlation of relapse and survival with amplification of Her-2/*neu* oncogene. Science, 235, 177-182.

Small, J. A., Scangos, G.A., Cork, L., Jay, G. and Khoury, G. (1986). The early region of human papovavirus JC induces dysmyelination in transgenic mice. Cell, 46, 13-18.

regulatory signals of the polyomavirus ge...

Songyang, Z., Shoelson, S. E., Chaudhuri, M., Gish, G., Pawson, T., Haser, W. J., King, F., Roberts, T., Ratnofsky, S., Lechleider, R. J., Neel, B. G., Birge, R. B., Fajardo, J. E., Chou, M. M., Hanafusa, H., Schaffhausen, B., & Cantley, L. (1993). SH2 domains recognize specific phosphopeptide sequences. Cell, 77, 767-778.

Sontag, E., Fedorov, S., Kamibayashi, C., Robbins, D., Cobb, M., & Mumby, M. (1993). The interaction of SV40 small tumor antigen with protein phosphatase 2A stimulates the MAP kinase pathway and induces cell proliferation. Cell, 75, 887-897.

Southern, E. M. (1975). Detection of specific sequences amoung DNA fragments seperated by gel electrophoresis. J. Mol. Biol., 98, 503-517.

Spandidos, D. A., & Wilkie, N. M. (1984). Malignant transformation of early passage rodent cells by a single mutated human oncogene. Nature (London), 310, 469-475.

Stein, D., Wu, J., Fuqua, S. A. W., Roonprapunt, C., Yajnik, V., D'Eustachio, P., Moskow, J. J., Buchberg, A. M., Osborne, C. K., & Margolis, B. (1994). The SH2 domain protein GRB-7 is co-amplified, overexpressed and in a tight complex with HER2 in breast cancer. EMBO J., 13, 1331-1340.

Stewart, T. A., Pattengale, P. K., & Leder, P. (1984). Spontaneous mammary adenocarcinomas in transgenic mice that carry and express MTV/*myc* fusion gene. Cell, 38, 627-637.

Su, W., Liu, W., Schaffhausen, B. S., & Roberts, T. M. (1995). Association of Polyomavirus middle tumor antigen with phospholipase C-γ1. J. Biol. Chem., 270, 12331-12334.

Sun, X. J., Rothenburg, P., Kahn, C. R., Backer, J. M., Araki, E., Wilden, P. A., Cahill, D. A., Goldstein, B. J., & White, M. F. (1991). Structure of the insulin receptor substrate IRS-1 defines a unique signal transduction protein. Nature (London), 352, 73-77.

Surh, C. D., & Sprent, J. (1994). T-cell apoptosis detected *in situ* during positive and negative selection in the thymus. Nature (London), 372, 100-103.

T'Ang, A., Varley, J.M., Chakraborty, S., and Fung, Y,-K.T. (1988). Structural rearrangement of the retinoblastoma gene in human breast carcinoma. Science, 242, 263-266.

Taylor, S. J., & Shalloway, D. (1994). An RNA-binding protein associated with Src through its SH2 and SH3 domains in mitosis. Nature (London), 368, 867-871.

Tooze, J. (1981). Molecular biology of tumor viruses. Cold Spring Harbour Laboritory 2nd ed.,.

Tremblay, P., Pothier, F., Hoang, T., Tremblay, G., Brownstein, S., Liszauer, A., & Jolicoeur, P. (1989). Transgenic mice carrying the mouse mammary tumor virus *ras* fusion gene: distinct effects in various tissues. Mol. Cell. Biol., 9, 854-859.

Trub, T., Choi, W. E., Wolf, G., Ottinger, E., Chen, Y., Weiss, M., & Shoelson, S. E. (1995). Specificity of the PTB domain of SHC for β turn-forming pentapeptide motifs amino-terminal to phosphotyrosine. J. Biol. Chem., 270, 18205-18208.

Turler, H., & Salomon, C. (1985). Small and middle T antigens contribute to lytic and abortive polyomavirus infection. J. Virol., 53, 579-586.

Urich, M., Shemerly, M. Y. M., Besser, D., Nagamine, Y., & Ballmer-Hofer, K. (1995). Activation and nuclear translocation of mitogen-activated protein kinases by polyomavirus middle-T or serum depend on phosphatidylinositol 3-kinase. J. Biol. Chem., 270, 29286-29292.

(1993). The mouse homeodomain protein Phox2 regulates Ncam promoter activity in concert with Cux/CDP and is a putative determinant of neurotransmitter phenotype. Development, 119, 881-896.

Van de Vijver, M., & Nusse, R. (1991). The molecular biology of breast cancer. Biochimica et Biophysica Acta., 1072, 33-50.

Van de Vijver, M. J., Peterse, Mooi, W., Lomans, J., Verbruggen, M., Van de Bersselaar, A., Devilee, P., Cornelisse, C., Bos, J.L., Yarnold, J. and Nusse, R. (1989). in Molecular Diagnostics of Human Cancer (Furth, M. and Greaves, M. eds.). , 385-391.

van der Geer, P., Wiley, S., Gish, G. D., Lai, V. K.-M., Stephens, R., White, M. F., Kaplan, D., & Pawson, T. (1996). Identification of residues that control specific binding of the Shc phosphotyrosine-binding domain to phosphotyrosine sites. Proc. Natl. Acad. Sci. USA, 93, 963-968.

Varley, J. M., Swallow, J.E., Brammer, W.J., Whittaker, J.L., and Walker, R.A. (1987). Alterations to either c-erbB-2(neu) or c-myc proto-oncogenes in breast carcinomas correlate with poor short-term prognosis. Oncogene, 1, 423-430.

Varley, J. M., Armour, J., and Swallow, J.R. (1989). The retinoblastoma gene is frequently altered leading to loss of expression in primary breast tumors. Oncogene, 4, 725-729.

Vonderhaar, B. K., & Greco, A. E. (1979). Lobulo-alveolar development of mouse mammry glands is regulated by thyroid hormones. Endocrinology, 2, 409-418.

Walter, G., Ruediger, R., Slaughter, C., & Mumby, M. (1990). Association of protein phosphatase 2A with polyoma virus medium tumor antigen. Proc. Natl. Acad. Sci. USA, 87, 2521-2525.

Wang, R. a. B., V.L. (1991). The polyomavirus early region gene in transgenic mice causes vascular and bone tumors. J. of Virology, 65, 5174-5183.

Waskiewicz, A. J., & Cooper, J. A. (1995). Mitogen and stress response pathways: MAP kinase cascades and phosphatase regulation in mammals and yeast. Curr. Opin. Cell Biol., 7, 798-805.

Webster, M. A., Cardiff, R. D., & Muller, W. J. (1995). Induction of mammary epithelial hyperplasias and mammary tumors in transgenic mice expressing a murine mammary tumor virus/activated c-*src* fusion gene. Proc. Natl. Acad. Sci., 92, 7849-7853.

Weinberg, R. A. (1985). The action of oncogenes in the cytoplasm and the nucleus. Science, 230, 770-776.

Whitman, M., Kaplan, D., Roberts, T., & Cantley, L. (1987). Evidence for two distinct phosphatidylinositol kinases in fibroblasts. Biochem. J., 247, 165-174.

Whitman, M., Kaplan, D. R., Schaffhausen, B., Cantley, L., & Roberts, T. M. (1985). Association of phosphatidylinositol kinase activity with polyoma middle-T competent for transformation. Nature (London), 315, 239-242.

Williams, J. M., & Daniel, C. W. (1983). Mammary ductal elongation: Differentiation of myoepithelium and basal lamina during branching morphogenesis. Dev. Biol., 97, 274-290.

Xia, Z., Dickens, M., Raigeaud, J., Davis, R. J., & Greenberg, M. E. (1995). Opposing effects of ERK and JNK-p38 MAP kinases on apoptosis. Science, 270, 1326-1331.

Yao, R., & Cooper, G. M. (1995). Requirement for phosphatidylinositol-3 kinase in the prevention of apoptosis by nerve growth factor. Science, 267, 2003-2006.

Yoakim, M., Hou, W., Liu, Y., Carpenter, C. L., Kapeller, R., & Schaffhausen, B. S. (1992). Interactions of Polyomavirus Middle T with the SH2 Domains of the pp85 Subunit of Phosphatidylinositol-3-Kinase. J. Virol., 66, 5485-5491.

Yu, H., Chen, J. K., Feng, S., Dalgarno, D. C., Brauer, A. W., & Schreiber, S. L. (1994). Structural basis for the binding of proline-rich peptides to SH3 domains. Cell, 76, 933-945.

Zhou, G., Bao, Z. Q., & Dixon, J. E. (1995). Components of a new human protein kinase signal transduction pathway. J. Biol. Chem., 21, 12665-12669.

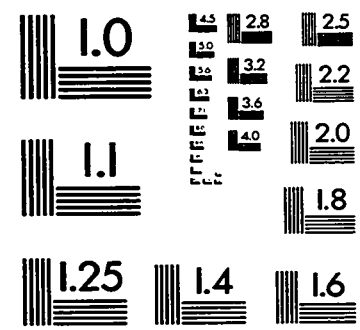

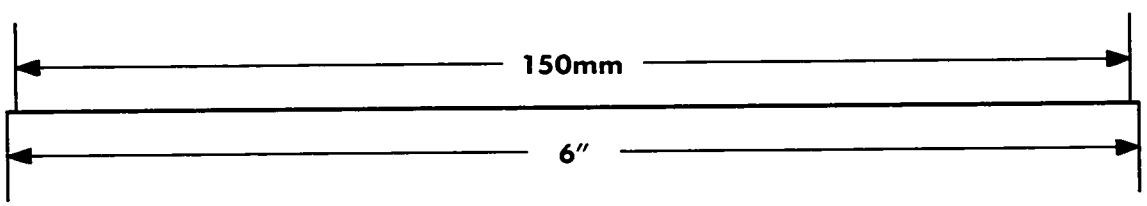

APPLIED IMAGE . Inc
1653 East Main Street
Rochester, NY 14609 USA
Phone: 716/482-0300
Fax: 716/288-5989